UNTRIPPED MANOEUVRE INDUCED ROLLOVER PREVENTION FOR SPORT UTILITY VEHICLES

by

VINCENT HERMANN WEHRMEYER

Submitted in partial fulfilment of the requirement for the degree of

MASTERS IN ENGINEERING (MECHANICAL ENGINEERING)

In the

FACULTY OF MECHANICAL AND AERONAUTICAL ENGINEERING

UNIVERSITY OF PRETORIA

February 2018

DECLARATION

I, Vincent Hermann Wehrmeyer

declare that the thesis which I hereby submit for the degree Master of Engineering at the University of Pretoria, is my own work and has not previously been submitted by me for a degree at this or any other tertiary institution.

Signature: ……. Date: …….. February 2018

ETHICS STATEMENT

The author, whose name appears on the title page of this dissertation, has obtained, for the research described in this work, the applicable research ethics approval.

The author declares that he has observed the ethical standards required in terms of the University of Pretoria's Code of ethics for researchers and the Policy guidelines for responsible research.

ABSTRACT

Title: Untripped manoeuvre induced rollover prevention for sport utility vehicles

Author: Vincent Hermann Wehrmeyer

Supervisor: Professor P.S. Els

Department: Mechanical and Aeronautical Engineering

Degree: Master of Engineering (Mechanical Engineering)

Keywords: Suspension height control, Hydro-pneumatic suspension, Roll detection, Rollover prevention, Sports Utility Vehicle

Rollover accidents account for a high number of serious injuries and fatalities and thus it is greatly important to reduce the number of occurrences. Although a large number of rollovers result from factors external to the vehicle design such as environmental obstacles there is a significant portion of rollover accidents which are preventable. O*n-road untripped rollovers* are directly related to the vehicle design. It is possible to do work in this area to improve vehicle-related safety factors.

During rollover, lateral acceleration acts on the centre of gravity of the vehicle over turning it about the outer wheels. Thus the method to reduce or prevent rollover of this study stemmed from decreasing the overturning moment by reducing the movement arm though which the lateral acceleration acts. This is achieved by lower the ride height of the test vehicle using slow active suspension control of the test vehicle (Land Rover Defender 110) fitted with a hydro-pneumatic suspension system.

An experimental validated mathematical model representing the test vehicle is created to develop a rollover prevention control system that reduces the vehicle's ride height and reduces the propensity to rollover. The control system applies one of three discrete suspension settings depending on the severity of the manoeuvre as well as lowering the ride height. The model is used to simulate the Fishhook 1B and the ISO 3888 Double Lane Change manoeuvres to evaluate the roll prevention system.

The rollover prevention control system improved the two wheel lift off speed of the vehicle through a Fishhook 1 B manoeuvre by 64%, the body roll angle of the vehicle through the Double Lane Change manoeuvre by 13% and the body roll rate by 25.7%. The control system significantly improved the vehicle's response with regard to smooth flat on-road untripped rollover. Further improvements are possible with the use of the proposed control system in conjunction with a fully active suspension system to allow for faster corrective action.

OPSOMMING

Titel: Untripped manoeuvre induced rollover prevention for sport utility vehicles

Outeur: Vincent Hermann Wehrmeyer

Studieleier: Professor P.S. Els

Department: Meganiese en Lugvaartkundige Ingenieurswese

Graadkursus: Meester van Ingenieurswese (Meganiese Ingenierswese)

Sleutelterme: Suspension height control, Hydro-pneumatic suspension, Roll detection, Rollover prevention, Sports Utility Vehicle

Oorrol ongelukke is verantwoordelik vir ‘n hoe aantal van ernstige beseerings en dodelike ongelukke en dus is dit van groot belang om die hoeveelheid ongelukke te verminder. Alhoewel meeste oorrol ongelukke is as gevolg van faktore anders as die voortuig se ontwerp, soos byvoorbeeld omgewingshindernisse, is daar ‘n groot percentasie van oorrol ongelukke wat vermybaar is. On-pad onbelemmerde rollovers is direk verwant aan die voertuigontwerp. Dit is moontlik om werk in hierdie area te doen om voertuigverwante veiligheidsfaktore te verbeter.

Tydens rolloverwerking tree laterale versnelling op die swaartepunt van die voertuig oor en draai dit om die buitenste wiele. Dus die metodiek in hierdie studie om oorrol te verminder of te verhoed, stem uit vermindering van die omkeer oomblik afgeneem, deur om die bewegingsarm waardeur die laterale versnelling werk, te verminder.

Dit word behaal deur die rithoogte van die toetsvoertuig te verlaag deur gebruik te maak van 'n stadig aktiewe opskortingsbeheer van die toetsvoertuig (Land Rover Defender 110) wat met 'n hidro-pneumatiese suspensie stelsel toegerus is.

'N eksperimentele gevalideerde wiskundige model wat die toetsvoertuig verteenwoordig, word geskep om 'n rollover-voorkomingsbeheerstelsel te ontwikkel wat die voertuig se rithoogte verminder en die geneigdheid om oor te skakel, verminder. Die beheerstelsel pas een van drie diskrete skorsingsinstellings toe, afhangende van die erns van die maneuver asook die verlaging van die rithoogte. Die model word gebruik om die Fishhook 1B en die ISO 3888 Double Lane Change maneuvers te simuleer om die rolvoorkomingsisteem te evalueer.

Die rollover-voorkomings-beheerstelsel het die twee-wiel oplig-snelheid van die voertuig verbeter deur 'n Fishhook 1 B-maneuver met 64%, die liggaamsrolhoek van die voertuig deur die Double Lane Change-maneuver met 13% en die liggaamsrolkoers met 25.7% te verbeter. Die beheersingsstelsel het die voertuig se reaksie aansienlik verbeter met betrekking tot gladde plat op-pad onbelemmerde oorrol. Verdere verbeterings is moontlik met die gebruik van die voorgestelde kontrolesisteem in samewerking met 'n ten volle aktiewe suspensie om vinniger regstellende aksie toe te laat.

ACKNOWLEDGEMENTS

I would like to express my gratitude to:

- Prof. Els, for his mentorship throughout my postgraduate studies.
- My parents Ella and Wilfred Wehrmeyer, for their support and encouragement in my pursuit of my Masters.
- My brother Wolfgang Wehrmeyer, for his advice and support.
- My fellow members of the Vehicle Dynamic Group-Carl Becker, Cor-Jacques Kat, Francois van der Westhuizen, Theunis Botha, Hermann Hamersma, Joachim Stallmann and Bernard Linström for their advice and support during testing.

TABLE OF CONTENTS

ABSTRACT iii
OPSOMMING iv
ACKNOWLEDGEMENTS v
TABLE OF CONTENTS vi
LIST OF FIGURES viii
LIST OF TABLES xiii
LIST OF SYMBOLS xiii
ABBREVIATIONS xiii
ROMAN SYMBOLS xiv
GREEK SYMBOLS xvi
SUBSCRIPTS xvi
1 INTRODUCTION 1
1.1 Context of the Research Problem 1
1.2 Problem Statement 2
1.3 Aim of the study 3
1.4 Scope of Research 3
1.5 Document Overview 3
2 LITERATURE STUDY 5
2.1 Rollover Mechanism 5
2.1.1 Rollover of a Rigid Vehicle 6
2.1.2 Rollover of a Suspended Vehicle 7
2.1.3 Transient Rollover 9
2.1.4 Rollover after Wheel Lift 11
2.1.5 14 Degree of Freedom Model 12
2.2 Roll Angle Estimations 12
2.2.1 Tyre Pressure/Deflection 12
2.2.2 Estimation of Roll Angle via Suspension Deflections 13
2.2.3 Estimation of Roll Angle from Lateral Acceleration 14
2.2.4 Estimation of Roll angle via Integration Measured Roll Rate 16
2.3 Rollover Prediction 16
2.3.1 Statics Stability Factor 16
2.3.2 Rollover Threshold on Look-up Tables 18
2.3.3 Roll Stability Advisor 19

2.3.4 Dynamic Stability Index 19
2.3.5 Rollover Prevention Energy Reserve 20
2.3.6 Rollover Prevention Metric 20
2.3.7 Time-To-Rollover 21
2.4 Rollover Prevention 23
2.4.1 Active Steering 23
2.4.2 Active Braking 25
2.4.3 Active Suspension Systems 28
2.4.4 Ideal Suspension Characteristics Settings 29
2.4.5 Centre of Gravity Position 31
2.5 Hydro-pneumatic Levelling Control 34
2.6 Conclusion 36
3 SIMULATION MODEL 38
3.1 Mathematical Model 38
3.1.1 Vehicle Properties 39
3.1.2 Suspension System 41
3.1.3 Hydraulic Circuit 46
3.2 Rollover Prevention Strategy 47
3.2.1 Roll Angle Estimation 49
3.2.2 Rollover Detection Strategy 50
3.2.3 Rollover Control Strategy 1 52
3.2.4 Rollover Control Strategy 2 55
3.3 Conclusion 59
4 SIMULATION MODEL VALIDATION 60
4.1 Experimental Setup 60
4.2 Test Manoeuvres 61
4.2.1 ISO 3888 Double Lane Change Manoeuvre 61
4.2.2 Step-Steer Manoeuvre 62
4.2.3 Slowly Increasing Steer 63
4.2.4 NHTSA Fishhook Manoeuvre 63
4.3 Validation Metric Based on Relative Error 67
4.4 Simulation Validation 67
4.4.1 Validation in Handling Mode 67
4.4.2 Validation in Ride Comfort Mode 70
4.5 Conclusion 72

5 SIMULATION RESULTS 73
5.1 The Step-Steer Manoeuvre 73
5.1.1 Roll Angle 73
5.1.2 Roll Rate 75
5.1.3 Yaw Rate 78
5.1.4 Lateral Acceleration 81
5.1.5 Wheel Lift 83
5.1.6 Conclusion 85
5.2 The Fishhook 1B 86
5.2.1 Determination of the Steering Angle Amplitude 86
5.2.2 Fishhook 1B Maximum Speed without Wheel Lift-Off 86
5.2.3 Fishhook 1B Control System Maximum Speed Without Wheel Lift-Off 87
5.2.4 Rollover Index 95
5.3 The ISO 3888 Double Lane Change 96
5.4 Conclusion 101
6 CONCLUSION AND RECOMMENDATIONS 103
6.1 Conclusion 103
6.2 Recommendation 103
7 REFERENCES 106
8 APPENDICES 110
8.1 Characteristics of hydraulic valves used in test vehicle circuit 110
8.2 Validation plots for higher speeds 112
8.3 Comparison for Fishhook 1B maximum run speeds 114
8.3.1 Fishhook 1B at 36 km/h 114
8.3.2 Fishhook 1B at 40 km/h 117
8.3.3 Fishhook 1B at 50 km/h 121
8.4 Double Lane Change Simulation Results for 60 and 70 km/h 124
8.4.1 Double Lane Change at 60 km/h 124
8.4.2 Double Lane Change at 70 km/h 128

LIST OF FIGURES

Figure 1.1: Percentage of Fatal Crashes & Fatalities per Type of Crash (RRTMC, 2009) 1
Figure 1.2: Severity per Type of Crash (RTMC, 2009) 2
Figure 2.1: Simple models reflecting vehicle roll motion during a) normal driving and b) rollover phase (Hac et. al, 2004) 6

Figure 2.2: Forces acting to roll over a vehicle (Gillespie, 1992) 6
Figure 2.3: Equilibrium lateral acceleration in rollover of a rigid vehicle (Gillespie, 1992) 7
Figure 2.4: Roll reactions on a suspended vehicle (Gillespie, 1992) 8
Figure 2.5: Equilibrium lateral acceleration in rollover of a suspended vehicle (Gillespie, 1992) 9
Figure 2.6: Roll response to a step input 10
Figure 2.7: Effects of damping ratio on rollover threshold in a step steer 10
Figure 2.8: Vehicle Body Roll and Suspension Deflections During a) a Right Turn on Smooth Road, b) Driving straight on Uneven Road (Hac et al., 2004) 14
Figure 2.9: A Simple Model of Vehicle Roll Motion (Hac et al., 2004) 15
Figure 2.10: Flow chart for the TTR calculation (Chen and Peng, 1999) 21
Figure 2.11: Detailed implementation for the TTR calculation (Chen and Peng 1999) 22
Figure 2.12: Feedforward Gain for Active Rear Steer System (Hac, 2002) 24
Figure 2.13: Functional Diagram of Vehicle Stability Enhancement System (Hac, 2002) 26
Figure 2.14: Active Roll Bars with Linear and Rotary Actuators (Hac, 2002) 28
Figure 2.15: Simulation Data of Two-Wheel Lift Velocity versus CG Height for the Blazer (Whitehead et al., 2004) 31
Figure 2.16: Simulation data of SIS Constant versus Weight Split (Whitehead et al., 2004) 32
Figure 2.17: Simulation data of two-wheel lift velocity versus weight split of a blazer in a Fishhook 1Amanoeuvre (Whitehead et al., 2004) 32
Figure 2.18: Simulation data showing the understeer curve for the various weight splits (Whitehead et al., 2004) 33
Figure 2.19: Basic setup of an electronically controlled levelling system (Bauer, 2011) 34
Figure 2.20: Interaction of controller and controlled system for axle suspension levelling (Bauer, 2011) 35
Figure 2.21: Logic and control behaviour of a P-controller (Bauer, 2011) 35
Figure 2.22: P-controller with deadband (Bauer, 2011) 36
Figure 2.23: Controller with double low pass filter (Bauer, 2011) 36
Figure 3.1: Location of centres of gravity and vehicle geometry (Uys et al., 2006) 40
Figure 3.2 Kingpin steer range 40
Figure 3.3 circuit diagram (Els 2006) 41
Figure 3.4 4S4Soft and Stiff spring characteristics (Els, 2006) 42
Figure 3.5 4S4 Damper characteristics (Els, 2006) 42
Figure 3.6: Modelling of the full vehicle front suspension in MSC.ADAMS (Thoresson, 2005) 44
Figure 3.7: Modelling of the full vehicle rear suspension in MSC.ADAMS (Thoresson, 2005) 45
Figure 3.8: Hydraulic circuit for a single suspension unit (Van der Westhuizen, 2012) 46
Figure 3.9: Flow diagram of the hydraulic setup in the test vehicle (Van der Westhuizen, 2012) 47
Figure 3.10: Rigid vehicle model (Dukkipati et al., 2008) 48
Figure 3.11: Vehicle rollover speed for step-steer steering angle 51
Figure 3.12: Rollover detection flow chart 52
Figure 3.13: Rollover prevention strategy 1, steady state rollover mode algorithm 54
Figure 3.14: Rollover strategy 1, dynamic rollover mode algorithm 55
Figure 3.15: PID and value control for rollover control strategy 2 57
Figure 3.16: Basic flow diagram of rollover control strategy 2 58
Figure 4.1: Fishhook 1a manoeuvre description (Forkenbrock et al., 2002) 64
Figure 4.2: Fishhook 1b manoeuvre description (Forkenbrock et al., 2002) 65
Figure 4.4: Land Rover Defender 110 Wagon doing a DLC manoeuvre in ride comfort mode 66

Figure 4.5: Vehicle path for 56.5 km/h validation test on handling suspension mode (speed, steering angle, path, lateral acceleration, yaw rate, roll rate and roll angle) 68
Figure 4.6: Suspension displacements and forces for 56.6 km/h validation test in handling mode 69
Figure 4.7: Vehicle path for 56.5 km/h validation test on ride comfort suspension mode (Speed, steering angle, path, lateral acceleration, yaw rate, roll rate and roll angle) 70
Figure 5.1: Maximum roll angle for step-steer simulation on ride comfort mode.....73
Figure 5.2: Maximum roll angle for step-steer simulation on energy removal mode.....74
Figure 5.3: Maximum roll angle for step-steer simulation on handling mode.....74
Figure 5.5: Maximum roll rate for step-steer simulation on ride comfort mode.....76
Figure 5.6: Maximum roll rate for step-steer simulation on energy removal mode.....76
Figure 5.7: Maximum roll rate for step-steer simulation on handling mode.....77
Figure 5.8: Roll rate comparison of various suspension modes executing a step steer manoeuvre of 13 degrees at a speed of 60 km/h 78
Figure 5.9: Maximum yaw rate for step-steer simulation on ride comfort mode.....78
Figure 5.10: Maximum yaw rate for step-steer simulation on energy removal mode.....79
Figure 5.11: Maximum yaw for step-steer simulation on handling mode.....79
Figure 5.12: Yaw rate comparison of various suspension modes executing a step steer manoeuvre of 13 degrees at a speed of 60 km/h 80
Figure 5.13: Yaw rate comparison of various step steer angles at a speed of 60 km/h for ride comfort mode 80
Figure 5.14: Maximum lateral acceleration for step-steer simulation on ride comfort mode 81
Figure 5.15: Maximum lateral acceleration for step-steer simulation on energy removal mode 81
Figure 5.16: Maximum lateral acceleration for step-steer simulation on handling mode 82
Figure 5.18: Maximum wheel lift for step-steer simulation on ride comfort mode (lower initial suspension force).....83
Figure 5.19: Maximum wheel lift for step-steer simulation on energy removal mode (lower initial suspension force).....84
Figure 5.20: Maximum wheel lift off for step-steer simulation on handling mode 84
Figure 5.21: Wheel lift comparison of various step steer angles at a speed of 60 km/h for ride comfort mode 85
Figure 5.22: Rear inner wheel lift comparison of various suspension modes executing a step steer manoeuvre of 13 degrees at a speed of 60 km/h.....85
Figure 5.23: Slowly Increasing Steer Angle.....86
Figure 5.25: Fishhook 1B manoeuvre on rollover prevention mode, vehicle path 88
Figure 5.26: Fishhook 1B manoeuvre on rollover prevention mode; lateral acceleration, roll rate, roll angle and yaw rate.....89
Figure 5.27: Fishhook 1B manoeuvre on rollover prevention mode, wheel lift.....89
Figure 5.28: Fishhook 1B manoeuvre on rollover prevention mode, suspension displacement 90
Figure 5.29: Fishhook 1B manoeuvre on rollover prevention mode, available strut pressure.....91
Figure 5.30: Fishhook 1B manoeuvre on rollover prevention mode, CG height change.....91
Figure 5.31: Fishhook 1B manoeuvre on rollover prevention mode, oil volume adjustment (incremental) 92
Figure 5.32: Fishhook 1B manoeuvre on rollover prevention mode, oil volume adjustment (total)...93
Figure 5.33: Fishhook 1B manoeuvre on rollover prevention mode, oil flow rates 93
Figure 5.34: Fishhook 1B manoeuvre on rollover prevention mode, suspension settings.....94
Figure 5.35: Fishhook 1B manoeuvre on rollover prevention mode, PID error tracking.....94

Figure 5.36: Fishhook 1B manoeuvre on rollover prevention mode, DSI and RPER 95
Figure 5.37: Fishhook 1B manoeuvre on rollover prevention mode, rollover prevention control system's rollover index.....96
Figure 5.38: Double Lane Change at 80 km/h, steer input 97
Figure 5.39: Double Lane Change at 80 km/h, vehicle path.....97
Figure 5.40: Double Lane Change at 80 km/h, lateral acceleration, roll rate, roll angle and yaw rate 98
Figure 5.41: Double Lane Change at 80 km/h, suspension displacement 99
Figure 5.42: Double Lane Change at 80 km/h, CG height change 99
Figure 5.43: Double Lane Change at 80 km/h, rollover index from control system 100
Figure 5.44: Double Lane Change at 80 km/h, DSI and RPER.....100
Figure 8.1: Performance graphs for the SV10-24 valve (Van der Westhuizen, 2012) 110
Figure 8.2: Performance graphs for the SV10-24 valve (Van der Westhuizen, 2012) 110
Figure 8.3: Flow vs. Pressure Drop for SV10-24 valve (Van der Westhuizen, 2012) 111
Figure 8.4: Flow vs. Pressure for the SV12-33 directional valve (Van der Westhuizen, 2012).....111
Figure 8.5: Flow vs. Pressure for the FPCC proportional valve (Van der Westhuizen, 2012).....111
Figure 8.6: Validation DLC 71 km/h on handling suspension setting 112
Figure 8.7: Validation DLC 71 km/h on ride comfort suspension setting 112
Figure 8.8: Validation DLC 76 km/h on handling suspension setting 113
Figure 8.9: Validation DLC 74 km/h on ride comfort suspension setting 113
Figure 8.10: Fishhook 1B at 36 km/h, speed input 114
Figure 8.11: Fishhook 1B at 36 km/h, Steer angle 114
Figure 8.12: Fishhook 1B at 36 km/h, Vehicle path 114
Figure 8.13: Fishhook 1B at 36 km/h, Lateral acceleration, roll velocity, roll angle and yaw rate.....115
Figure 8.14: Fishhook 1B at 36 km/h, Wheel lift off 115
Figure 8.15: Fishhook 1B at 36 km/h, Suspension displacement 116
Figure 8.16: Fishhook 1B at 36 km/h, CG height change 116
Figure 8.17: Fishhook 1B at 36 km/h, Rollover index from control system 116
Figure 8.18: Fishhook 1B at 36 km/h, DSI and RPER.....117
Figure 8.19: Fishhook 1B at 40 km/h, speed input 117
Figure 8.20: Fishhook 1B at 40km/h, Steer angle.....117
Figure 8.21: Fishhook 1B at 40km/h, Vehicle path 118
Figure 8.22: Fishhook 1B at 40km/h, Lateral acceleration, roll velocity, roll angle and yaw rate.....118
Figure 8.23: Fishhook 1B at 40km/h, Wheel lift off 119
Figure 8.24: Fishhook 1B at 40km/h, Suspension displacement 119
Figure 8.25: Fishhook 1B at 40km/h, CG height change 120
Figure 8.26: Fishhook 1B at 40km/h, Rollover index from control system 120
Figure 8.27: Fishhook 1B at 40km/h, DSI and RPER.....120
Figure 8.28: Fishhook 1B at 50 km/h, speed input 121
Figure 8.29: Fishhook 1B at 50km/h, Steer angle.....121
Figure 8.30: Fishhook 1B at 50km/h, Vehicle path 121
Figure 8.31: Fishhook 1B at 50km/h, Lateral acceleration, roll velocity, roll angle and yaw rate.....122
Figure 8.32: Fishhook 1B at 50km/h, Wheel lift off 122
Figure 8.33: Fishhook 1B at 50km/h, Suspension displacement 123
Figure 8.34: Fishhook 1B at 50km/h, CG height change 123
Figure 8.35: Fishhook 1B at 50km/h, Rollover index from control system 123
Figure 8.36: Fishhook 1B at 50km/h, DSI and RPER.....124

Figure 8.37: Double Lane Change at 60 km/h, speed 124
Figure 8.38: Double Lane Change at 60 km/h, steer input 125
Figure 8.39: Double Lane Change at 60 km/h, vehicle path 125
Figure 8.40: Double Lane Change at 60 km/h, lateral acceleration, roll rate, roll angle and yaw rate 125
Figure 8.41: Double Lane Change at 60 km/h, wheel lift 126
Figure 8.42: Double Lane Change at 60 km/h, suspension displacement 126
Figure 8.43: Double Lane Change at 60 km/h, CG height change 127
Figure 8.44: Double Lane Change at 60 km/h, rollover index from control system 127
Figure 8.45: Double Lane Change at 60 km/h, DSI and RPER 127
Figure 8.46: Double Lane Change at 70 km/h, speed 128
Figure 8.47: Double Lane Change at 70 km/h, steer input 128
Figure 8.48: Double Lane Change at 70 km/h, vehicle path 128
Figure 8.49: Double Lane Change at 70 km/h, lateral acceleration, roll rate, roll angle and yaw rate 129
Figure 8.50: Double Lane Change at 70 km/h, wheel lift 129
Figure 8.51: Double Lane Change at 70 km/h, suspension displacement 130
Figure 8.52: Double Lane Change at 70 km/h, CG height change 130
Figure 8.53: Double Lane Change at 70 km/h, Rollover index from control system 131
Figure 8.54: Double Lane Change at 70 km/h, DSI and RPER 131

LIST OF TABLES

Table 3-1: MSC.ADAMS vehicle model's degrees of freedom 39
Table 3-2: Properties of the test vehicle (Uys et al., 2006) 39
Table 4-1: Parameters measured for vehicle validation 61
Table 4-2: ISO 3888 Double Lane Change manoeuvre course section dimensions 62
Table 4-3: Summary of Rollover Resistance Manoeuvre Scores (Forkenbrock et al., 2002) 63
Table 4-4: Peak %RE for handling mode 68
Table 4-5: Suspension validation metrics for 56.5 km/h validation test in handling mode 69
Table 4-6: %RE peak values for 56.6 km/h validation test on suspension ride comfort mode 71
Table 4-7: Suspension validation metrics for 56.6 km/h validation test in ride comfort mode 72
Table 5-1: Step-steer manoeuvre, maximum roll angle before rollover 75
Table 5-2: Step-steer manoeuvre, maximum roll rate before rollover 77
Table 5-3: Step-steer manoeuvre, maximum yaw rate before rollover 80
Table 5-4: Step-steer manoeuvre, maximum lateral acceleration before rollover 82
Table 5-5: Fishhook 1B maximum speed without wheel lift off 87
Table 5-6: Analysis of test maneuvers 101

LIST OF SYMBOLS

ABBREVIATIONS

Abbreviation	Description
$4S_4$	Four-State Semi-Active Suspension System
4WS	Four wheel steer
AARB	Active Anti-Roll Bar
ABS	Anti-lock braking system
ARB	Anti-rollover braking
ARS	Active rear steer
BWR	Benedict Webb Rubin (real gas equation)
CG	Centre of Gravity
DBC	Dynamic Body Control
DLC	Double Lane Change
DOF	Degree of freedom
DSF	Damping Static Factor
DSTC	Dynamic Stability Traction Control
ESC	Electronic stability control

GV	Gas Volume
InF	Infinite values
MV	Manipulated variable
NaN	Not a number
NHTSA	National Highway Traffic Safety Administration
NN	Neural Network
PID	Proportional Integral Derivative controller
RE	Relative error
RPER	Rollover Prevention Energy Reserve
RPM	Rollover Prevention Metric
RSA	Roll stability advisor
RSC	Roll Stability Control
SIS	Slowly Increasing Steer
SSF	Statics Stability Factor
SUV	Sports-utility vehicle
TTR	Time-to-Rollover
VDG	Vehicle Dynamics Group
VSC	Vehicle Skid Control
VSE	Vehicle stability enhancement

ROMAN SYMBOLS

Symbol	Description
a_y	Lateral acceleration
$a_{y(\max)}$	Maximum body lateral acceleration threshold
a_{ym}	Combined lateral and gravitational acceleration the vehicle experiences
b	Lateral distance between struts
c_{roll}	Roll angular damping coefficient
e	Error value
E_k	Instantaneous kinetic energy prior to rollover

E_v	Potential energy at the tipping point
F_y	Lateral force
F_z	Vertical force on wheel
F_{zo}	Vertical force on the outside wheel
F_{zi}	vertical force on the inside wheel
g	Gravitational constant
h	Height of the center of gravity
$h_1 or\ h_{roll}$	Height difference between the CG and the roll center
h_r	Roll center height above the ground
K	Derivative gain for a PID controller
K_f	Front roll stiffness
K_I	Integral gain for a PID controller
K_P	Proportional gain for a PID controller
k_{roll}	Roll angular stiffness coefficient
K_r	Rear roll stiffness
K_s	Suspension unit stiffness
$k_{tyreroll}$	Roll stiffness resulting from tyre stiffness
I_B	Mass moment of inertia of the vehicle about the outside wheel contact patch
I_{xx}	Roll mass moment of inertia about the center of gravity
M	Mass of the vehicle
m	Measured value
p	Predicted value
r	Distance between the CG and the point of rotation
t	Track width
T_o	Lateral kinetic energy
T_1	Rotational energy
v	Vehicle speed
V	Velocity

W	Weight of the vehicle
z	Half the track width
z_{actual}	Measure strut displacement
$z_{desired}$	Desired strut displacement
Z_{FL}	Front left suspension displacement height
Z_{FR}	Front right suspension displacement height
Z_{RL}	Rear left suspension displacement height
Z_{RR}	Rear right suspension displacement height

GREEK SYMBOLS

Symbol	Description
δ	Steer angle at wheels
Δz	Change in suspension deflection
θ	Body roll angle
$\theta_{threshold}$	Maximum body roll angle threshold
θ_{a_y}	Estimation of the roll angle from lateral acceleration
θ_Z	Estimation of the roll angle from the suspension displacements
$\theta_{\dot{\theta}}$	Estimation of the roll angle from integration of the roll rate
$\dot{\theta}$	Body roll rate
$\dot{\theta}_{threshold}$	Maximum body roll rate threshold
$\ddot{\theta}$	Body roll acceleration
κ	Static tip angle
μ	Kinetic friction coefficient between the wheels and the road
φ	Road lateral elevation angle

SUBSCRIPTS

Subscripts	Description

FL	Front left
FR	Front rear
i	Inner
o	Outer
RL	Rear left
RR	Rear right
x	Longitudinal direction
y	Lateral direction
z	Vertical direction
Z	Suspension displacement

1 INTRODUCTION

1.1 Context of the Research Problem

Rollover accidents are one of the most significant safety problems on the road. Rollover accidents account for a high number of serious injuries and fatalities. Rollovers are caused by various factors such as excessive speeds in cornering, traversing critical slopes and tripping. The high number of fatalities has led to investigations into the causes and severity of vehicle crashes.

The **Road Traffic Management Corporation (2009)** in South Africa reported on the types of fatal crashes to support information on the prevalent conditions and possible factors contributing to crashes. The percentage of fatal crashes in terms of type of crash for 2009 is depicted in Figure 1.1:

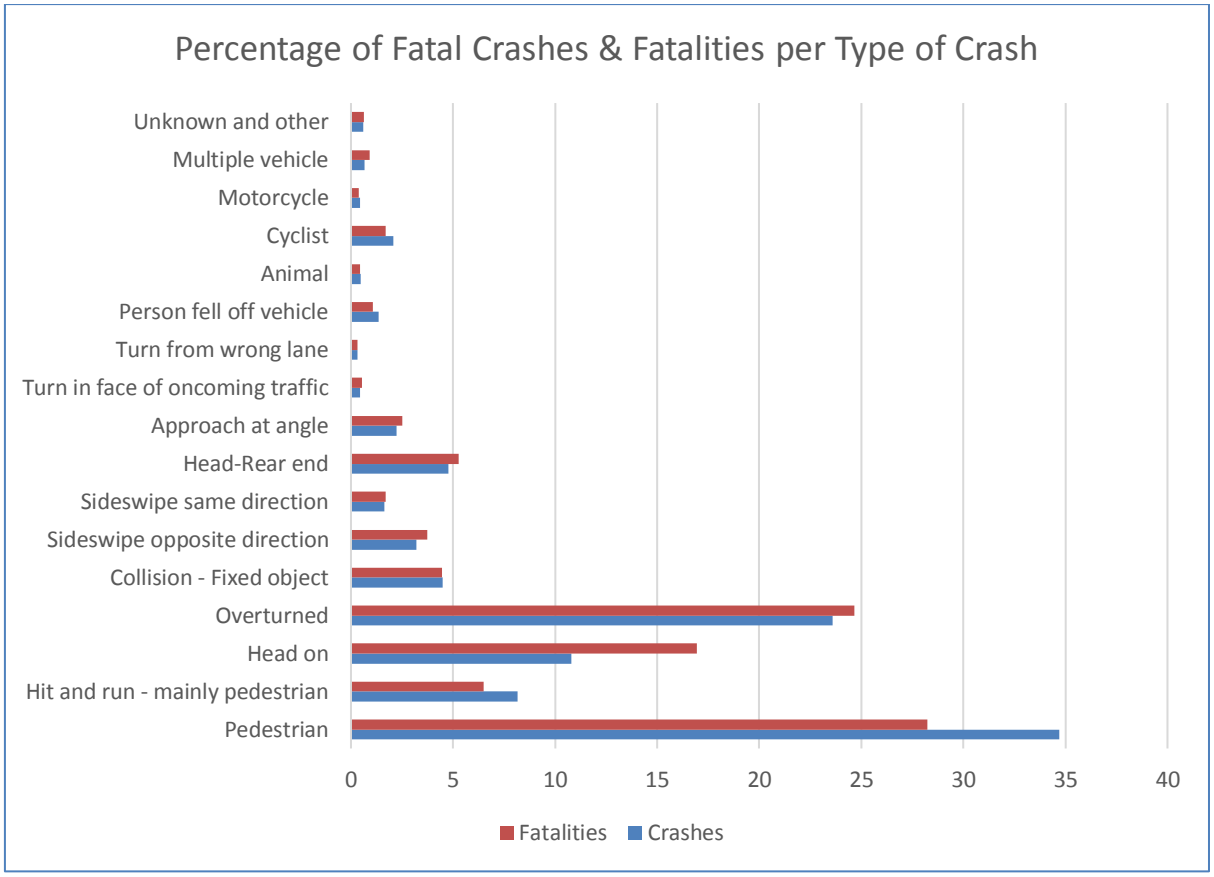

Figure 1.1: Percentage of Fatal Crashes & Fatalities per Type of Crash (RTMC, 2009)

They concluded that rollover accidents in 2009 were responsible for the second highest percentage of fatal crashes as well as fatalities per type of crash. Therefore, not only do rollover accidents present a frequently-occurring type of accident, but the severity of their nature is also evident from the data. This is illustrated in Figure 1.2, which compares the severity of different types of crashes in terms of a proportional rating.

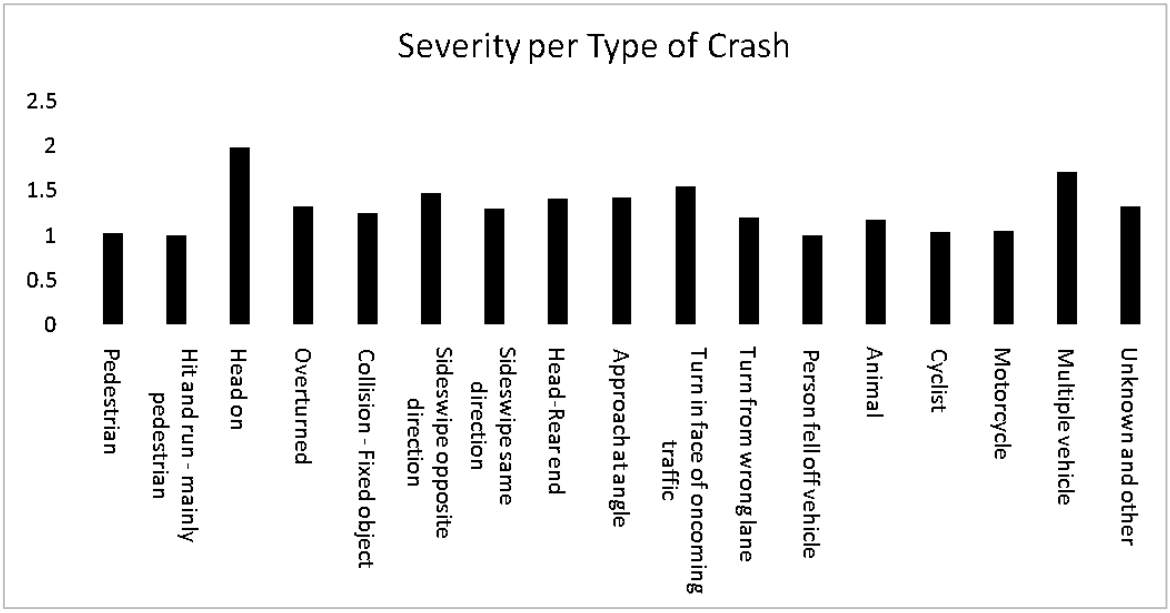

Figure 1.2: Severity per Type of Crash (RTMC, 2009)

The report concluded that vehicles that had overturned were induced most likely by unsafe and illegal overtaking manoeuvres, fatigue, poor judgement, poor visibility or poor vehicle and road conditions. It is not always possible to account for the environment or the condition of the driver; however, it is possible to improve the vehicle such that it can intelligently act to prevent rollovers.

According to the **National Highway Traffic Safety Administration** (NHTSA) **(Rollover Data Special Study Final Report, 2011)**, although rollover crashes are accountable for 3% of vehicle crashes, they are responsible for approximately one-third of all occupant deaths in the USA. This highlights the great need for research to improve vehicle design in order to reduce the number of casualties.

The NHTSA estimates that at least ten percent of rollovers are what is termed *on-road untripped rollover* ***(cf. Jin et al., 2016)***. This means that the vehicle overturns on a smooth road due to loss of grip or momentum but without being caused by collision with another object such as a rock. It is induced by extreme manoeuvres during critical driving situations (e.g. excessive speed during cornering, obstacle avoidance and severe lane change manoeuvres **(Jin et al., 2016)**. This is only a small portion of rollovers; however, since these rollovers are a direct reflection of the vehicle design and are not dependent on external circumstances, it is possible to do work in this area to improve vehicle-related safety factors. Untripped rollovers are preventable and thus are an unnecessary occurrence. The aim of the NHTSA is to achieve a set of standards that are a function of vehicle parameters, which can be used as a benchmark in vehicle design and production **(Rollover Data Special Study Final Report, 2011)**.

1.2 Problem Statement

The research topic for this thesis stemmed from the literature study, which indicated that one way of minimising the possibility of rollover and improve overall rollover characteristics of a vehicle is to lower its centre of gravity (CG). This identified a potential research area, i.e. to investigate an intelligent method to lower the CG of a SUV, the Land Rover Defender 110, fitted with a hydro-pneumatic suspension system (the $4S_4$) during potentially severe manoeuvres.

1.3 Aim of the study

The aim of this study, therefore, is to investigate the reduction of the CG height using a semi-active hydro-pneumatic suspension installed on a Land Rover Defender 110 in order to reduce the effects of rollover. The vehicle is a suitable test vehicle since it has a relatively high CG and soft suspension, making it prone to rollovers.

The main aim of the study can be divided into two secondary aims:

- To simulate the prevention of rollover by lowering the CG of a Sports Utility Vehicle;
- To develop an algorithm that will predict the propensity of rollover for a vehicle on its limits and activate a rollover prevention strategy.

These aims in turn clarify the scope of the research project.

1.4 Scope of Research

In achieving the aims set out above, the study incorporates three aspects:

- Firstly, a mathematical model representing the test vehicle is developed using the multi-dynamic software package MSC.ADAMS/VIEW **(MSC.Software, 2013)**.
- Secondly, this model is then validated with experimental data from physical tests.
- Finally, computer simulation is done on the model in order to develop a rollover prevention control system that reduces the vehicle's ride height and reduces the propensity to rollover.

Simulations such as those achieved with ADAMS/VIEW shorten the development time and cycle, reduce testing costs and reduce the risk involved in rollover tests **(Dukkipati et al., 2008)**. The simulation rollover prevention control system will include a detection algorithm, a prediction algorithm and a prevention algorithm. The detection algorithm will consider lateral acceleration, roll rate, vehicle speed and steering angle to determine the severity of the manoeuvre. For the prediction algorithm, a combination of vehicle measurements used in a threshold look-up table is best suited for the particular application at hand. Obviously, a prediction system that can calculate the time to rollover would be more desirable, but due to the complex nature of such a system, it would be time-consuming beyond the scope of this thesis. The prevention algorithm will use slow active control levelling of the fitted hydro-pneumatic suspension system (the $4S_4$) to lower the centre of gravity of the vehicle. Two discrete suspension settings with regard to spring rate and damping will be utilised. The manoeuvres investigated in this thesis include the step steer manoeuvre, the Fishhook 1B manoeuvre and the ISO 3888 Double Lane Change manoeuvre.

1.5 Document Overview

In chapter 1, the research topic is introduced in the context of the importance of vehicle design to prevent rollover and the thesis's aim of creating a simulation model using the multi-dynamic software package MSC.ADAMS/VIEW to address the possibility of lowering the CG in order to prevent rollover is outlined.

In chapter 2, the results of the literature study are reported. Different rollover mechanisms varying in complexity are discussed, as well as different means of estimating the roll angle which underpins most rollover detection and prediction algorithms. Thereafter, different methods of rollover prediction and prevention are outlined. The chapter concludes with a discussion of a hydro-pneumatic levelling control system in anticipation of the requirements of the study.

In chapter 3, the development of the mathematical model used in the investigation is discussed. Thereafter a report is given of the simulation design in terms of estimation of roll angle, the design of the rollover detection strategy and the design of rollover control strategies.

Chapter 4 reports on the experimental work undertaken to provide validation of the mathematical model, together with an explanation of types of manoeuvres that relate vehicle rollover to severity and identification, of those investigated in this thesis.

Chapter 5 presents the simulation results for the three different manoeuvres outlined in chapter 4, namely the Step Steer Manoeuvre, the Fishhook 1B manoeuvre and the ISO3888 Double Lane Change manoeuvre.

In chapter 6, the conclusions of the study in terms of the research question and aims are presented. Limitations of the present study and recommendations for future research are also discussed.

2 LITERATURE STUDY

Accounting for work already done in the field of rollover prevention is of importance to determine what ideas were studied and what possibilities exist for improvements.

In chapter 2.1, the physical mechanism of rollover is investigated using various models. This is followed in chapter 2.2 by a discussion on existing methods of roll angle detection and calculation. In chapter 2.3, different indices used in rollover prediction models are introduced, and in chapter 2.4, means of rollover prevention are discussed. Finally, a discussion of hydro-pneumatic levelling control systems is given in chapter 2.5 in preparation for the requirements of the present study. The chapter concludes by giving a summary of the literature review.

2.1 Rollover Mechanism

Rollover may be defined and is dependent on various vehicle parameters and conditions.

Gillespie (1992) defines rollover as that which occurs when a vehicle rotates 90 degrees or more about its longitudinal axis such that the body makes contact with the ground, where the resulting action is manoeuvre-induced. Rollover is considered to begin when the inside wheel lifts off and is irretrievable when the lateral acceleration reaches zero. The pivot about which the body roll occurs and the lateral forces are transferred from the axle to the sprung mass is called the roll centre.

According to **Dukkipati et al. (2008)**, the vulnerability to rollover is affected by the vehicle's tyres, the vehicle's characteristics, environmental conditions and the driver. On-road rollovers are normally caused by dangerous driving manoeuvres. These manoeuvres are induced by high lateral acceleration or by yaw instability. During yaw instability the tyres produce saturation forces that cause sliding and rollover. Most rollovers occur under conditions such as:

- Travelling at high speed on a curved road;
- Undertaking severe cornering manoeuvres;
- Travelling on a collapsing road;
- Suddenly providing steer input for a vehicle with a low level of stability;
- Losing control due to a rapid decrease of friction such as driving on an icy road, laterally sliding off the road;
- Sliding from a cliff.

According to **Hac et al. (2004)**, there is a weak coupling between the primary causes of rollover. The primary causes of rollover are defined as excitation due to road irregularities, which enters through the wheels, and the inertial forces induced by vehicle manoeuvres, which act directly on the CG.

This is illustrated in Figure 2.1. Under normal driving conditions (a), the body rotates about the roll centre and the overturning moment is balanced by the restoring moment developed primarily by the suspension. In the rollover phase (b), the entire vehicle rotates about the axis defined by the contact patches of the outside tyres. The restoring torque of the suspension vanishes and is replaced instead by the torque due to gravity.

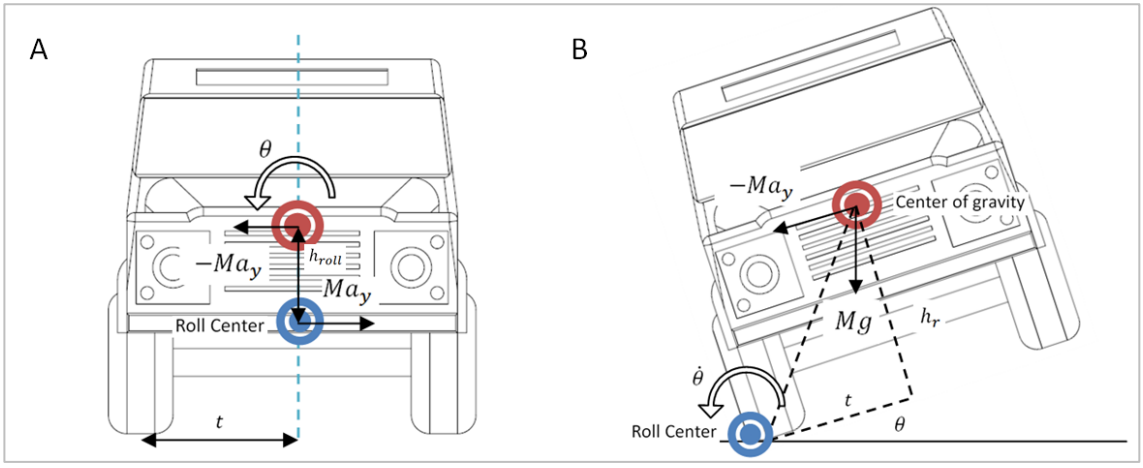

Figure 2.1: Simple models reflecting vehicle roll motion during a) normal driving and b) rollover phase (Hac et. al, 2004)

With an understanding of how rollover works, mathematical models can be developed to model rollover. The rigid vehicle rollover model is used in the early stage of development.

2.1.1 Rollover of a Rigid Vehicle

The rigid vehicle model is the most common roll-plane model due to its simplicity and parameterization and it represents the theoretical upper bound on vehicle stability **(Shim & Ghilke, 2007)**. This estimation of rollover assumes a rigid vehicle by neglecting the suspension and tyre deflections, and assumes a steady-state turn with no roll acceleration present in the turn. This analysis over-estimates the roll threshold of the vehicle by neglecting relative roll movement between the sprung and unsprung mass **(Gillespie, 1992)**.

The forces on the vehicle are depicted in Figure 2.2:

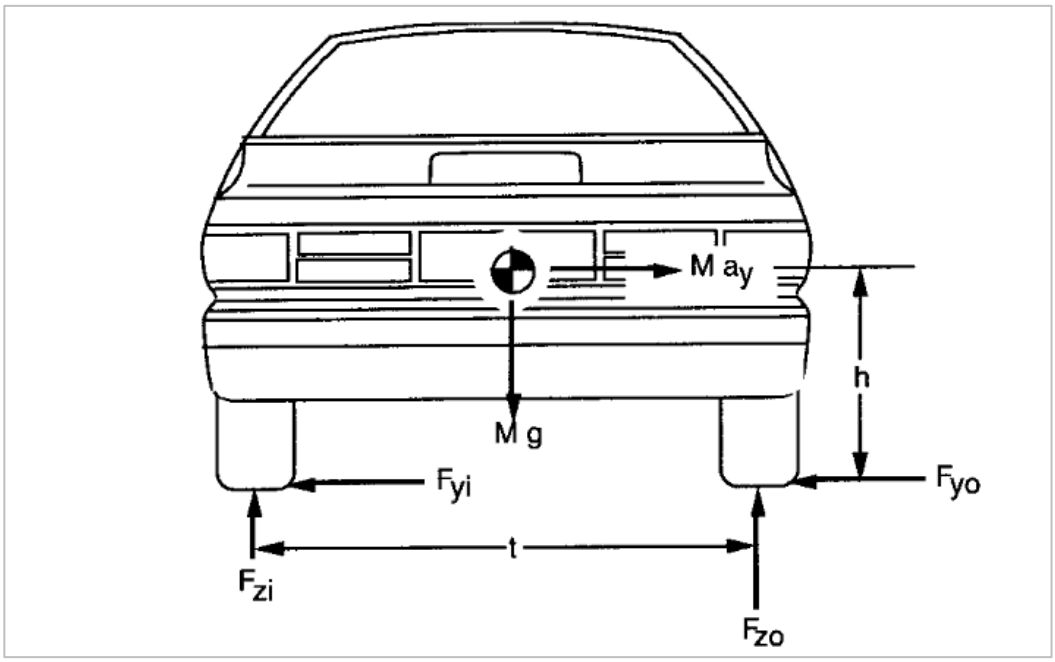

Figure 2.2: Forces acting to roll over a vehicle (Gillespie, 1992)

According to Gillespie **(1992)**, the maximum lateral acceleration the vehicle is able to experience while resisting rollover is defined for a rigid body as:

$$\frac{a_y}{g} = \frac{\left(\frac{t}{2}\right) + \theta h - \frac{F_{zi}}{Mg} t}{h}$$ **Equation 2-1**

where

- $a_y$is the lateral acceleration
- g is the gravitational constant $[9.81 \frac{m}{s^2}]$
- t is the vehicle's track width
- h is the height of the centre of gravity of the vehicle
- φis the road lateral elevation angle
- M is the vehicle's mass
- F_{zi} is the vertical force on the inside wheels

Note that the small angle assumption is used.

Equation 2-1 overestimates lateral acceleration at rollover in the sense that the lateral acceleration predicted for rollover of the vehicle is higher than the actual value at which rollover would actually occur, i.e. rollover will likely occur before this predicted value.

This lateral acceleration threshold occurs when the inside vertical wheel forces goes to zero, which is known as the cornering condition limit **(Gillespie, 1992)**. Once this lateral acceleration threshold is exceeded, the vehicle begins to roll. The vehicle may have various lateral acceleration values below the rollover threshold before rollover starts **(Gillespie, 1992)**.

The relationship between roll angle and lateral acceleration is illustrated in Figure 2.3:

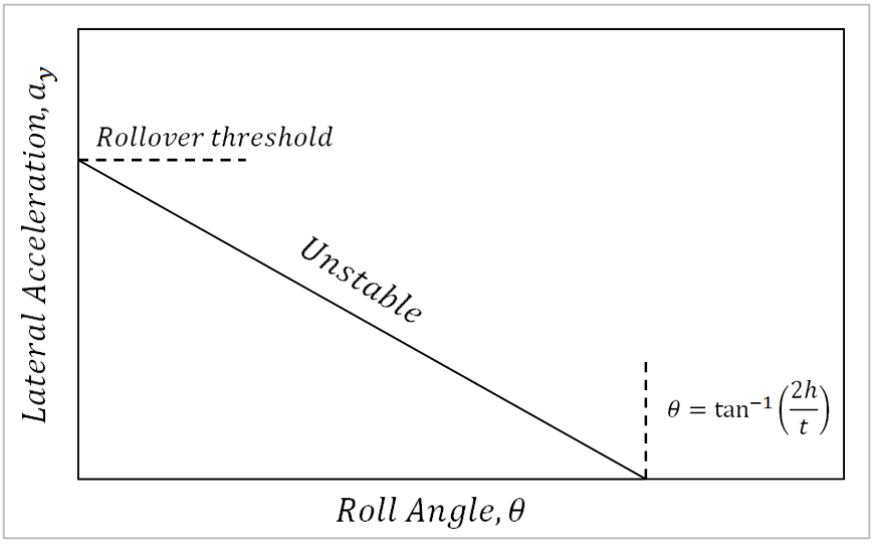

Figure 2.3: Equilibrium lateral acceleration in rollover of a rigid vehicle (Gillespie, 1992)

Equation 2-1 is only a first order estimation that gives a basic preview of the lateral acceleration that would cause the vehicle to rollover. A better approximation is obtained by including the suspension of the vehicle in the calculations.

2.1.2 Rollover of a Suspended Vehicle

Improving the current model to include the effects of suspension adds complexity to the equation, since by including the suspension, the vehicle body may rotate relative to the suspension. This causes

the body to be pulled outwards, resulting in compression of the outer suspension and tyres and extension of the inner suspension and tyres. The suspended vehicle model assumes that the sprung mass rotates around the roll centre **(Shim & Ghilke, 2007)**.

Modelling of the suspension results in lateral load transfer and thus a change in the CG outwards, leading to a smaller rollover resistance moment. This model is valid if the lateral acceleration changes much slower than the vehicle response to roll. The highest rollover threshold is achieved by maintaining the sprung mass roll rate at the highest possible stiffness **(Gillespie, 1992)**.

The lateral acceleration defined for this rollover mechanism is given by the summation of moments about the outside wheels (**Gillespie, 1992)**:

$$\frac{a_y}{g} = \frac{t}{2h}\left(\frac{1}{1+\dot{\theta}\left(1-\frac{h_r}{h}\right)}\right)$$ **Equation 2-2**

where:

- θ is the roll angle
- $\dot{\theta}$is the roll rate
- h_r is the roll centre height above the ground
- h is the centre of gravity height

The forces present in rollover of a suspended vehicle are illustrated in Figure 2.4:

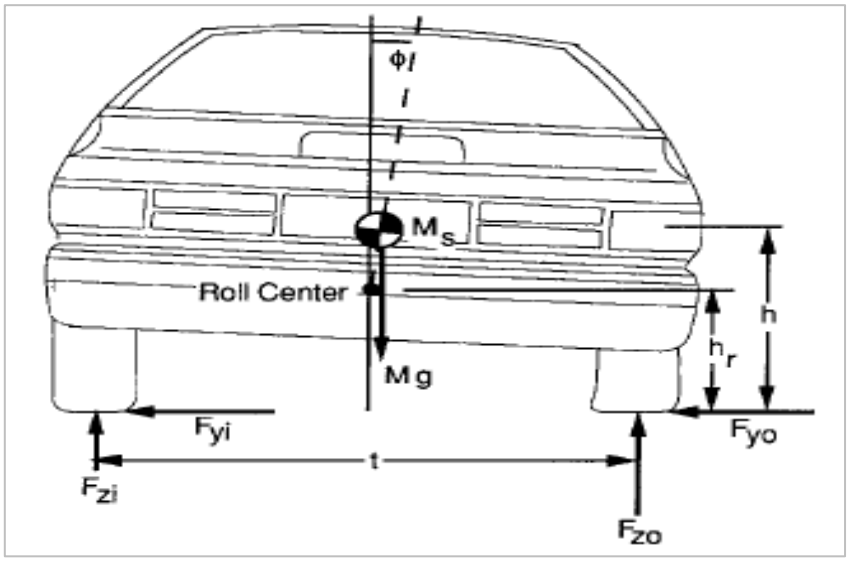

Figure 2.4: Roll reactions on a suspended vehicle (Gillespie, 1992)

The difference in distance between the roll centre height and height of the CG is important with regard to roll since this distance is the moment arm through which the lateral acceleration acts to overturn the vehicle.

It should be noted that detailed modelling of the tyre and the suspension system is required to determine the lateral shifts of the CG, the tyre vertical force action point and the roll centre. The difference in behaviour of the front and rear axles should also be considered **(Gillespie, 1992)**. Solid axle suspension systems (such as the test vehicle) tend to have high roll centres which tend to reduce the effects of lateral shifts **(Gillespie, 1992)**.

Figure 2.5 illustrates the adjusted relationship between roll angle and lateral acceleration:

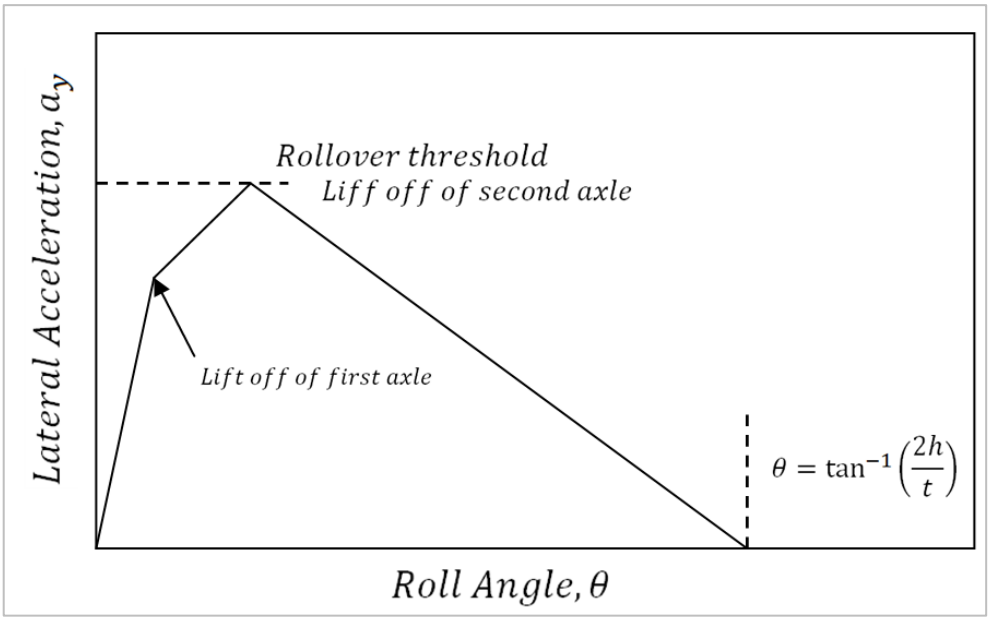

Figure 2.5: Equilibrium lateral acceleration in rollover of a suspended vehicle (Gillespie, 1992)

It is evident from Figure 2.5 that inclusion of suspension effects reduces the calculated lateral acceleration threshold.

Until this point, only simple rollover mechanisms in steady state analysis have been considered. In quasi-static state or steady state rollover analysis, the initial rollover moment assumes that the rotational velocity and acceleration are neglected **(Dukkipati et al., 2008).** The addition of transient effects adds greater complexity to the rollover mechanism.

2.1.3 Transient Rollover

Transient rollover, i.e. changes in lateral acceleration over time during the roll, occurs when the forces acting on the vehicle change while the roll is in progress. Two simple examples of time-varying lateral acceleration include when a vehicle slides with locked brakes and then experiences a sudden return of the cornering forces when the brakes are released, or when the road surface on which the vehicle is driving changes from a low to a high friction coefficient.

Transient rollover is typically examined using lateral acceleration as a step input **(Gillespie, 1992)**. According to **Jazar (2008)** a step input is a sudden change in the steer angle from zero to a nonzero constant value. Such an action causes overshooting of the roll angle due to inertial forces, resulting in a lower rollover threshold. This is illustrated in Figure 2.6:

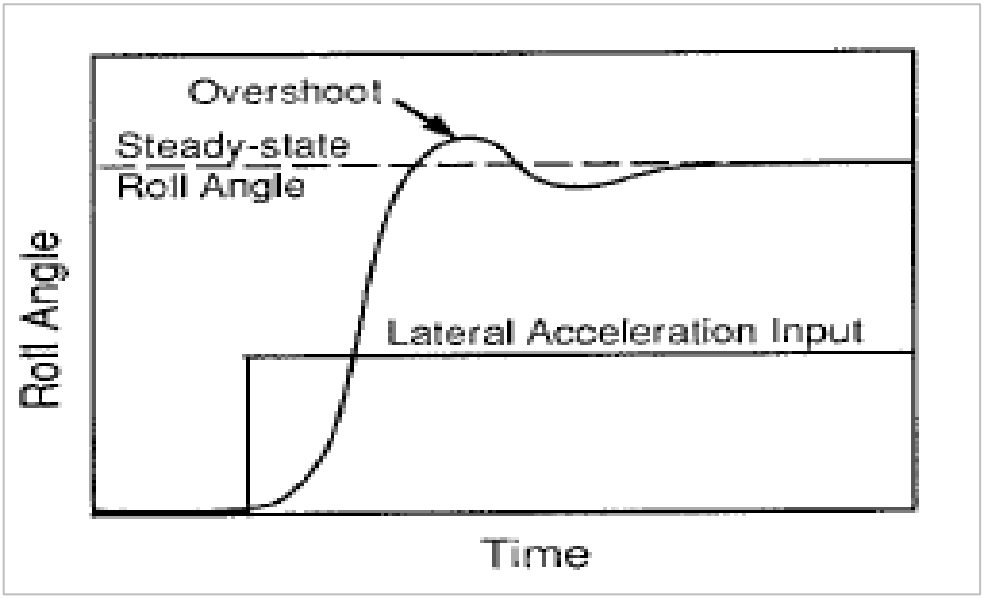

Figure 2.6: Roll response to a step input

Three factors contribute to transient effects on rollover, namely the damping ratio, the resonance frequency and yaw motions. Firstly, according to **Gillespie** (**1992**), the rollover threshold is dependent on the damping coefficient. Thus high damping increases the threshold and improves roll prevention **(Gillespie, 1992)**. This is illustrated in Figure 2.7, where a consistent relationship between damping and rollover threshold is evident for a range of vehicles of differing CG heights.

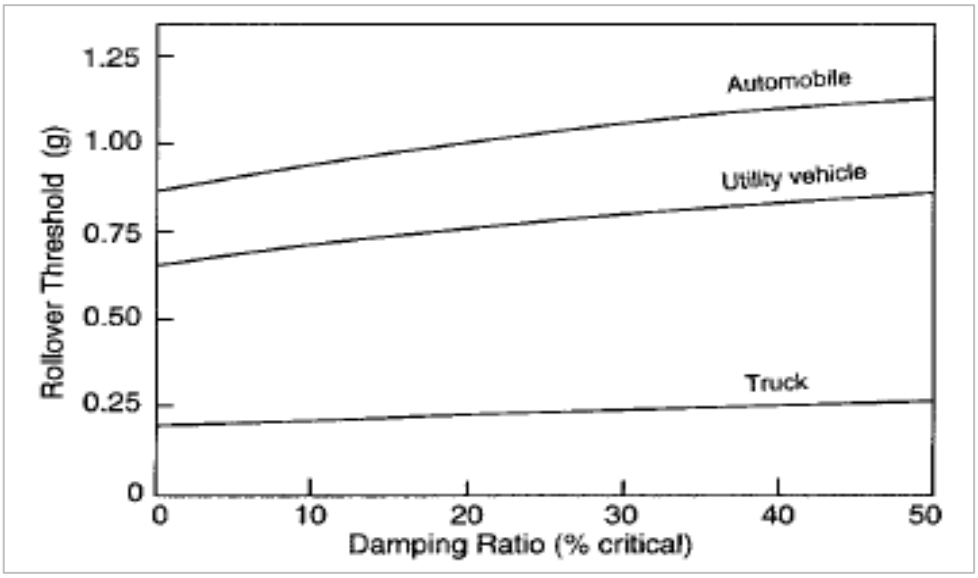

Figure 2.7: Effects of damping ratio on rollover threshold in a step steer

Secondly, if the effects of roll resonance on the rollover threshold are taken into account, the resulting sinusoidal lateral acceleration is dependent on the roll resonance frequency. The quasi-static model threshold therefore essentially corresponds to a zero frequency input. The roll resonance frequency varies according to the type of vehicle. According to **Gillespie** (**1992**), utility vehicles typically have roll resonance frequencies around 1.5 Hz.

Thirdly, the transient lateral acceleration is affected by yaw. A phase lag exists between the front and the rear wheels of a vehicle. In turning, the front wheels develop lateral forces almost immediately,

but the rear wheels first need to build up their side angle. Lateral acceleration is thus diminished by this phase lag, which reduces the rollover tendency. However, the yaw motions of the vehicle may result in lateral acceleration causing roll motion. This in turn alters the yaw response by changing the tyre cornering forces due to load transfer effects. This is particularly evident in sinusoidal inputs.

As discussed in chapter 2.1, rollover begins when the inner wheels start to lift. After wheel lift-off, there is a change in roll behaviour compared to when all four wheels were still in contact with the ground.

2.1.4 Rollover after Wheel Lift

To investigate rollover after wheel lift, use is made of a two-body system possessing two degrees of freedom, where the relative angles between the sprung and unsprung masses on the one hand, and between the unsprung mass and the road surface on the other hand, account for the degrees of freedom.

At the point of rollover, the relative motion between the sprung and unsprung mass becomes negligible **(Uys, 2007)**. The rollover motion thereby changes from rotation about the roll centre of the vehicle to the outer wheels.

The following equation may be used to estimate roll rate after wheel lift off **(Uys 2007)**:

$$\dot{\boldsymbol{\theta}} \leq \sqrt{\frac{\boldsymbol{2Mgr[1-\cos(\kappa-\theta)]}}{\boldsymbol{I_{xx}+Mr^2\sin^2(\kappa-\theta)}}}\,|\boldsymbol{\theta}| \leq \boldsymbol{\kappa} \qquad \textbf{Equation 2-3}$$

where:

- θ is the roll angle
- $\dot{\theta}$ is the roll rate
- r is the distance between the CG and the point of rotation, as illustrated in Figure 2.8
- $\kappa = arc\tan\left(\frac{t}{h}\right)$ is the static tip angle
- Where:
    - t is half the track width
    - h is the CG height
    - g is the gravitational constant

Wheel lift is considered to have occurred with the vehicle rotating about the contact patches of the outer wheels and the inner wheels lifting of the ground. However there are various degrees of wheel lift. Wheel lift off may occur for a short period and not be detrimental with regards to rollover, or it may result from a manoeuvre severe enough to overturn the vehicle. Hence it is useful to divide wheel lift into three categories, namely: minor, moderate and major two-wheel lift. Minor two-wheel lift occurs when two wheels leave the road surface for a fraction of a second with amplitudes of less than two inches. Moderate two-wheel lift is defined as being somewhat between minor and major two-wheel lift. Major two-wheel lift occurs when the outriggers of a test vehicle are required to counteract roll motion by contacting the ground. The suspension characteristics of the vehicle thus greatly influence the occurrence of two-wheel lift and hence the actual definition of when major two-wheel lift occurs depends on the height at which the outriggers are set **(Forkenbrock et. al., 2002)**.

2.1.5 14 Degree of Freedom Model

The rigid and suspended vehicle models do not accurately represent the lateral and yaw dynamics well because of coupling of the yaw-roll motion due to the transient lateral load transfer. Thus higher order models are required for better representation. The 14DOF vehicle model considers the suspension at each corner and can predict pitch and heave, allows the modelling of nonlinear springs and dampers, can simulate the normal force inputs and can predict vehicle behaviour even after wheel lift-off **(Shim & Ghilke, 2007)**.

The assumption that the roll centre is a certain distance from the sprung mass CG height can have an impact on the response compared to if the roll centre is assumed to be fixed with respect to ground or variation in roll centre height due to geometry changes.

To implement rollover prevention, a system that defines when rollover is occurring and when to implement the rollover prevention is required. This involves monitoring and estimation of the roll angle. This is discussed in the next section.

2.2 Roll Angle Estimations

According to **Dukkipati et al. (2008)**, the main functions of a rollover sensing system are to accurately estimate the vehicle's dynamics (roll rate, roll angle, lateral and vertical acceleration, etc.) and to accurately and at the right time activate the rollover restraint system. Many rollover prediction and detection algorithms rely on an estimate of roll angle. The roll angle of the vehicle cannot be measured directly and thus needs to be estimated from other measurements. According to **Hac et al. (2004)**, to reduce rollover probability, the estimate should be reliable within a range of -20 to +20 degrees roll angle.

According to **Hac et al. (2004)**, the main excitations of rollover are road excitations and inertial forces acting on the vehicle from dynamic manoeuvres. Various methods of rollover detection systems have been reported in the literature. In this section, four of the most common methods are discussed, namely direct measurement of tyre pressure changes, estimation via suspension deflections, estimation from lateral acceleration and estimation from measuring the integrated roll rate.

According to **Hac et al. (2004),** using a single sensor to provide estimates usually results in reliable feedback from only one of the rollover mechanisms. They conclude that no single method can produce satisfactory results for all operating conditions.

The first example discussed is the use of pressure sensors in the tyres to determine the vehicle's orientation.

2.2.1 Tyre Pressure/Deflection

As the vehicle manoeuvres, pressure sensors placed in the vehicle's tyre can be used to determine the vehicle's orientation by monitoring the rate and magnitude of pressure changes in the tyres. These sensors can detect and thus monitor relatively small changes in vehicle movement, leaks, improper inflation of the tyres as well as load transfer from tyre to tyre, and alert the driver when conditions fall outside of the desired parameters. Monitoring dynamic tyre pressure changes in this way allows for the orientation of the vehicle to be monitored and thereby for a rollover prevention to be implemented **(Clark, J. 2004)**.

A second method of detecting the orientation of the vehicle may be done using the relative displacements of the suspension.

2.2.2 Estimation of Roll Angle via Suspension Deflections

Hac et al. (2004) conclude that using suspension deflections, the roll angle can be estimated based on geometry according to the following equation:

$$\boldsymbol{\theta} = (\mathbf{\Delta z_{LF}} - \mathbf{\Delta z_{RF}} + \mathbf{\Delta z_{LR}} - \mathbf{\Delta z_{RR}})/(\boldsymbol{2t}) \qquad \textbf{Equation 2-4}$$

where

- Δz is the suspension deflection of the respective strut
- t is the track width

This method determines the roll angle of the body with respect to the plane defined by the centres of wheels and does not take the axle roll due to tyre deflection into account. To correct for this, an estimate of the axle roll is included using the equation for lateral acceleration **(Hac et al., 2004)**, giving:

$$\boldsymbol{\theta} = \frac{\mathbf{\Delta z_{LF}} - \mathbf{\Delta z_{RF}} + \mathbf{\Delta z_{LR}} - \mathbf{\Delta z_{RR}}}{\boldsymbol{2t}} - \boldsymbol{M a_{ym} h / k_{tyreroll}} \qquad \textbf{Equation 2-5}$$

where:

- $k_{tyreroll}$ is the roll stiffness resulting from tyre stiffness
- M is the vehicle's mass
- h is the height of the roll axis
- a_{ym} is the combined lateral and gravitational acceleration the vehicle experiences

The advantages of this model of detection are its simplicity, good transient and steady-state cornering estimates on smooth roads, low sensitivity to parameter variation and the fact that the estimate tracks the roll angle with respect to the road. However, it can give unsatisfactory results when there is significant wheel motion, such as a bump in the road, which may cause the estimator to interpret this as body roll from inertial forces. Thus, two drawbacks for this model include poor estimation on rough roads and underestimation for large roll angles **(Hac, Brown & Martens, 2004)**.

The effect of road bumps on the suspension is illustrated in Figure 2.8:

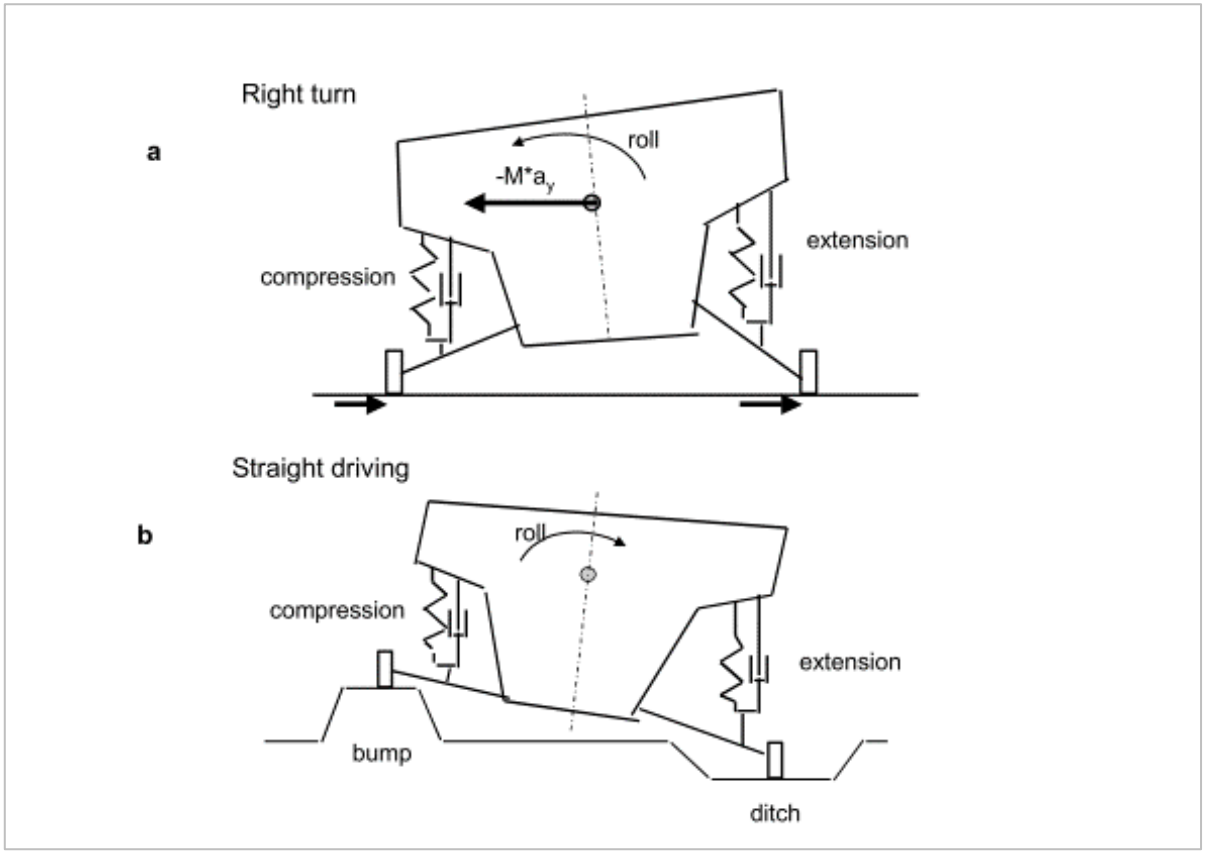

Figure 2.8: Vehicle Body Roll and Suspension Deflections During a) a Right Turn on Smooth Road, b) Driving straight on Uneven Road (Hac et al., 2004)

It is evident from the Figure 2.8 above that while the model can reasonably detect roll angle when turning on a straight road (a), the angled suspension resulting from encountering a bump or ditch while driving straight (b) gives a false reading.

2.2.3 Estimation of Roll Angle from Lateral Acceleration

Although the absolute roll rate is measurable, the roll angle and roll rate with respect to the road needs to be estimated. Typically these estimates are derived from the measurement of lateral acceleration, longitudinal acceleration, vertical acceleration, and roll rate sensors **(Hac et al., 2004)**.

Lateral acceleration is the main inducer of rollover on smooth roads. Lateral acceleration can be represented using a single-DOF model where the roll motion is caused by the inertial force due to the lateral acceleration.

The equation of motion for inertial force due to lateral acceleration is given as **(Hac et al., 2004)**:

$$\boldsymbol{I_{xx}\ddot{\theta} + c_{roll}\dot{\theta} + k_{roll}\theta = -Ma_{ym}h_r} \qquad \textbf{Equation 2-6}$$

where:

- M is the mass of the vehicle
- I_{xx} is the roll mass moment of inertia
- c_{roll} is the roll angular damping of the system
- k_{roll} is the roll angular stiffness of the system
- h_r is the roll centre height above ground

However, gravity also contributes to the roll moment and the gravitational component is used to account for the bank angle **(Hac et al., 2004)**. This means that only considering the lateral acceleration limits the model's performance and may thereby fail to prevent rollover from vertical road inputs.

The combined lateral and gravitation acceleration the vehicle experiences is given as **(Hac et al., 2004)**:

$$\boldsymbol{a_{ym} = a_y + g * \sin\theta} \qquad \textbf{Equation 2-7}$$

where:

- a_y is the lateral acceleration
- g is the gravitational force
- θ is the roll angle

The combined moments of gravity and inertia are illustrated in Figure 2.9:

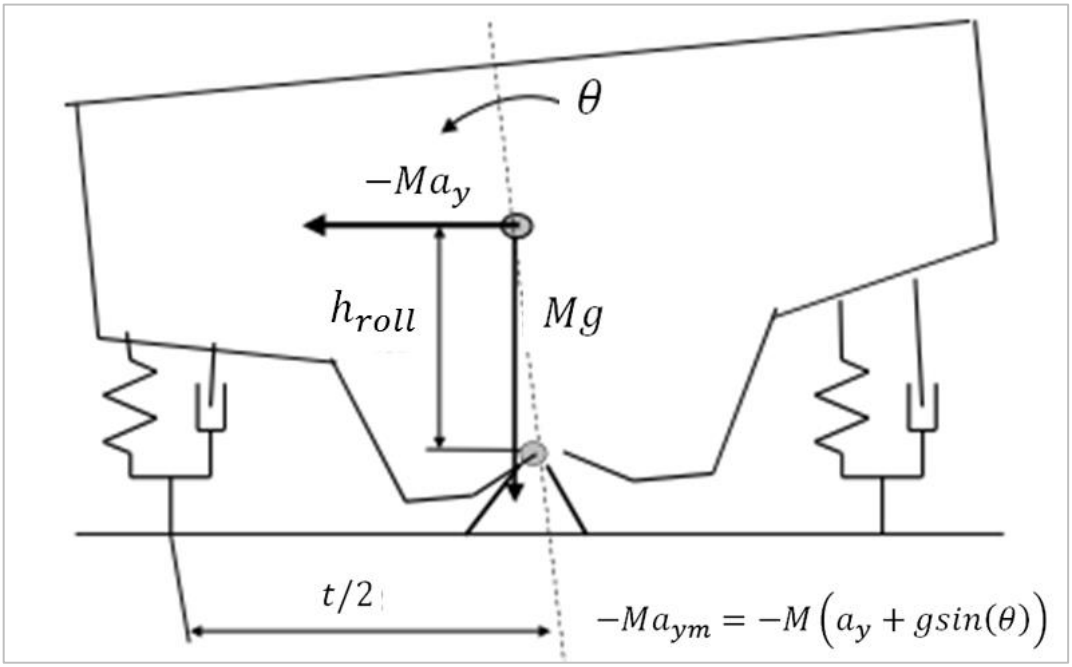

Figure 2.9: A Simple Model of Vehicle Roll Motion (Hac et al., 2004)

During handling, the equation of motion (Equation 2-6) may be simplified to **(Hac et al., 2004)**:

$$\boldsymbol{\theta = -\left(\frac{Mh_r}{k_{roll}}\right) a_{ym}} \qquad \textbf{Equation 2-8}$$

where:

- M is the sprung mass of the vehicle
- h_r is the height of the roll axis

An estimate for roll rate may be obtained from the equation of motion or by differentiating the reduced equation of motion.

Hac et al. (2004), conclude from their study that estimations of roll angle from lateral acceleration are sufficient for handling manoeuvres on smooth roads with all wheels on the ground (i.e. roll angles below about 8 degrees). The model assumes that the wheels remain on the ground, which

results in poor estimation after two-wheel lift. Notwithstanding, this estimate provides a simple method of estimating roll during normal cornering manoeuvres on smooth road with the consideration of bank angle included. It has bounded effects from changes in vehicle parameters. The model is therefore inadequate when the vehicle is driven straight and excited by road inputs, or when roll becomes severe enough the induce wheel lift **(Hac et al., 2004)**.

A fourth means of estimating the roll angle is by means of integrating the measured roll rate.

2.2.4 Estimation of Roll angle via Integration Measured Roll Rate

Roll angle of the vehicle may be derived from the measured roll rate signal; however, some consideration to certain aspects should be noted.

Firstly, when measuring the roll rate signal, it should be noted that integration of the signal can be sensitive to sensor bias since the bias is integrated over time. Integration should therefore be replaced with pseudo-integration. Pseudo-integration reduces the effect of sensor bias, but also tends to reduce the steady-state slowly varying roll angle signal or underestimate the roll angle in steady-state turns **(Hac et al., 2004)**.

Secondly, roll rate sensors measure absolute rates of rotation and not relative to the ground, thus an estimate of bank angle should be included in the measure. Bank angle estimation is achieved by taking the difference between the measured roll rate and the estimated roll rate from the lateral acceleration model **(Hac et al., 2004)**.

According to **Hac et al. (2004)**, this method of integration produces a good estimate when roll rate changes quickly both for small and large angles and it is also not sensitive to vehicle parameter variation. However, it gives unsatisfactory results for steady-state turns and it has sensitivity towards sensor bias and change in bank angle.

In this section, various methods to determine the orientation of the vehicle have been discussed. However, none give a measure to the propensity of how close the vehicle is to rollover. This is not to say that they are not influential to detecting or predicting rollover. According to **Zhang et al. (2017)**, rollover detection and rollover mitigation control are the two important stages of vehicle rollover prevention. The next section is devoted to discussions on predicting rollover risk.

2.3 Rollover Prediction

In this section, a number of parameters are discussed that allow prediction of vehicle rollover risk.

According to **Hac et al. (2004)**, early rollover detection is important since this means that the corrective action does not have to be severe. Compromise in path following can be reduced, delays in rollover prevention methods can be compensated for and false activations can potentially be avoided. However, as **Dukkipati et al. (2008)** note, the phenomenon of rollover is difficult to predict since it involves factors external to the vehicle itself, such as the road friction coefficient, foreign obstacles, inclination angles and various driver steering patterns.

2.3.1 Statics Stability Factor

It is important to determine whether a vehicle will slide before it rolls on a flat road and this can be determined from the Static Stability Factor (SSF). The vehicle will slide before it rolls if the SSF is larger than the coefficient of friction between the road and the tyres. However, it is not always possible to determine the coefficient of friction **(Cronjé, 2009)**.

The SSF may be thought of as a comparison of the maximum lateral acceleration from the rigid body rollover mode with the maximum lateral acceleration attainable from the friction between the tyres and the road.

The maximum attainable lateral acceleration from able friction is given as **(Gillespie, 1992)**:

$$\frac{a_y}{g} = \mu \qquad \textbf{Equation 2-9}$$

where:

- a_y is the lateral acceleration limit due to friction
- μ is the kinetic friction coefficient between the wheels and the road
- g is the gravitational constant [$9.81 m/s^2$]

According to **Ackermann and Odenthal (1998)**, the track width ratio (the ratio of half-track width to the height of the CG) is the most influential vehicle parameter in predicting vehicle rollover risk. Incorporating the track width into the above equation, the maximum attainable lateral acceleration before rollover occurs may therefore be derived as **(Gillespie, 1992)**:

$$\frac{a_y}{g} = \frac{t}{2h} \qquad \textbf{Equation 2-10}$$

where:

- $a_y$is the lateral acceleration limit due to rollover
- $t$is the vehicle trackwidth
- h is the height of the center of gravity of the vehicle

The expression $\frac{t}{2h}$ is known as the rollover threshold and its inverse $\frac{2h}{t}$ is known as the roll propensity **(Dukkipati et al., 2008)**. These terms will be referred to throughout the text.

Combining these maximum lateral accelerations the SSF is defined as:

$$SSF = \frac{t}{2h} \qquad \textbf{Equation 2-11}$$

Using an expression derived from the rigid body assumption and the available friction, it is then possible to determine if the vehicle will roll before it slides. Thus, if the friction coefficient is less than the SSF, the vehicle will slide before it rolls, i.e.:

$$\mu < \frac{t}{2h} \ (for\ slide\ before\ roll) \qquad \textbf{Equation 2-12}$$

Although the SSF does relate some of the vehicles properties to roll and does give some insight to the rollover behaviour, it is not always an accurate representation. **Whitehead et al. (2004)** showed that two vehicles with the same SSF but different weight distributions had substantially different two-wheel lift-off velocities, thereby demonstrating that although the SSF is an important property of roll propensity, CG height and track width are not the only parameters that play an important role. There is therefore no guarantee that improving the static rollover threshold will improve transient rollover response **(Gillespie 1989)**.

The above relationship may be modified to incorporate the suspension effects for a more accurate representation in steady state corning **(Uys 2007)**:

$$\mu < \frac{t}{2h}\left(\frac{1}{1+\dot{\theta}\left(1-\frac{h_r}{h}\right)}\right)$$ **Equation 2-13**

Alternatively, according to **Gillespie (1992)**, suspension effects can be approximated by making a 10% reduction in the SSF, i.e.:

$$0.9(SSF) \geq \mu$$ **Equation 2-14**

The friction coefficient μ is typically found to be 0.88 for a dry, clean surface.

The SSF provides a good initial indicator of rollover probability, but is not accurate enough to be the sole indicator since it does not take into account the various degrees of severity a manoeuvre may possess.

There are a number of other static predictions of rollover not discussed in this document. These include the Tilt Table Ratio and the Side Pull Ratio. Of the static tests, **Dukkipati et al. (2008)** reported the Side Pull Ratio to be the best static estimator of rollover. Static analysis involves lateral acceleration and the vehicle in a quasi-static state, but because they do not take all factors into account, tend to significantly over-estimate roll thresholds.

2.3.2 Rollover Threshold on Look-up Tables

Acknowledging that it is difficult to define a single expression that is accurate and reliable enough to define rollover for all vehicles, it may be feasible to define thresholds such as lateral acceleration or roll angle that report the propensity of rollover. Such a system may employ a look-up table index.

According to Chen and Peng (1999), the development of accurate rollover threat indices is an important technique for the prevention of rollover, since it determines when the rollover prevention is implemented. Most algorithms that warn against rollover are based on acceleration, i.e. when either the lateral acceleration of a vehicle or the roll angle exceeds a particular threshold, the warning is issued.

According to Hac et al. (2004), previously proposed methods of predicting impending rollover measure the lateral acceleration, vertical acceleration, roll rate and longitudinal acceleration using sensors as well as a pendulum to predict roll angles close to critical values. However, they found these methods to be inaccurate in the range of 5-20 degrees, which is of importance in rollover prevention. Instead, they propose a rollover index that is a combination of the estimated roll angle, roll rate and lateral acceleration and thus is sensitive to both manoeuvre- and road-induced rollover. Their rollover index indicates the probability of rollover in a given dynamic situation and is scaled from normal driving, represented by a zero value, to one or above when rollover is certain.

The index therefore provides an indication of the severity of the manoeuvre, allowing for various roll preventions to be implemented at different degrees of severity. This enables the distinction between steady-state and transient rollover threat. According to **Uys (2007)** the relationship between transient and steady-state rollover thresholds is non-linear, thus care should be taken when designing for both parameters.

Using a combination of measures can be useful for evaluating various manoeuvres that induce rollover.

2.3.3 Roll Stability Advisor

The Roll Stability Advisor (RSA) system is based on the lateral acceleration threshold. It determines the rollover acceleration threshold based on real-time measurements of the status of the vehicle **(Chen, B and Peng, H, 1999)** and thereby provides real-time measurement and analysis regarding vehicular roll.

When a vehicle is fitted with the system, the loaded roll stability limit of the vehicle is automatically determined and the rollover threshold is displayed for the driver, who thereby is able to receive real-time updates on the severity of a manoeuvre and may therefore take corrective action to reduce rollover risk **(Ervin, 1998)**. Audio signals and sometimes steer torque are used to inform the driver when he approaches the limit. In high-risk situations, a driver is normally unable to pay visual attention to the display and thus the display will show the prior manoeuvre for review when the driver is no longer in a risky situation **(Ervin, 1998)**.

RSA addresses a driver's general inability to perceive the loaded stability level in response to roll-inducing demands. Although this system does not actively intervene to reduce risks, use of the RSA system can condition a driver to predict manoeuvre responses and anticipate the vehicle response. The hypothesis is that within a reasonable term of use, the driver will be able to intuitively grasp rollover conflicts and will only need to look at the display when new load conditions need to be calibrated **(Ervin, 1998)**.

2.3.4 Dynamic Stability Index

The SSF is used to determine whether a vehicle will slide before it roll and is derived from the rigid vehicle model. In a similar manner, the Dynamic Stability Index is derived from the steady-state suspended vehicle rollover model described in chapter 2.1.2. It is used to determine whether rollover will occur.

Adding rotational energy to the steady-state suspended equation, this gives **(Dukkipati et al., 2008)**:

$$\frac{a_y}{g} + \frac{I_{xx}\ddot{\theta}}{Mgh} = \frac{t}{2h} \qquad \textbf{Equation 2-15}$$

From the above equation, the dynamic stability index (DSI) is defined as **(Dukkipati et al., 2008)**:

$$DSI = \frac{a_y}{g} + \frac{I_{xx}\ddot{\theta}}{Mgh} \qquad \textbf{Equation 2-16}$$

where:

- a_y is the lateral acceleration
- I_{xx} is the roll moment of inertia
- M is the sprung mass of the vehicle
- t is the track width
- h is the height of the vehicles CG
- $\ddot{\theta}$ is the roll acceleration

Rollover will occur if the dynamic stability index (DSI) is larger than the static stability factor (SSF). The DSI includes the effects roll velocity and acceleration that contribute to rollover, as well as the lateral acceleration contribution **(Dukkipati et al., 2008)**. According to **Dukkipati et al. (2008)**, it provides a practical metric to describe dynamic rollover propensity.

2.3.5 Rollover Prevention Energy Reserve

It is possible to use rollover energy to determine whether there is enough energy in the system to overturn the vehicle laterally. This may be achieved with the Rollover Prevention Energy Reserve.

The Rollover Prevention Energy Reserve (RPER) is a function used to measure the dynamic rollover stability of a vehicle in order to employ a rollover prevention strategy. The RPER function is comprised of the potential energy at the tip-over position of the vehicle minus the total instantaneous potential energy and rolling kinetic energy of the vehicle **(Dukkipati et al., 2008)**.

$$\boldsymbol{RPER = E_v - E_k} \qquad \textbf{Equation 2-17}$$

The kinetic rollover energy is comprised of the lateral velocity of the vehicle and the roll rate. It is represented as **(Dukkipati et al., 2008):**

$$\boldsymbol{E_k = \frac{1}{2} M V^2 + \frac{1}{2} I_B \dot{\theta}} \qquad \textbf{Equation 2-18}$$

where:

- E_v is the potential energy at the tipping point
- E_k is the instantaneous kinetic energy prior to rollover
- m is the mass of the vehicle
- V is the lateral velocity of the vehicle
- I_B is the mass moment of inertia of the vehicle about the outside wheel contact patch
- $\dot{\varphi}$ is the rotational velocity of the vehicle

The mass moment of inertia at rollover may be calculated as:

$$\boldsymbol{I_B = I_{xx} + M(h^2 + \frac{t^2}{4})} \qquad \textbf{Equation 2-19}$$

where:

- I_{xx} is the roll mass moment of inertia about the CG
- h is the height of the CG from the ground
- t is the track width

If the instantaneous RPER is positive the vehicle is not under rollover threat, however if it is negative the vehicle is likely to roll. The rate at which the RPER changes to negative and the rate it reduces to zero is an indication on the severity of the rollover.

Although the RPER provides a useful measure to describe the dynamic rollover threshold, its disadvantages are that it is time consuming and expensive to measure the energy, and it is also difficult to predict the energy storage of the tyre and the dissipation of energy in the system **(Dukkipati et al., 2008)**.

2.3.6 Rollover Prevention Metric

Rollover may also be predicted by comparing the lateral kinetic energy of a body to its rotational energy. This is done using the Rollover Prevention Metric (RPM), which uses the percentage difference between the lateral kinetic energy and the initial rotational energy to predict a threshold for rollover **(Dukkipati et al., 2008)**, i.e.:

$$\boldsymbol{RPM = 100\left(\frac{T_o - T_1}{T_o}\right)\%} \qquad \textbf{Equation 2-20}$$

where:

- The lateral kinetic energy $$T_0 = \frac{1}{2}MV^2$$ **Equation 2-21**
- The rotational energy $$T_1 = \frac{1}{2}I_B\dot{\theta}^2$$ **Equation 2-22**
- The conservation of momentum $$MVh = I_B\dot{\theta}_0$$ **Equation 2-23**

Substituting **Equation 2-23** into **Equation 2-22** gives:

$$T_1 = \frac{\left(\frac{1}{2}\right) M^2V^2h^2}{I_{xx}}$$ **Equation 2-24**

Hence, substituting **Equation 2-24** into **Equation 2-20** gives:

$$RPM = 100\left(1 - \frac{Mh^2}{I_{xx}}\right)\%$$ **Equation 2-25**

It is noted from the above equation that RPM is not a function of lateral acceleration, but reports a percentage value.

The problem with most rollover detection algorithms is that they are instantaneous measures. Being able to determine the current rollover propensity is important, however it would be advantageous to be able to predict the future behaviour of the vehicle with regard to rollover.

2.3.7 Time-To-Rollover

One such predictive algorithm is the Time-to-Rollover (TTR), which estimates the time to tyre lift-off. The time taken for the vehicle's sprung mass to reach its critical roll angle when the steering angle is fixed is defined as the TTR **(Chen & Peng, 1999)**. The true-TTR is determined at a certain point in time prior to when the roll angle exceeds the defined threshold. If a TTR can be calculated in real-time, the rollover threat can accurately be determined **(Chen & Peng, 1999)**.

Chen and Peng (1999) compute a TTR index in real-time, verifying their model using test data from the Vehicle Research and Test Centre of NHTSA for two sports-utility vehicles (SUV). Their algorithm is given in Figure 2.10:

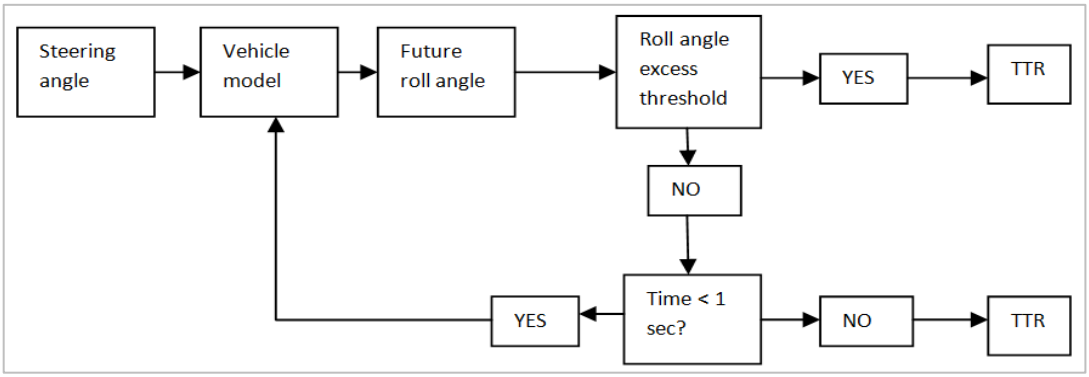

Figure 2.10: Flow chart for the TTR calculation (Chen and Peng, 1999)

The TTR is computed from a simple model and then corrected by an artificial Neural Network (NN). The integrated model is depicted in Figure 2.11:

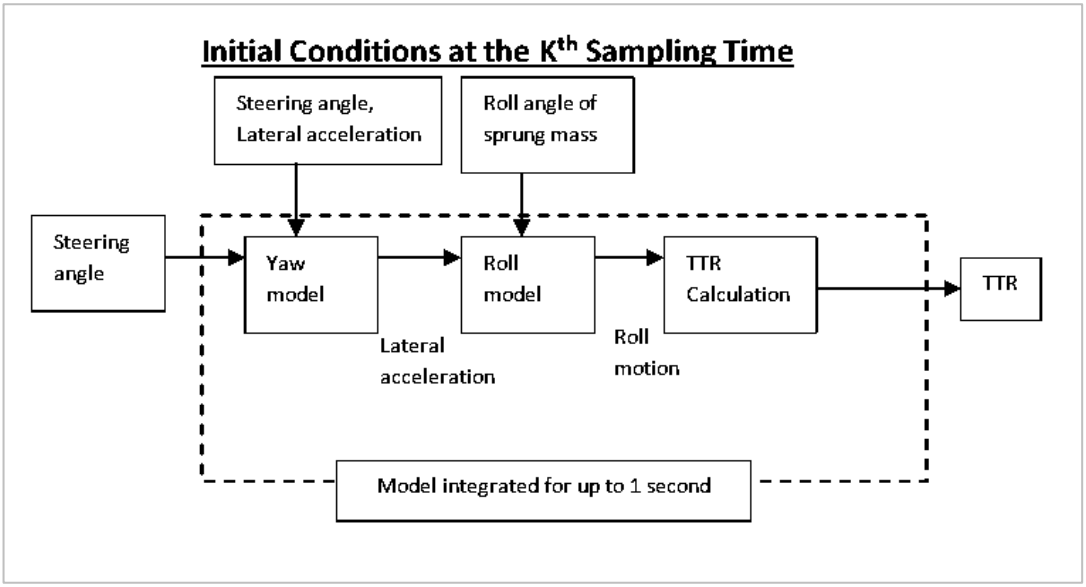

Figure 2.11: Detailed implementation for the TTR calculation (Chen and Peng 1999)

The TTR model offers an enormous advantage in being able to potentially predict rollover. However, its disadvantage is that there is a trade-off between prediction preview time and accuracy, i.e. the larger the prediction preview time, the less accurate is the prediction. Moreover, the model is complicated by the need to incorporate vehicle yaw and roll models in order to estimate the response from a steering input.

Imine et al. (2014) proposed a method of prediction based on the calculation of the load transfer ratio (LTR) specifically for heavy vehicles. The advantages of this approach is its simplicity. The LTR is defined as the proportion of load on one side of the vehicle to the other in a transient manoeuvre and is based on vertical force inputs. They develop a higher-order-sliding-mode (HOSM) observation tool to estimate the vertical forces and confirmed the tool's robustness using zigzag and braking tests. The system issues a warning to the driver to reduce speed if the LTR exceeds a predefined limit.

Imine et al.'s (2014) approach for heavy vehicles was further improved by **Zhang et al. (2017)**. By mapping the contour line of LTR for wheel lift thresholds, they were able to create a prediction system from the set of instantaneous measures. They investigated the LTR in the roll phase plane for various ramp steering and step steering manoeuvres. The LTRs were observed to be located approximately in a straight line. The contour line load transfer ratio (CL-LTR) defined using a ramp input lateral acceleration for static rollover and a step-input lateral acceleration for dynamic rollover, are defined for a 1 DOF roll model. From these results, extensions for a full vehicle model are derived. A CL-LTR based vehicle rollover index (CLRI) is derived by evaluating a vehicle's state in the roll phase plane relative to its CL-LTR thresholds. CLRI returns an estimated time that the vehicle will take to reach the CL-LTR threshold. The prediction of vehicle rollover threat is achieved by setting a prediction time and the vehicle is considered to be in danger of rollover if the time calculated for the CLRI is less than the selected prediction time **(Zhang et al., 2017)**.

Once the means of detection and prediction of rollover have been defined, the next step is to define a correlating rollover prevention system. This is done in the next section.

2.4 Rollover Prevention

Before effective action to reduce rollover can be implemented, a combination of factors should be controlled. If these factor and effects are not known, it would be premature to impose an arbitrary limit on the rollover threshold of the vehicle **(Gillespie 1989)**. However, once the factors are determined and rollover is detectable, rollover prevention strategies may be put in place to intervene.

According to **Hac et al. (2004)**, rollover prevention should intervene when the body roll angle roughly corresponds to the two-wheel lift-off. Thus is it important to know the roll angle and roll rate of the vehicle body with respect to the road.

Rollover prevention systems may be classified into two basic classes, namely passive and active. Passive systems merely use prediction algorithms to warn the driver to take corrective action in the presence of impending rollover risk. In contrast, active systems actively reduce the vehicle's rollover tendency, e.g. by controlling the vehicle's yaw motion using four-wheel steering and differential braking, as well as directly controlling the vehicle's roll motion using active roll bars and active suspension **(Shim & Ghike, 2007)**. Active roll-prevention controls are proposed by **Chen and Peng (1999)** for application on SUV's and **Samson and Cebon (1998)** for application on heavy vehicles. These early systems consisted of hydraulically tiltable fifth wheel couplings and hydraulic actuators, lateral acceleration feedback and different techniques to control load shift in heavy vehicles, such as tilting the vehicle into the turn **(Sampson & Cebon 1998).**

According to **Dukkipati et al. (2008)**, the most effective way to keep a vehicle from rolling over is to make the centre of gravity of the vehicle as low as possible, and or to make the vehicle wider and use tyres with less lateral force generation capabilities. Similarly, **Van der Westhuizen (2012)** recommends reducing the centrifugal force on the CG by reducing the cornering speed, or reducing the lateral force generated by the tyres by changing the load transfer. Imine et al. (2012) consider the three main factors affecting roll stability as the centre height of gravity, track width and suspension kinematics.

For the purposes of the present study, active rollover prevention systems which intervene between the inputs of the driver and the response of the vehicle to reduce rollover propensity were reviewed. Both existing systems that have shown potential rollover reduction, as well as studies that may be developed and improved on are reviewed. The four main areas investigated below include active steering, braking and suspension systems, as well as changing the position of the vehicle's centre of gravity.

2.4.1 Active Steering

The first possible method of intervention between the inputs of the driver and the response of the vehicle is to evaluate and correct the steering inputs of the vehicle such that the severity of the manoeuvre is reduced and rollover is prevented. Excessive steering commands may result in an unstable vehicle motion. Thus to reduce the possible instability, active steering systems can reduce or reverse the steer angle input of the driver **(Dukkipati et al., 2008)**. Active steering allows the relationship between the steering inputs from the driver to be altered before transferring the steering inputs to the wheels. Apart from improving high speed stability by reducing the effects of normal steer angle responsiveness, these systems may also be used to improve low speed steering manoeuvres (such as parking) by reducing the input steering angle.

In the study of **Ackermann and Odenthal (1998)**, active steering was investigated in which the CG height is of particular importance. This was aimed to reduce the risk of rollover in the transient overshoot behaviour in the case of increased velocity or increased height of the vehicle's CG. The control system appropriately reduces the steering input at the wheels from the user input.

Rapid change in sign of the steering angle at high speeds induces oversteer and loss of control. This causes the front axle lateral force to be in the opposite direction of the rear axle because of lag, which generates a large yaw moment on the vehicle (Gasper et al. 2004, 2005). To advance the phase of the rear lateral force generation, the rear wheels are steered in-phase with the front ones. This reduces the yaw rate and its rate of change. It is desirable to keep the lags in lateral acceleration and yaw rate approximately equal throughout the entire range of speeds **(Hac, 2002)**.

Imine et al. (2012) have recently developed an active steering control based on calculating the load transfer ratio (LTR) that uses a high-order sliding mode observer to estimate lateral acceleration and centre height of gravity. Their model assumes a small roll angle and linear suspension and tyre dynamics. Their simulations show improved rollover prevention in zigzagging and ramping tests. However, their model has not yet been empirically verified.

Active rear steer (ARS) or four wheel steer (4WS) systems improve the vehicle yaw response. ARS limits vehicle oversteer and improves handling. The aim is to enhance manoeuvrability at low speeds, improve stability at high speeds and improve vehicle transient response to steering inputs **(Hac, 2002)**. 4WS systems can be hydraulically controlled or controlled by planetary gear, to vary the rear-to-front steer ratio **(Furukawa et al., 1989)**.

A "vehicle-speed-sensing 4WS" is a vehicle that can vary its rear-to-front steer angle ratio according to vehicle speed **(Furukawa et al., 1989)**.At low speeds, the rear wheels are steered out of phase or in the opposite direction to the front wheels in order to reduce the turning radius. The gain of the steer angle is negative at low speeds, positive at high speeds and sets a larger steering angle at the rear wheels at low speeds when the front wheels are steered sharply **(Hac, 2002)**. This is illustrated in Figure 2.12:

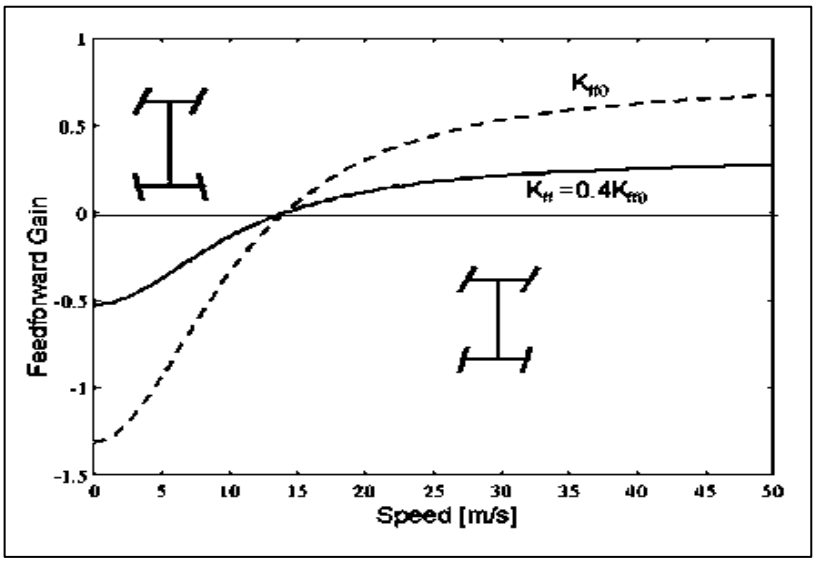

Figure 2.12: Feedforward Gain for Active Rear Steer System (Hac, 2002)

The transient response of the vehicle driven by a 4WS does not vary appreciably from that of a two-wheel steering (2WS) vehicle with respect to the characteristics of the yaw rate, but it does differ significantly with respect to the characteristics of the lateral acceleration.

Four wheel steering improves the responsiveness in cornering. However, it should be noted that it may increases the potential for rollover by exciting roll resonance **(Gillespie, 1992)**. Thus the control system implemented must be done in such a manner that improves safety and not the inverse. Reduction in vehicle speed greatly reduces attainable lateral acceleration and thus reduces the propensity of the vehicle to rollover. However, during a high speed manoeuvre in which the driver loses control of the vehicle, the driver may not have the knowledge or capability to brake intelligently to return the vehicle to control. Thus an active braking system would be beneficial.

2.4.2 Active Braking

A second method of rollover prevention is the implementation of an active braking system. According to **Chen and Peng (2010)**, differential braking is considered the most effective way to manipulate tyre force to reduce lateral acceleration of the vehicle. It can reduce the forward speed that contributes to lateral acceleration, something which four-wheel steering, active suspension and active stabilizer are unable to do. **Shim and Velusamy (2011)** note that active braking control methods are estimated to reduce single-vehicle crashes of passenger cars by 34% and of SUVs by as much as 59%.

Differential braking works by applying a braking moment to the outer front wheel while the vehicle is turning that reduces yaw rate. Longitudinal braking force results from the non-zero tyre slip ratio, thus applying the brake moment changes the tyre slip ratio of the wheel. The maximum lateral tyre force is determined from the longitudinal tyre force. The longitudinal force is increased due to breaking and the lateral force is consequently reduced (Gasper et al., 2004, 2005). Thus, increasing the longitudinal braking force produces a moment that reduces the lateral tyre force and yaw rate, and ultimately reduces the lateral acceleration and thereby the danger of rollover.

In differential braking, braking is applied to either the right or left wheel of the front axle, controlling the yaw motion of the vehicle. Differential braking aims to understeer the vehicle. In contrast, full braking can have some combination of braking forces that make the vehicle understeer less or even oversteer. Direct yaw control is used to implement differential braking. The anti-lock braking system (ABS) generates the desired yaw moment by commands from the direct yaw moment control. The yaw moment is achieved by longitudinal braking forces. The longitudinal braking forces are determined from tyre slip ratios for ABS through a two-dimensional look-up table, which uses the tyre vertical load and the desired longitudinal force to generate the desired tyre slip ratio. Finally, the brake system controls the slip ratio from the ABS.

Active braking may be applied to both front brakes simultaneously, as is the case in Anti-Rollover Braking (ARB). ARB systems activate the front brakes of the vehicle before rollover starts. This reduces the cornering capabilities of the front tyres, creating an understeer characteristic and a reduction in vehicle speed. The brakes are then released once the rollover warning drops below a certain threshold **(Dukkipati et al., 2008)**. However, Gasper et al. (2005) note that the disadvantage of this solution is that the switching of the brake can cause a dangerous slip of the vehicle. Although a solution is to decrease the critical value for which the brake is activated, this results in the brake activation occurring more frequently and over longer durations.

Active braking may be used to keep the intended path as well as reduce rollover. An example of commercial active braking can be seen in Electronic Stability Control (ESC), a control system that monitors the driver's inputs compared to the actual response of the vehicle. According to **Forkenbrock et al. (2004)**, ESC is also referred to as Vehicle Skid Control (VSC) or Dynamic Stability Traction Control (DSTC). ESC will intervene when the driver is about to lose control of the vehicle. When the vehicle starts to leave its intended path, braking is applied judicially at individual wheels to restore the line of travel. ESC helps prevent rollovers and spin-outs **(Farmer, 2004)**.

If the concept of ESC is extended to suppress rollover as its main function, Roll Stability Control (RSC) is derived. RSC can be thought of as an extension of a conventional ESC system, but with conceptually different control logic. Whereas ESC involves yaw stability control and assists the driver with path following, RSC is designed to suppress on-road untripped rollovers. RSC requires measurement of the vehicle's roll motion and subsequent brake application hard enough to change the vehicle's path in order to reduce lateral acceleration. This may cause path deviation, whereas ESC will try and maintain the path.

The front brakes can be applied to reduce lateral acceleration. Brake-based vehicle stability enhancement system (VSE) improves the vehicle yaw response, while simultaneously reducing the tendency of the vehicle to oversteer as well as the lateral slip. Thus the probability of rollover is expected to be reduced. VSE controls the braking inputs at or near the limit of adhesion by judicially applying brakes at individual wheels independently of the driver. The aim is to reduce difference in vehicle behaviour between the limits of the vehicle and the linear range of handling and thereby to make the vehicle more predictable and controllable.

The control system must compare the desired vehicle response to the estimated measured response and take corrective action when the difference is at a predetermined threshold **(Hac, 2002)**. This is illustrated in Figure 2.13:

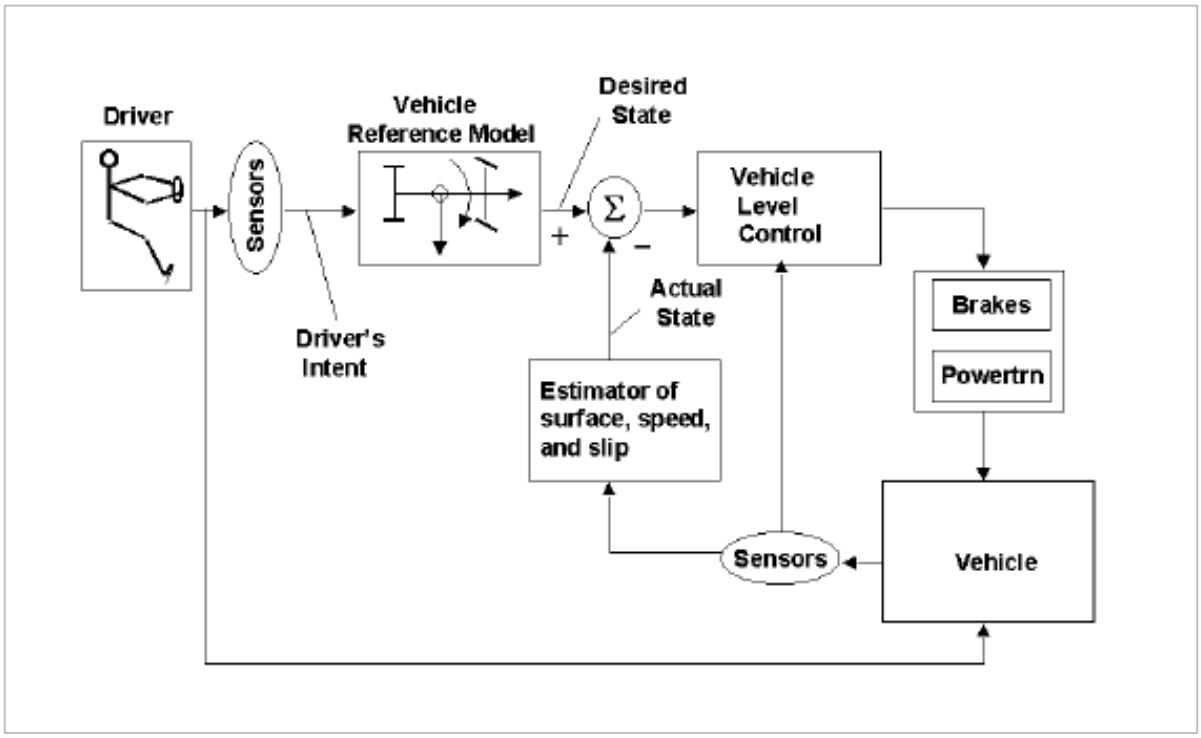

Figure 2.13: Functional Diagram of Vehicle Stability Enhancement System (Hac, 2002)

The driver inputs typically include the steering angle, brake pedal force and throttle position. The vehicle response is measured in terms of lateral acceleration, yaw rate and wheel speeds (from which the vehicle reference speed is derived). Additional sensors are built into the brake and power-train subsystems. The vehicle model then generates the desired vehicle response in terms of the desired yaw rate and the desired side-slip angle or side-slip rate. The estimation block then estimates the vehicle reference speed, surface coefficient of adhesion, vehicle side-slip angle and side-slip rate. The vehicle level control block compares the desired values of yaw rate and side-slip angle with the measured or estimated values and calculates the necessary corrective action, which is normally expressed in a yaw moment. To generate the yaw moment, closed-loop control of yaw rate and usually side-slip angle or side-slip rate is used. **Nishio et al. (2001)** provides a method of estimating the side-slip angle. The system level controller uses a closed-loop controller to achieve the values of wheel slip or wheel torques as determined by the vehicle level controller.

Grip (2009) describes the side-slip angle as the angle between the longitudinal orientation of the vehicle and the direction of travel at the CG. A vehicles side-slip angle can be measured using a device known as on Optical Correlation Sensor. According to **Grip (2009)**, there are a number of methods to estimate the side-slip angle. Two such methods are estimates based on an Extended Kalman Filter (EKF) with a road-tyre friction model, and a linear observer where the vehicle velocity is used as an input to a Kalman filter based on the kinematic equations of motion.

The VSE system does not target rollover directly, but rather reduces oversteer, since excessive oversteer normally leads to rollover **(Hac, 2002)**. The stability enhancement algorithms control the yaw rate and slip angle or slip rate and do not include the roll angle explicitly. However, by limiting the side-slip angle, the lateral velocity is reduced and this reduces the probability of vehicle rolling over. For untripped rollover, maximum lateral force is required to generate a peak lateral acceleration that would be great enough to initiate rollover. On a dry surface, the maximum lateral force generated is at large slip angles – typically between 10-20 degrees. For this slip angle range to be achieved at the rear axle, the vehicle must be oversteering. Manoeuvres with two-wheel lift-off have significantly larger yaw rates than manoeuvres where the vehicle remains stable, with the peak lateral acceleration roughly the same.

Hac (2002) showed that although the VSE system significantly improves vehicle response to manoeuvre-induced rollovers, a combination of VSE and ARS (active rear wheel steering) was even more stable and showed no tendency to rollover, even with very small side-slip angles.

There exist a number of variations in the design of active braking. **Lu and Brown (2004)** patented a control system that influences the stability of vehicle rollover. The control system determines the estimated roll angle based on speed, lateral acceleration, roll rate, yaw rate, longitudinal acceleration or a combination of these measures. In a high-risk rollover situation, the tyre force vectors are changed by judicial braking and rear steering. The tyre moment is reduced to counter the net moment of the vehicle and to reduce roll of the vehicle. The system is designed to be easily implemented into a steer-by-wire system. By contrast, the control model developed by Gasper et al. (2005) is based on the linear parameter varying (LPV) model of yaw-roll dynamics of heavy vehicles which directly measures the forward velocity, and a predictive system that compares lateral load transfer (LTR) to critical values using a short time interval. If the LTR exceeds preprogramed critical values, the brake is activated.

2.4.3 Active Suspension Systems

Being able to resist the roll motion of a vehicle during a potentially risky manoeuvre is a great advantage. One way to achieve this is to have the suspension exert an independent force that creates a moment to counter the roll. Active suspensions are thus an improvement to the normal suspension characteristics, i.e. an active suspension is a suspension system to which a control system has been added to create forces in the suspension. The some control systems uses electro-hydraulic equipment (hydraulics, hydro-pneumatics, pneumatics, electro-mechanics, etc.) to generate forces in the suspension in order to counteract roll moments. Active suspension systems were developed due to high demand both for more ride comfort and more stable handling. A rollover index is defined for the vehicle so that in critical situations under rollover danger, an emergency roll prevention control is activated in the suspension **(Dukkipati et al., 2008)**. Because active suspension systems provide extra force input, they demand a high amount of energy and power **(Cronjé, 2008)**. Thus, although they are highly effective, these systems are also highly complex and expensive.

The Active Anti-Roll Bar (AARB) **(Cronjé, 2008)** illustrated in Figure 2.14 is based on the passive roll-bar system found on most production vehicles. It is also referred to as Dynamic Body Control (DBC) **(cf. Hac, 2002)**.

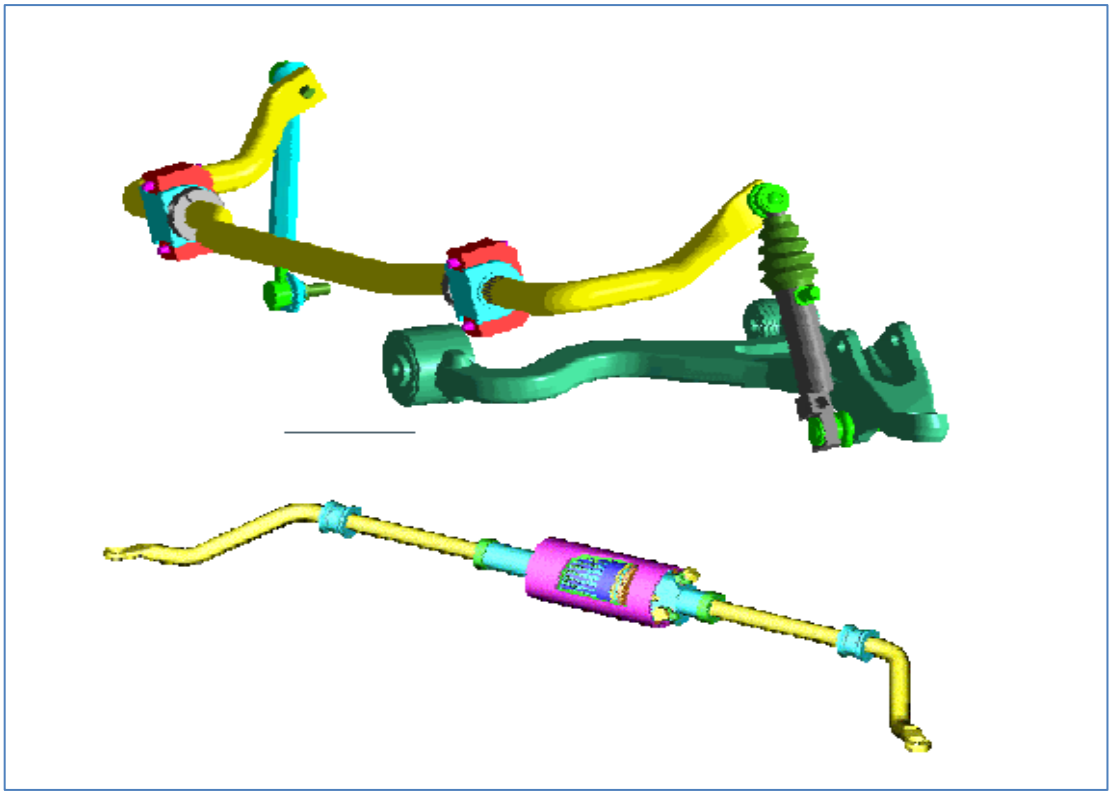

Figure 2.14: Active Roll Bars with Linear and Rotary Actuators (Hac, 2002)

These systems primarily improve the ride and handling of a vehicle by using linear or rotary hydraulic actuators on conventional roll-bars to provide forces that resist vehicle roll. A two-way valve controls the actuator chamber by supplying hydraulic pressure to it via a pump. For straight-line driving, the roll-bar assemblies can rotate relatively freely with the roll-bars unpressurised. In cornering, the measured lateral acceleration determines the camber of the actuator, creating a torque to oppose roll motion. This roll-resistant moment may be distributed between the front and the rear as a function of vehicle yaw response. Two main limitations of DBC with regard to manoeuvre-induced rollovers are power limits and torque limits **(Hac, 2002)**. Power limitations negatively influence the

response to reduce roll angle in quick transient manoeuvres**,** in that response speed is limited by the power of hydraulic pump. Torque limitations mean that the vehicle body will still experience some roll in steady-state cornering with large lateral acceleration.

The use of an anti-roll bar was implemented to improve the handling characteristics of an off-road vehicle without sacrificing ride comfort **(Cronjé & Els, 2009)**. To improve the handling capabilities, the lateral acceleration generated by the vehicle should be increased; however the roll-over propensity should be reduced such that the vehicle slides before rollover is induced. The method proposed by **Cronjé and Els (2009)** is to reduce the roll angle of the vehicle by increasing roll stiffness. This increases the vertical load transfer and decreases the lateral acceleration. The drawback of the anti-roll bar is that it is not very adaptable to other characteristics; however, it is cost-effective and requires low flow and pressure. The AARB demonstrated an 80% improvement in the body roll angle for a double lane change at 80Km/h on a smooth road and 41% improvement for a double lane change on Belgian paving at 50km/h.

Sampson and Cebon (2003a, 2003b) develop a theoretical model based on a stiff U-shaped anti-roll bar (ARB) connected to the trailing arms of the vehicle suspension and indirectly connected to the vehicle chassis by hydraulic actuators. In their simulation model (based on 8 degrees of freedom: two sprung mass and two unsprung mass roll degrees of freedom for the tractor unit, one sprung and one unsprung mass roll degree of freedom for the trailer and one yaw degree of freedom for each tractor and trailer), they find the optimal control was to set the normalised load at the maximum angle allowed by the suspensions. They developed and refined a controller based on a linear quadratic Gaussian approach combined with a loop transfer recovery procedure, but did not experimentally investigate the performance of their controller. Their linear model is somewhat simplistic in that they assume roll stiffness and damping of the suspension system to be constant for different manoeuvers. Their theoretical model was experimentally verified by **Miege and Cebon (2011).** They found best results for activating both tractor and trailer drive axles.

Van der Westhuizen (2012) proposes that it is possible to cause the vehicle to slide rather than to roll over by reducing the body roll angle of the vehicle. This will increase the load transfer and thus decrease the lateral force that can be generated by the tyres. He used slow active suspension control to reduce the body roll angle on a vehicle fitted with a hydro-pneumatic suspension system. Sliding is not desirable for vehicle control, but it dissipates energy and thus reduces the vehicle's speed which reduces rollover probability.

2.4.4 Ideal Suspension Characteristics Settings

Rollover characteristics of a vehicle are affected by the suspension characteristics, hence it is important to investigate what set of suspension settings minimises rollover risk. There is a well-known trade-off in suspension design between handling stability and ride comfort. A relatively stiff suspension usually gives good handling but a poor ride. **Uys (2007)** investigated the effects of various suspension settings for the hydro-pneumatic semi-active $4S_4$ suspension system (discussed in further detail in chapter 2.5) with regard to various spring stiffness and damping values. Normally, low damping suspensions have a high spring stiffness, which is recommended to counter roll. However, in the case of the $4S_4$, **Uys (2007)** reported that high damping was found to limit rollover propensity and therefore recommended a combination of high damping and low spring stiffness for steady state cornering. This confirms previous results by **Ackermann and Odenthal (1998),** who also found that hardening the damping with respect to the roll acceleration and suspension rates for active suspension reduced rollover risk with respect to suspension characteristics. Damping removes energy

from the roll motion, thus lowering steady-state roll. Hence the higher the damping, the more energy is removed from the system during roll motions. Similarly, the higher the roll stiffness, the lower the relative roll angle of the body relative to the suspension will be.

Uys (2007) summarized the recommended suspension Gas Volume (GV) (which affects the suspension stiffness) and the Damping Static Factor (DSF) (which affects the suspension damping) for the $4S_4$ hydro-pneumatic suspension system developed by **Els (2006)**. These figures are presented in Table 2.1:

Table 2-1: Summary of the Gas Volume and Damper Scale Factors to determine the lowest maximum parameter (Uys, 2007)

For lowest maximum…	Damping Scale Factor	Gas Volume [litres]
Roll angle	3	0.3
Roll rate	3	0.1
Yaw rate	3	0.6
Lateral acceleration	3	0.6
Wheel lift (inner rear)	2	0.6
Wheel lift (inner front)	3	0.6
Wheel lift (outer rear)	3	0.6
Wheel lift (outer front)	3	0.1
Note: The lowest maximum refers to the setting that resulted in the investigated parameter having the smallest value of the maximum of the parameter for the range of DSF and GV investigated.		

From the table, **Uys (2007)** recommends a DSF of 2-3 (for high damping) and a GV of 0.6 litres (for low stiffness). With regard to vehicle rollover propensity, the velocity of the suspension plays a greater role than suspension displacement. It may be possible that large suspension displacements limit the wheel lift in that although there may be more body roll, the wheels remain grounded.

Recent studies have attempted to overcome this trade-off between handling and ride comfort through the use of hydraulic or mechanical interconnections between the individual wheel stations. **Smith, Zhang and Hu (2011)** show that a well-designed suspension system can greatly reduce vehicular rollover propensity and that by using interconnected (hydraulically) suspension models (cf. Smith and Walker, 2004; Yao et al. 2015), greater flexibility can be achieved in controlling stiffness and damping independently, e.g. by increasing roll stiffness without affecting bounce stiffness and giving a good handling performance and moderate compensation in ride comfort. However they also show that there is a limit to the benefits achieved by such systems; in the hydraulic interconnected system, fluid compressibility being a limiting factor.

Vehicle suspension plays an important role in both body-wheel motions (i.e. the relative motion between a vehicle's body and its wheels) and integral multi-body motions or planar dynamics. Hence, controllable suspension systems that directly govern a vehicle's relative motion between the vehicle body and the wheel such as bounce, roll, pitch and warp offer considerable advantage over non-controlled systems. Using a 10-degree-of freedom (DOF) vehicle model, **Zhang, Wang and Du (2014)** propose a motion-mode energy method (MEM) to identify predominating modes for vehicle dynamics analysis and control, with the aim to make active suspension systems, particularly reconfigurable hydraulically interconnected suspension systems, more affordable and energy conservative. They achieved this by employing a switchable controller (using active/semi-active actuators) to detect and control the dominating vehicle modes (bounce, pitch and roll motions). However they caution that more work still need to be undertaken in order to refine aspects of

practical implementation, e.g. by developing and testing algorithms to estimate vehicle state vector and tyre deflection.

Although beyond the scope of the current study, it is noted that recent research on interconnected systems have indicated improved energy efficiency as well as improved handling and ride comfort characteristics (Smith & Walker 2004; Yao et al. 2015). Yao et al. (2015) propose a dual mode interconnected suspension (DIS) which incorporates a default mode as well as an anti-pitch mode. The simulation results of their proposed system show benefits to both reducing vehicle roll/pitch motion as well as improving ride comfort.

2.4.5 Centre of Gravity Position

The investigation of the rollover mechanism and the detection and prediction of rollover showed a significant correlation between rollover and the CG height. According to **Dukkipati et al. (2008)**, the most effective way to keep the vehicle from rolling over is to make the centre of gravity of the vehicle as low as possible, and or to make the vehicle wider and use tyres with less lateral force generation capabilities. However, due to most vehicles having passive (fixed ride height) suspension systems, not many investigation have been carried out.

Uys (2007) investigated the effects of varying the ride height of a vehicle with respect to the vehicle's roll propensity using a simulation model and found that a higher CG makes the vehicle more prone to higher roll rates and smaller phase lags. He concluded that the greatest improvement in the reduction of ride height was made by reducing the rear inner wheel lift during a modified Fishhook 1A manoeuvre. (A full description of different types of manoeuvres is provided in chapter 4.2 and will therefore not be discussed here.) He also observed a good correlation between ride height and rollover tendency.

Whitehead et al. (2004) reported that varying the CG of the vehicle vertically affects the two-wheel lift-off speed in that the latter decreases as the CG height is raised. Their results are depicted in Figure 2.15. This is congruent with the SSF discussed in chapter 2.3.1, since the SSF varies proportionally when the wheel base length is held constant and the CG is varied. The SIS (Slowly Increasing Steer) constant was measure at the tyre and remained constant with CG height changes.

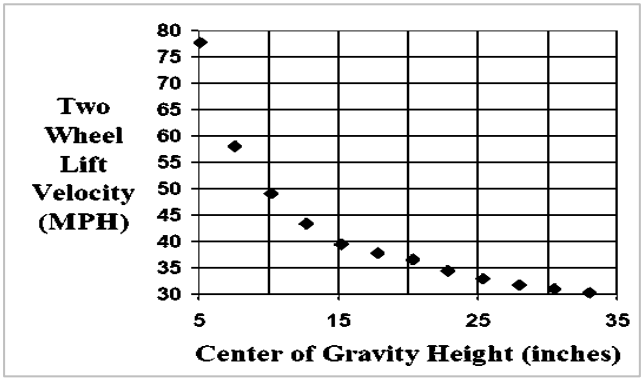

Figure 2.15: Simulation Data of Two-Wheel Lift Velocity versus CG Height for the Blazer (Whitehead et al., 2004)

According to **Whitehead et al. (2004)**, in order to isolate the effects of the understeer curve (due to changing the weight split) from other factors, the roll centre, suspension stiffness and damping are set the same for the front and the rear. The wheel base is held constant. The variation of the CG longitudinally varies the SIS constant and the two-wheel lift velocity.

The relationship between SIS and front-axle percentage weight is given in Figure 2.16, which shows that the closer to the front of the vehicle the CG is, the greater the SIS constant:

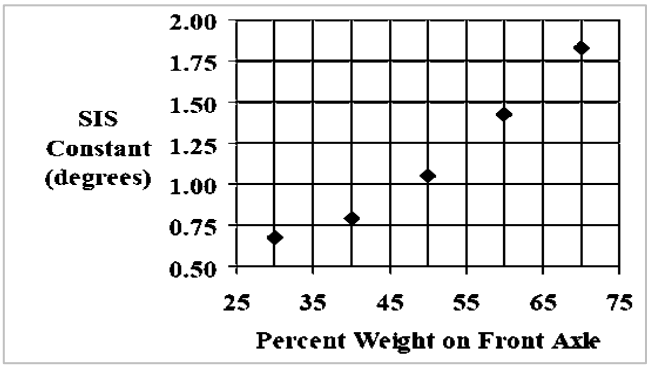

Figure 2.16: Simulation data of SIS Constant versus Weight Split (Whitehead et al., 2004)

Figure 2.17 depicts the relationship between the two-wheel lift velocity and front-axle percentage weight. The closer the CG is to the front of the vehicle, the greater is the two-wheel lift-off velocity.

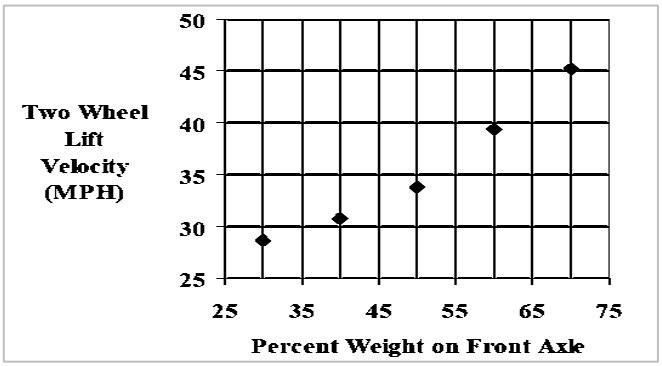

Figure 2.17: Simulation data of two-wheel lift velocity versus weight split of a blazer in a Fishhook 1A manoeuvre (Whitehead et al., 2004)

An increase in the SIS causes the Fishhook 1a to become an even more severe manoeuvre. The authors show that with the CG shifted horizontally to the rear, the vehicle oversteers more and rolls at a lower velocity, demonstrating a correlation between understeer and roll propensity. This is illustrated in Figure 2.18 and can be described by the cornering equation (Equation 2-1) and the understeer gradient **(Gillespie, 1992)**.

$$\delta = \frac{L}{R} + K\left(\frac{V^2}{Rg}\right) \qquad \textbf{Equations 2-25}$$

where:

- L is the wheel base
- R is the radius or the turn
- K is the understeer gradient
- V is the forward velocity
- g is the gravitational constant

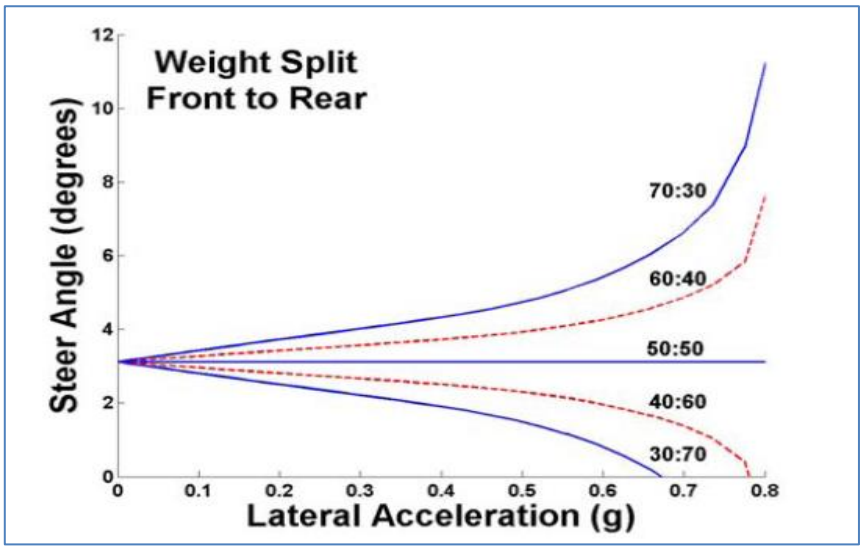

Figure 2.18: Simulation data showing the understeer curve for the various weight splits (Whitehead et al., 2004)

The lowering of the CG also reduces the load transfer. **Gillespie (1992)** presents the relationship for vertical force on the inside and outside wheels during cornering:

$$\boldsymbol{F_{zo} - F_{zi} = 2F_y \frac{h_r}{t} + 2k_{roll} \frac{\theta}{t}} \qquad \textbf{Equation 2-26}$$

where:

- F_{zo} is the vertical force on the outside wheel
- F_{zi} is the vertical force on the inside wheel
- F_y is the lateral force
- h_r is the roll centre height
- k_{roll} is the roll stiffness of the suspension
- t is the track width
- θ is the roll angle of the body

The roll stiffness may be determined as **(Gillespie 1992)**:

$$\boldsymbol{k_{roll} = 0.5 * K_s b^2} \qquad \textbf{Equation 2-27}$$

where:

- K_s is the suspension unit stiffness
- b is the lateral separation between the springs

Equation 2-26 shows that the load transfer is a function of both CG height (the first term on the right hand side of the equation) and roll angle (the second term on the right hand side or the equation). The lateral force generation is a function of the vertical force, and thus related to load transfer at a slip angle. Thus reducing the CG height will lower both the lateral tyre force generation and the rollover moment.

In the final section below, hydro-pneumatic levelling control systems are explored in order to provide background for the present study. In the present study, the CG height adjustment of the hydro-

pneumatic test vehicle (Land Rover Defender 110) must be controlled to achieve the desired design height. This is done by adding or removing hydraulic fluid from the suspension units.

2.5 Hydro-pneumatic Levelling Control

Height-control levelling with hydro-pneumatic suspension is advantageous since the mass of the gas remains constant and the volume decreases under load. This results in a stiffer spring characteristics when the suspension is under load. According to **Bauer (2011)** the levelling control should fulfil its function without being intrusive. This requires a compromise between stable control and low sensitivity to ground irregularities. A vehicle is a statically indeterminate system making it difficult to balance. The control algorithms are one of the best-kept secrets of the suppliers or users of a suspension system. A basic levelling system for a hydro-pneumatic suspension system is depicted in Figure 2.19.

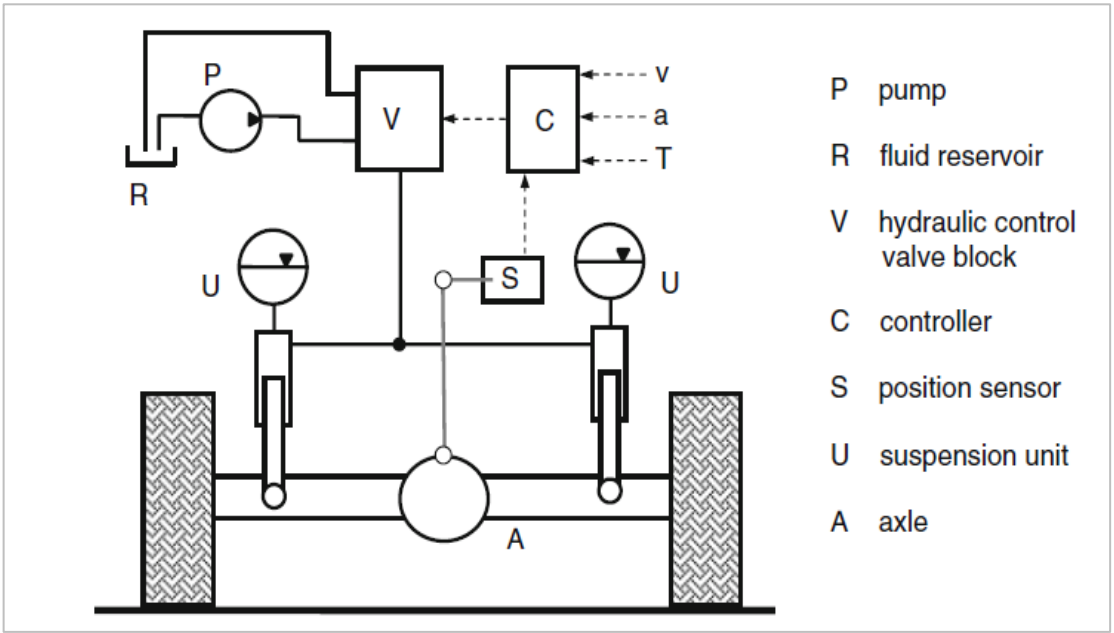

Figure 2.19: Basic setup of an electronically controlled levelling system (Bauer, 2011)

A block value determines the in/out flow of hydraulic fluid, which respectively raises or lowers the suspension. A control system (depicted in Figure 2.20) determines whether to adjust the height level by comparing measurements of the suspension position sensors with the required positions.

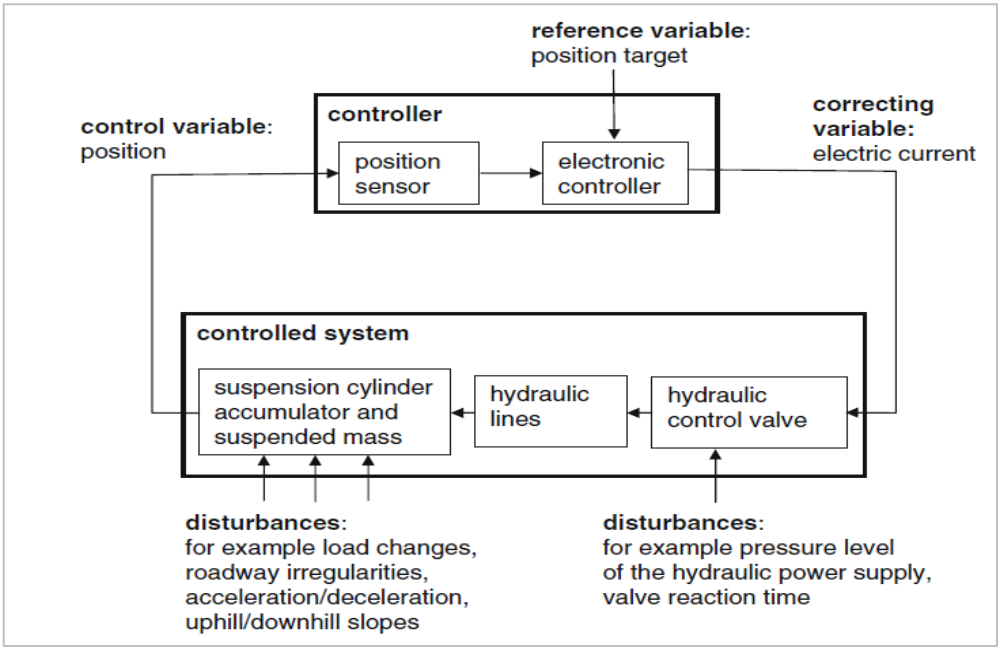

Figure 2.20: Interaction of controller and controlled system for axle suspension levelling (Bauer, 2011)

A level controller can be designed to replicate level control of a mechanical system by using proportional control. This is depicted in Figure 2.21.

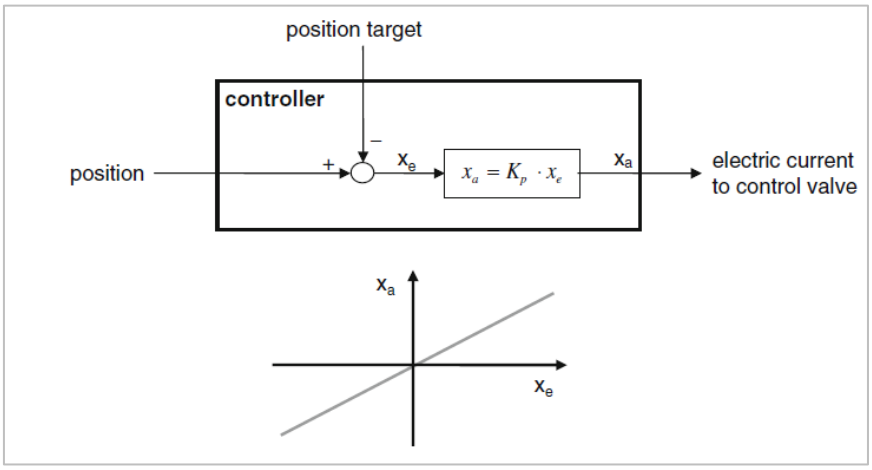

Figure 2.21: Logic and control behaviour of a P-controller (Bauer, 2011)

However the problem of a proportional controller is that is requires permanent readjustment **(Bauer, 2011)**. One possible solution to this problem is to incorporate a deadband around the desired design postion to calm the control algorthim and reduce energy consumption in the presence of ground irregularities, as depicted in Figure 2.22:

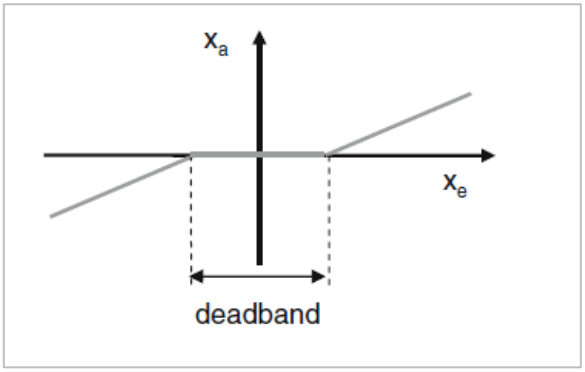

Figure 2.22: P-controller with deadband (Bauer, 2011)

A double low pass filter can help reduce false activations and optimise height adjustment compensation. This is depicted in Figure 2.23:

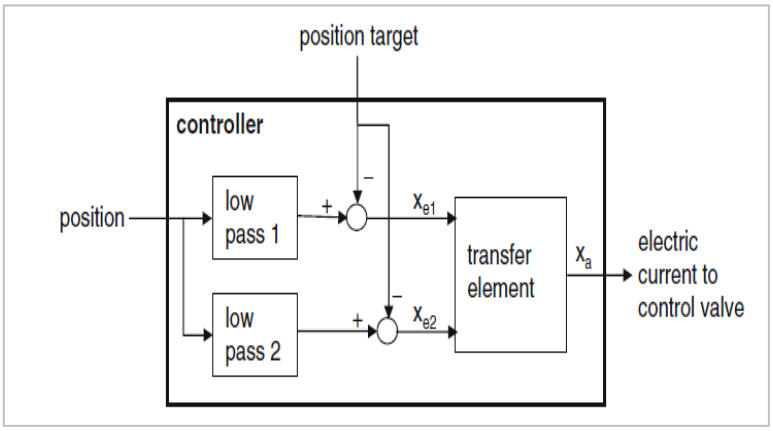

Figure 2.23: Controller with double low pass filter (Bauer, 2011)

Bauer (2011) recommends a long average of 6 seconds sampling period for activation of the height adjustment and a shorter average of 0.8 seconds sampling period to avoid overshoot of the height adjustment. Thus, when the suspension position leaves the desired position, readjustment is not made until the long average value leaves the tolerance bound range of ±7.5% around the design position relative to the overall suspension travel. To avoid long activation of the valves, the control valves are de-energized when the short average value re-enters the tolerance band.

2.6 Conclusion

In this chapter, the rollover mechanism was discussed using a number of models that vary in complexity and therefore applicability. The rigid body model may be used in steady-state turns where there is no roll acceleration. This model estimates roll to occur at higher lateral acceleration than the true value. The suspended vehicle model is valid when lateral acceleration changes slower than roll response. The transient model accounts for overshoot that lowers the rollover threshold. The 14 DOF model may be used to predict vehicle behaviour even after wheel lift-off. Thus the vehicle manoeuvre under investigation should be understood in terms of which model would be best suited.

Secondly, because many algorithms require an estimate for the roll angle of the vehicle in order to detect and predict rollover, four methods of estimating the roll angle were discussed, namely direct measurement of tyre pressure changes, estimation via suspension deflections, estimation from lateral acceleration and estimation from measuring the integrated roll rate. It was noted that no

single method is adequate under all road conditions. Since lateral acceleration and roll rate estimations are complimentary in the sense that one produces a good estimate when the other can expect to perform poorly, they can be combined. Similarly, by using model-based techniques, lateral acceleration containing inertial information may also be combined with suspension sensor estimates containing road input information. Thus it is possible to obtain a roll angle estimate from other measured signals. However, this estimate must still be implemented into an algorithm to predict when rollover will occur or detect the severity of the state of the vehicle.

Thirdly, various means of predicting rollover were discussed. Firstly, since it is preferable to have the vehicle lose traction and slide out rather than rollover, the SSF provides a useful measure to determine when the maximum lateral acceleration attainable from the friction between the tyres and the road is exceeded. A second method is to implement a rollover index, which provides rollover propensity detection for manoeuvre- and road-induced rollover and may be adjusted to suit the vehicle. Because of the complex nature of rollover, prediction methods that account for various *dynamic* motions are preferred over static tests, which only consider selected variables. These include the DSI, the RSA, the RPER, RPM and TTR algorithms. Some of these more complex techniques require vehicle modelling and extensive measurements. The TTR model offers the advantage in that it is able to predict rollover time rather than simply measure proximity to rollover. This is helpful as it assists to overcome equipment delays and may avoid false activations, but has the disadvantage of requiring the implementation of complicated yaw and roll vehicle models to estimate steering input responses.

Fourthly, various means of preventing rollover were explored. Rollover may be avoided by introducing active steering or active braking, adding a control mechanism to achieve active suspension or by lowering or adjusting the CG of the vehicle. With respect to suspension characteristics, hardening the dampening with corresponding low spring stiffness gave the greatest potential in reducing rollover risk. With respect to adjusting the CG, it was found that reducing the CG height will lower both the lateral tyre force generation and the rollover moment.

3 SIMULATION MODEL

The investigation of on-road untripped manoeuvre-induced rollover was done though simulation using an existing mathematical model adapted for the purpose. Simulations do not require expensive and dangerous tests, and eliminates variability effects that influence the behaviour of the vehicle **(Hac, 2002)**. Using a mathematical model allows for fast and relative easy parameter adjustments. In addition, some test manoeuvres require a substantial testing area, where as space constraints are not problematic for simulations.

The setup of the mathematical model is discussed in detail in chapter 3.1, in terms of overall vehicle properties, the suspension system and the hydraulic circuit. In each case, the physical parameters of the test vehicle are first described, thereafter the means used to model them are explained.

In chapter 3.2, parameters defined using simulations that are used in developing the control system for rollover prevention are discussed. These include the roll angle estimation, a rollover detection strategy and two rollover control strategies. The rollover prevention strategies are defined and developed into a control system which adjusts the centre of gravity using the slow active suspension control developed for the test vehicle by **Van der Westhuizen (2012)**. Hydraulic fluid is added from a pressurised accumulator or removed to atmospheric pressure from individual suspension struts to achieve height adjustment.

3.1 Mathematical Model

In order do simulations, a model that represents the physical test vehicle needs to be created. The test vehicle for the study is a Land Rover Defender 110 fitted with a $4S_4$ hydro-pneumatic suspension system. According to **Dukkipati et al. (2008),** rollover accidents for SUVs and small trucks are higher than that of passenger cars, thus the test vehicle is a good candidate for the task. The model is an ongoing project built up by previous students and has had parameters and coding added over the years to increase its accuracy and complexity.

A dynamic mathematical model of the Land Rover 110 test vehicle was created in MSC.ADAMS/View **(MSC.Software, 2011) to** study the system and predicted the behaviour of the vehicle. The dynamic model aims to achieve essential features realistically, but without over-complication **(Thoresson, 2003)**. The model was initially developed by **Thoresson (2007)** and upgraded to include changes made to the test vehicle by **Uys (2007)**, **Cronjé (2008)**, **Botha (2011)** and **Van der Westhuizen (2012)**. The model is co-simulated with the MSC.ADAMS/Controls interface linked to MSC.ADAMS/View with MATLAB and SIMULINK. MSC.ADAMS solves the vehicle dynamics, while the calculations for the suspension characteristics and controls are executed in MATLAB and SIMULINK.

In this study, the ADAMS model was designed to study lateral vehicle dynamics and body roll. In order to develop the mathematical model, certain vehicle parameters are needed. These were accurately measured on the test vehicle during earlier studies and then implemented for the model. The final product implemented for this study is a non-linear full vehicle model which has 15 unconstrained degrees of freedom, 16 moving parts, 6 spherical joints, 8 revolute joints, 7 Hooke's joints and a motion defined by the steering driver.

Table 3.1 shows the relative degrees of freedom of the mathematical model.

Table 3-1: MSC.ADAMS vehicle model's degrees of freedom

Body	Degree of Freedom	Associated Motions
Vehicle Body (2 rigid bodies)	7	Body torsion Longitudinal, lateral, vertical Roll, pitch, yaw
Front Axle	2	Roll, vertical
Rear Axle	2	Roll, vertical
Wheels	4x1	Rotation

The model's accuracy is affected by the roll centre, tyre inclination angle and jacking forces. These effects are common limitations in vehicle models. The roll centre acts as both a point of application of forces as well as a kinematic constraint. The roll centre influences the net roll moment acting on the sprung mass as well as the load transfer at the tyres **(Shim & Ghike, 2007)**. The current vehicle model incorporates these effect by modelling the kinematics of the vehicle suspension which is discussed in chapter 3.2.1.The model incorporates a non-linear Pacejka 89 tyre model fitted with estimated tyre data. However, to reduce model complexity, longitudinal tyre dynamics are not included. This is sufficient for the simulations performed in this study, since lateral tyre forces were the main focus.

3.1.1 Vehicle Properties

The motion of a rigid body is highly affected by its moments of inertia. Thus to develop an accurate mathematical model of the test vehicle, it is very important to have a good representation of the moments of inertia.

The Land Rover's roll, pitch and yaw moments of inertia and CG were determined experimentally by **Uys et al. (2006)** and are tabulated in Table 3.2:

Table 3-2: Properties of the test vehicle (Uys et al., 2006)

Property	Value
Pitch moment of inertia	3339 [kg m^2]
Yaw moment of inertia	2478 [kg m^2]
Roll moment of inertia	744 [kg m^2]
Centre of gravity height	1.000 [m]
Track width	1.4859 [m]
Front body mass	682.2133 [kg]
Rear body mass	893.6054 [kg]
Torsional stiffness between bodies	250 [Nm/degree]
Anti-roll bar stiffness	134 [Nm/degree]
Weight distribution	Close to 50\50

It must be noted that during experimental testing, the vehicle is fitted with outriggers to avoid rollover for safety reasons. The outriggers do affect the vehicle's mass moments of inertia and CG position and therefore are included in the model.

The Land Rover's physical dimensions are shown in Figure 3.1:

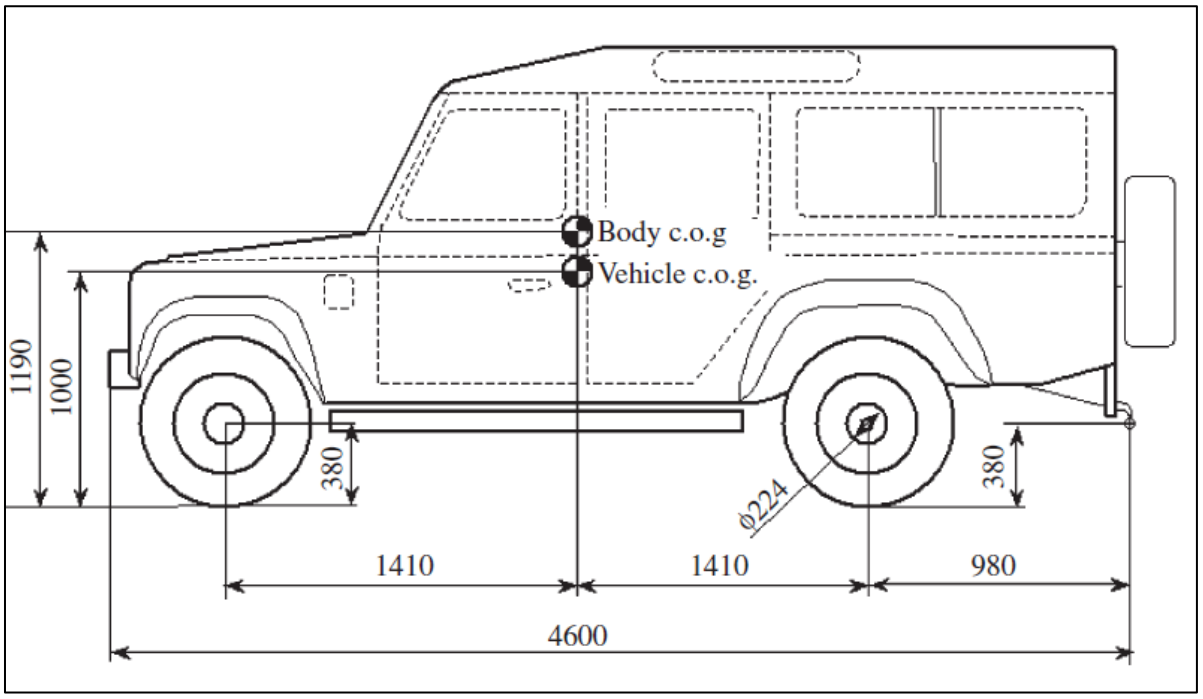

Figure 3.1: Location of centres of gravity and vehicle geometry (Uys et al., 2006)

For the mathematical model, the moments of inertia of the vehicle body were implemented from the data above for the physical Land Rover 110. The vehicle body is modelled as two rigid bodies connected along the roll axis at chassis height by a revolute joint and a torsional spring to capture body torsion in roll.

The steering mechanism was modelled with the steering inputs given directly at the wheels or king pin. Thus the steering ratio between the steering wheel and the front wheels is required.

According to **Uys (2007)**, for a maximum steering-wheel angle of 1080 degrees, the angle at the kingpin must be 50 degrees, as depicted in Figure 3.2. Thus the steering ratio is calculated as:

$$\boldsymbol{Steeringratio = \frac{1080^o}{50^o} = 21.6}$$ **Equation 3-1**

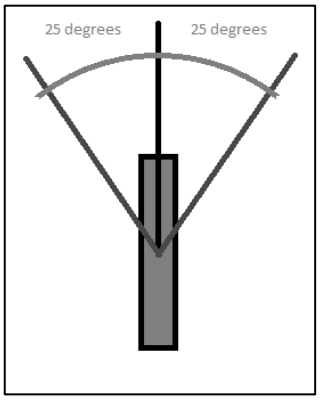

Figure 3.2 Kingpin steer range

The second task was the modelling of the suspension system.

3.1.2 Suspension System

The test vehicle is fitted with a semi-active suspension system. The Four-State Semi-Active suspension system abbreviated as the $4S_4$ system was developed and designed by Els **(Els, 2006)**. The $4S_4$is a hydro-pneumatic suspension system that exhibits two discrete spring characteristics and two discrete damper characteristics, and allows switching between these characteristics. Solenoid valves are used to channel hydraulic fluid which creates the different characteristics **(Cronjé & Els, 2009)**.

The $4S_4$ circuit diagram is given in Figure 3.3 in order to clarify the working mechanism of the suspension system. The accumulators act as springs by compressing gas. Changing the gas volumes changes the individual spring rates. To achieve a low spring rate in the unit, both accumulators are used in compression. To achieve a high spring rate, only the 0.1 litre accumulator is used with valve 3 and 4 sealing off the 0.4 accumulator. Damping is created by absorbing energy as the hydraulic fluid passes through orifices. Thus, to achieve low damping in the suspension unit, bypass valves (valve 1 and valve 2) are used to short the circuit so that the hydraulic fluid is not forced through the damper. High damping is achieved by closing the bypass valves and forcing the fluid through the damper. The damping in the system may be upgraded by installing proportional valves or servo valves. The ride height of the vehicle may be adjusted by adding or extracting oil from the unit **(Els, 2006)**.

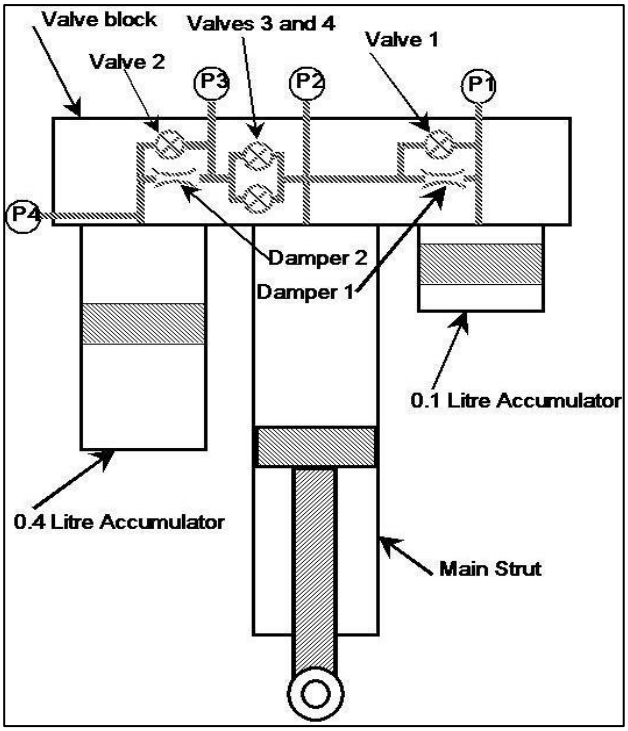

Figure 3.3 Circuit diagram (Els 2006)

The system allows for the suspension characteristics to be switched in less than 100 milliseconds while driving. The ride comfort mode has been optimized to minimize the vertical accelerations. The handling mode has been optimized to minimize body roll angle in a Double Lane Change (DLC) manoeuvre. The system improved the roll angle of the vehicle compare to the baseline vehicle by 78 percent and the ride comfort between 50-80 percent over Belgian paving **(Els, 2006)**.

The spring and damper characteristics for the different settings discussed above are plotted in Figures 3.4 and 3.5 respectively.

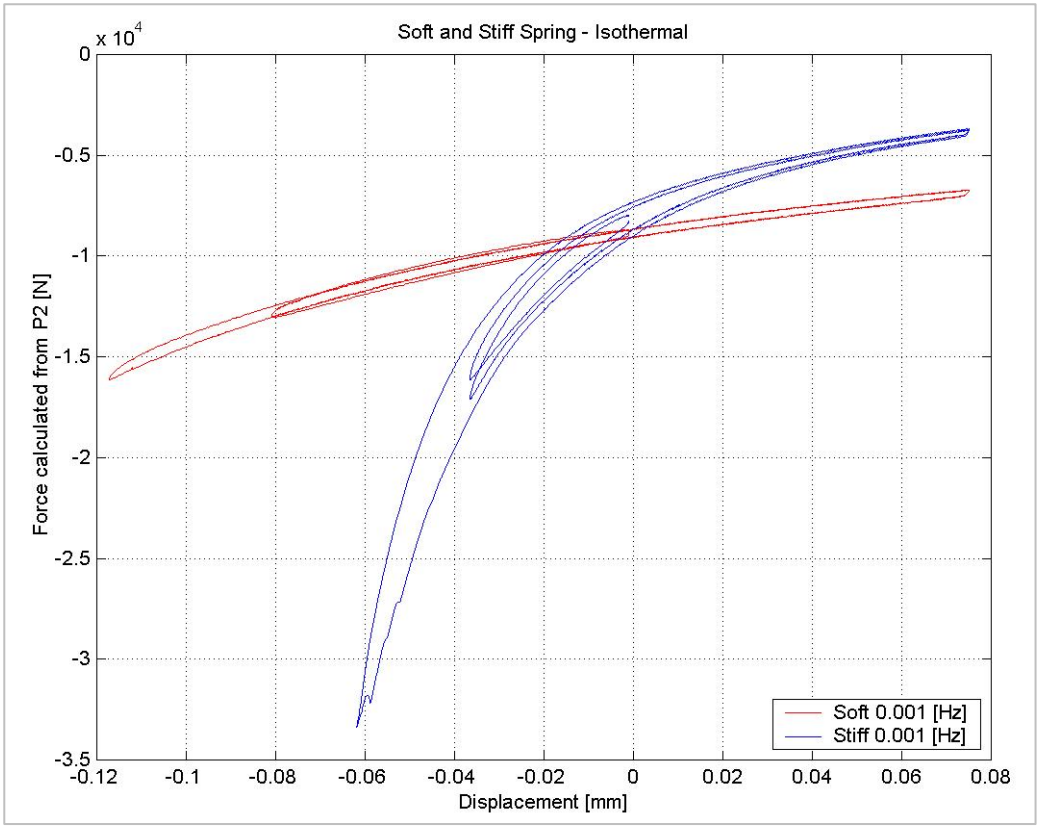

Figure 3.4 4S$_4$ Soft and stiff spring characteristics (Els, 2006)

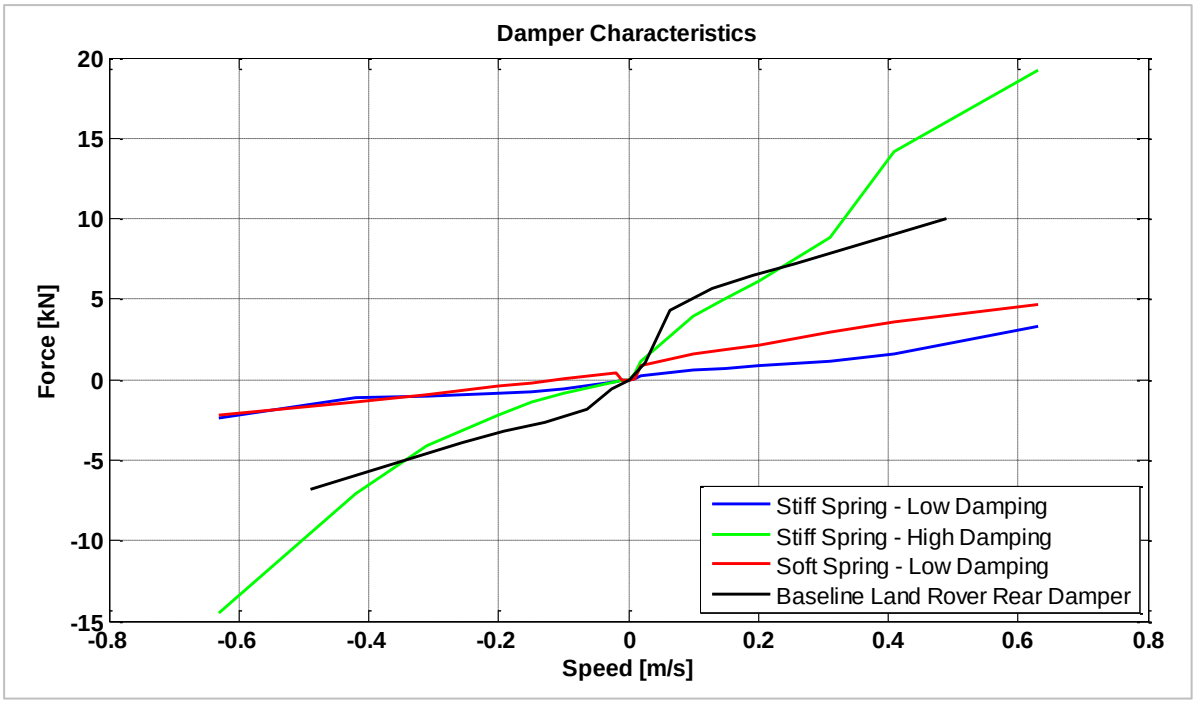

Figure 3.5 4S$_4$ Damper characteristics (Els, 2006)

In the model, the suspension system was mathematically modelled to include spring and damper characteristics, mass properties and tyre characteristics and to account for the damper force, strut friction, spring force and bump stop force. Friction in the joints, connection points and seals are not modelled, which may cause the simulated model to move with more ease than the test vehicle in reality **(Cronjé, 2009)**.

The damper force is calculated as a piecewise quadratic approximation and a function of strut velocity. The friction force in the individual struts is calculated by means of a lookup table as a function of strut velocity. The bump stop force is calculated as a first order polynomial. The spring force may be approximated using either the ideal gas equation or the Benedict Webb Rubin (BWR) real gas equation which can both be represented as functions of the strut displacement. For the purpose of this study, the adiabatic ideal gas model was used to model the hydro-pneumatics and the oil is assumed to be incompressible.

The model uses kinematic joints with torsional spring characteristics to model the suspension bushings. The front suspension is modelled by means of a rigid axle which is fixed longitudinally by two leading arms connected to the body with rubber bushes. The bushes' stiffness's are included in the model. The rear suspension is modelled with rigid axles with two trailing arms. An A-arm connected with a revolute joint to the body and a spherical joint to the axle fixes the lateral direction. The trailing arm bushes' stiffness's are also modelled. The suspension units are mathematically modelled in MATLAB and linked in the SIMULINK model. The SIMULINK model is then linked to the MSC.ADAMS model using the MSC.ADAMS Control environment.

The front suspension of the mathematical model is given in Figure 3.6

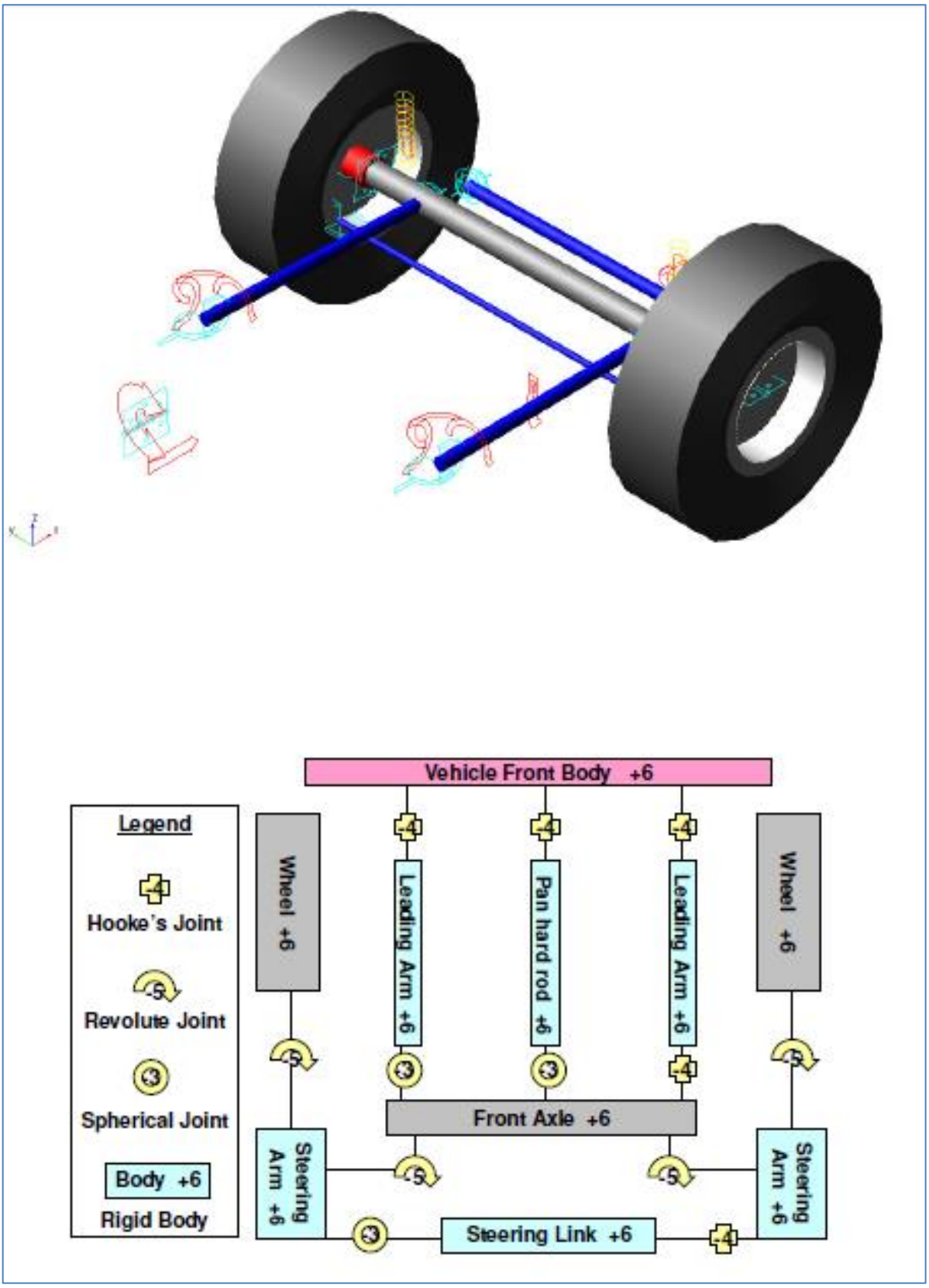

Figure 3.6: Modelling of the full vehicle front suspension in MSC.ADAMS (Thoresson, 2005)

Figure 3.7 shows the rear suspension model in MSC.ADAMS:

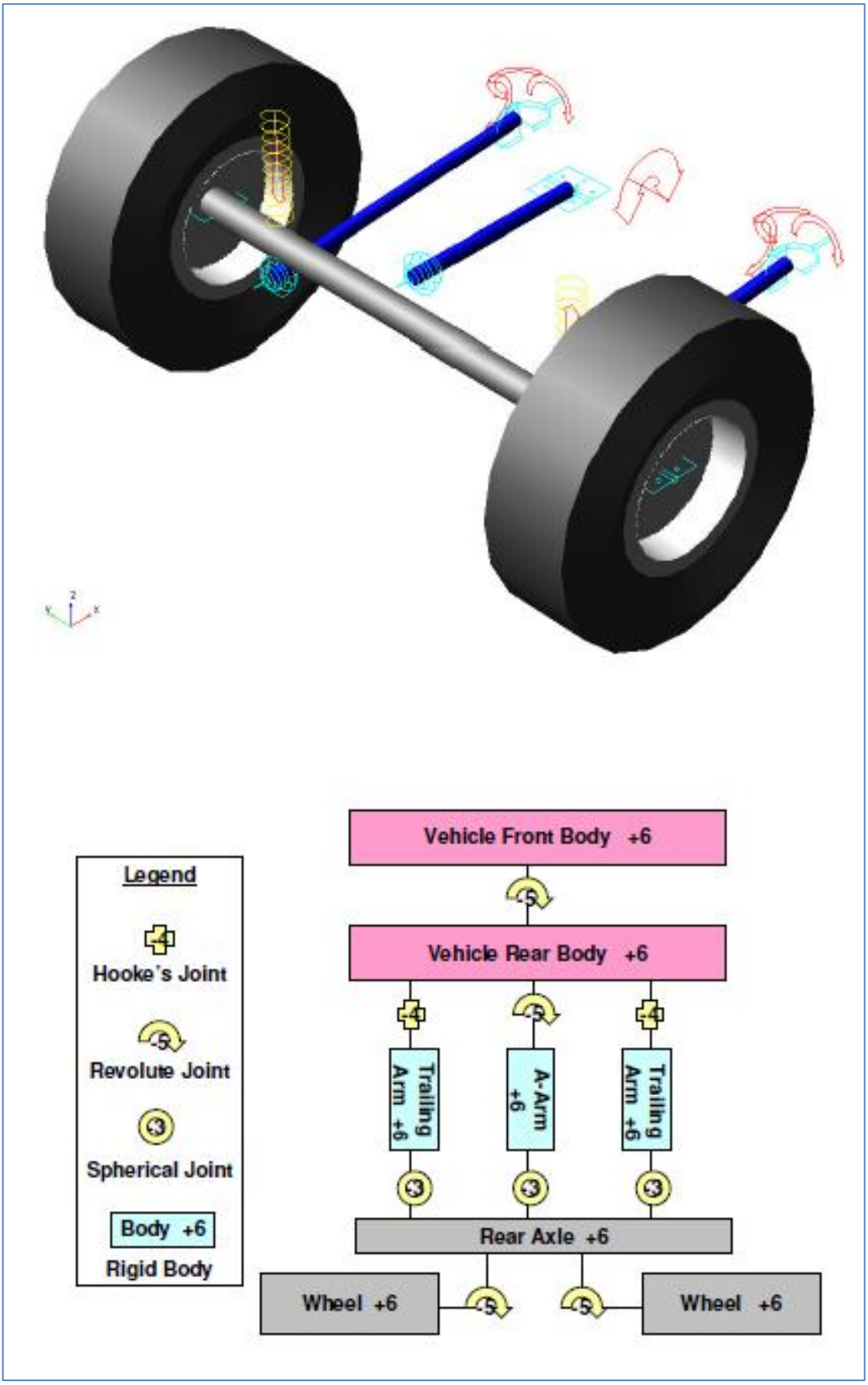

Figure 3.7: Modelling of the full vehicle rear suspension in MSC.ADAMS (Thoresson, 2005)

In the next section, the modelling of the hydraulic circuit is reported.

3.1.3 Hydraulic Circuit

For the purposes of this study, the hydraulic system (depicted in Figure 3.8)used in the simulation model to pump in or out of the $4S_4$ suspension units for slow active control was adopted from the model developed by **Van der Westhuizen (2012).**

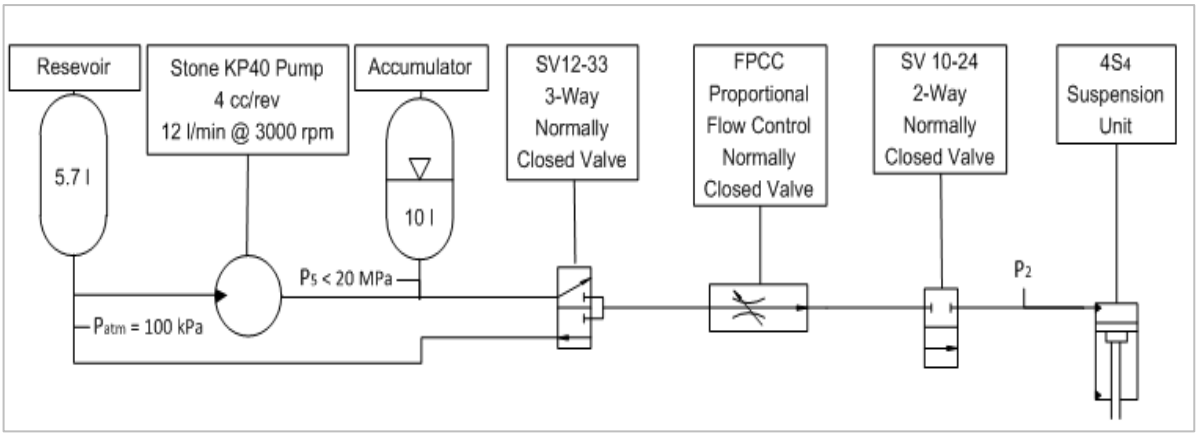

Figure 3.8: Hydraulic circuit for a single suspension unit (Van der Westhuizen, 2012)

In this system, oil is pumped at 12 l/min by a Stone KP40 **(Stone Hydraulics, 2012)** gear pump and stored in a pressurised bladder type accumulator which supplies the strut with oil. Directional valves (SV12-33) **(Stone Hydraulics, 2012)** are used to add oil to the strut from the accumulator or remove oil from the strut to the oil reservoir. The in and out flow is controlled by a proportional valve (FPCC). A two way valve (SV10-24) is used to close the system when suspension control is not used. The valve characteristics for flow are modelled using a lookup table and are given in Appendix 7.1.

The pressure at P2 represents the pressure due to the vertical wheel force. The pressure at P5 represents the maximum pressure the pump is able to supply (12MPa). The oil can be added at a flow rate proportional to the pressure difference between the accumulator and the suspension unit's cylinder and removed at a flow rate proportional to the pressure difference between the suspension unit and the atmosphere. The hydraulic circuit allows the system to drain oil from the struts at a maximum flow rate of 23 *l*/min and supply the strut with oil at a maximum rate of 12 *l*/min. This has a direct influence on ride height adjustment rates.

The complete flow diagram for the hydraulic system is given in Figure 3.9:

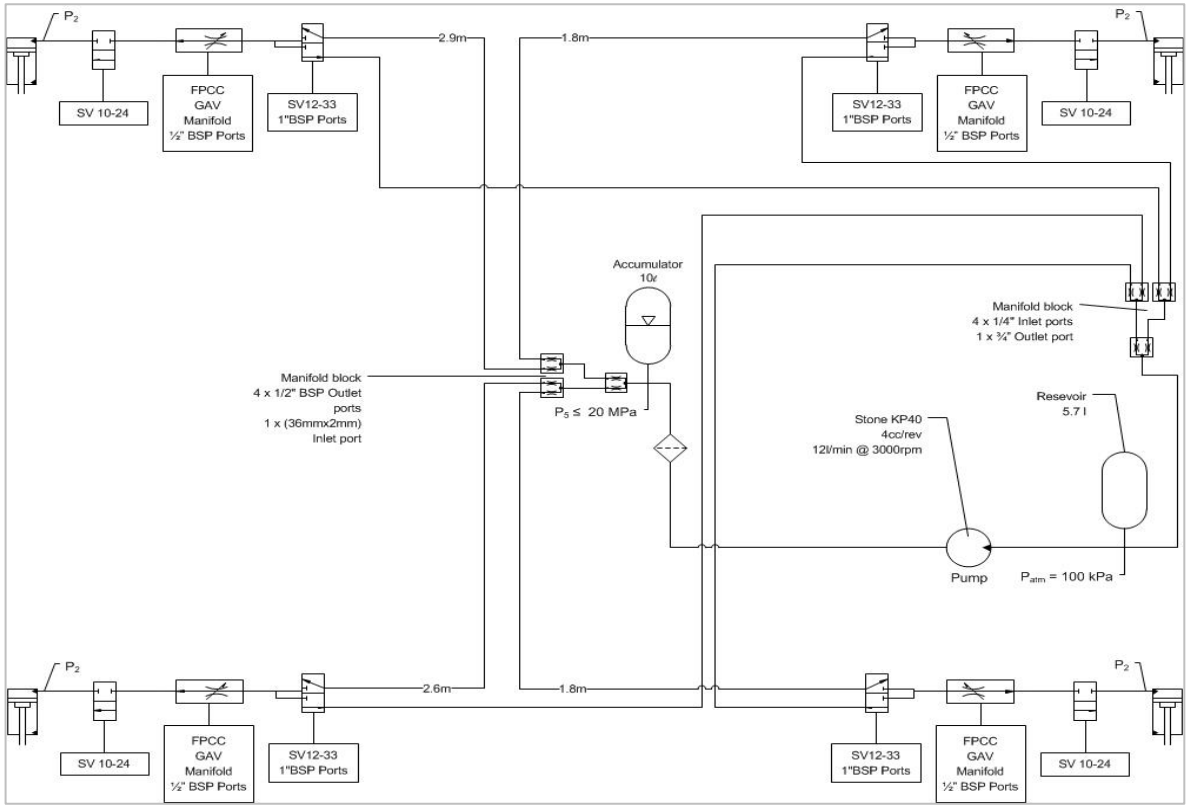

Figure 3.9: Flow diagram of the hydraulic setup in the test vehicle (Van der Westhuizen, 2012)

The algorithm developed by **Van der Westhuizen (2012)** to determine the accumulator pressure based on the Benedict Webb Rubin real gas equation was appropriated in the simulation model for the present study.

With the requirement of a mathematical model fulfilled, the manoeuvres used to investigate rollover are discussed in the next section.

3.2 Rollover Prevention Strategy

Since rollover is a complex mechanism that is hard to predict, the construction of a rollover prevention system requires the consideration of a number of parameters. In this study, the parameters related to rollover are the CG height of the vehicle, the suspension characteristics, the body roll angle, the body roll rate, the body lateral acceleration, the body yaw rate, the vehicle speed and the front wheels steering angle.

It is proposed to lower the height of the CG of the vehicle by using slow active control of the semi-active $4S_4$ suspension system. As discussed in chapter 3.1.2 above, the CG height in the test vehicle can be lowered by extracting oil from the suspension system and raised by adding oil to the suspension units. The $4S_4$ is a single-acting cylinder creating non-linearity in cornering for height adjustment. The control system will lower the CG height as a function of roll angle, roll rate, lateral acceleration, and longitudinal velocity and steer angle. The control system should calculate a CG height that reduces the roll angle of the vehicle and eliminates wheel lift off. The vehicle should hug the ground during cornering. The lowering of the vehicle will also act as feedback to the driver to acknowledge that the vehicle is close to the limit of possible rollover.

In steady state cornering, soft suspension characteristics (soft spring and low damping) allow the tyres to maintain ground contact at larger lateral accelerations. However, in dynamic manoeuvres,

the body roll inertia overshoots the vehicular roll angle and thus hard suspension characteristics (hard spring and high damping) would be better suited. From simulations, **Uys (2007)** determined that the greatest influence on the vehicle's behaviour was the roll centre height and suspension nonlinearity. With regard to the suspension characteristics, increasing the front roll stiffness adds to understeer in the limit of cornering. This could add to rollover prevention. **Uys (2007)** found though simulation that, in a turn, the test vehicle tended to extend on the outer wheels more than compress on the inner wheels. This will impact the roll angle of the vehicle.

Rollover can be initiated by the driver reacting in a way that causes the vehicle to overturn due to a combination of excessive speed and steering inputs. The prevention strategy should therefore consider the speed and steering input given to the vehicle.

Maintaining the F_{zi} (vertical load on the inside wheels) at half the weight of the vehicle in the presence of lateral acceleration can be done by changing the road elevation angle φ. This elevation principle may be applied to the suspension heights. The angle to maintain the weight distribution is **(Gillespie, 1992)**:

$$\boldsymbol{\theta = \frac{a_y}{g}} \qquad \textbf{Equation 3-3}$$

Thus this angle is used to lean the vehicle into corners in an attempt to reduce rollover. In cornering, the aim is to shift the vehicle's CG inside the vehicle's centreline or as close as possible. This will aid the moment acting against the centrifugal force acting on the vehicle. However, shifting of the CG too fast should be avoided. This reflects on the importance of reducing body roll outwards in the corners. If the CG of the vehicle can be lowered such that the most weight can be transferred to the inner front wheel, the vehicle will understeer more and reduce the rollover effects.

In the rollover phase, lateral acceleration acts at the CG, together with tyre lateral forces acting on the outer wheels to overturn the vehicle. Thus the limits of lateral acceleration should be known. Lateral acceleration of a vehicle at normal operation is below $6m/s^2$ **(Botha, 2011)**.

For steady state rollover on a flat road, the maximum lateral acceleration may be determined as follows **(Dukkipati et al., 2008)**:

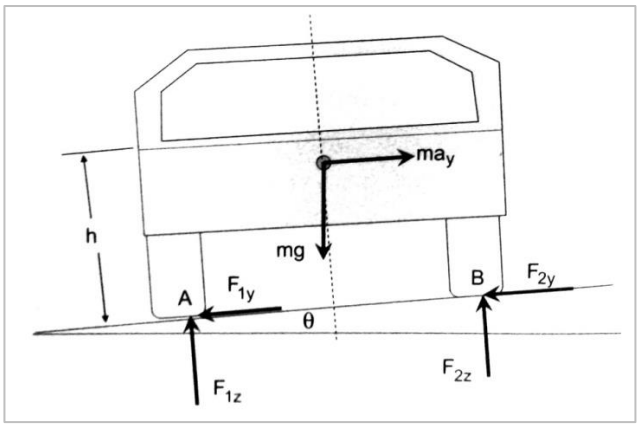

Figure 3.10: Rigid vehicle model (Dukkipati et al., 2008)

First order estimate of the static rollover threshold:

$$\frac{a_y}{g} = \frac{t}{2h} + \varphi$$ **Equation 3-4**

where:

- a_y lateral acceleration threshold
- t is the track width
- h is the vehicle's centre of gravity height
- φ is the bank angle of the road

From the rigid vehicle model, the lateral acceleration threshold is determined for the test vehicle as:

$$a_y = 0.7262g = 7.124\ m/s^2$$

The tracking of rollover should be able to differentiate between steady-state and transient roll behaviour. Thus it is essential that there be a defined degree of rollover, such as a rollover index.

3.2.1 Roll Angle Estimation

Before a rollover detection strategy can be defined, the roll angle of the vehicle body must be estimated. As discussed in chapter 2.2, roll angle must be estimated using various vehicle parameters, since there is no direct method of measuring it accurately. For comparison purposes, the integrated roll rate was used for the simulations. The roll angle in the control system uses a combination of suspension displacements, lateral acceleration and roll rate to determine the roll angle. An estimate is derived for each parameter as defined in the literature study.

Roll angle estimation from lateral acceleration:

$$\theta_{a_y} = \frac{Mh_1 a_y}{K_f + K_r - Wh_1}\left(\frac{180}{\pi}\right)\ [degrees]$$ **Equation 3-5**

where:

- M is the vehicle's mass
- K_f is the front roll stiffness
- K_r is the rear roll stiffness
- W is the weight of the vehicle
- a_y is the lateral acceleration
- h_1 is the height difference between the CG and the roll centre
- θ_{a_y} is the estimation of the roll angle from lateral acceleration

Roll angle estimation from suspension displacement:

$$\theta_Z = \left(\frac{tan\left(\frac{Z_{FR}-Z_{FL}}{t}\right) + tan\left(\frac{Z_{RR}-Z_{RL}}{t}\right)}{2}\right)\left(\frac{180}{\pi}\right)\ [degrees]$$ **Equation 3-6**

where:

- Z_{FR} is the front right displacement height
- Z_{FL} is the front left displacement height
- Z_{RR} is the rear right displacement height
- Z_{RL} is the rear left displacement height
- t is the track width
- θ_Z is the estimation of the roll angle from the suspension displacements

Roll angle estimation from roll rate:

$$\boldsymbol{\theta_{\dot{\theta}} = \int_{t_i}^{t_f} \dot{\theta} dt \ [degrees]}$$ **Equation 3-7**

where:

- $\dot{\theta}$ is the measure roll rate
- $\theta_{\dot{\theta}}$ is the estimation of the roll angle from integration of the roll rate

If the estimated roll angle is less than 8 degrees for which the suspension displacement and lateral acceleration estimates are accurate, the average of the two is used as the roll angle estimation. If the estimated roll angle exceeds 8 degrees, the estimation from the integrated roll rate is used to define the roll angle.

3.2.2 Rollover Detection Strategy

Before a prevention strategy can be implemented, it is important to differentiate the degree of rollover propensity. This is done via a rollover detection system.

The rollover detection system used in the rollover prevention control system uses roll angle, roll rate, lateral acceleration, vehicle speed and steering angle at the kingpin or front wheels to detect the degree of rollover. The detection system makes use of the measured vehicle parameters and their thresholds to report a rollover index. The index ranges from zero to one, where zero indicated no risk of potential rollover and one indicated definite rollover. The rollover index reports an average rollover threat with regard to the measured parameters.

For this study, the rollover thresholds are determined from step-steer manoeuvre simulations with the mathematical model in the ride comfort mode and constant ride height, this mode was observed to be highly prone to rollover tendencies. The step-steer manoeuvre results are discussed in greater detail in chapter 4.2.2.

The maximum body roll angle threshold is determined from the maximum body roll angle obtainable before vehicle rollover occurred.

$$\theta_{threshold} = 14 \ degrees$$

The maximum body roll rate threshold is determined from the maximum body roll rate obtainable before vehicle rollover occurred.

$$\dot{\theta}_{threshold} = 27 \ degrees/sec$$

The maximum body lateral acceleration threshold is determined from the maximum body lateral acceleration obtainable before vehicle rollover occurred.

$$a_{y(\max)} = 7.25 \ m/s^2$$

This is in close correlation to the analytical threshold for lateral acceleration in steady-state rollover on a flat road.

To include excessive speeds for a particular steering angle, the speeds at which rollover occurred (for the step-steer manoeuvre simulations) are plotted verse their respective steer angles.

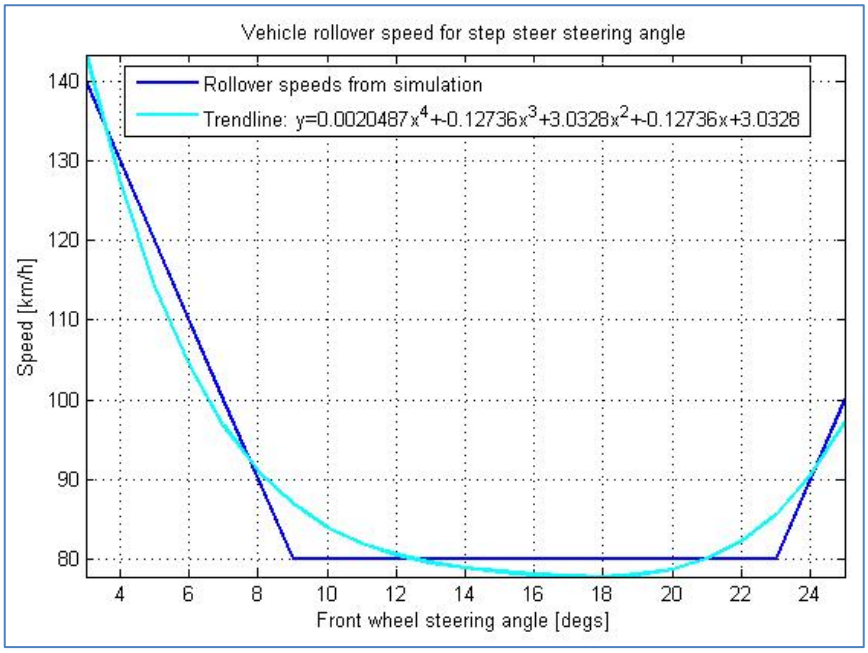

Figure 3.11: Vehicle rollover speed for step-steer steering angle

The speed thresholds for various steering inputs are recorded for step-steer manoeuvre simulation. A polynomial trend line of the fourth order was fitted to the data to evaluate the speed thresholds at any given steer angle.

Trend line:

$$\boldsymbol{Steer\ and\ speed\ index} = \mathbf{0.0020487}\boldsymbol{\delta}^{\mathbf{4}} + \mathbf{0.12736}\boldsymbol{\delta}^{\mathbf{3}} + \mathbf{3.0328}\boldsymbol{\delta}^{\mathbf{2}} + \mathbf{0.12736}\boldsymbol{\delta} + \mathbf{3.0328} \quad \textbf{Equation 3-8}$$

The steering angle is used as an input into the trend line and the speed threshold is obtained as the output. This gives an estimate for the speed that would result in rollover for a given steering angle input during a simulated step-steer manoeuvre.

The final index becomes a combination of the four thresholds. Each threshold makes an equal contribution to the rollover index.

$$\boldsymbol{Rollover\ index} = \left[\frac{\left|\frac{\boldsymbol{\theta}}{\boldsymbol{\theta_{max}}}\right| + \left|\frac{\dot{\boldsymbol{\theta}}}{\dot{\boldsymbol{\theta}}_{\boldsymbol{max}}}\right| + \left|\frac{\boldsymbol{a_y}}{\boldsymbol{a_{y(max)}}}\right| + \left|\frac{\boldsymbol{V}}{\boldsymbol{steer\ and\ speed\ index}}\right|}{\mathbf{4}}\right] \quad \textbf{Equation 3-9}$$

where:

- θ is the body roll angle
- $\dot{\theta}$ is the body roll rate
- a_y is the lateral acceleration
- V is the vehicle speed

The rollover index derived above is not derived from any equation of motion, but is rather a comparison derived from mathematical simulations of how close the vehicle is to a combination of limits. Thus, to determine its validity, it was compared in the simulations to the Dynamic Stability Index (DSI)(described in chapter 2.3.4) and the Rollover Prevention Energy Reserve (RPER) discussed

in chapter 2.3.5.It is noted that if V≠0 (e.g. for steady-state straight driving), then the rollover index ≠ 0.

3.2.3 Rollover Control Strategy 1

Being able to detect potential rollover and the degree of severity allows for the design of a rollover prevention system that can implement prevention methods at various levels of potential rollover. This session discusses two main strategies investigated.

In the first method proposed for preventing rollover, the algorithm consisted of differentiating between steady-state and dynamic driving. Thus the rollover index was utilised to calibrate between the two modes. The detection algorithm is presented in Figure 3.12:

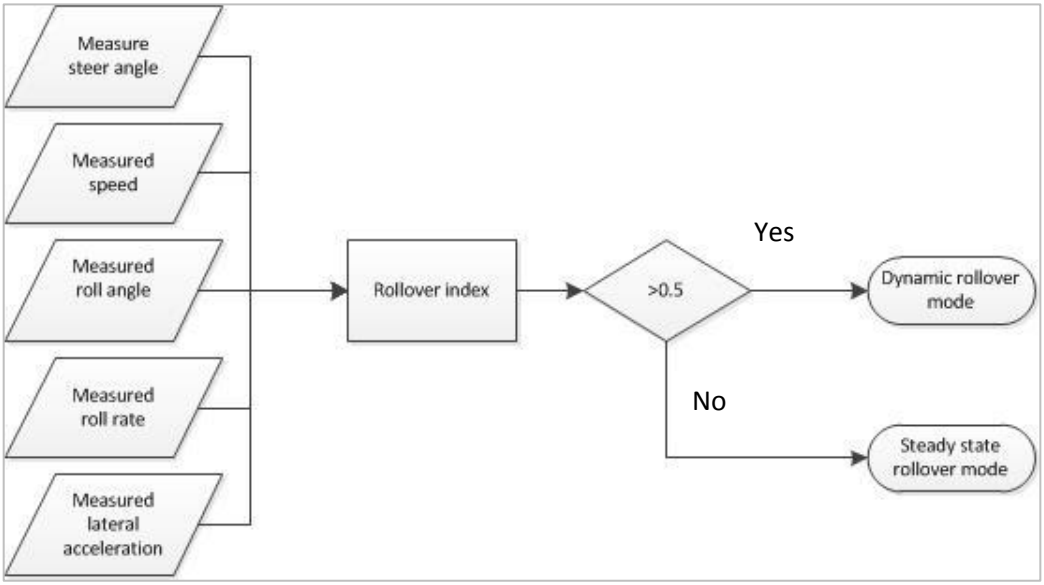

Figure 3.12: Rollover detection flow chart

The index uses the inputs and their respective thresholds (determined from step-steer simulations) to scale the severity of rollover from zero to one, where zero represents no possibility of rollover and one, certainty of rollover. The algorithm differentiates dynamic rollover from steady-state rollover when the defined rollover index exceeds the value of 0.5. This value represents the rollover index with a safety factor of 2.

In steady-state driving, the suspension is set to ride comfort mode, thus low damping and soft spring characteristics are used. In the case of steady state cornering, the algorithm detects the side defined as the inner and outer vehicle track from the direction of the lateral acceleration. The aim of the steady state driving mode is to maintain the minimum roll angle so that the vehicle remains level to the ground as well as to reduce ride height. The desired ride height is adjusted proportionally to the speed of the vehicle. Hydraulic fluid is added or removed by opening values to adjust the ride height. The pressure drop across the values is used to determine the flow rates of the hydraulic fluid during height adjustment. The pressure in the strut is measured as well as the pressure in the accumulator to obtain the pressure drop. If the measured suspension displacement varies from the desired suspension displacement, within in a tolerance range of 10%, hydraulic fluid is either added or removed from the struts until the desired height level is achieved.

To reduce the constant adjustment of the suspension units due to road irregularities and inertial effects on the vehicle, a low-pass filter is used to filter the suspension displacement and the roll

angle. To avoid overshoot in height adjustment, another low-pass filter with a slightly higher frequency is then used to filter the suspension displacement and roll angle. As noted in chapter 2.5, **Bauer (2011)** recommends for levelling control a proportional controller with a dead-band great enough to account for disturbances and that sufficient suspension travel is allowed. If the low-pass filters are set too high, the system will have false activations. However, if too low, the control compensation will be too slow. **Bauer (2011)** recommended a 6 second low-pass filter while the levelling system is inactive and a 0.8 second low-pass filter while the system is active. These signal filtering periods were applied in the rollover prevention algorithm.

If there is still a significant roll angle and roll rate in the defined steady-state of the control algorithm, the suspension damping is switched from low damping to high damping. This aids to absorb and dissipate rotational energy acting on the vehicle, reducing rollover risk. The struts are lowered in a manner that the vehicle's roll angle is within a tolerance of 10% of the desired roll angle, where the desired roll angle is determined from the lateral acceleration. However the desired roll angle becomes saturated at 4 degrees if the roll direction is changed suddenly, i.e.:

$$\boldsymbol{\varphi = \frac{a_y}{g}\ for\ \varphi} < 4\ degrees \qquad \textbf{Equation 3-12}$$

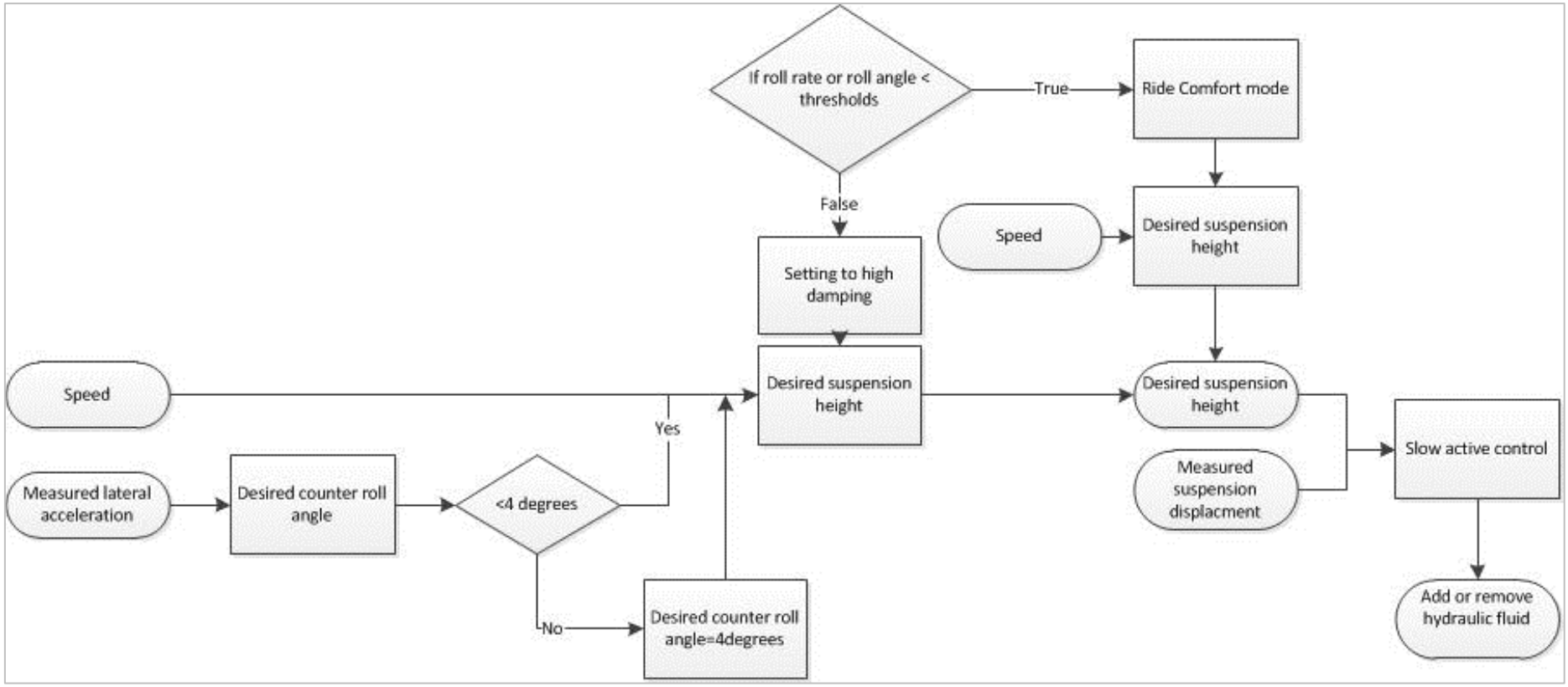

Figure 3.13: Rollover prevention strategy 1, steady state rollover mode algorithm

For rollover index ratings over 0.5, the dynamic rollover driving mode is initiated. This mode aims to reduce rollover risk from larger moments acting to overturn the vehicle. Thus the suspension settings are adjusted for increased stability. The damping characteristics of all four struts are set to high damping to absorb and dissipate maximum roll energy. As noted in chapter 2.4.3, **Uys (2007)** recommended using a soft spring characteristic and a high damping characteristic to allow for greater energy dissipation in his study of off-road vehicular rollover. This recommendation was utilized in the control system. In an attempt to reduce the yaw moment on the vehicle, which contributes to vehicle rollover, the front outer suspension strut of the vehicle was set to a high stiffness characteristic. This aids the understeer characteristic of the vehicle and lowers the yaw motion.

The suspension levelling in the dynamic mode aims to keeps the vehicle level by adding or removing hydraulic fluid from the struts. The strut heights are compared to one another (left side to right side) and if there is a difference greater than 50mm, the higher strut is drained and the lower strut inflated until they are within the tolerance range.

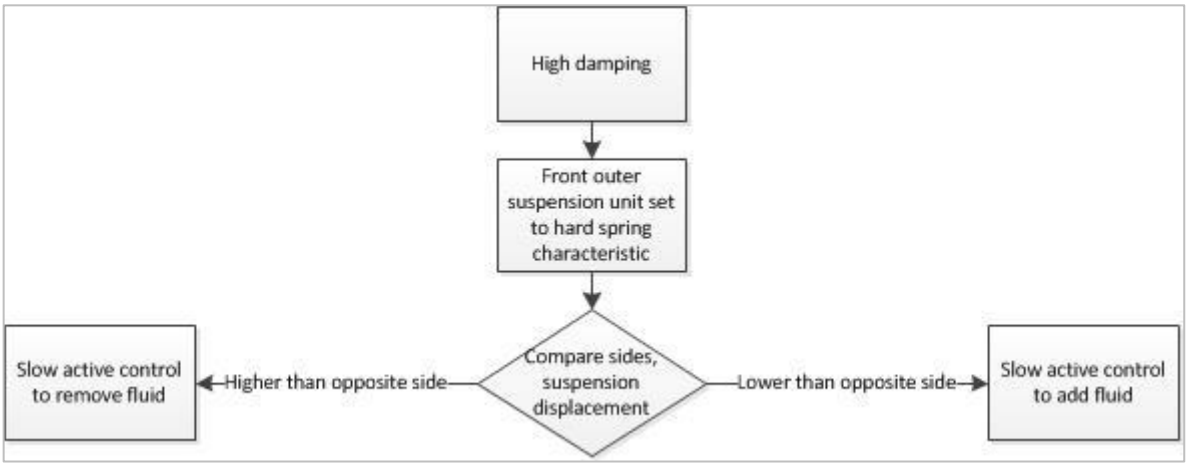

Figure 3.14: Rollover strategy 1, dynamic rollover mode algorithm

Although this strategy greatly increased the speed at which the vehicle could perform the Fishhook 1B manoeuvre, rollover still occurred, which was undesirable.

This control system comprised numerous iterations to improve rollover prevention. Such iterations considered various other suspension setting configurations, various dead-bands and various levels of driving modes. However, the complex nature of rollover would require numerous computational expensive optimisation iterations for even the slightest improvements and thus it was decided to incorporate a PID (Proportional Integral Derivative) controller to control the desired suspension height.

3.2.4 Rollover Control Strategy 2

The final iteration and so-called second control strategy is based on a similar structure as the first control strategy. The major differences shall be discussed.

The system control is done by the PID controller. The control is applied individually to each suspension strut. The error value is defined as the difference between the measured suspension displacement and the desired displacement.

$$\boldsymbol{MV(t) = K_P e(t) + K_I \int_0^t e(\tau) d\tau + K_D \frac{d}{dt} e(t)} \quad \textbf{Equation 3-13}$$

$$\boldsymbol{e(t) = z_{desired} - z_{actual}} \quad \textbf{Equation 3-14}$$

where

- v is the vehicle speed in [km/h]
- $MV(t)$ determines the ideal hydraulic fluid adjustment (Manipulated variable)
- $e(t)$ is the error value
- K_P is the proportional gain
- K_I is the integral gain
- K_D is the derivative gain
- $z_{desired}$ is the desired strut displacement
- z_{actual} is the measure strut displacement

The desired height change is a function of vehicle speed and lateral acceleration. The longitudinal speed component of the desired height change is defined as:

$\boldsymbol{if}\ (\boldsymbol{Speed} <= 30\ km/h)$

$\boldsymbol{z_{desired\ (Speed)} = 0}$

$\boldsymbol{elseif}\ (\boldsymbol{30 km/h} < Speed <= 80 \boldsymbol{km/h})$

$\boldsymbol{z_{desired} = -0.0016 * (Speed(km/h)) - 30)\ [m]}$

$\boldsymbol{else}$

$\boldsymbol{z_{desired\ (Speed)} = -0.08\ [m]}$

The lateral acceleration component of the desired height change acts to lean the CG to the inner wheels:

$$\boldsymbol{z_{desired\ (a_y)} = (\pm \frac{b}{2} \sin\left(\frac{a_y}{9.81}\right))} \quad \textbf{Equation 3-15}$$

$$\boldsymbol{z_{desired} = z_{desired\ (Speed)} + z_{desired\ (a_y)}} \quad \textbf{Equation 3-16}$$

where

- b is the lateral distance between struts
- a_y is the lateral acceleration

The second term $(\pm \frac{b}{2} \sin\left(\frac{a_y}{9.81}\right))$ is positive if the strut is define to be on the outer track in cornering and negative for the inner track. The inner and outer tracks are determined from the direction of lateral acceleration. The lateral acceleration is passed thought a low pass filter to remove noise.

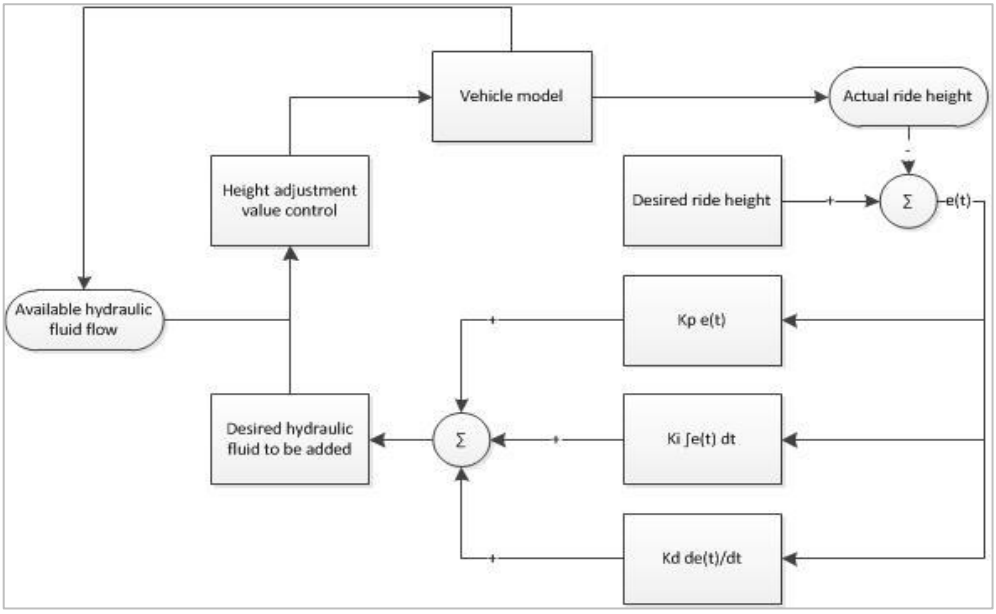

Figure 3.15: PID and value control for rollover control strategy 2

The PID controller uses the difference between desired and actual ride height to calculate the volume of hydraulic fluid to be added to the individual suspension units or the required value opening for that iteration. The available flow rate is then estimated from the suspension unit's pressure difference and the value characteristics. Using the available flow rate with the desired flow rate the value position is then determined to provide the desired hydraulic fluid flow.

The rollover index derived in Equation 3-9 above was used to determine the severity of the rollover on a scale from zero to one. The rollover prevention control operates in two main modes, steady-state rollover prevention mode and the dynamic rollover prevention mode. However for Rollover Control Strategy 2 the dynamic mode range is increased and split into two phases. The steady-state rollover prevention mode is active when the rollover index rating is between [0; 0.35), and the dynamic mode is active for the range [0.35; 1).

In steady state cornering, the $\pm\frac{b}{2}\sin\left(\frac{a_y}{9.81}\right)$ term is limited to 0.035m. This done that the vehicle does not experience adverse effects, such as the cornering direction is changing abruptly. The suspension settings are set to ride comfort, i.e. a soft spring characteristic (GV=0.5) and a low damping characteristic (DSF=0.25).

The PID gains in steady state cornering are set to:

- $K_P = -8e-4$
- $K_I = -6e-4$
- $K_D = -8e-4$

This applies to all four struts.

In the dynamic roll prevention mode, the $(\pm\frac{b}{2}\sin\left(\frac{a_y}{9.81}\right))$ term is limited to an absolute maximum of 0.00881m. The dynamic roll prevention mode is subdivided into two sections. The first is in the rollover index rating range of [0.35; 0.5) and the other in the range of [0.5, -1].

For the first dynamic range, the PID gains in dynamic cornering are set to:

- $K_P = -8e-4$
- $K_I = -12e-4$
- $K_D = -8e-4$

This is applies for all strut except the front outer one which has the gains

- $K_P = -8e-5$
- $K_I = -12e-5$
- $K_D = -8e-5$

The suspension characteristics in the first dynamic range is set to high damping for all strut and soft spring characteristics for all struts except the outer front strut which has a hard spring stiffness characteristic. This is done to remove rotational energy. In dynamic mode, it is best that the vehicle remains as level as possible to avoid rollover from a sudden change in direction. The suspension displacement is filtered to avoid false activations from sudden suspension disturbances. To reduce suspension displacement overshoot from the control system, a low pass filter with a higher frequency is used when the suspension displacement adjustment is active compared to when it is inactive.

For the second range of the dynamic rollover control (rollover index rating =>0.5), the suspension is set to handling mode for all of the suspension units. When the control system is switched from the ride comfort mode to the handling mode, it should be noted that the gain or hydraulic fluid adjustment is considerably reduced. The PID gains are set to:

- $K_P = -8e-5$
- $K_I = -12e-5$
- $K_D = -8e-5$

This ensures that the vehicle has maximum handling capacities together with CG height reduction.

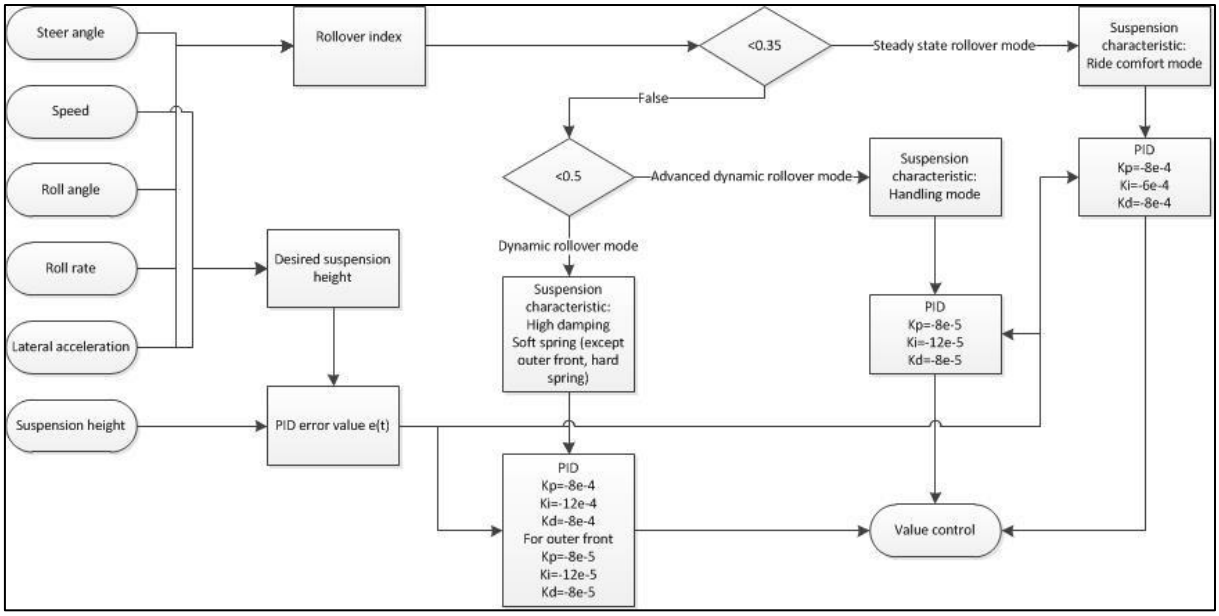

Figure 3.16: Basic flow diagram of rollover control strategy 2

This control strategy includes a sampling time of 30ms to account for valve response times. This is incorporated in the algorithm by setting the valve opening at a constant position for the duration of the sampling time. Various valve sample times were investigated. The faster response times gave the

best results. A sample time of 25ms would be preferable; however, the valves on the test vehicle have a minimum sample time of 30ms **(Van der Westhuizen, 2012)**. **Van der Westhuizen (2012)** recommended using a sampling time of twice the minimum sampling time. The 60ms sampling time was investigated and was observed to be sufficient for small suspension displacement divergences from the desired suspension displacement. However, for large divergences, such as those seen at large displacements, the sampling time causes the PID control to diverge, draining the maximum possible oil from the struts. Although this aids rollover prevention, it diverges from the purpose of a control system, which is to have a desired and predictable system response.

The maximum available flow rates are a function of accumulator pressure, atmospheric pressure and suspension strut pressure and are not constant. This affects height adjustment considerably, making it a nonlinear function. The lowering capabilities of the inner struts during cornering is reduced as the pressure difference between the strut pressure and the atmospheric pressure is considerably reduced, thus reducing the flow rate of the hydraulic fluid removed from the strut. Raising capabilities of the outer struts is reduced as well, since the strut pressure is increased and the pressure difference between the accumulator pressure and strut pressure decreases. The accumulator pressure does not stay constant either and thus the accumulator must be mathematically modelled. **Van der Westhuizen (2012)** modelled the accumulator using the real gas Benedict Webb Rubin (BWR) equation. **Van der Westhuizen's (2012)** code was used directly with the appropriate inputs to calculate the accumulator pressure in the simulations.

3.3 Conclusion

In this chapter, the mathematical modelling of the Land Rover Defender 110 using the simulation package MSC.ADAMS/View in order to investigate rollover though simulation was reported and explained. The lateral dynamics of the model are the most important with regard to rollover. The model incorporates the suspension system, the vehicle body and tyres. The model is used to perform simulation test manoeuvres to evaluate rollover and improve the response of the vehicle to rollover.

Secondly, the development of a rollover detection and prevention system was discussed in detail as the main focus of this chapter. The system uses the measured inputs of vehicle speed, steering angle, lateral acceleration, roll rate, suspension displacement and suspension pressures together with slow active control to adjust ride height and change suspension characteristics to prevent rollover.

The validation of the mathematical model was made through comparison of experimental determined results. This is discussed in chapter 4. This determines the correction of the mathematical model to the physical test vehicle in terms of how well the results of the model represent reality. The simulation results from the manoeuvres discussed in this chapter are reported in chapter 5.

4 SIMULATION MODEL VALIDATION

This chapter reports on the validation of the mathematical model simulation data when compared to recorded data collected during the test vehicle's execution of the ISO3888 Double Lane Change (DLC) manoeuvre **(International Organisation for Standardisation, 1975)**. Mathematical models seldom represent real systems exactly due to assumptions and model simplifications, but should still provide acceptable accuracy. Hence validation is needed to determine the accuracy and credibility of the mathematical modelling predicting the dynamic responses of the test vehicle. For the purpose of this study, the lateral dynamics of the vehicle are of particular importance and thus the validation correlated lateral acceleration, roll rate, roll angle and yaw rate. Correlation of suspension displacement and suspension forces are also important in order to validate tyre force generation and suspension characteristics. As explained in chapter 3.2.1, the body roll angle of the vehicle is determined by integration of the roll rate and not from direct measurement. The measured vehicle speeds and steering angles were used as inputs for the simulation.

4.1 Experimental Setup

The validation maneuvers were performed at Gerotek, a division of Armscor Defense Institutes SOC Ltd that has a large testing facility where vehicle design and development may be monitored under typical South African conditions **(Armscor Defence Institutes, 2014).** The testing required a relatively large setup with complex recording instrumentation and thus was done by the whole Vehicle Dynamics Group of the University of Pretoria, with the senior members planning and instructing the team. The student under instruction assisted with rigging of the test equipment and installation/fitment of some of the test equipment. The data acquisition was done by the group's senior members

Figure 4.1: VBOX and IMU base station

The transducers listed in Table 4.1 were implemented in the vehicle to record data:

Table 4-1: Parameters measured for vehicle validation

Parameter	Transducer
Vehicle Speed	Racelogic Velocity BOX 3 (VBOX3) Differential Global Positioning System
Vehicle position	VBOX3 DGPS
Vehicle heading	VBOX3 DGPS
Body CG lateral acceleration	Accelerometer (Crossbow 4g)
Body roll velocity	Solid state gyroscope (CRS03)
Body yaw velocity	Solid state gyroscope (CRS03)
Left front suspension displacement	Linear Displacement Transducer (Celesco)
Right front suspension displacement	Linear Displacement Transducer (Celesco)
Left rear suspension displacement	Linear Displacement Transducer (Celesco)
Right rear suspension displacement	Linear Displacement Transducer (Celesco)
Left front suspension force	Pressure Transducer in Suspension strut (Wika)
Right front suspension force	Pressure Transducer in Suspension strut (Wika)
Left rear suspension force	Pressure Transducer in Suspension strut (Wika)
Right rear suspension force	Pressure Transducer in Suspension strut (Wika)
Front steeling angle at wheels	Potentiometer (Celesco)

These were used to record the response of the test vehicle for the validation manoeuvre.

4.2 Test Manoeuvres

Static tests are one of two fundamental methods for predicting or evaluating rollover tendencies. The static stability factor, tilt table ratio, side pull ratio or critical sliding velocities provide simple indications of rollover. The second set of fundamental methods for predicting or evaluating rollover tendencies are dynamic tests where the vehicle is induced to two-wheel lift-off. Static tests lack consideration of the effects of suspension or chassis control systems **(Hac, 2002)**. Thus this study focuses on the dynamic tests. The dynamic test manoeuvres that are investigated in this thesis are the ISO 3888 Double Lane Change manoeuvre, the Step-steer manoeuvre, the Slowly Increasing Steer (SIS) manoeuvre and the NHTSA Fishhook 1B manoeuvre. The SIS manoeuvre is required for the Fishhook 1B manoeuvre.

4.2.1 ISO 3888 Double Lane Change Manoeuvre

The mathematical model requires at least one experimental validation to deem the results from other simulation testing valid. The Double Lane Change manoeuvre was chosen for this purpose and the experimental work and model validation are discussed in this chapter. The Double Lane Change manoeuvre is also used as a secondary test for rollover propensity in the simulation, whereas the primary test for rollover propensity is the Fishhook 1B.

The likelihood of two-wheel lift-off increases with increasing steering angle and vehicle yaw rate in lane change manoeuvres **(Marine et al., 1999)**. The Double Lane Change (DLC) manoeuvre is used to measure the handling and roll sensitivity of a vehicle. It excites almost all dynamics, while providing very little time to reach a steady state. The DLC manoeuvre is illustrated in Fig 4.2. To execute a DLC manoeuvre, the vehicle is driven straight at a particular speed and after two meters the driver releases the throttle. No braking or acceleration is done during the remainder of the test. The driver changes lanes onto a parallel road and then returns. The test run is considered invalid if a marking cone is bypassed or struck. The speed is incremented in 1mph from 35 mph until the runs are no longer valid **(Forkenbrock et al., 2002)**.

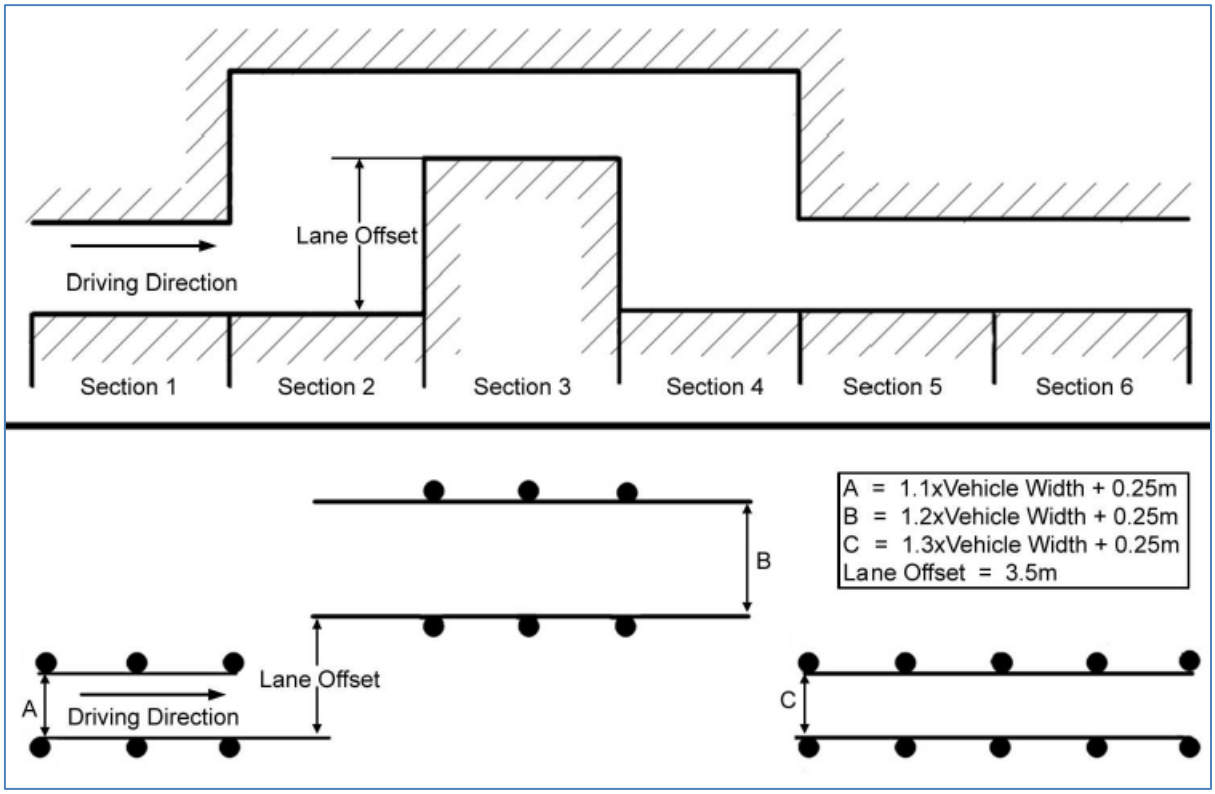

Figure 4.2: ISO 3888 Double Lane Change manoeuvre course dimensions (Botha, 2011)

Table 4-2: ISO 3888 Double Lane Change manoeuvre course section dimensions

Section	Section 1	Section 2	Section 3	Section 4	Section 5	Section 6
Length	15m	30m	25m	25m	15m	15m

For the test vehicle, a DLC at 40km/h was considered the border between linear and nonlinear response; hence, a DLC at 70km/h is considered to be a very nonlinear response of the vehicle **(Botha, 2011)**.

4.2.2 Step-Steer Manoeuvre

The rollover prevention and detection control system was defined using parameters obtained from simulations of a step-steer input manoeuvre. The step-steer manoeuvre is used to define important rollover parameters, namely the roll angle, roll rate, yaw rate, lateral acceleration and wheel lift, in order to determine indications of rollover, as well as to characterise a vehicle with regard to rollover thresholds of the respective parameters. For the purpose of developing a rollover detection algorithm, simulations were used to investigate the response of the vehicle with respect to roll angle, roll rate, yaw rate, lateral acceleration and wheel lift. This was done using step-steering inputs.

The Step-Steer manoeuvre is used investigate the relationship between speed and steer angle. In the Step-Steer manoeuvre, the vehicle speed is kept constantand the vehicle given steering inputs at a fixed angle for a range of steer angles. According to **Jazar (2008)**, a step input is a standard test for examining dynamic system behaviour. In vehicle dynamics, a step input is defined as a sudden change in the steer angle from zero to a nonzero constant value. The transient behaviour of the vehicle may be considered by the input of a step-steer.

The present study does an in-depth investigation on the Step-Steer manoeuvre, using over 230 simulations to acquire data. The results of the Step-Steer manoeuvre are used in defining the limits of the vehicle with regard to rollover. This is done by studying the maximum value of the parameter of interest. Simulations were run for steer angles at the front wheels from 1 to 25 degrees (the maximum steering angle of the test vehicle) at increments of 2 degrees and for speeds from 40 to 140km/h (just above the vehicle's maximum speed of around 130 km/h) at increments of 20 km/h. The simulation starts by allowing the vehicle to get up to entry speed with an acceleration of 2.78 m/s^2. Once the desired entry speed is reached, it is maintained constant for 5 seconds to allow for some settling before the steer input is delivered. The steer input is then held constant for 10 second or until the vehicle overturns.

4.2.3 Slowly Increasing Steer

The lateral dynamics of a vehicle may be characterised by the Slowly Increasing Steer (SIS) manoeuvre. The driver enters the manoeuvre at 50 mph (80 km/h) and maintains the speed throughout the manoeuvre. The steering angle is increased from zero to 270 degrees (3 steering wheel rotations) at a rate of 13.5 degrees per second, held constant for two seconds and thereafter returned to zero at a desired rate. The maximum quasi-steady-state lateral acceleration of the vehicle may be determined from this manoeuvre. The manoeuvre, however, requires considerable testing space and for this reason is not always a physically possibility **(Forkenbrock et al., 2002)**. This makes simulation an ideal investigation method.

According to **Whitehead et al. (2004)** the steering magnitude, based on the vehicle's response, is determined from the steering wheel angle when the vehicle experiences 0.3g lateral acceleration. This steering wheel angle is then used as a multiplication factor for the steering input of the Fishhook manoeuvre.

4.2.4 NHTSA Fishhook Manoeuvre

In order to reduce the rollover propensity of the test vehicle, it is necessary define a method to report the manoeuvre-induced response. The highest speed at which the vehicle can complete the selected manoeuvre without two-wheel lift off is used to define its rollover propensity. According to **Whitehead et al. (2004)** the NHTSA selected the Fishhook to be the primary candidate, which deals with un-tripped on-road rollovers and provides a relative comparison between different vehicles or vehicle configurations:

Table 4-3: Summary of Rollover Resistance Manoeuvre Scores (Forkenbrock et al., 2002)

Assessment Criterion	NHTSA J-Turn	Fishhook 1a	Fishhook 1b	Nissan Fishhook	Ford Path-Corrected Limit Lane Change	ISO 3888 Part 2 Double Lane Change	Consumers Union Short Course Double Lane Change	Open-Loop Pseudo-Double Lane Change
Objectivity and Repeatability	Excellent	Excellent	Excellent	Good	Bad	Bad	Bad	Satisfactory
Performability	Excellent	Good	Excellent	Satisfactory	Satisfactory	Good	Satisfactory	Satisfactory
Discriminatory Capability	Excellent*	Excellent	Excellent	Excellent	Good	Very Bad	Very Bad	Very Bad
Appearance of Reality	Good	Excellent	Excellent	Excellent	Excellent	Excellent	Excellent	Excellent

In this study, the Fishhook 1B was mainly used to define improvement to rollover from the control system implemented. The Fishhook 1B requires an input for the steering magnitude to be used, which is obtained from the Slowly Increasing Steer (SIS).

The steering wheel steer rates are based on the roll angle natural frequency and are fixed at 720 degrees per second. According to **Whitehead et al. (2004)**, the Fishhook 1A manoeuvre (depicted in Figure 4.1) has an initial steering input followed by a steering input in the opposite direction. The vehicle is driven until it reaches a steady speed known as the entrance speed and then the vehicle coasts through the rest of the manoeuvre after the initial steering input has been given. The steering angle input is described as a zero steer angle followed by a steering angle that is specified by 6.5 times the steering angle at which 0.3 g is experience by the vehicle in the Slowly Increasing Steer manoeuvre, at a rate of 720 degrees per second. This angle is then held for a period of 0.250 seconds (known as the dwell time) and then the vehicle is steered in the opposite direction at the same rate and same angle magnitude. This is held for 3 seconds and then returned to a zero steering angle.

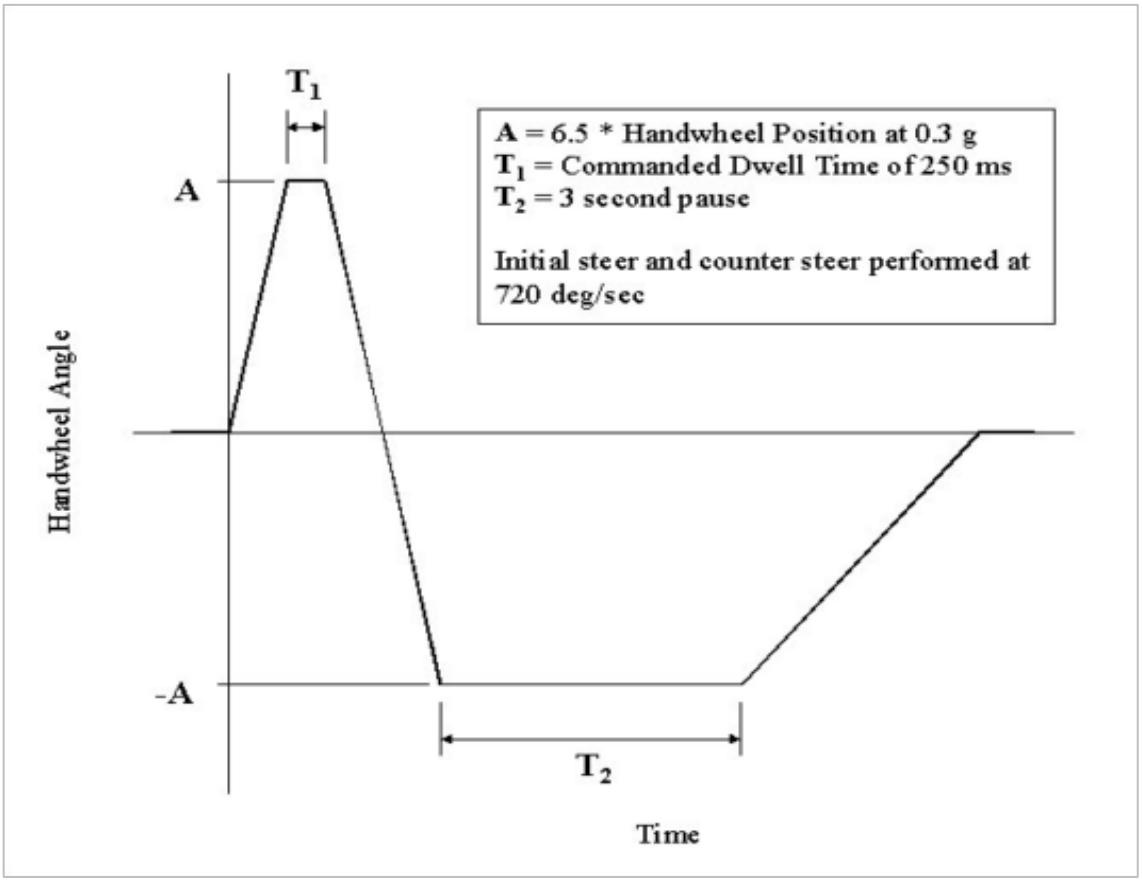

Figure 4.1: Fishhook 1a manoeuvre description (Forkenbrock et al., 2002)

The speed is incremented from 35 mph (56 km/h) to 50 mph (80 km/h) in increments of 5 mph. However, if two-wheel lift-off occurs, the entrance speed reduces by increments of 1 mph. During the Fishhook, if either outrigger touches the ground, the outrigger is raised 0.75 inches and the test is repeated at the same entrance speed **(Forkenbrock et al., 2004)**.

According to **Whitehead et al. (2004)**, the Fishhook 1A is repeatable and easily programmed for an open loop input. The Fishhook 1B requires roll velocity for a closed loop feedback control system and is not as easily done as the Fishhook 1A. The Fishhook 1B (depicted in Figure 4.2) arises from the Fishhook 1A; however, the initial dwell time is varied according to the response of the vehicle. The steering wheel angle magnitudes and rates are chosen in the same manner as for the NHTSA Fishhook 1A, but the dwell time is determined by the roll motion of the vehicle instead of the 250 milliseconds. The dwell time is determined when the roll rate equals or goes below 1.5 degrees per second for the initial steer **(Forkenbrock et al., 2002)**.

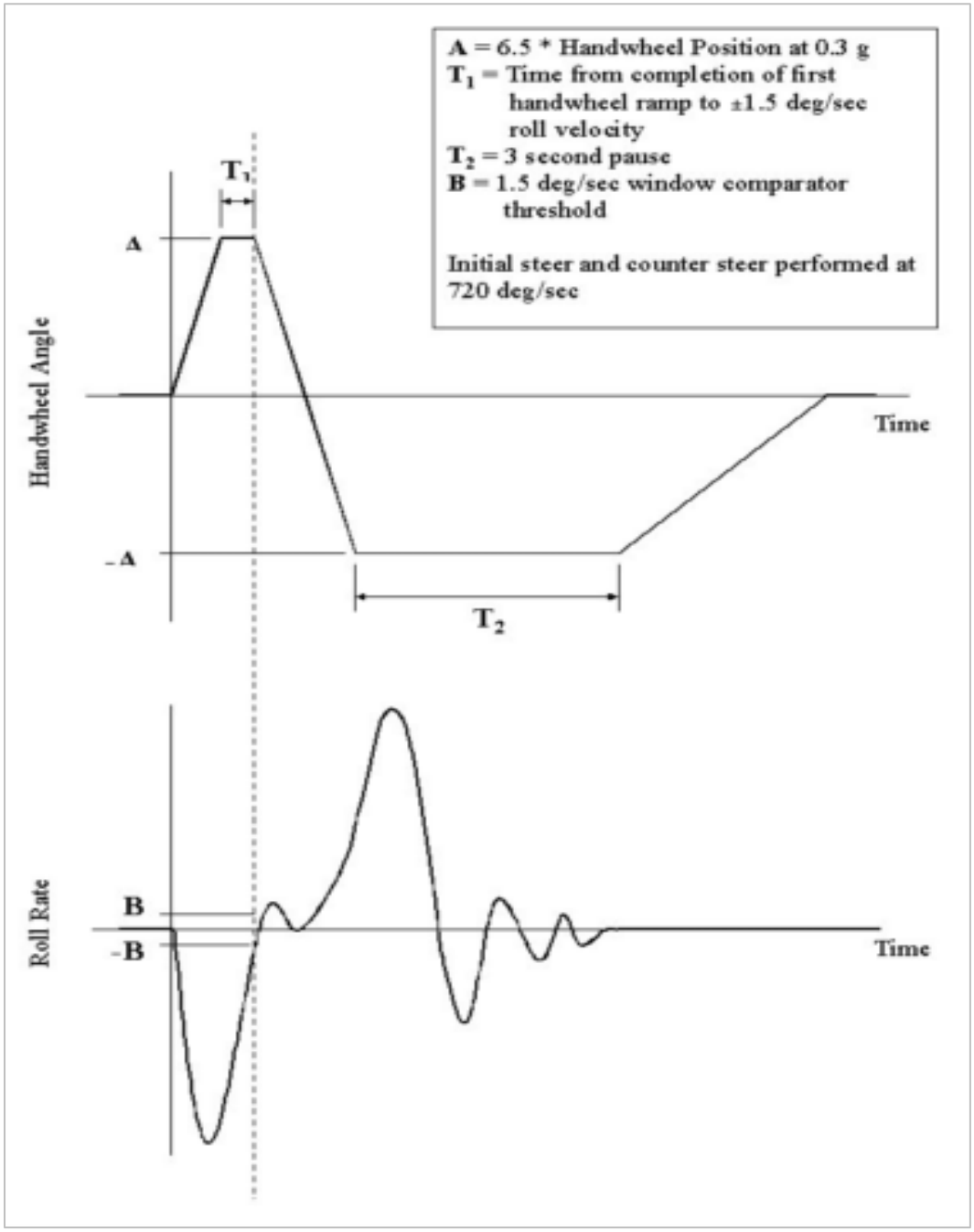

Figure 4.2: Fishhook 1b manoeuvre description (Forkenbrock et al., 2002)

Although the steering rates of the Fishhook manoeuvres are fast, they are considered to be within the capabilities of a driver. The NHTSA consider the Fishhook 1B to be the most effective of the Dynamic Rollover Propensity tests and it is thus known as "NHTSA Road-Edge Recovery Manoeuvre" **(Forkenbrock et al., 2002)**.

In the next section, construction of a rollover prevention system is discussed.

4.3 Validation test

The Fishhook 1B manoeuvre is considered the best validation for studying rollover, but requires large tracks of land to execute it. Since the testing facility did not have sufficient area available, the ISO 3888 DLC manoeuvre discussed in chapter 4.2.1 was performed instead. The manoeuvre was performed at various speeds for two suspension settings. Firstly, the *handling* suspension setting

(Figure 4.3), i.e. hard spring and hard damping, is designed to provide the best vehicle response, but is not always comfortable for the driver.

Figure 4.3: Land Rover Defender 110 Wagon doing a DLC manoeuvre in handling mode

Secondly, in the *ride comfort* setting (Figure 4.4), the suspension units are set to soft spring characteristics using both accumulators, and damping is set to low. This mode (usually the standard vehicle setting) provides optimum comfort over rough terrain by isolating the driver from road inputs.

Figure 4.4: Land Rover Defender 110 Wagon doing a DLC manoeuvre in ride comfort mode

It is evident from the photos that the vehicle performed the DLC manoeuvre more easily with less tilt of the outriggers when in the handling mode than in the ride comfort mode. A good mixture of displacements, velocities and accelerations were obtained from the measured data.

Before the results of the simulations are discussed, the method used to evaluate the degree of validations is explained.

4.4 Validation Metric Based on Relative Error

The degree of validation was determined from the relative error base validation metric. The relative error (RE) compares the predicted value (p) to the experimentally measured value (m) **(Kat, 2012)**:

$$\boldsymbol{RE} = \left|\frac{\boldsymbol{p}-\boldsymbol{m}}{\boldsymbol{m}}\right| \qquad \textbf{Equation 4-1}$$

$$\%\boldsymbol{RE} = \left|\frac{\boldsymbol{p}-\boldsymbol{m}}{\boldsymbol{m}}\right| * \mathbf{100} \qquad \textbf{Equation 4-2}$$

where:

- RE is the relative error
- p is the predicted value from the mathematical model
- m is the experimentally measured value
- $\%RE$ is the percentage relative error

If the predicted value approaches the measured value, the limit of the RE approaches zero. If the predicted value is much greater than the measured value, the RE approaches positive infinity. If the predicted value is much less than the measured value, the RE approaches negative infinity. This method provides a useful way to validate data and compare predictive models, but presents difficulties when periodic systems are compared or when values are equal to or near zero, since these situations cause non-constant %RE over the independent variables (different %RE values for each data point), NaN's ($\frac{0}{0} - not\ a\ number$) and InF's ($\frac{1}{0} - infinite\ values$) **(Kat, 2012)**.For non-constant %RE over the independent variables, one may either determine the probability of %RE being below the mean %RE ($m\%RE^m$) or below a specified %RE ($m\%RE^s$). The specific %RE is usually used when the predictive model is required to have a specified accuracy requirement **(Kat, 2012)**, which is not the case in this study. Hence, the mean %RE was taken as the validation metric.

The mean %RE is calculated using histograms by plotting %RE frequency against each %RE. A cumulative histogram of %RE frequency against %RE is used to determine the probability of all the %RE values being less than the mean %RE **(Kat, 2012)**.

With a validation metric in place, comparison of the measured and simulated data was done for each of the two suspension modes to validate the mathematical model.

4.5 Simulation Validation

The mathematical model was given two measured inputs from the experimental data, namely the longitudinal speed and the front wheel steering angle. Simulations were run at 1000Hz, i.e. at a time step of 0.001 seconds, to match the sampling frequency of the data recordings during the test vehicle runs. Validation runs were done for a range of input speeds. For the sake of conciseness, only the 56.5 km/h run data are discussed in this chapter in detail, with data for higher speeds given in Appendix 7.3. As discussed above, the %RE reports excessively large signals or values at or near zero. This was observed for the yaw rate, roll rate, roll angle, suspension displacements and lateral acceleration comparisons and thus only the mean %RE of the peaks were used for the validation metric instead of the mean %RE for the full interval. Since the steering angle and longitudinal speed are inputs, there is zero difference between simulation and experimentally measured values.

4.5.1 Validation in Handling Mode

The results of the vehicle path validations for the 56.5km/h run in the handling suspension mode (are presented in Figure 4.5(vehicle path validations).

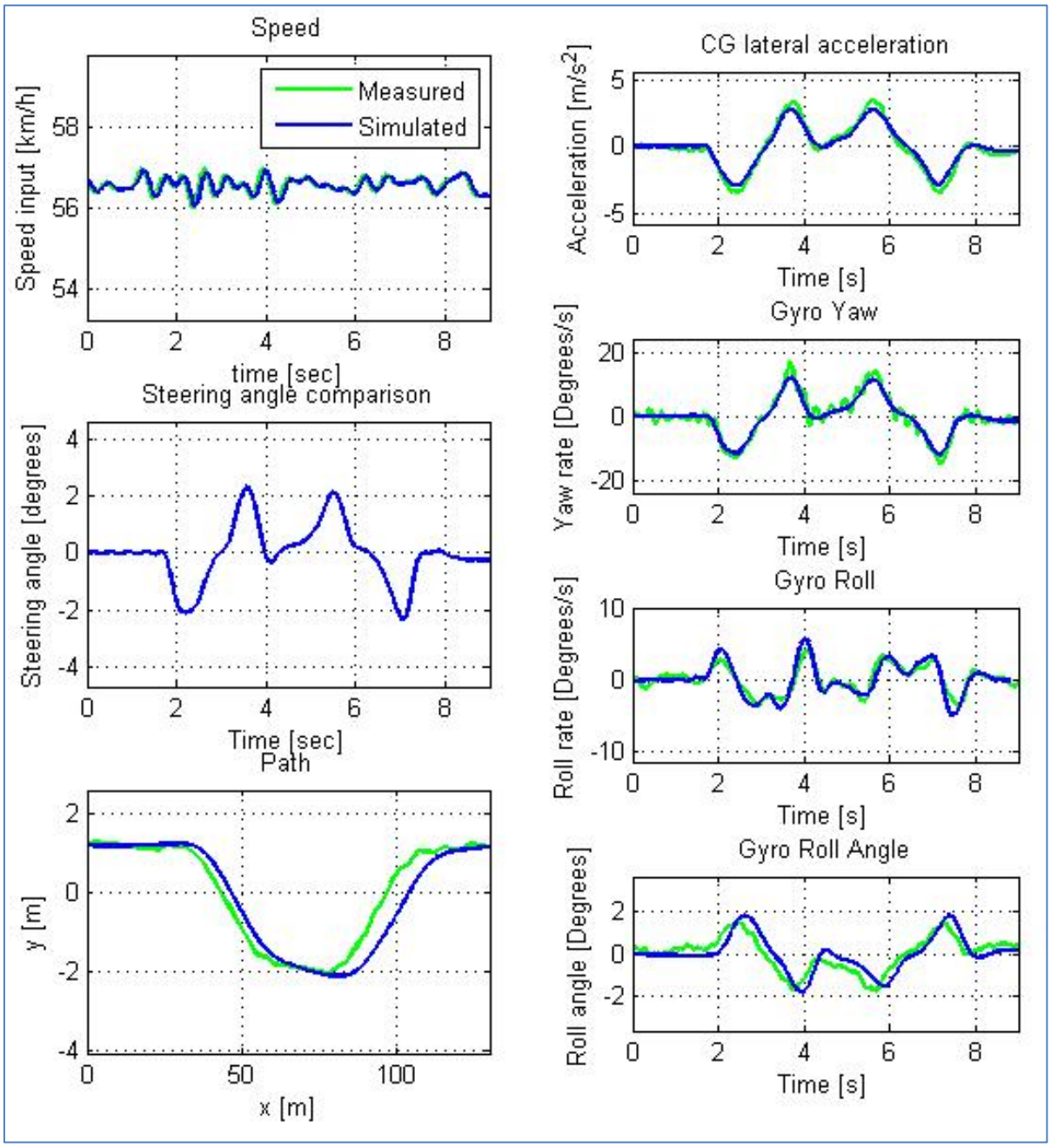

Figure 4.5: Vehicle path for 56.5 km/h validation test on handling suspension mode (speed, steering angle, path, lateral acceleration, yaw rate, roll rate and roll angle)

The mathematical model slightly underestimates the lateral acceleration and yaw rate responses of the vehicle, whereas the roll rate and roll angle are slightly over estimated. The calculated peak %RE values are given in Table 4.4:

Table 4-4: Peak %RE for handling mode

Parameter	Mean Peak %RE
Lateral acceleration	13 %
Roll rate	20 %
Roll angle	12 %
Yaw rate	15 %

The greatest deviation is noted in roll rate prediction. The correlations for suspension displacements and forces are presented in Figure 4.6:

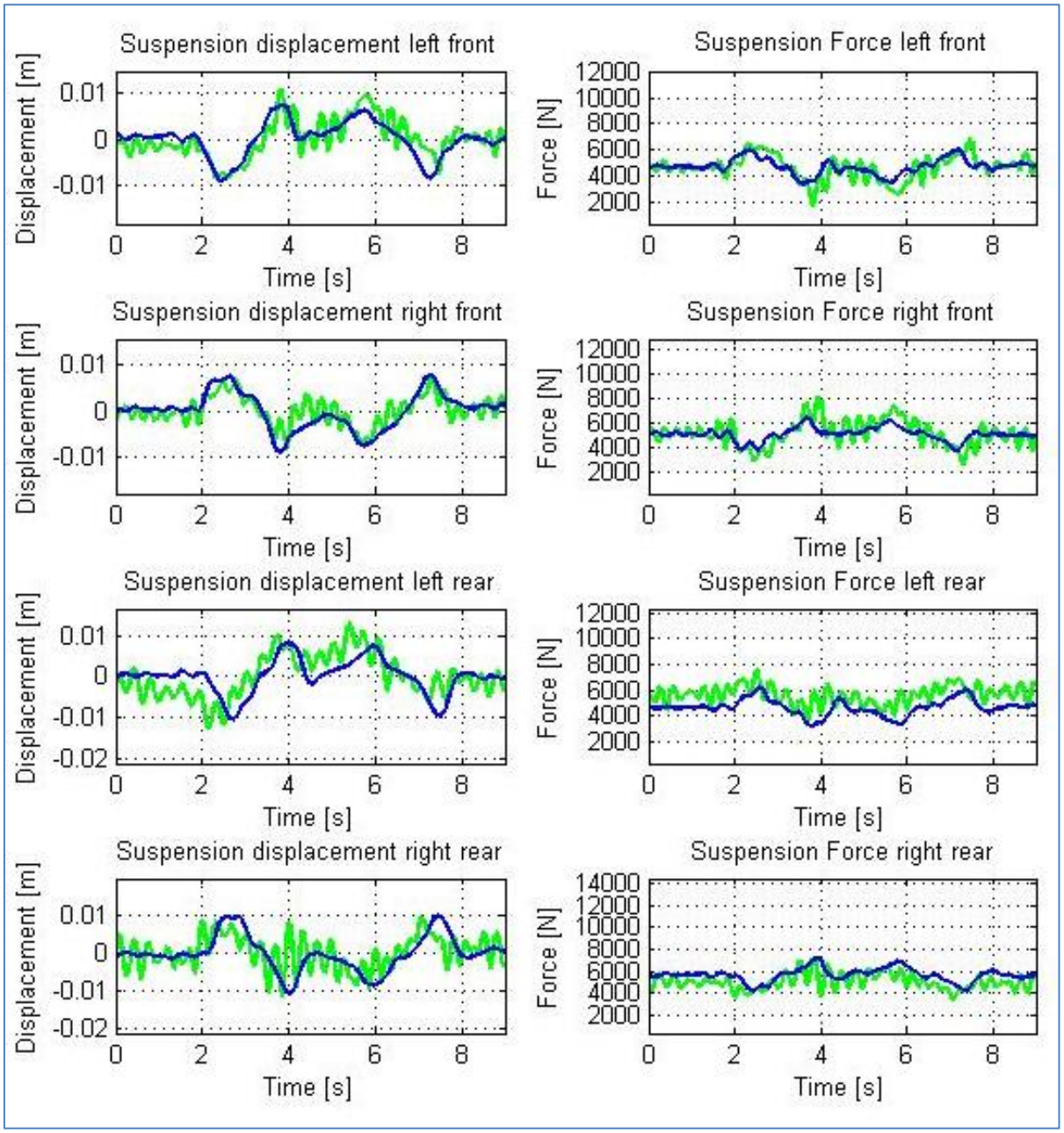

Figure 4.6: Suspension displacements and forces for 56.6 km/h validation test in handling mode

The validation metrics are tabulated in Table 4.5:

Table 4-5: Suspension validation metrics for 56.5 km/h validation test in handling mode

Strut	Mean Peak %RE suspension displacement	Mean %RE suspension forces
Front left	23 %	$m\%RE^m = 9\ \%\mathrm{P}(69\ \%)$
Front right	8 %	$m\%RE^m = 8\ \%\mathrm{P}(72\ \%)$
Rear left	27 %	$m\%RE^m = 17\ \%\mathrm{P}(58\ \%)$
Rear right	7 %	$m\%RE^m = 13.\%\mathrm{P}(58\ \%)$

The suspension displacement and forces correlate well on the right and less on the rear left suspension unit.

4.5.2 Validation in Ride Comfort Mode

The same procedure was followed for the vehicle in the ride comfort mode. The vehicle path correlations for the DLC manoeuvre at 56.6 km/h are presented in Figure 4.7:

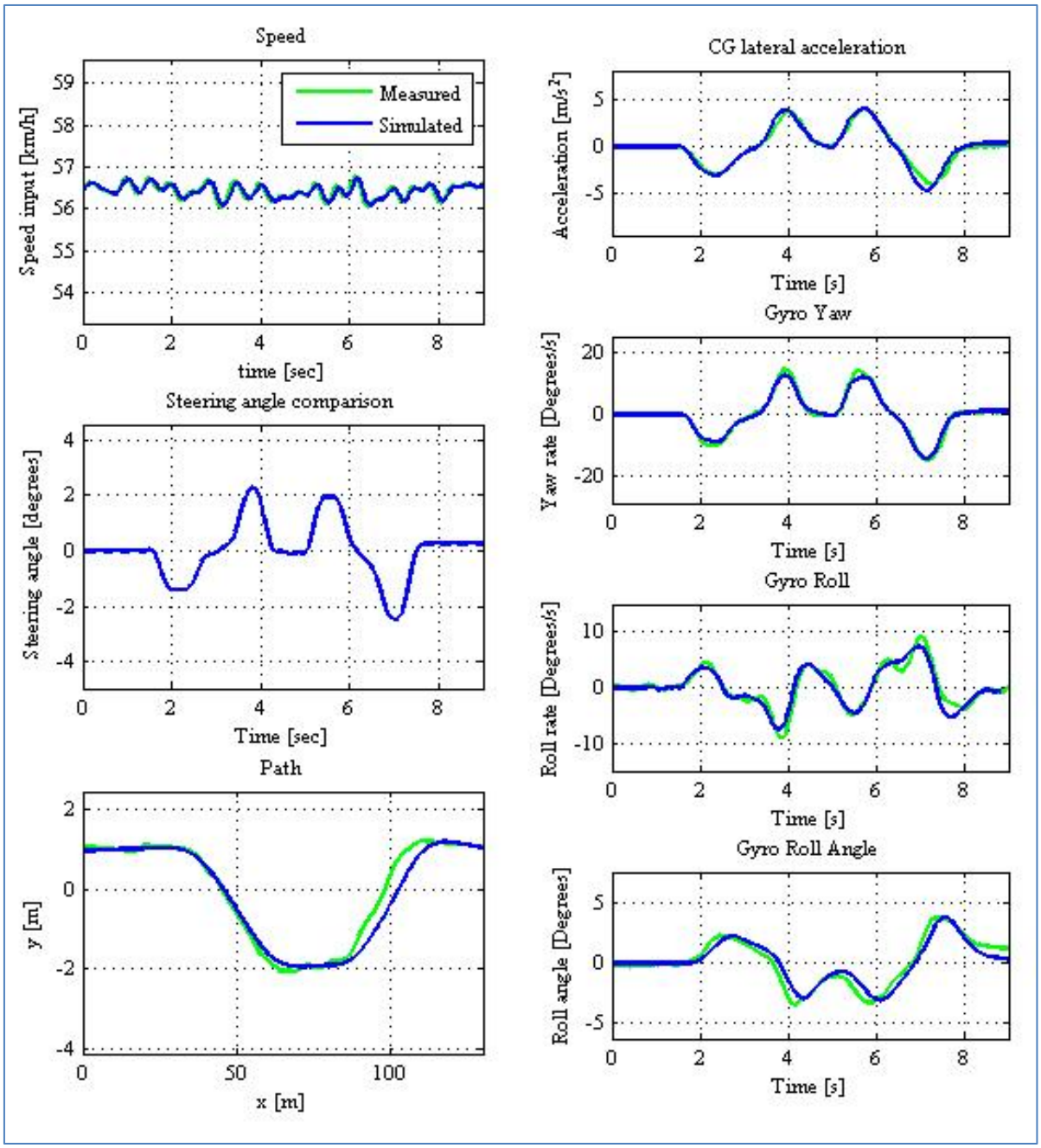

Figure 4.7: Vehicle path for 56.5 km/h validation test on ride comfort suspension mode (Speed, steering angle, path, lateral acceleration, yaw rate, roll rate and roll angle)

The simulation slightly overestimated the lateral acceleration of the vehicle and slightly underestimated the roll rate, roll angle and yaw rate of the vehicle, but on the whole good correlation was achieved. The peak %RE values are given in Table 4.6:

Table 4-6: %RE peak values for 56.6 km/h validation test on suspension ride comfort mode

	Mean peak %RE
Lateral acceleration	7 %
Roll rate	13 %
Roll angle	6 %
Yaw rate	11 %

The correlations for suspension displacements and forces are presented in Figure 4.8:

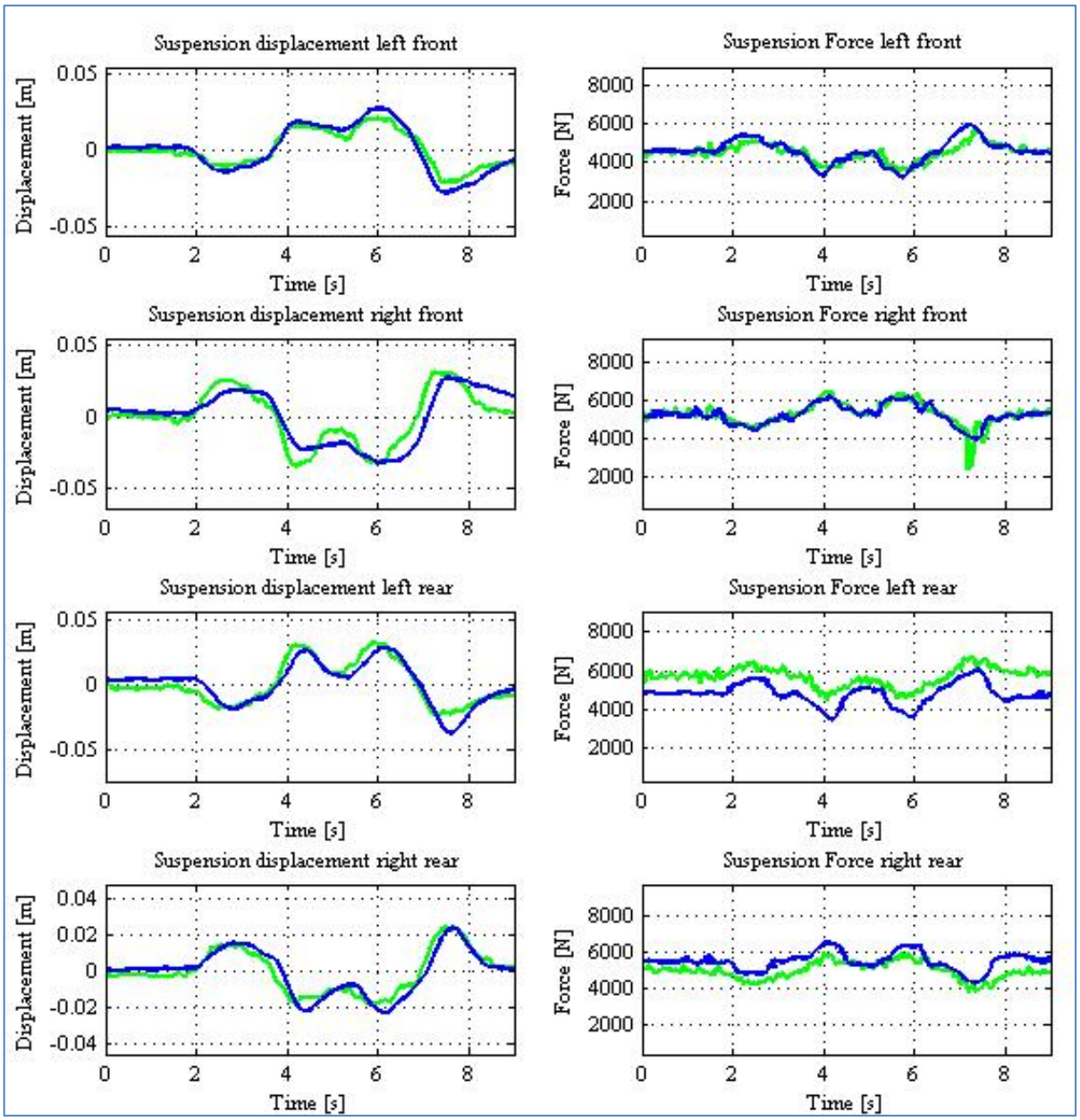

Figure 4.8: Suspension forces for 56.6 km/h validation test on ride comfort mode (Suspension displacements and forces)

The suspension validation metrics are tabulated in Table 4.7**:**

Table 4-7: Suspension validation metrics for 56.6 km/h validation test in ride comfort mode

	Mean Peak %RE suspension displacement	Mean %RE suspension forces
Front left strut	21 %	$m\%RE^m = 5\ \%\mathrm{P}(64\ \%)$
Front right strut	24 %	$m\%RE^m = 4\ \%\mathrm{P}(82\ \%)$
Rear left strut	19 %	$m\%RE^m = 16\ \%\mathrm{P}(55\ \%)$
Rear right strut	16 %	$m\%RE^m = 12\ \%\mathrm{P}(59\ \%)$

A good correlation was observed for both suspension displacements and forces. The front right suspension unit displayed the worst displacement correlation and the left rear suspension unit the worst forces correlation. This was likely due to deviation of the static gas pressure and deviation of the gas mass of the according suspension units.

4.6 Conclusion

In this chapter, the simulation model was validated using experimental data from the test vehicle for the DLC manoeuvre for two suspension settings, firstly for high damping and spring (the handling mode) and secondly, for low damping and spring (the ride comfort mode) at different velocities and steering angles.

The results of the simulation validations showed that although there was slight deviation in the absolute position, there was generally good correlation for vehicle path and the outputs of yaw rate, roll rate, roll angle and lateral acceleration for both suspension modes. It may be concluded that good correlation is obtained with an acceptable error between 10-20%.

There are various factors that influenced the suspension displacement and forces during the test runs, and which may therefore have caused deviations between measured and simulated results. Two of these factors are road surface inconsistencies and variations in the gas mass of the hydro-pneumatic suspension between the test vehicle and mathematical model. Firstly, deviations may arise from defects on the road surface such as stones, twigs and casting lines. These may have caused sudden spikes in the data. Secondly, the suspension modelling is highly dependent on the amount of gas in the accumulators and the preload pressure of the gas. **Els (2006)** emphasises that the installation procedure of the suspension units is no trivial task and that the mass of gas in the accumulators may easily deviate from the exact desired amount. The model is statically indeterminate which makes it extremely difficult to obtain excellent results for all four suspension units, since the gas mass on the physical vehicle may deviate from the mathematical model. This phenomenon may be observed by the front suspension displacements and forces having better correlations than the rear suspension. The model is deemed accurate enough to be used with confidence in future simulation.

In the following chapter, the simulation results for the different manoeuvres are reported.

5 SIMULATION RESULTS

In this chapter, simulations results are reported for three manoeuvres discussed in chapter 4, namely the step-steer manoeuvre, the Fishhook 1B manoeuvre and the Double Lane Change (DLC) manoeuvre. The simulations were done for three suspension settings, namely handling mode, ride comfort mode and energy removal mode. As discussed in chapter 4.4, the handling mode consists of hard spring characteristics and high damping for the suspension setup. Thus only the 0.1 litre accumulator is active and the hydraulic fluid is forced through the damper by closing the bypass valve. The ride comfort mode consists of a soft spring characteristic and a low damping characteristic. Thus both accumulators of the $4S_4$ are used, providing a gas volume of 0.5 litres. Low damping is achieved by opening the bypass value. The energy removal mode consists of a soft spring characteristic and a high damping characteristic. This mode allows relatively large body motions, but damps out energy to remove inertial effects. This setting was derived by **Uys (2007)** in an attempt to reduce rollover for steady-state cornering.

5.1 The Step-Steer Manoeuvre

The manoeuvre was simulated for speeds ranging from 40 km/h to 140 km/h with increments of 20 km/h. The step-steering angle (measured at the kingpin of the front wheels) was varied from 1 degree to 25 degrees with increments of 2 degrees, turning to the left. Using the manoeuvre, roll angle, roll rate, yaw rate, lateral acceleration and wheel lift for the three suspension modes could be compared.

5.1.1 Roll Angle

The first parameter investigated with regard to rollover was the body roll angle of the vehicle. The results obtained from the simulations are displayed as surface plots in Figure 5.1 for the ride comfort mode, Figure 5.2 for the energy removal mode and Figure 5.3 for the handling mode.

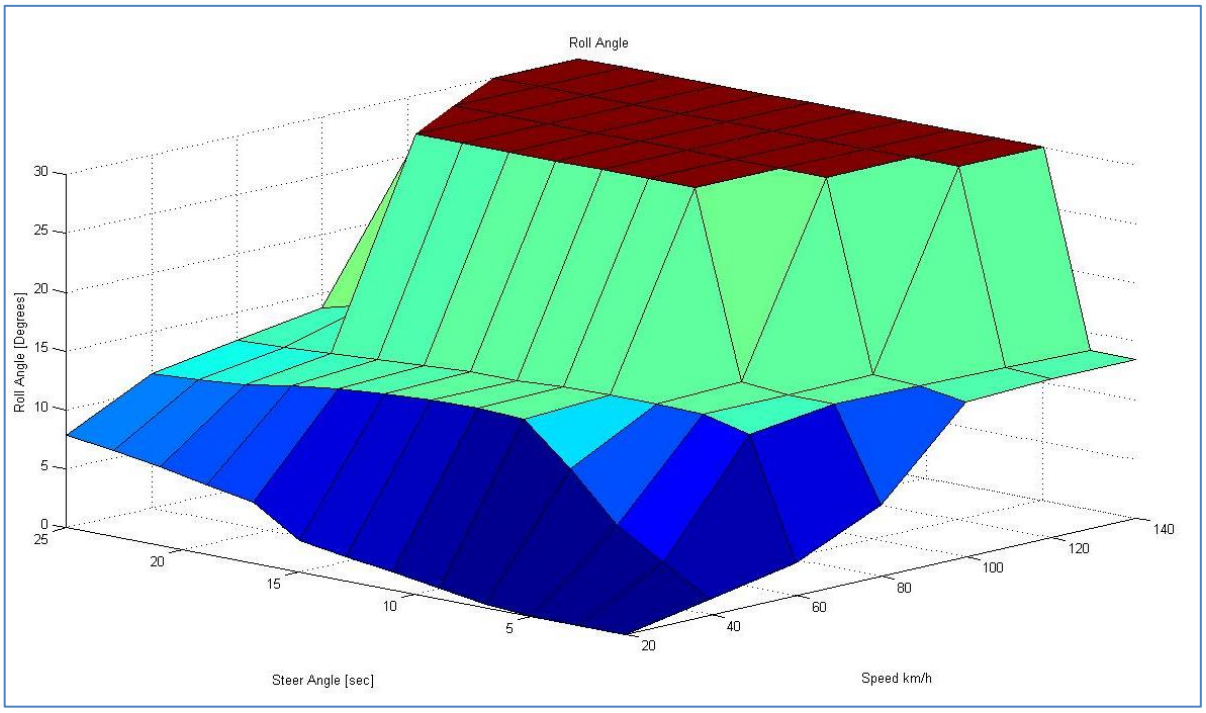

Figure 5.1: Maximum roll angle for step-steer simulation on ride comfort mode

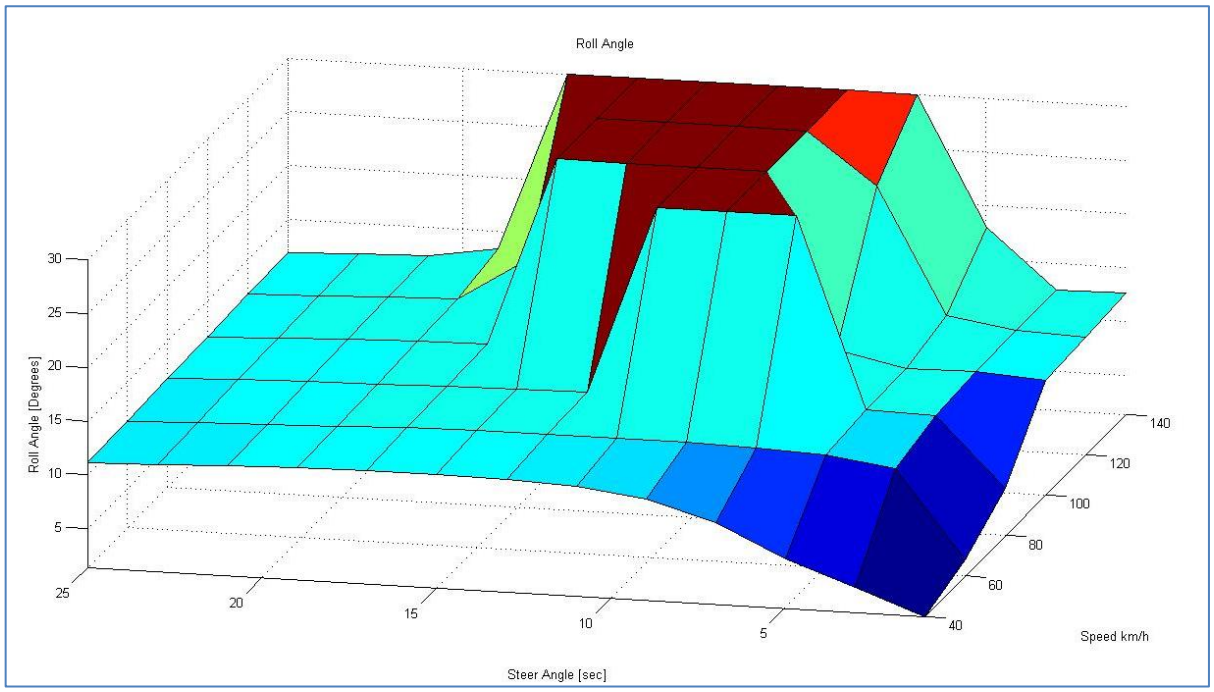

Figure 5.2: Maximum roll angle for step-steer simulation on energy removal mode

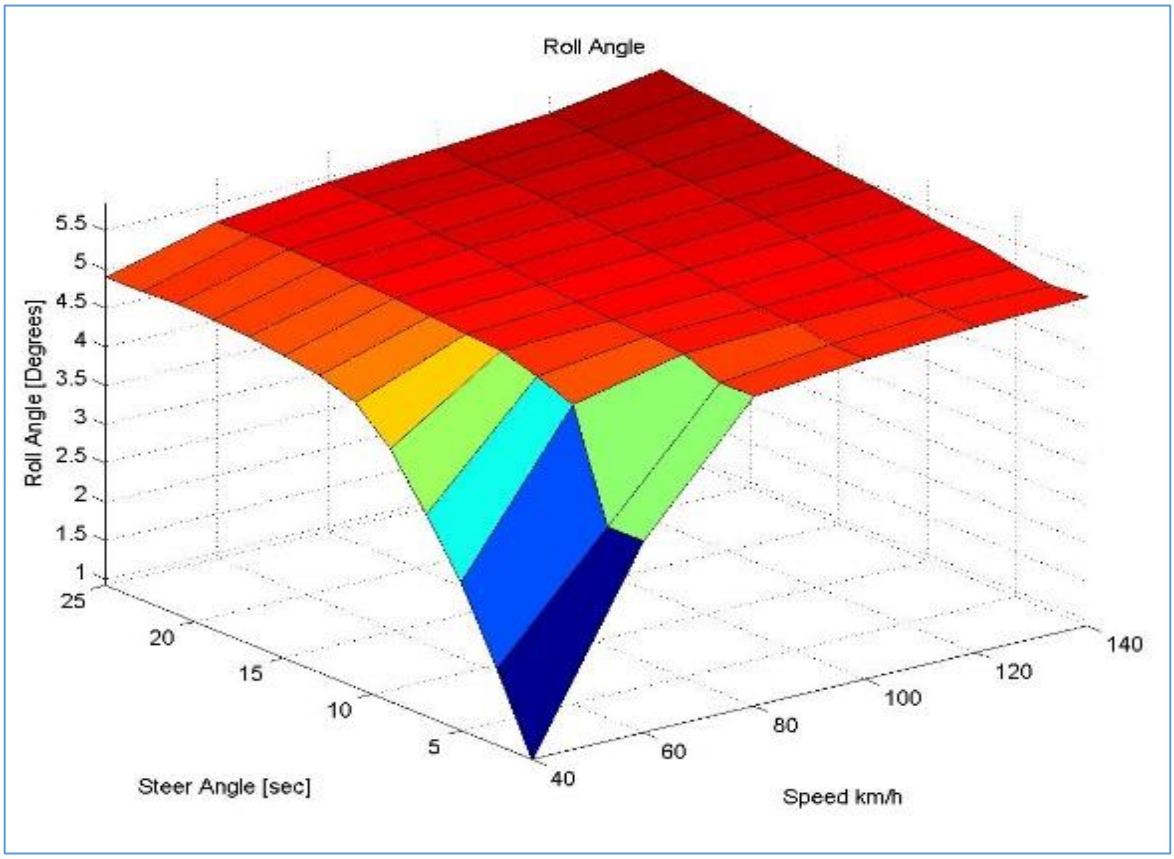

Figure 5.3: Maximum roll angle for step-steer simulation on handling mode

In Figure 5.1 and Figure 5.2 the vehicle rolled over for some of the simulations. The rollovers may be observed where the roll angle is limited to 30 degrees and creates a table top on the plot. From the simulations, it was found that roll angle prior to rollover is the largest for the ride comfort mode and smallest for the handling mode, for which the vehicle spun out. As Figure 5.3 shows, the vehicle never overturned in handling mode; however, it did lose control and spun out. A sudden increase in

roll angle indicates that rollover has occurred, and a trend may be observed in that there is a slow rise in roll angle as the vehicle approaches rollover.

Table 5.1 shows the maximum roll angle experienced by the vehicle before rollover occurred.

Table 5-1: Step-steer manoeuvre, maximum roll angle before rollover

	Ride comfort mode	Energy removal mode	Handling mode
Maximum roll angle before rollover is induced	14 degrees	25 degrees	6 degrees with no rollover

The maximum roll angles occur at 3 separate locations, illustrating that change in suspension characteristics have nonlinear effects. It should be noted that for the step-steer simulations, the model was able to complete all simulations in the handling mode without rolling over. The maximum roll angle seen for the handling mode was 6 degrees. The roll angles were maintained low enough to reduce load transfer to the out wheels, thus reducing the lateral tyre force generation enough to allow the vehicle to slide before roll. This demonstrates that the SSF does not hold true for all circumstances and that suspension plays an important role. The handling mode has thus substantial potential to reduce the risk of rollover. This is further illustrated in Figure 5.4 for individual simulations where the roll angle for the handling mode is less than the other modes.

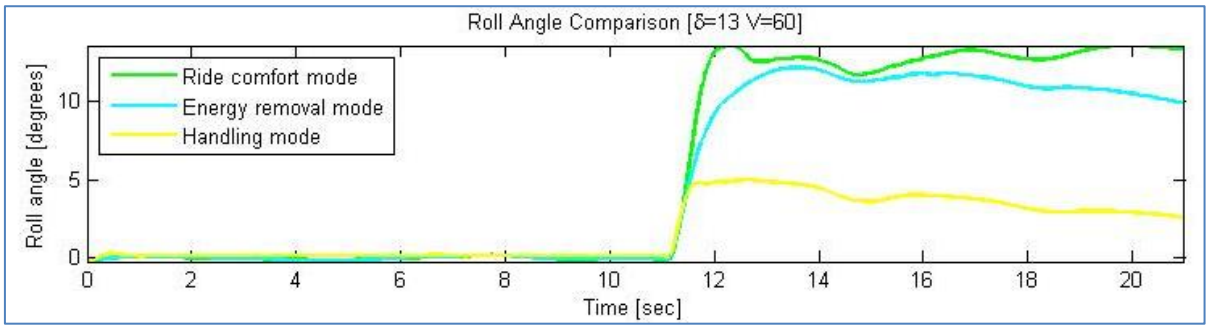

Figure 5.4: Roll angle comparison of various suspension modes executing a step steer manoeuvre of 13 degrees at a speed of 60 km/h

It was also noted that the relative roll angle between the body and the axles saturates at a point due to suspension geometry.

5.1.2 Roll Rate

The next parameter that was investigated was roll rate. Roll rate has a great effect on the vehicle with regard to rollover as it accounts for inertial overshoot, which often lead to the vehicle overturning. The results of the simulations are displayed in Figures 5.5 (ride comfort mode), 5.6 (energy removal mode) and 5.7 (handling mode).

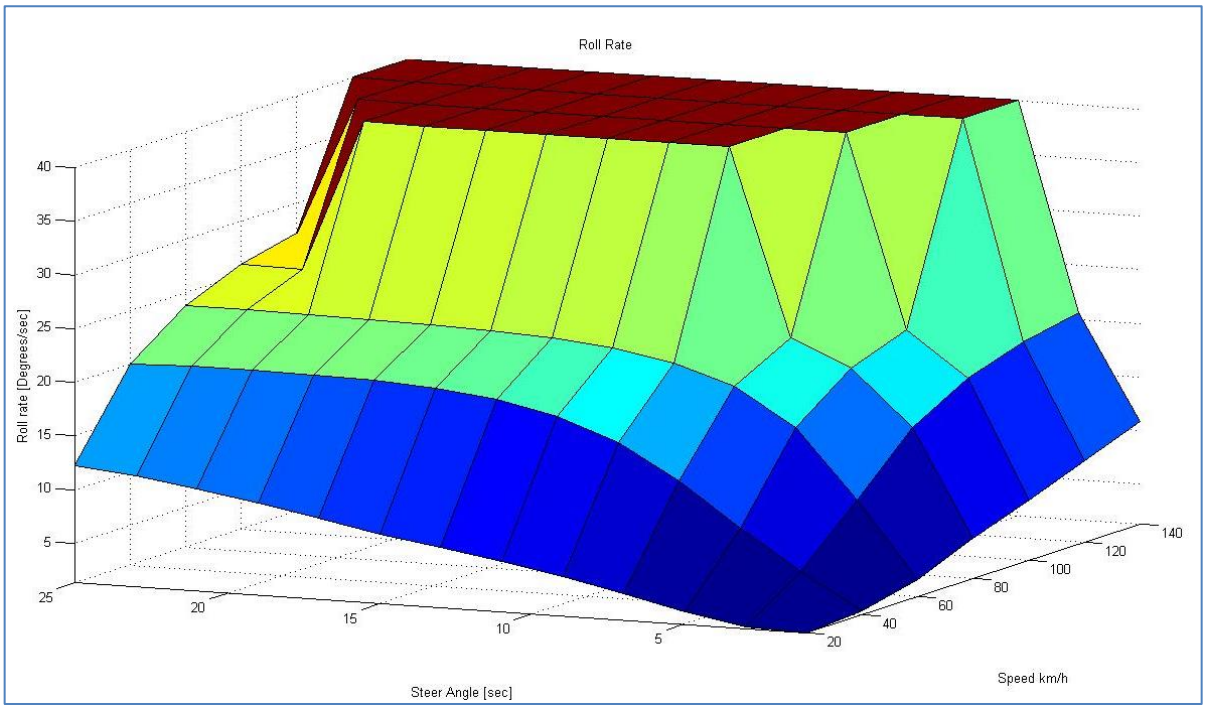

Figure 5.5: Maximum roll rate for step-steer simulation on ride comfort mode

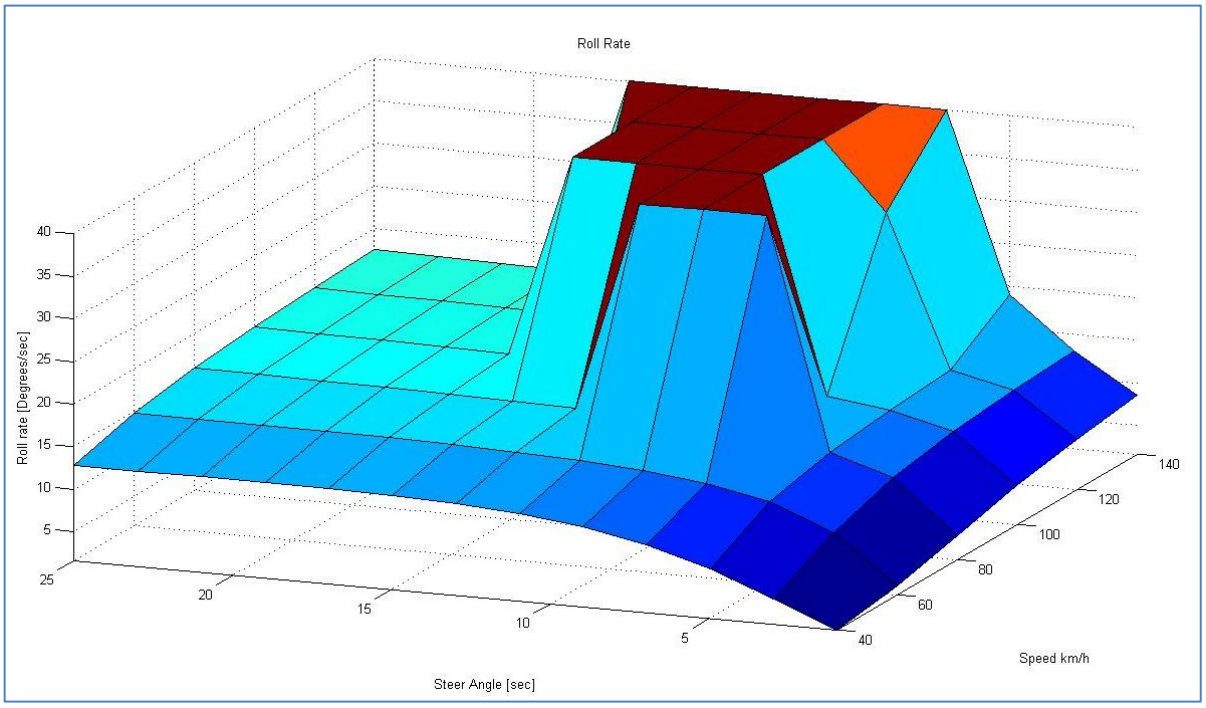

Figure 5.6: Maximum roll rate for step-steer simulation on energy removal mode

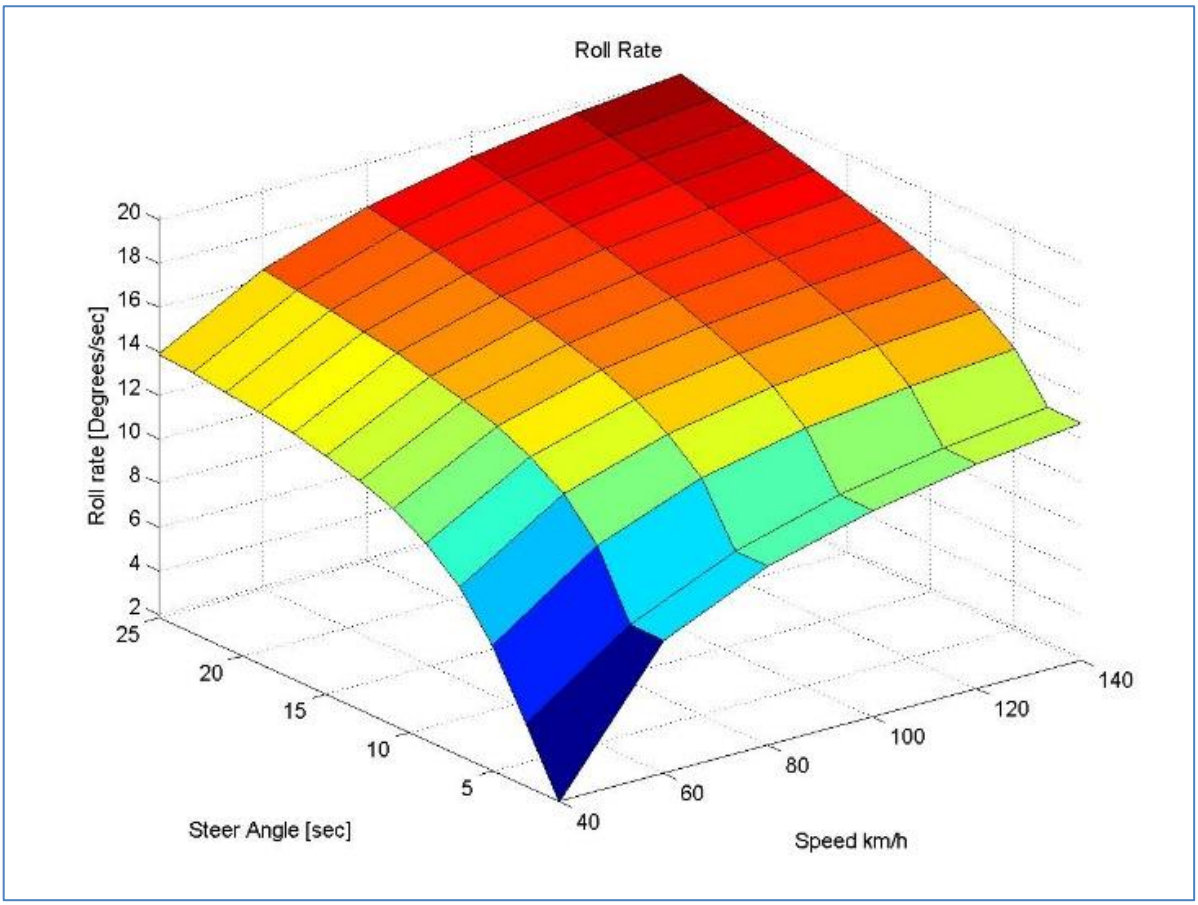

Figure 5.7: Maximum roll rate for step-steer simulation on handling mode

Again rollover may be observed in Figure 5.5 and Figure 5.6 where the plot is limit to a roll rate of 40 degrees per second. The results of the simulations showed that maximum roll rate is smallest for the handling mode and largest for the ride comfort mode. Maximum roll rate gives a similar indication of rollover as roll angle, but the gradient change in the former is more marked. Thus, prior to rollover, maximum roll rate is a better indicator of rollover than maximum roll angle. The maximum roll rates for each mode are displayed in Table 5.2:

Table 5-2: Step-steer manoeuvre, maximum roll rate before rollover

	Ride comfort mode	Energy removal mode	Handling mode
Maximum roll rate before rollover	27 degrees/s	19 degrees/s	20 degrees/s with no rollover

The largest maximum roll rate before rollover was observed in the ride comfort mode and the smallest in the energy removal mode. The handling mode maximum value is close to that of the energy removal mode. This is illustrated in Figure 5.8.This could be attributed to them having the same damping in roll motion. The energy removal exhibited the highest maximum roll angle and the lowest maximum roll rate, demonstrating its ability to allow for large roll motions in a larger variety of steer angles and speeds. The high roll rates in the ride comfort mode lead to vehicle roll overshooting and thus toppling over.

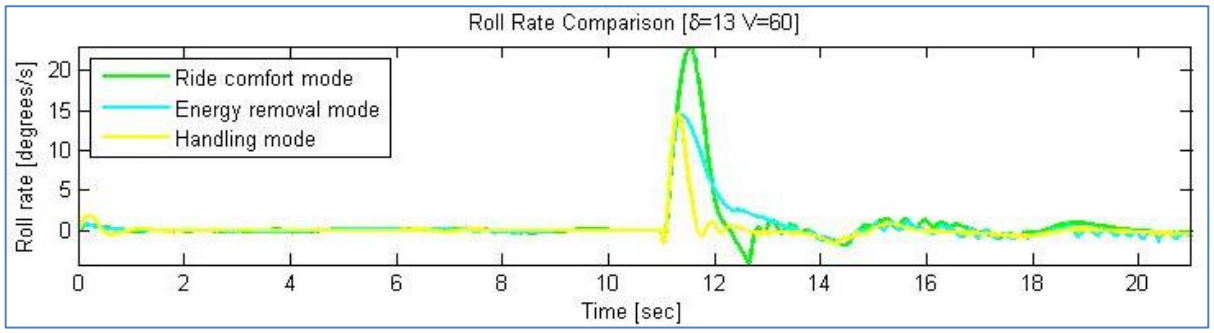

Figure 5.8: Roll rate comparison of various suspension modes executing a step steer manoeuvre of 13 degrees at a speed of 60 km/h

5.1.3 Yaw Rate

Yaw rates are important with regard to over-steer, which often leads to rollover. The simulation results are presented in Figures 5.9 (ride comfort mode), 5.10 (energy removal mode) and 5.11 (handling mode):

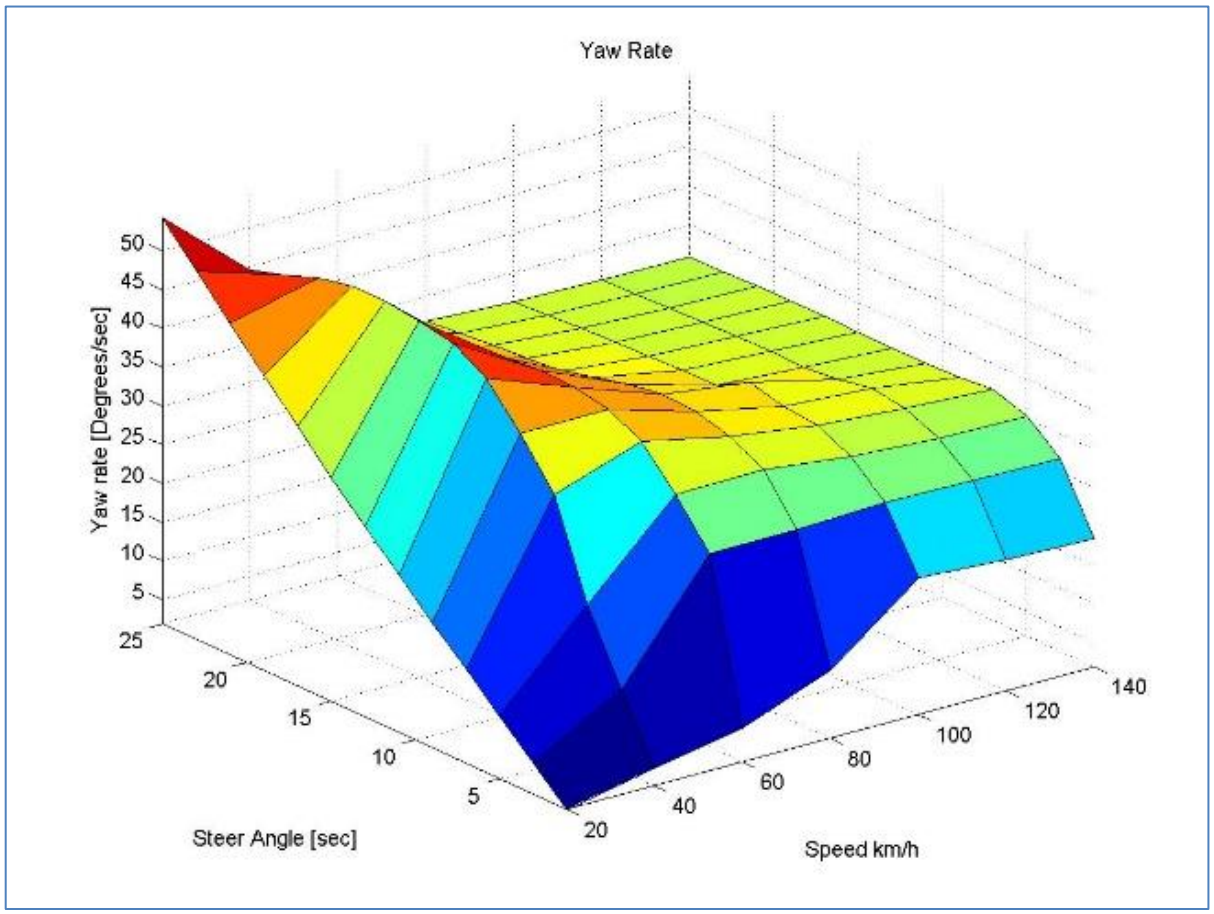

Figure 5.9: Maximum yaw rate for step-steer simulation on ride comfort mode

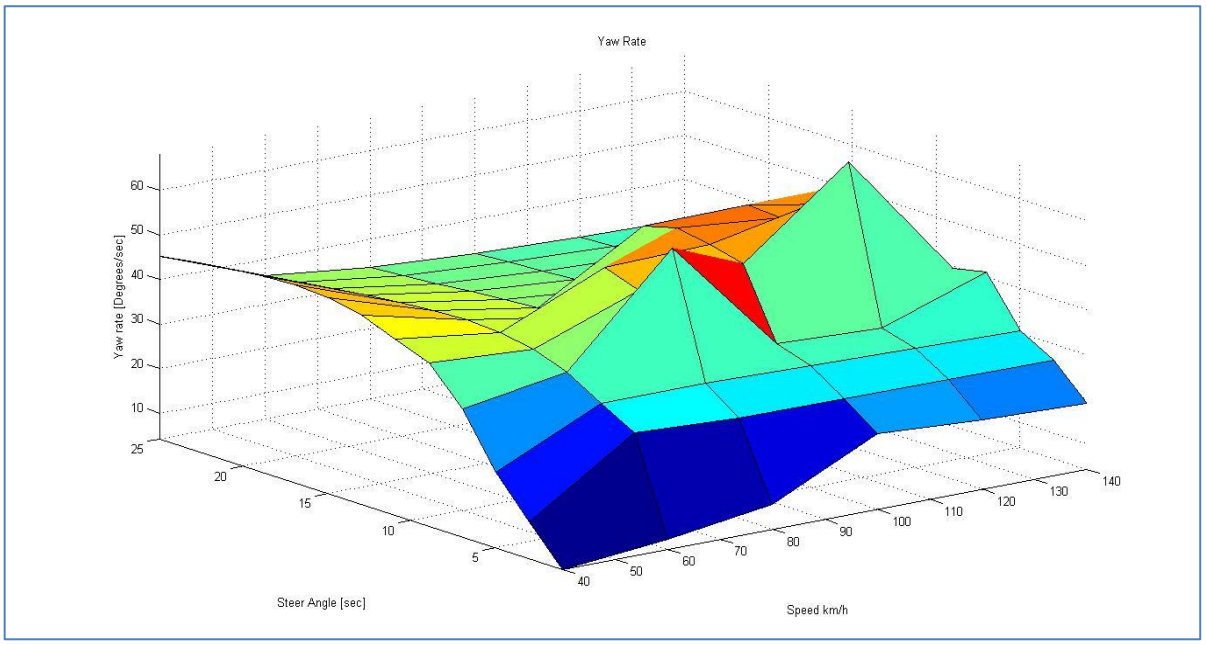

Figure 5.10: Maximum yaw rate for step-steer simulation on energy removal mode

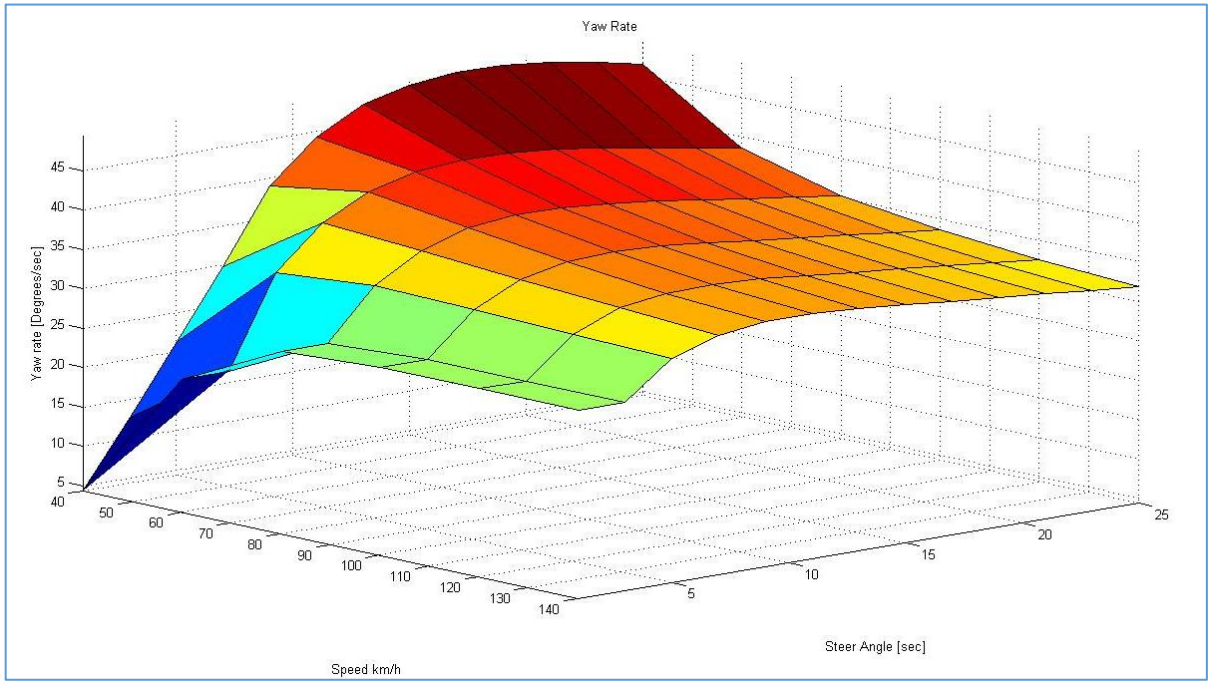

Figure 5.11: Maximum yaw for step-steer simulation on handling mode

Maximum yaw rate does not show any indication of rollover. However, the largest maximum may still be seen on ride comfort mode and the smallest for energy removal mode. Although the maximum yaw rate plots lack detail of rollover prediction, for individual simulations, as illustrated in Figure 5.12 and Figure 5.13, the yaw rate exhibited oscillation before rollover occurred.

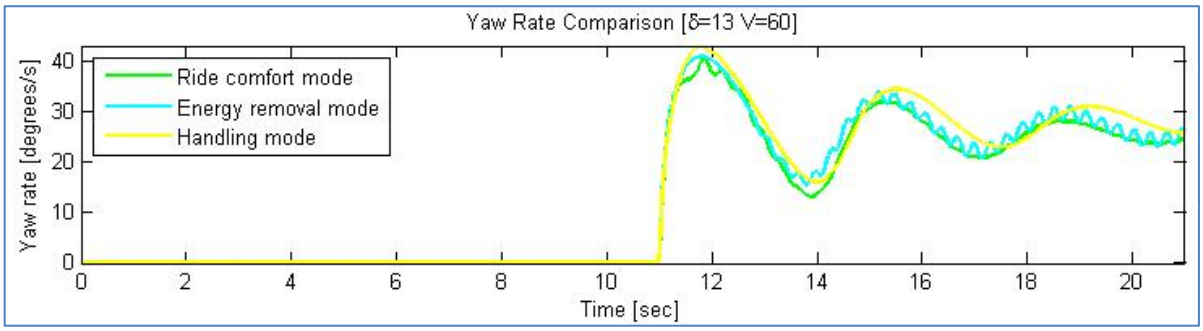

Figure 5.12: Yaw rate comparison of various suspension modes executing a step steer manoeuvre of 13 degrees at a speed of 60 km/h

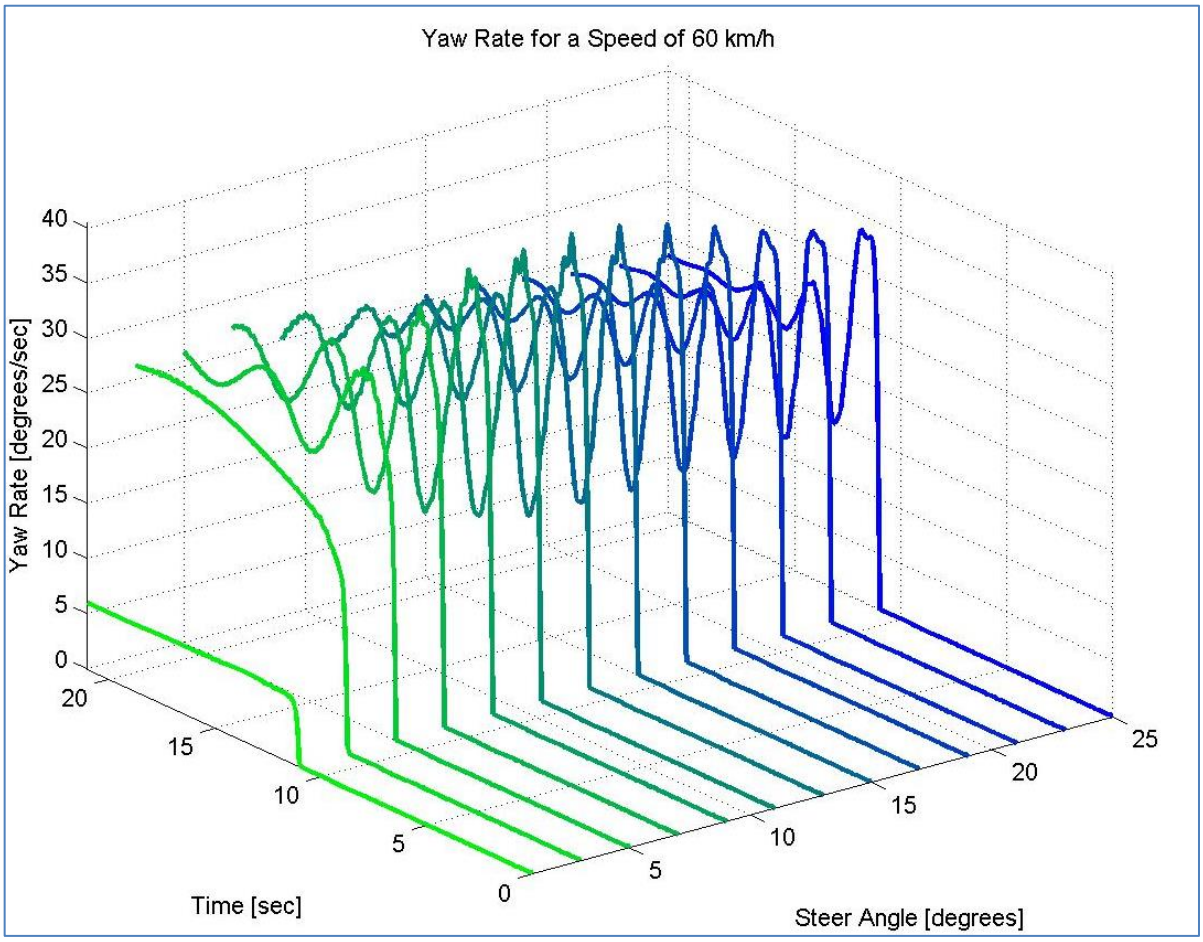

Figure 5.13: Yaw rate comparison of various step steer angles at a speed of 60 km/h for ride comfort mode

The maximum yaw rates derived from the simulations for each mode are presented in Table 5.3:

Table 5-3: Step-steer manoeuvre, maximum yaw rate before rollover

	Ride comfort mode	Energy removal mode	Handling mode
Maximum yaw rate before rollover	55 degrees/s	48 degrees/s	22222 degrees/s with no rollover

The largest maximum yaw rate in general is observed at 40km/h and above steering angles of 10 degrees, although the energy removal mode does exhibit some deviations from this trend. The maximum yaw rate decreases for these steer angles as speed increases, most likely due to lack of traction.

5.1.4 Lateral Acceleration

Lateral acceleration is a parameter often measured on production vehicles and is used to define static and dynamic measures of rollover. The simulation results are presented in Figures 5.14 (for ride comfort mode), 5.15 (for energy removal mode) and 5.16 (for handling mode):

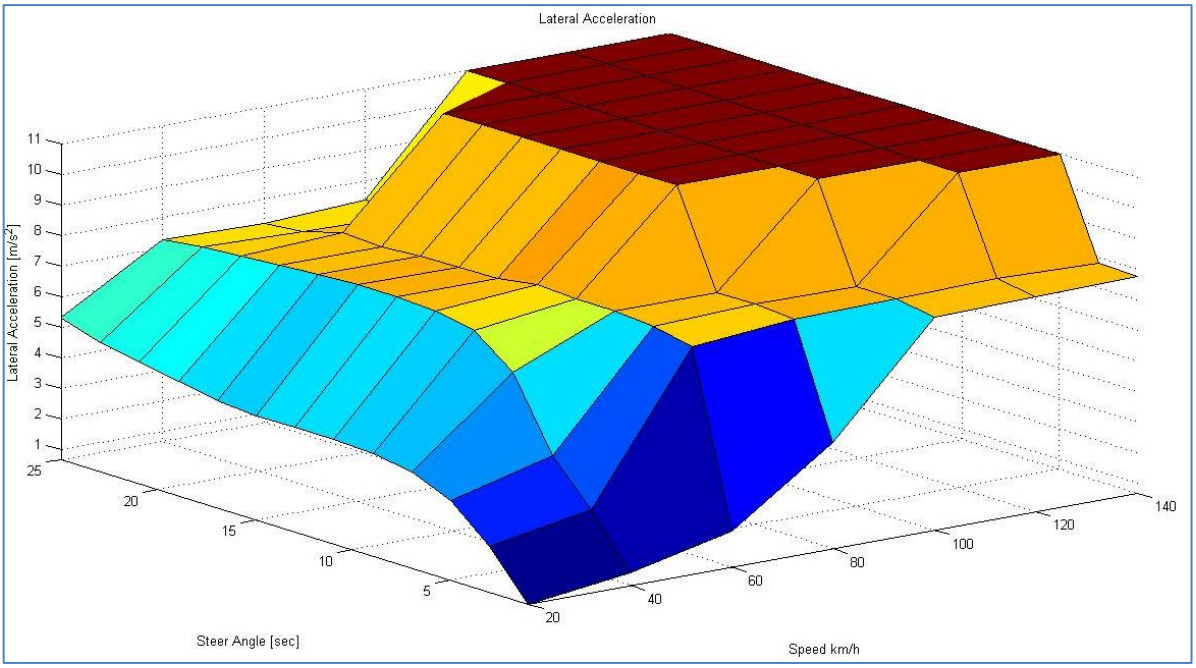

Figure 5.14: Maximum lateral acceleration for step-steer simulation on ride comfort mode

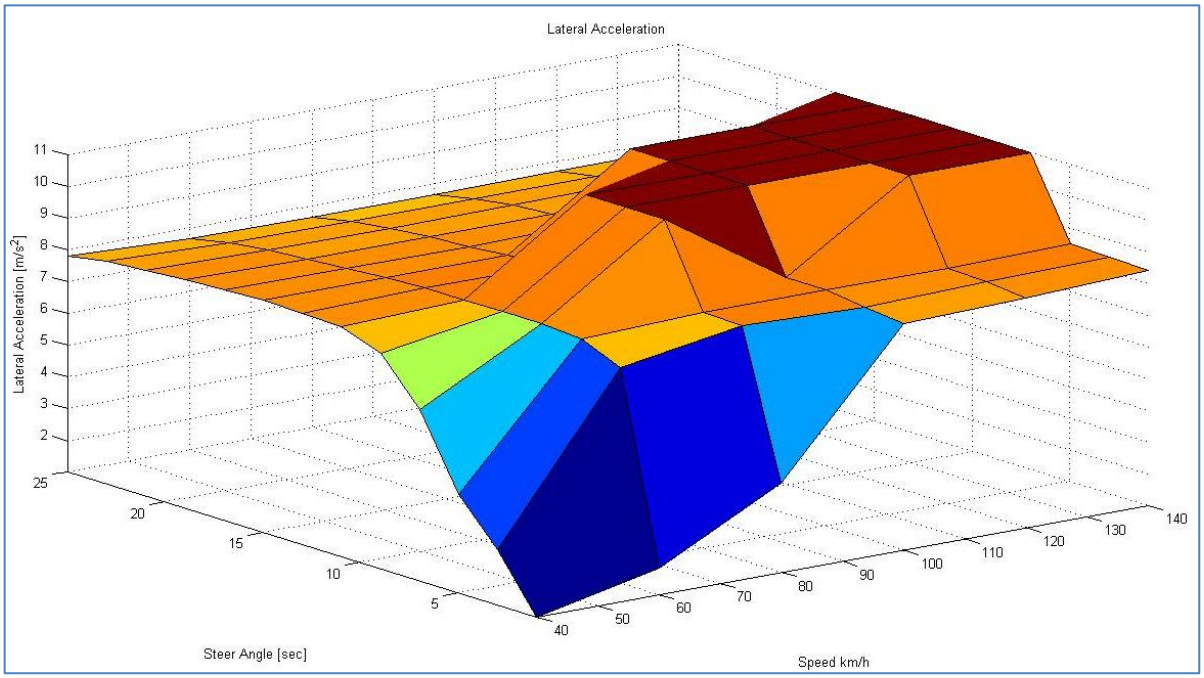

Figure 5.15: Maximum lateral acceleration for step-steer simulation on energy removal mode

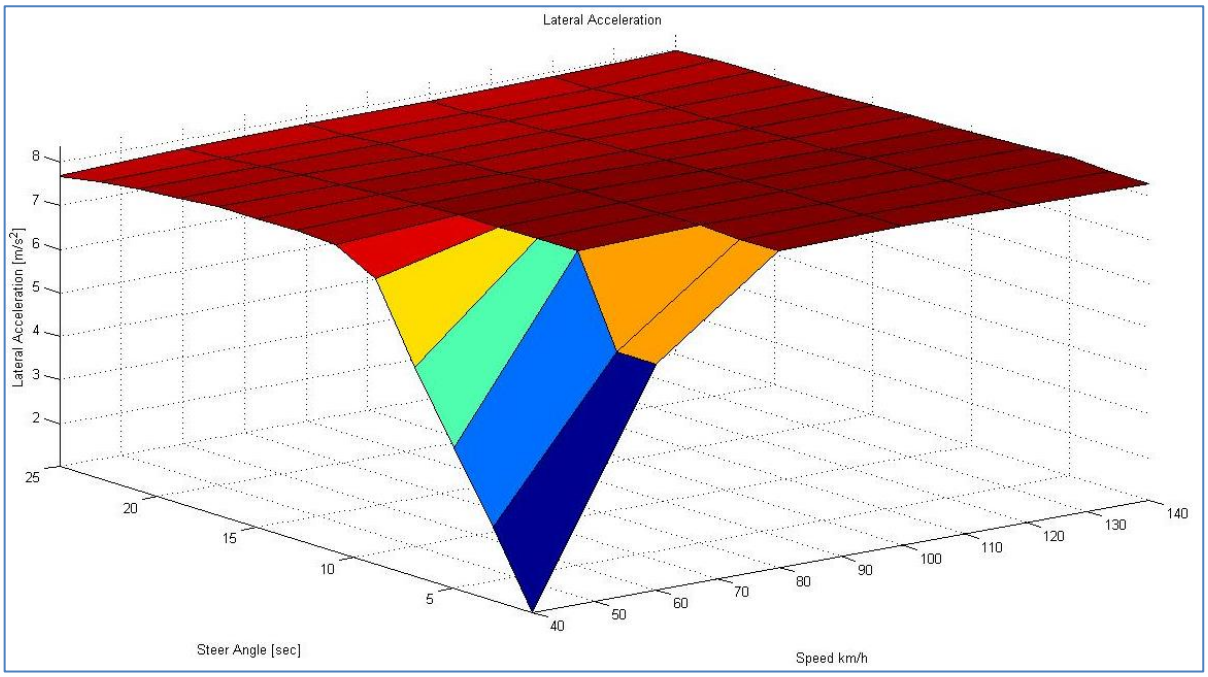

Figure 5.16: Maximum lateral acceleration for step-steer simulation on handling mode

Figure 5.14 and Figure 5.15 limit the plot to 11 m/s^2, for the simulations in which rollover occurred. Maximum lateral acceleration seems to saturate around $8m/s^2$ for all modes. Although some trend is visible with increasing lateral acceleration up till the point of saturation, once saturation occurs, rollover may or may not occur. Although the lateral acceleration should reduce to zero after rollover, in the case of the model, it increases because contact has not been defined between the road and the body in the simulation program and thus the body still accelerates through the road. This explains why such unrealistic accelerations are observed in the plots for simulations in which the vehicle rolled over. The maximum lateral acceleration values derived from the simulations are presented in Table 5.4:

Table 5-4: Step-steer manoeuvre, maximum lateral acceleration before rollover

	Ride comfort mode	Energy removal mode	Handling mode
Maximum lateral acceleration before rollover	$7.25m/s^2$	$8.5m/s^2$	$8.3m/s^2$ with no rollover

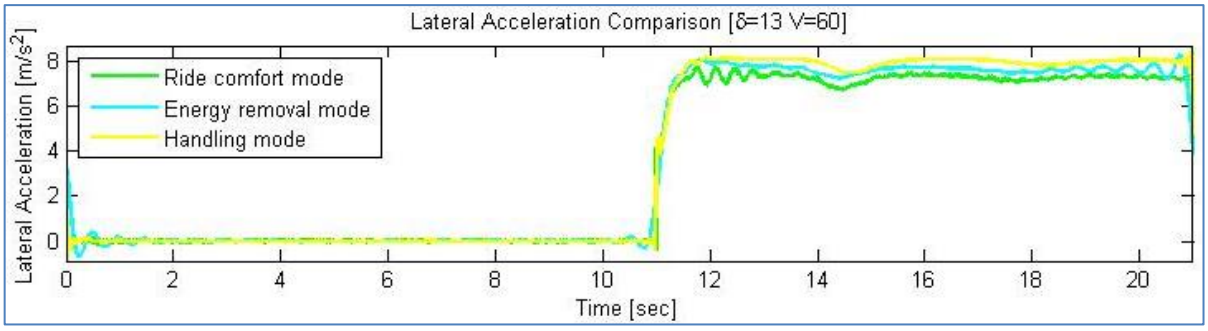

Figure 5.17: Yaw rate comparison of various suspension modes executing a step steer manoeuvre of 13 degrees at a speed of 60 km/h

Figure 5.17 illustrates how a vehicle with a softer suspension setting is likely to rollover at lower lateral accelerations than a vehicle with stiffer suspension settings as discussed in chapter 2.1.2.

5.1.5 Wheel Lift

Uys (2007) reported the inner wheel lifts to be the critical parameters used to determine vehicle rollover propensity. The simulation results are presented in Figures 5.18 (for ride comfort mode), 5.19 (for energy removal mode) and 5.20 (for handling mode):

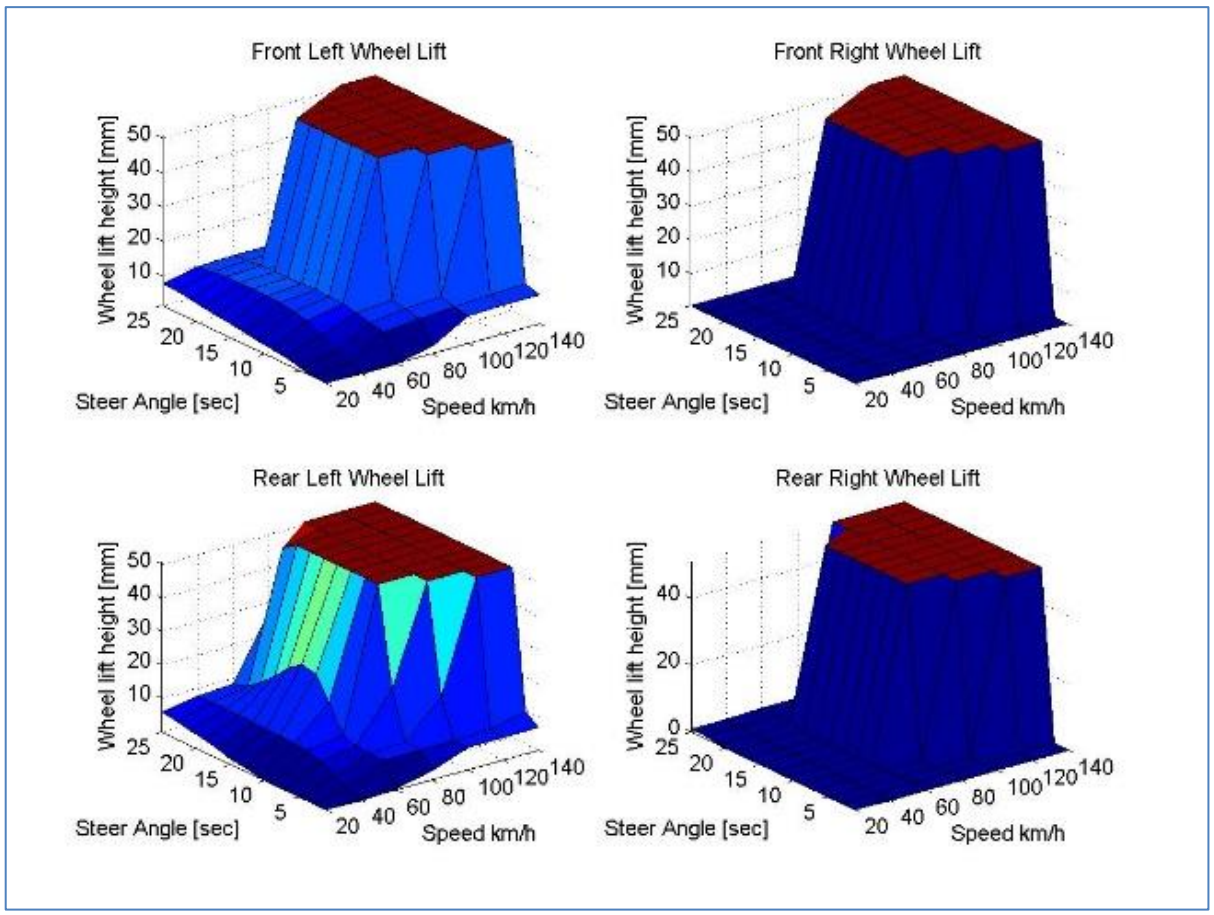

Figure 5.18: Maximum wheel lift for step-steer simulation on ride comfort mode (lower initial suspension force)

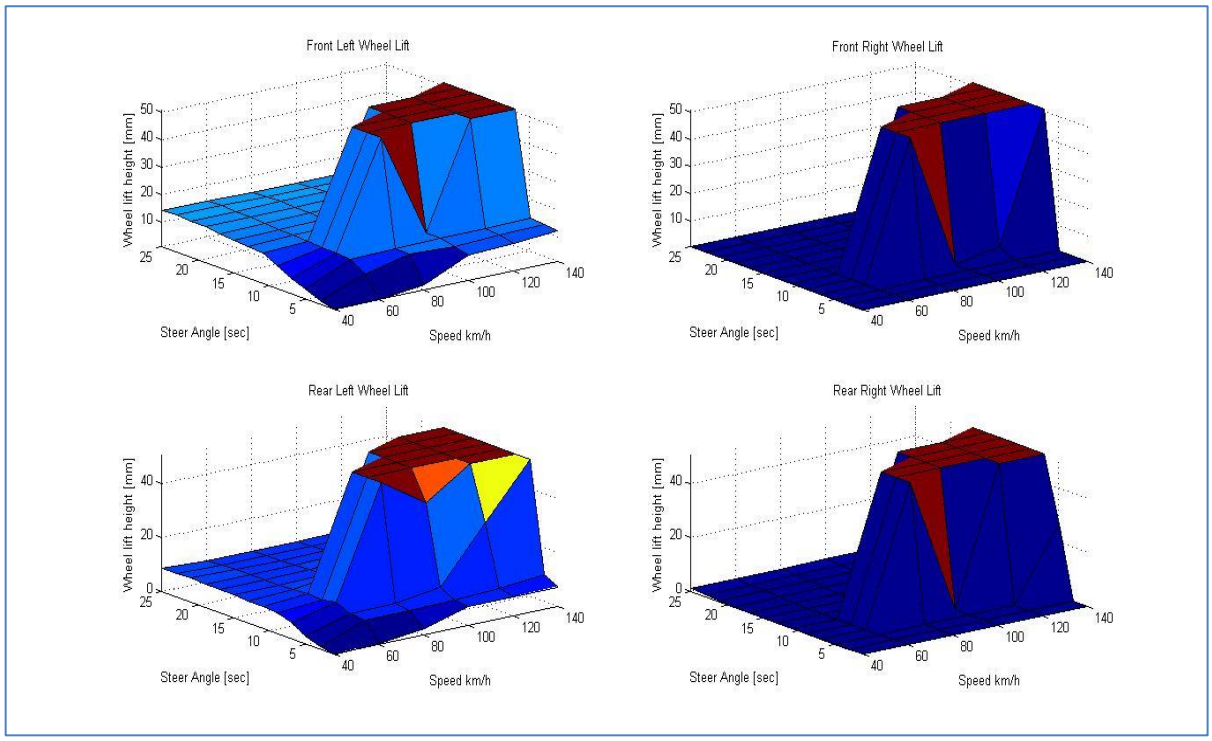

Figure 5.19: Maximum wheel lift for step-steer simulation on energy removal mode (lower initial suspension force)

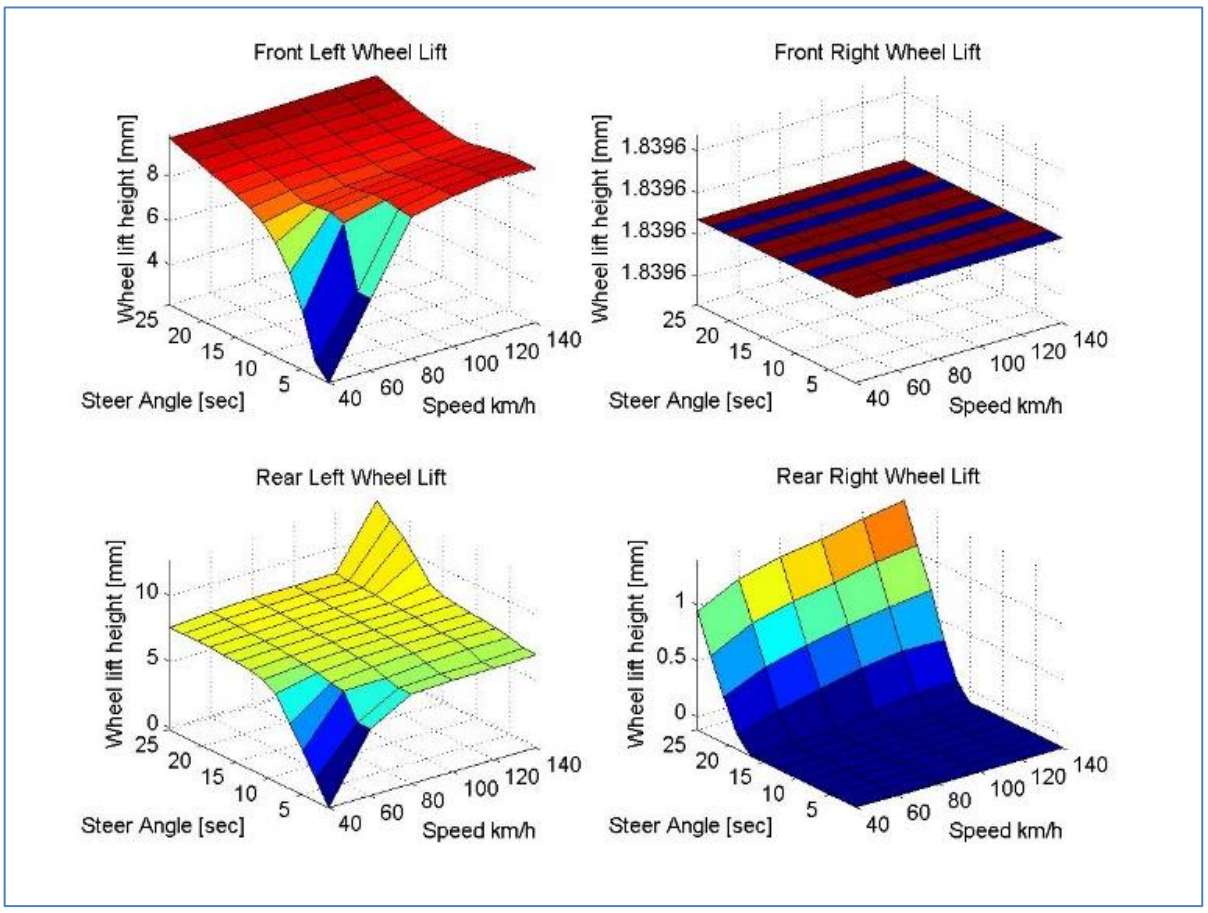

Figure 5.20: Maximum wheel lift off for step-steer simulation on handling mode

The best indication of rollover in ride comfort mode may be observed to be the rear inner maximum wheel lift; however, the same cannot be said for the other suspension settings. This is due to the smoothness in which it transitions into rollover for the ride comfort mode. When individual simulations were reviewed, the wheel lift is also observed to oscillate before rollover is induced. This was observer in Figure 5.21, where the speed is maintained at 60km/h and the magnitude of the step steer angle varied.

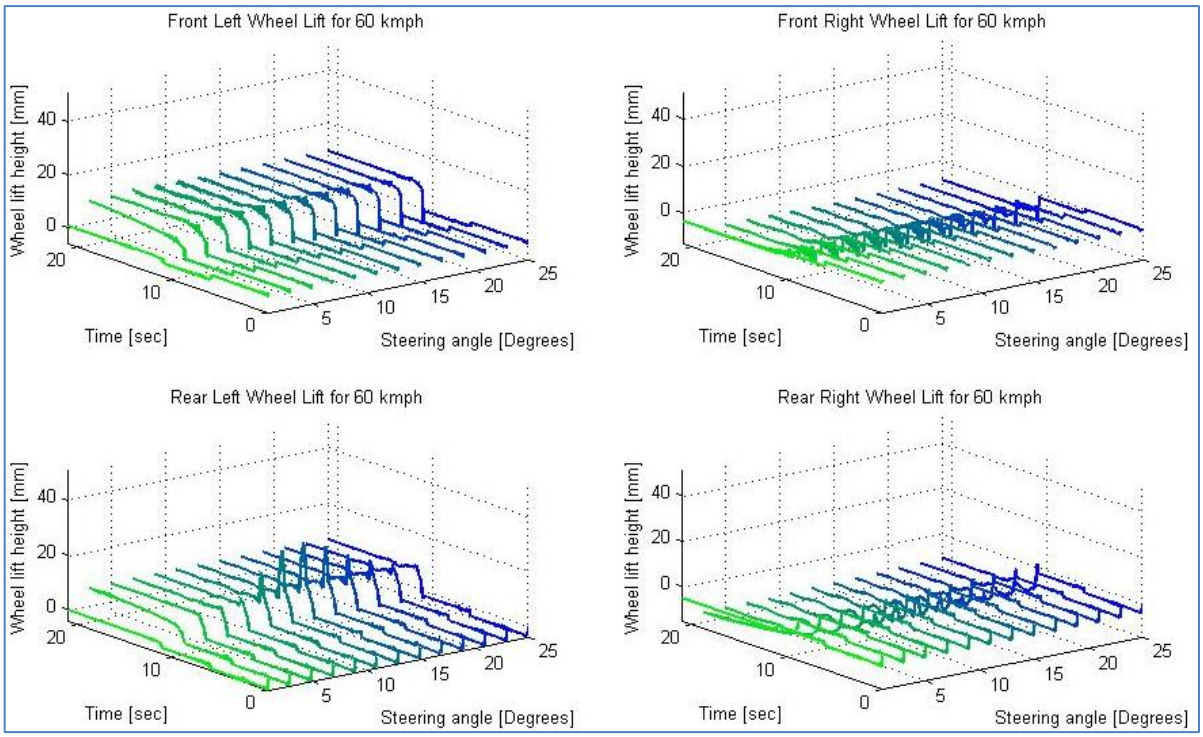

Figure 5.21: Wheel lift comparison of various step steer angles at a speed of 60 km/h for ride comfort mode

Figure 5.22 illustrates the wheel lift of the investigate suspension settings. It is know that the ride comfort mode was the closest to rolling over and thus wheel lift offers a good indication of the state of rollover.

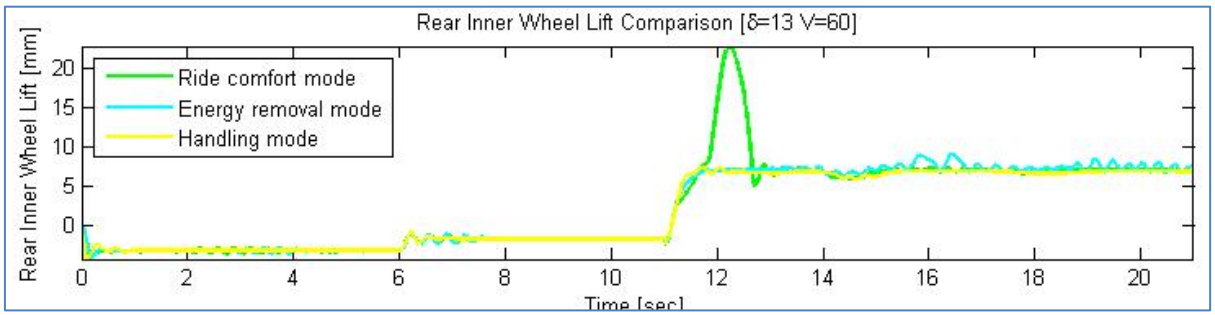

Figure 5.22: Rear inner wheel lift comparison of various suspension modes executing a step steer manoeuvre of 13 degrees at a speed of 60 km/h

5.1.6 Conclusion

The maximum values of lateral acceleration roll rate and roll angle provide a good threshold that can be used to detect rollover. The maximum values before rollover for the ride comfort mode are used as thresholds for defining the index of rollover severity. From the simulations, the best predictor of rollover appears to be the maximum roll rate.

In the next sections, the results for the simulation of the Fishhook 1B manoeuvre are reported.

5.2 The Fishhook 1B

Having established rollover parameters for the three modes of the simulation model by using the step-steer manoeuvre, the Fishhook 1B manoeuvre simulations were primarily undertaken to evaluate the two rollover prevention control systems proposed in chapter 3.2.3 and 3.2.4 respectively that attempt to reduce rollover propensity by adjusting the suspension height, based on a rollover index. The first prevention control system also increases damping to prevent rollover by calculating and monitoring the rollover angle and rate, whereas the second prevention control system adds a PID controller on each strut to add or remove hydraulic fluid. The vehicle is bought to entry speed before executing the manoeuvre.

5.2.1 Determination of the Steering Angle Amplitude

The Fishhook 1B uses the SIS manoeuvre steering input that generates 0.3g lateral acceleration.

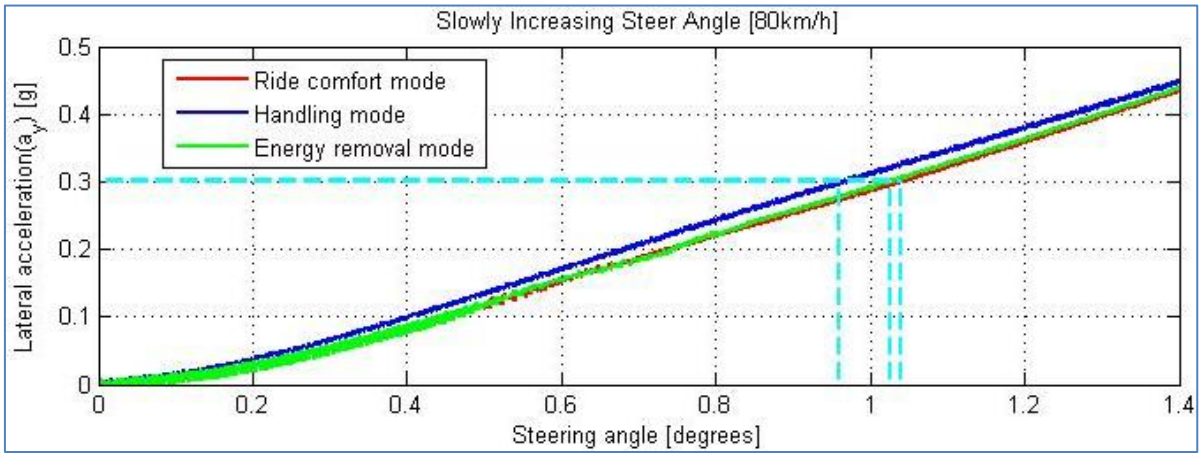

Figure 5.23: Slowly Increasing Steer Angle

The SIS steering input was designed for passenger cars and thus as compensation for the use of an SUV, twice this angle was used in the simulations. For all the suspension modes tested, the SIS steering angles were rounded off to the closest whole number of degrees. From the simulation tests, it was observed that the SIS steering angle from simulations was not representative of the potential severity of rollover with regard to rollover for the test vehicle. According to **Whitehead et al. (2004)**, the SIS steer angle is negligibly affected by the change in CG height and can be assumed to have no influence on the SIS angle. The Fishhook uses an angle of 6.5 times the SIS 0.3g steering angle (1 degree according to Figure 5.23), thus the maximum steering angle used for the Fishhook 1B was 13 degrees. This angle also correlates to the steering angle that gave a high number of rollovers in the step-steer manoeuvre.

5.2.2 Fishhook 1B Maximum Speed without Wheel Lift-Off

Simulations were undertaken to investigate the maximum speed for each mode at which the modelled vehicle performed the manoeuvre without raising its wheels more than 50 mm. The results are tabulated in Table 5.5:

Table 5-5: Fishhook 1B maximum speed without wheel lift off

	Ride comfort mode	Energy removal mode	Handling mode	Control system strategy 1	Control system strategy 2
Maximum speed without two-wheel lift-off	36 km/h	46 km/h	51 km/h	64 km/h	84 km/h
Vehicle rollover speed (two-wheel lift-off > 50 mm)	37 km/h	47 km/h	52 km/h	65 km/h	Remains untripped for all speeds tested (40-140 km/h)

The ride comfort mode was the first setup to raise two wheel lift off more than 50 mm. Rollover was induced with very little increase to vehicle speed for all modes except the second control strategy which remained close to 50 mm wheel lift-up until 140 km/h and passed the maximum vehicle speed without incurring rollover.

Control strategy 2 therefore improved possible vehicle speed before rollover by at least 133% compared to ride comfort mode and 64% compared to the handling mode. The simulation results of this control system are therefore presented in detail in the next section.

Appendix 7.4 presents figures for comparisons of the maximum speed simulations of the different suspension settings. Thus the different suspension setting can be compared at various simulation speeds for the Fishhook 1B.

5.2.3 Fishhook 1B Control System Maximum Speed Without Wheel Lift-Off

The steering angle is set initially by a path-following controller to ride along a straight line until the manoeuvre steering inputs are applied. Small changes in suspension geometry due to weight shifts add minor steer angle offsets; thus the path-following controller is necessary to maintain straight driving. The simulated steer angle is depicted in Figure 5.24:

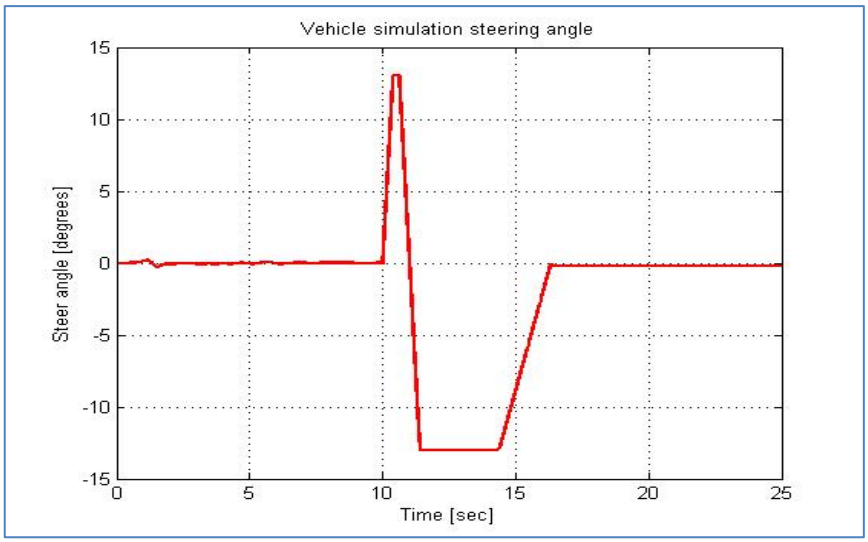

Figure 5.24: Fishhook 1B manoeuvre on rollover prevention mode, steer angle

The figure illustrates a (positive) left steering input, followed by a (negative) right steering input.

In Figure 5.25, the yaw angle of the model vehicle at a speed of 84km/h (maximum speed without lift-off) is tracked relative to the path using asterisks to represent its wheels:

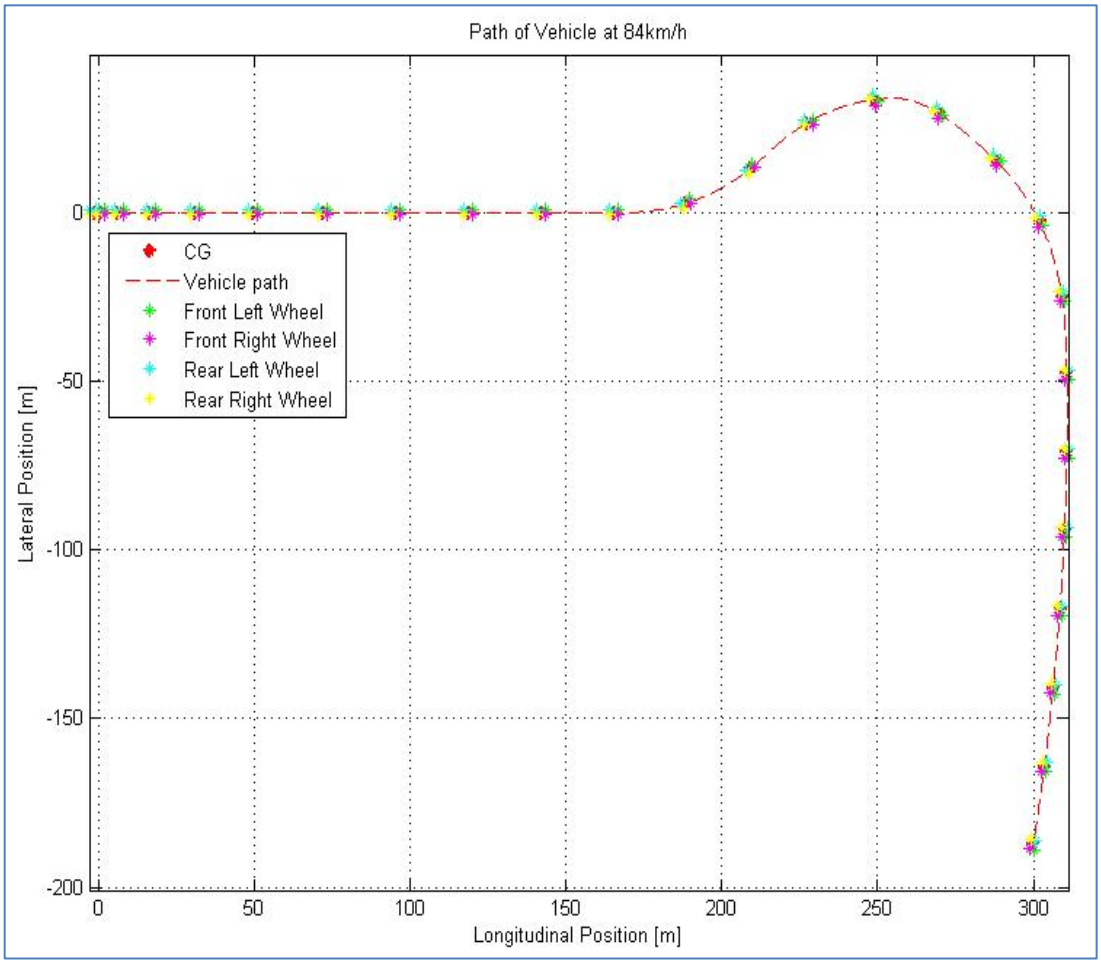

Figure 5.25: Fishhook 1B manoeuvre on rollover prevention mode, vehicle path

The curvature of the path indicates that there is substantial vehicle sliding before traction is regained. During the manoeuvre, the vehicle undergoes sliding, the large yaw angles created resulting in a decrease in the forward velocity. This is expected when the friction circle is considered, which states that the maximum acceleration of the vehicle is limited with regard to the combination of lateral and longitudinal acceleration.

As observed in chapter 5.1.4, lateral acceleration reaches traction limits around 8m/s^2. At this acceleration, significant oscillation is observed in both roll rate and roll angle. This can be interpreted as due to the fact that the vehicle is on the limit of tyre force generation and has spurts of traction forces. The vehicle shudders significantly but remains untripped.

The control system also exhibits shaky behaviour due to the independent strut adjustments. The adjustment of one strut changes the response of the other three, i.e. they all have an effect on each other. In physical testing, only the vertical response of the vehicle would be considered, since the physical system for height adjustment will have additional unknown effects (e.g. equipment delays and maximum accumulator pressures) that are not modelled due to their complex nature.

The lateral acceleration, roll rate, roll angle and yaw rate oscillations for the control system at 84 km/h are presented in Figure 5.26:

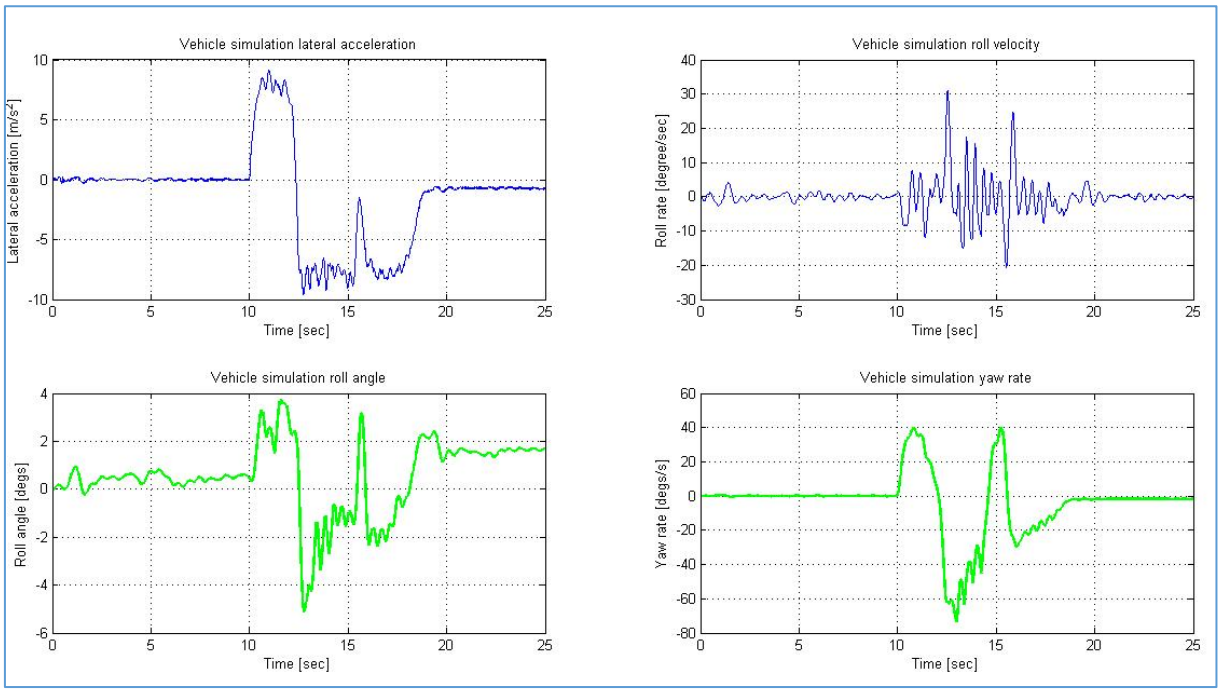

Figure 5.26: Fishhook 1B manoeuvre on rollover prevention mode; lateral acceleration, roll rate, roll angle and yaw rate

In chapter 5.1.3, the yaw rate was observed to oscillate violently before rollover in the step-steer simulations. The same phenomenon is observed in the yaw rate for the Fishhook 1B above. Thus from the yaw rate, it is observed that the vehicle is on the limit of rollover during the second dwell period. This speed is the highest speed observed before wheel-lift greater than 50 mm occurred.

Figure 5.27 depicts the wheel displacements. A negative displacement represents tyre compression and positive displacement represents the wheel lift distance.

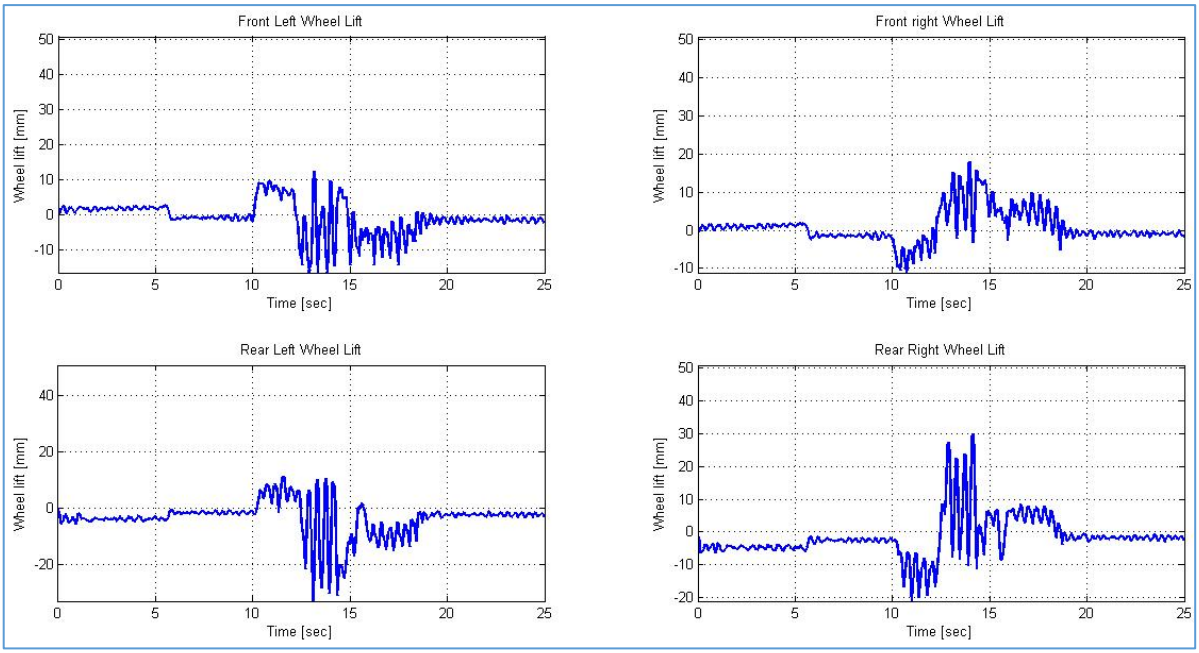

Figure 5.27: Fishhook 1B manoeuvre on rollover prevention mode, wheel lift

Figure 5.28 presents the suspension displacements for the prevention control system at 84 km/h and compares them with the desired suspension displacement values with respect to the vehicle's speed

as well as with the desired counter roll angle. The reduced ride height results in the model's suspension having a softer characteristic than in reality. The lowering of the suspension should be more responsive in reality than in simulation, since the function used to calculate suspension forces in the model cannot differentiate between oil adjustments and suspension displacement due to road or inertia inputs.

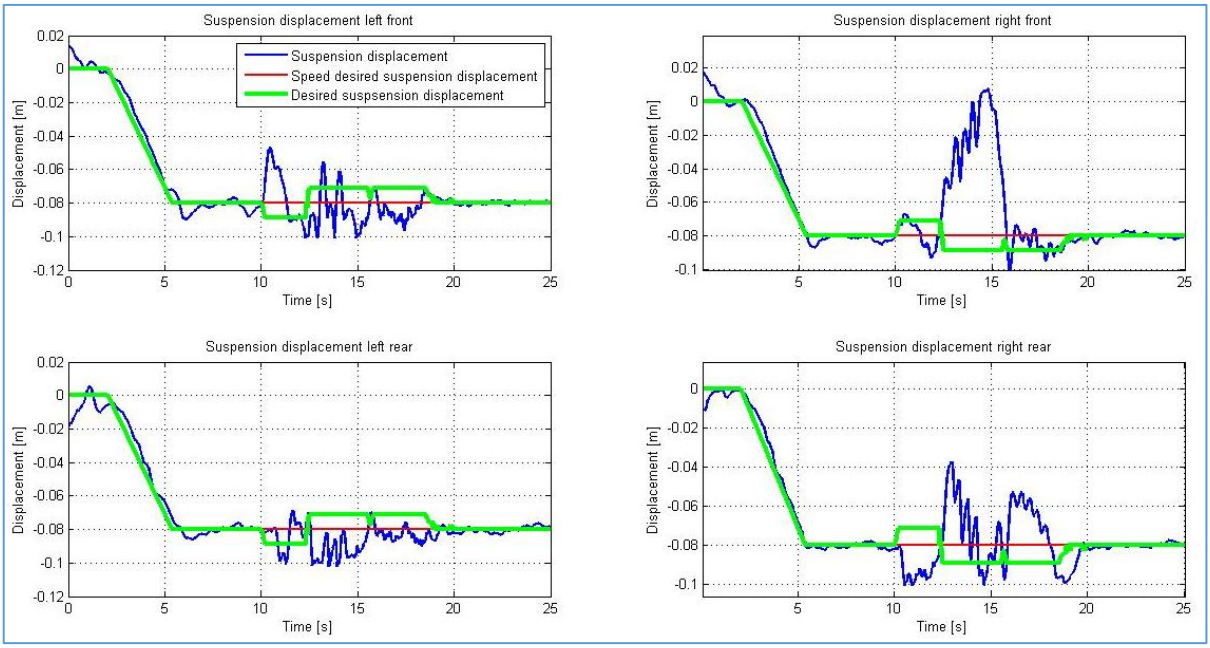

Figure 5.28: Fishhook 1B manoeuvre on rollover prevention mode, suspension displacement

The suspension follows the desired heights relatively well until the manoeuvre steer angles are applied. The speed at which the manoeuvre is executed required oil flow rates greater than the simulated system was able to provide. This may be observed from the available pressure difference that needs to be positive to allow oil to be added or removed. After the steer inputs are completed, the control system is able to converge once again to the desired suspension height. The deviation of the suspension displacement can therefore be ascribed to sudden inertia forces and the limit of oil flow rates.

The suspension height adjustments rates are dependent on the available pressures. To extend the strut and raise the vehicle corner, the pressure in the hydraulic fluid accumulator needs to be greater than the pressure in the strut. This pressure difference is referred to as the oil-adding pressure difference. To compress the strut or lower the vehicle corner, the pressure in the strut needs to be greater than the atmospheric pressure. This pressure difference is referred to as the oil-removal pressure. The pressure differences during cornering at 84 km/h are depicted for each strut in Figure 5.29:

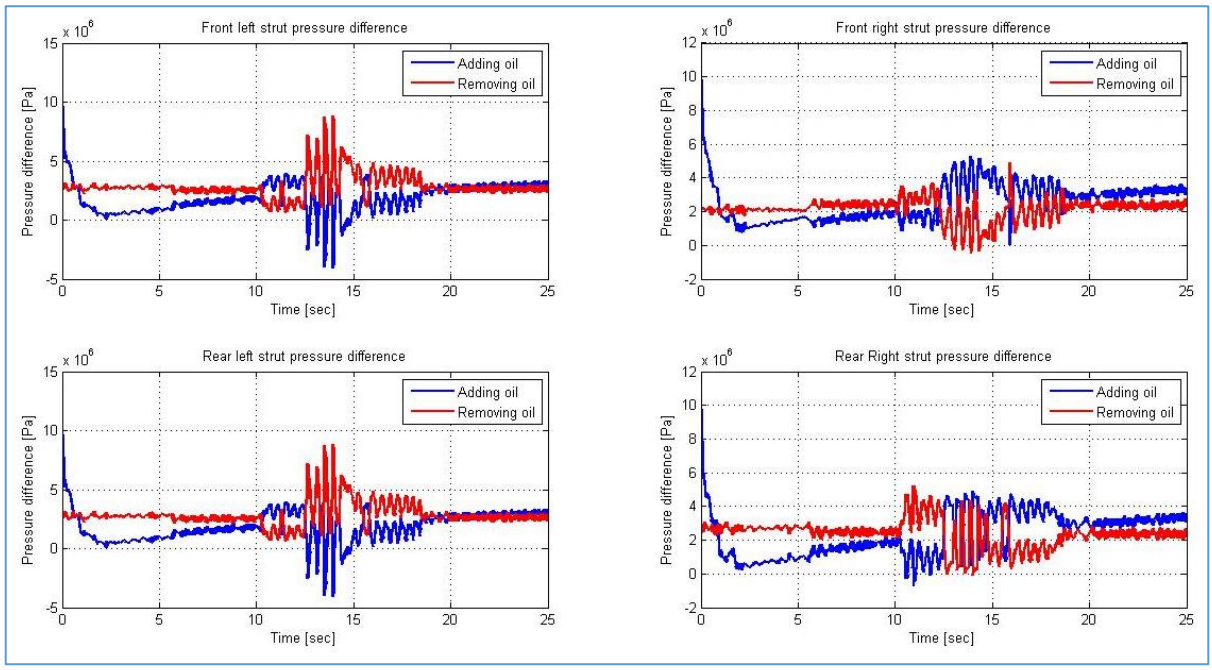

Figure 5.29: Fishhook 1B manoeuvre on rollover prevention mode, available strut pressure

Observing the deviation of the suspension displacement from the desired height in terms of available pressure differences, it is noted that, in cornering, the oil-adding pressure of the outer struts (where oil needs to be added) is close or below zero. For the inner struts, the oil-removal pressure is also close to zero. This limits the performance of the control system.

The change in CG height during the manoeuvre at 84 km/h is depicted in Figure 5.30:

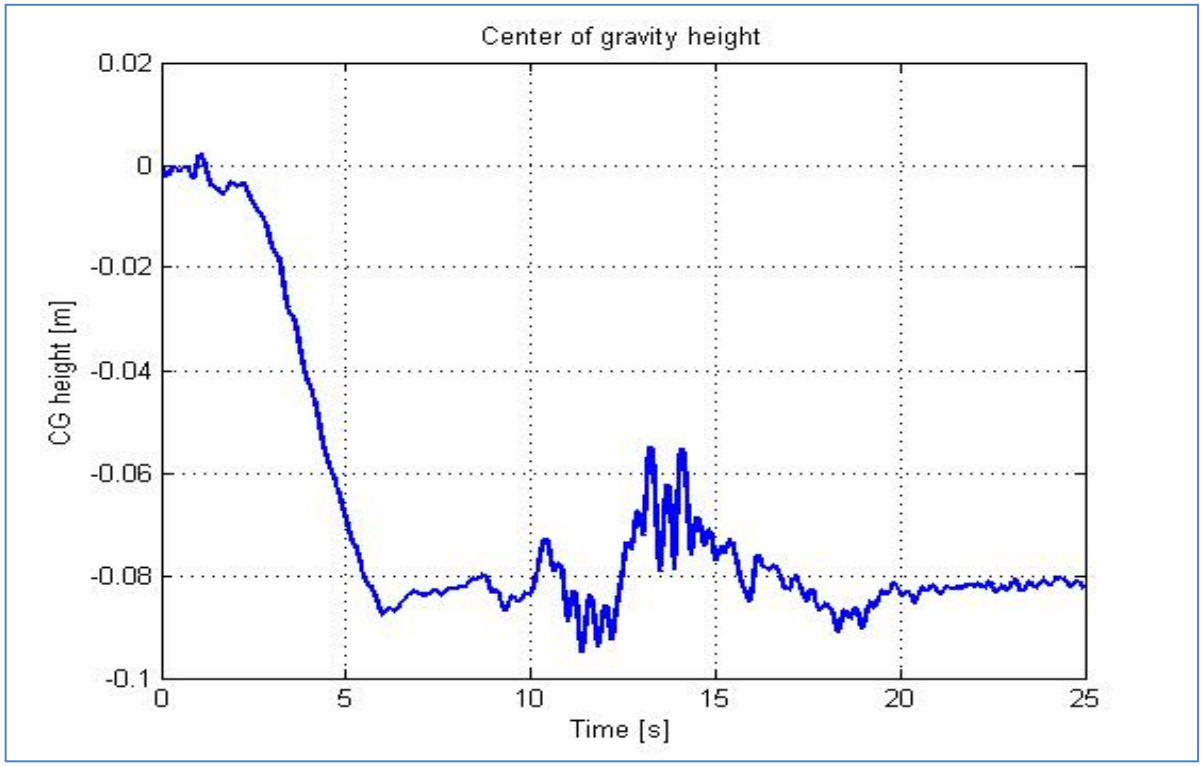

Figure 5.30: Fishhook 1B manoeuvre on rollover prevention mode, CG height change

At speeds of 80 km/h and above (and thus at 84 km/h), the control system has a maximum height reduction of 80mm to allow for an additional 40mm compression travel. From the data, the CG height does not show much oscillation.

The oil volume adjustments for each strut are presented in Figure 5.31:

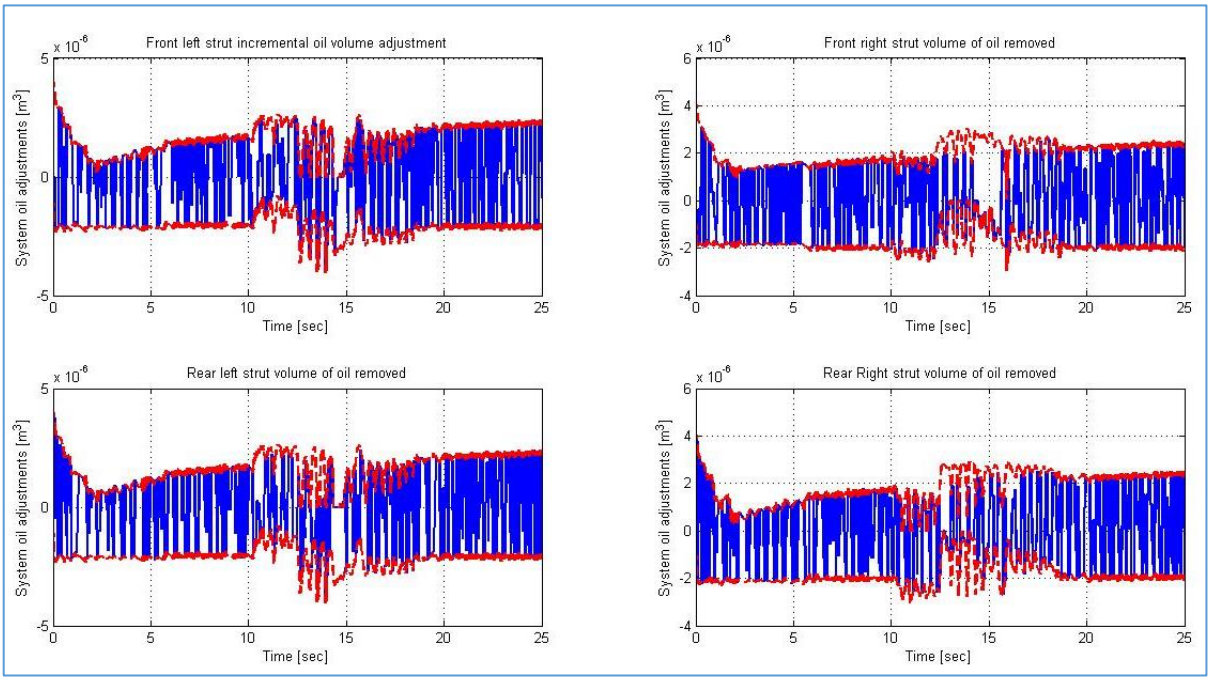

Figure 5.31: Fishhook 1B manoeuvre on rollover prevention mode, oil volume adjustment (incremental)

The volume adjustments from the PID are active for most of the time. This means that the valves will need a constant power supply. From the total volume change in the struts, it is evident that the adjustments are not smooth. Possible solutions could be to increase the damping of the PID controller or to take the average volume change over an interval; however, this may affect response times when a sudden height change is required. Thus the smoothness of the oil volume change is reduced to compensate for a quicker reaction time.

The total volume adjustments are presented in Figure 5.32:

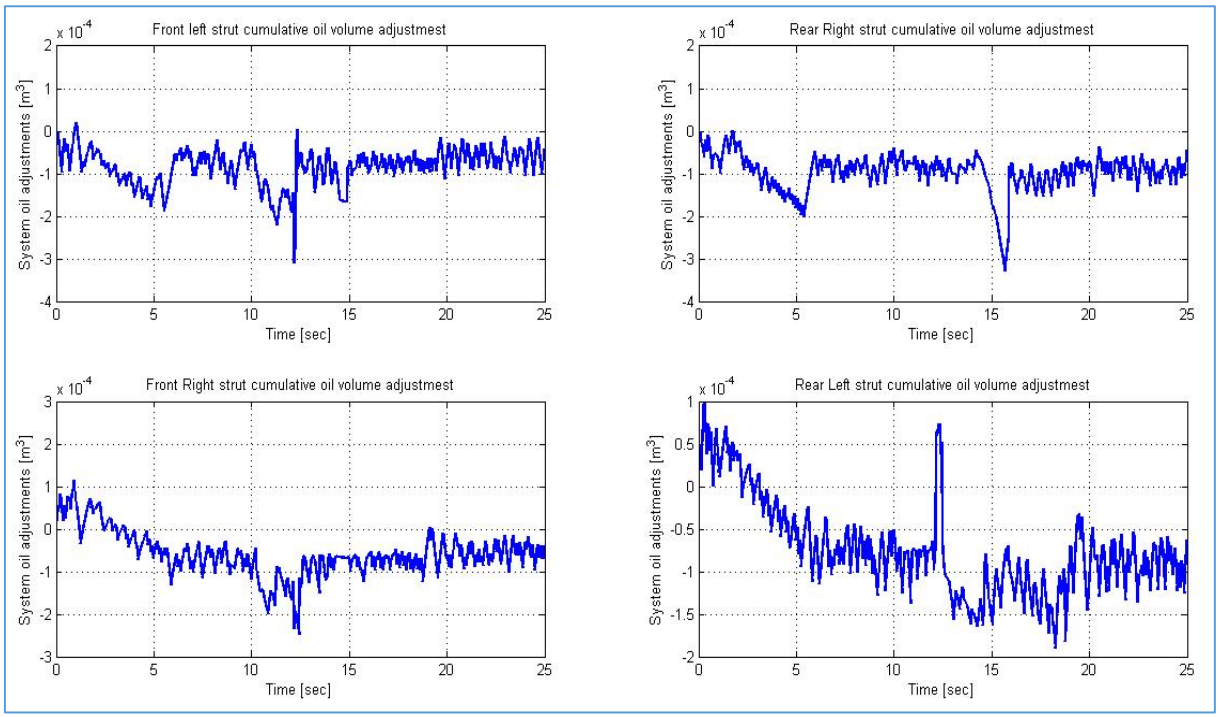

Figure 5.32: Fishhook 1B manoeuvre on rollover prevention mode, oil volume adjustment (total)

The flow rate (presented in Figure 5.33) is bounded by the available flow rate, which in turn is limited by the respective pressure differences.

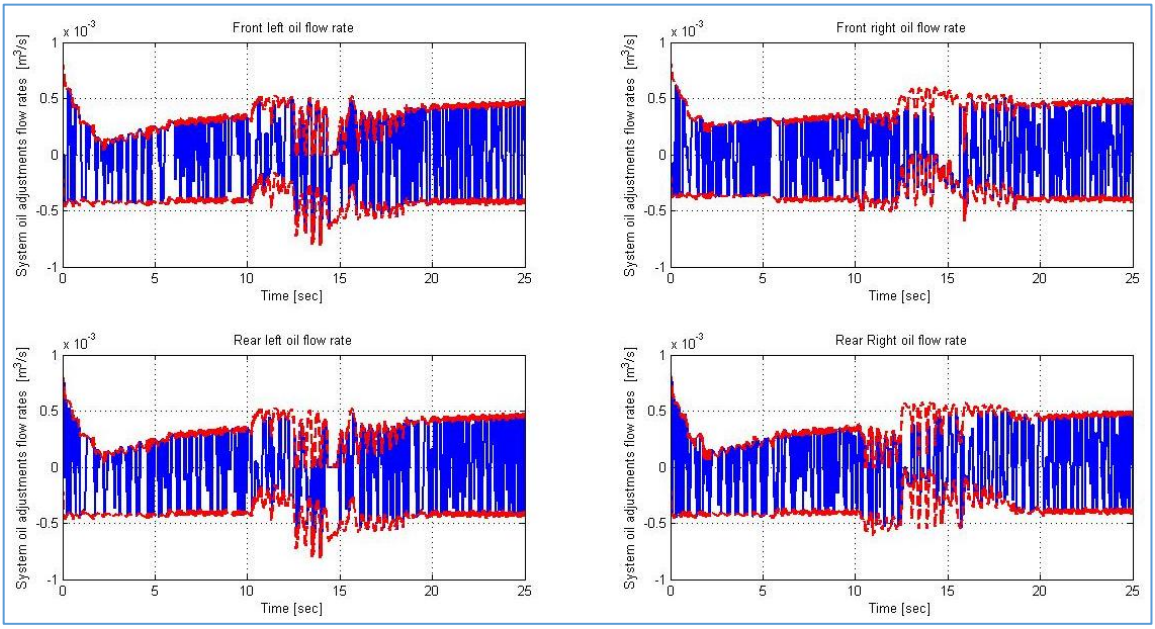

Figure 5.33: Fishhook 1B manoeuvre on rollover prevention mode, oil flow rates

Since the valves cannot add and remove oil at the same time, they are open for either one or the other action, or closed for both. This therefore limits the degree to which ideal suspension height can be attained.

The suspension settings are presented in Figure 5.34:

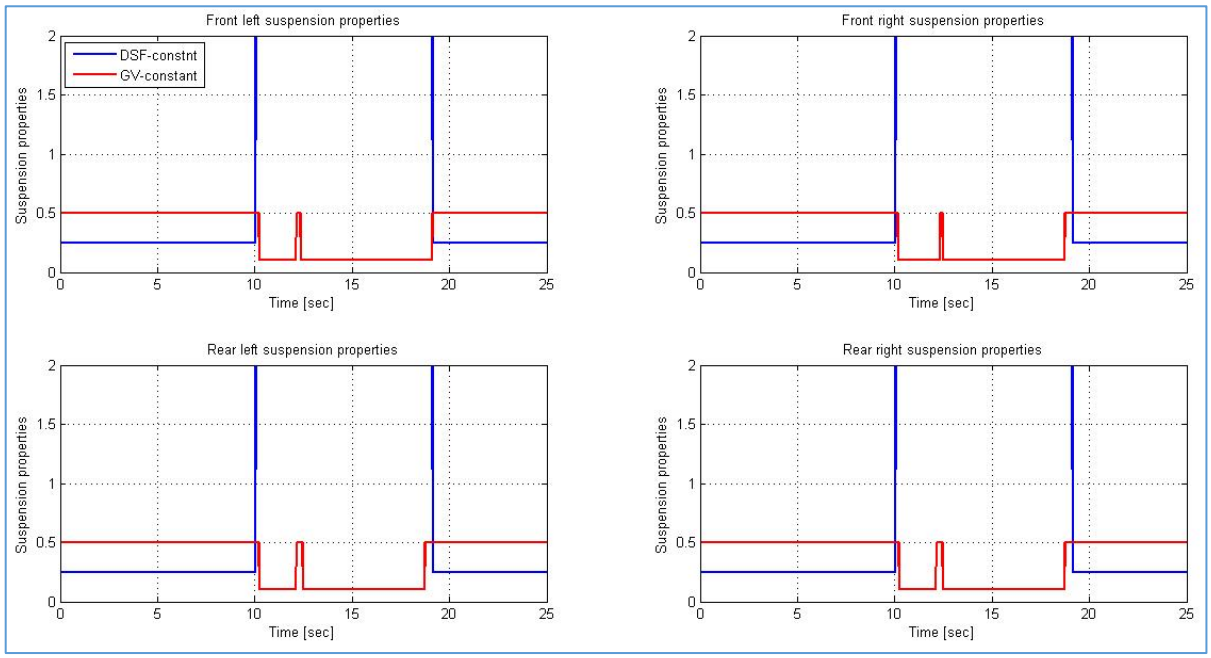

Figure 5.34: Fishhook 1B manoeuvre on rollover prevention mode, suspension settings

The data shows that the control system initiates high damping settings for the duration of the dynamic part of the manoeuvre and low damping for the remaining time. Thus roll energy is removed when needed and ride comfort can be maintained when good handling is no longer priority. The high damping is maintained for a short while after activation to account for possible counter-steer behaviour to remove energy from overshoot roll motions.

Similarly, the soft spring setting is used for when handling is not a priority and the hard for when it is crucial to reduce the roll angle and thus the load transfer to the outer wheels.

The gains of the PID control may be tuned and manually optimised using the respective error values in the PID control. Figure 5.35 depicts the PID error tracking during the simulation:

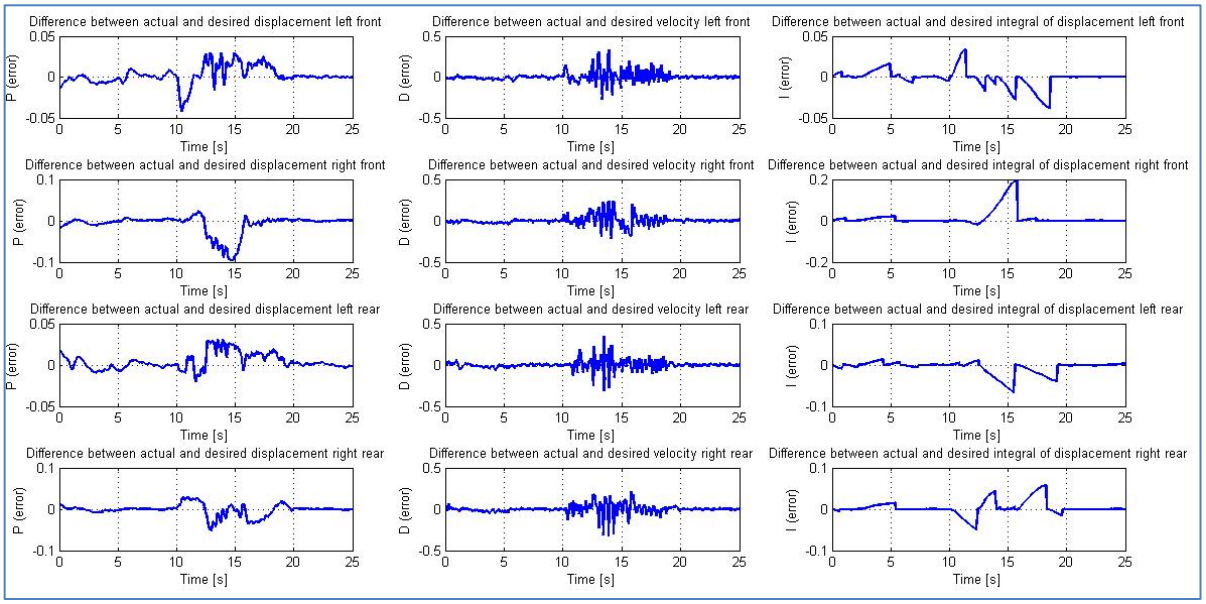

Figure 5.35: Fishhook 1B manoeuvre on rollover prevention mode, PID error tracking

The accumulator pressure of the hydraulic fluid from the slow active control system is of significant importance as it affects the maximum flow rate into the struts. As noted in chapter 3.1.3 above, the algorithm used to determine the accumulator pressure.

5.2.4 Rollover Index

The rollover index derived in chapter 3.2.2 as a function of thresholds was compared to the DSI and RPER to explore its ability to determine the threat of rollover. The SSF and DSI values for the manoeuvre are compared in Figure 5.36(a) and the RPER index is presented in Figure 5.36(b).

As stated in chapter 2.3.4, rollover is considered to occur when the DSI is greater than the SSF. The SSF is defined from the simulation value of the CG height. Thus, according to the DSI, the vehicle should have rolled after t=10 seconds; however, it remained upright. Although the DSI over-estimated the roll propensity of the modelled vehicle with the control system in place, it was an adequate predictor for the ride comfort mode without height adjustment.

The RPER predicts rollover in a similar region to the DSI, but is harder to interpret as the severity of rollover propensity is dependent on the slope of the RPER where it crosses zero.

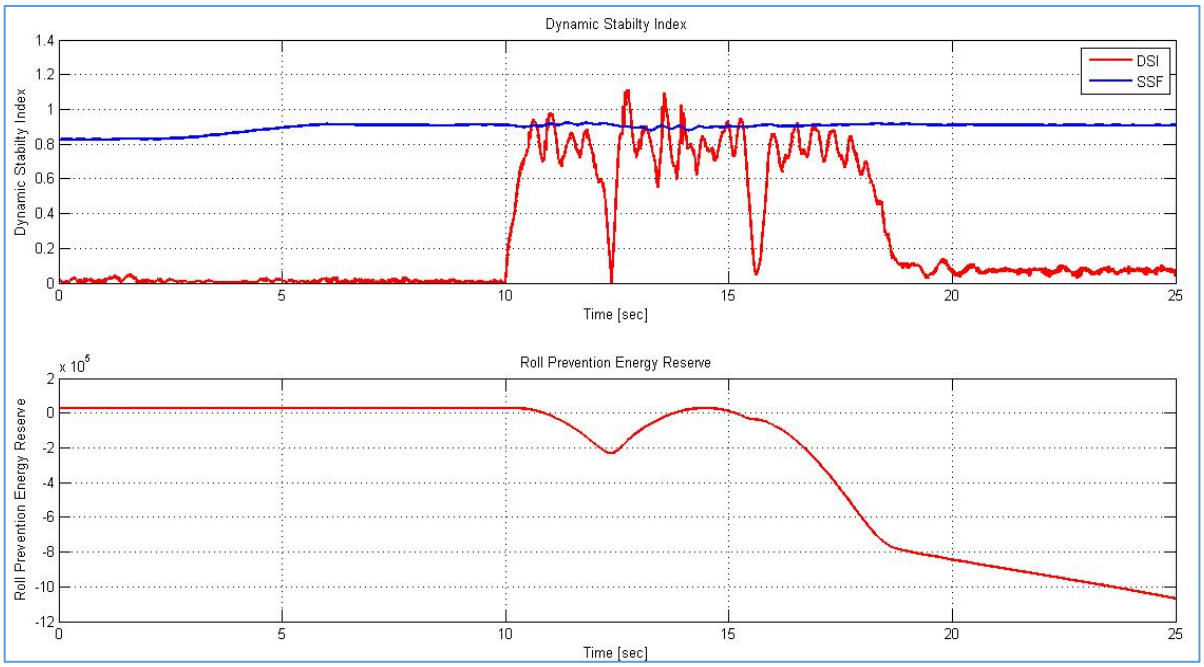

Figure 5.36: Fishhook 1B manoeuvre on rollover prevention mode, DSI and RPER

The rollover index defined from thresholds and used in the control algorithm is presented in Figure 5.37(a). In the plot below it (Figure 5.37(b)), the control algorithm position (cf. chapter 3.2.4) that was active in the control system throughout the simulation is displayed.

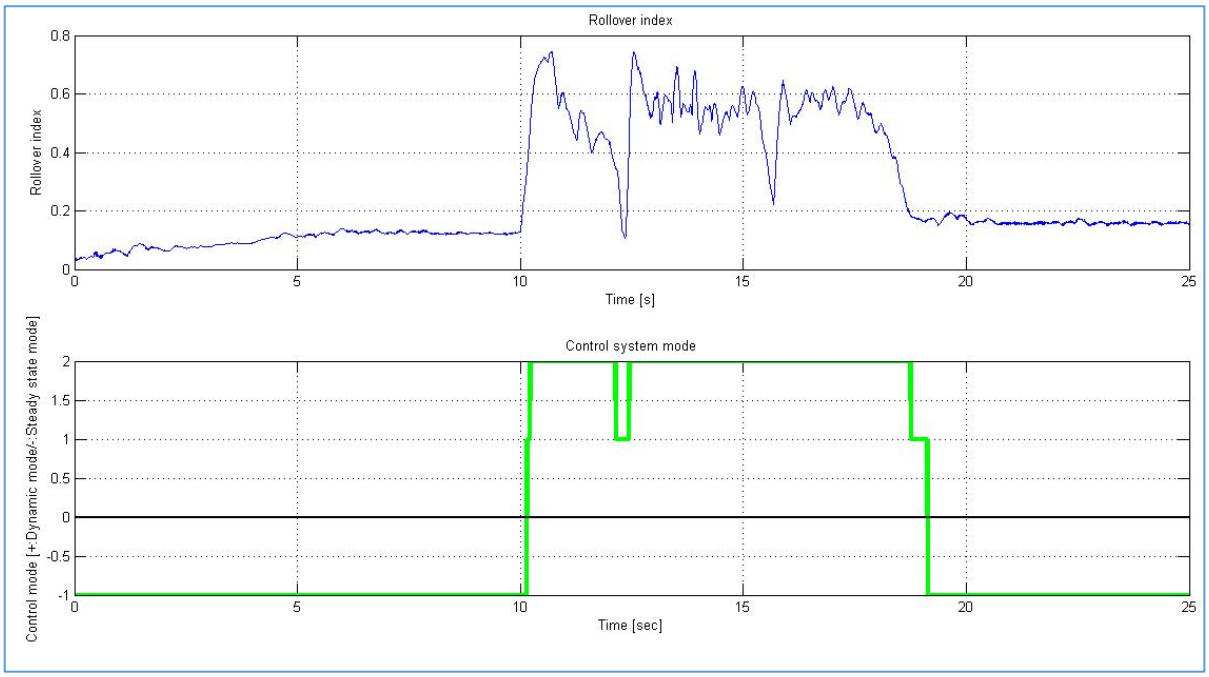

Figure 5.37: Fishhook 1B manoeuvre on rollover prevention mode, rollover prevention control system's rollover index

Both indices give a good reflection of the severity of the manoeuvre and the duration spent in it. As noted in chapter 3.2.2, the rollover index gives a non-zero value even during straight steady-state driving due to its dependence on vehicle speed (cf. Equation 3.9). The rollover severity of the initial overshoot that is responsible for many rollovers is well represented here as the initial peak of the rollover index. The index's maximum value occurs at the start of the steer inputs and decreases until the second steer input is given.

In the next section, the simulated ISO3888 DLC manoeuvre is discussed.

5.3 The ISO 3888 Double Lane Change

The DLC manoeuvre was simulated in order to evaluate the handling properties and roll sensitivity of the control system. The DLC simulations were performed at 60, 70 and 80 km/h and the ride comfort mode, handling mode and energy removal mode suspension settings were compared with the control system. These simulations used a driver model to perform the path following of the DLC. From the simulations performed, the 80 km/h simulation results are discussed below, since this is the limit for the control system height reduction, as well as the manoeuvre speed that exhibits the most dynamic behaviour for the speeds evaluated. The data for the DLC simulations at 60 and 70 km/h are presented in Appendix 7.5.

The steering performance for the four modes is presented in Figure 5.38:

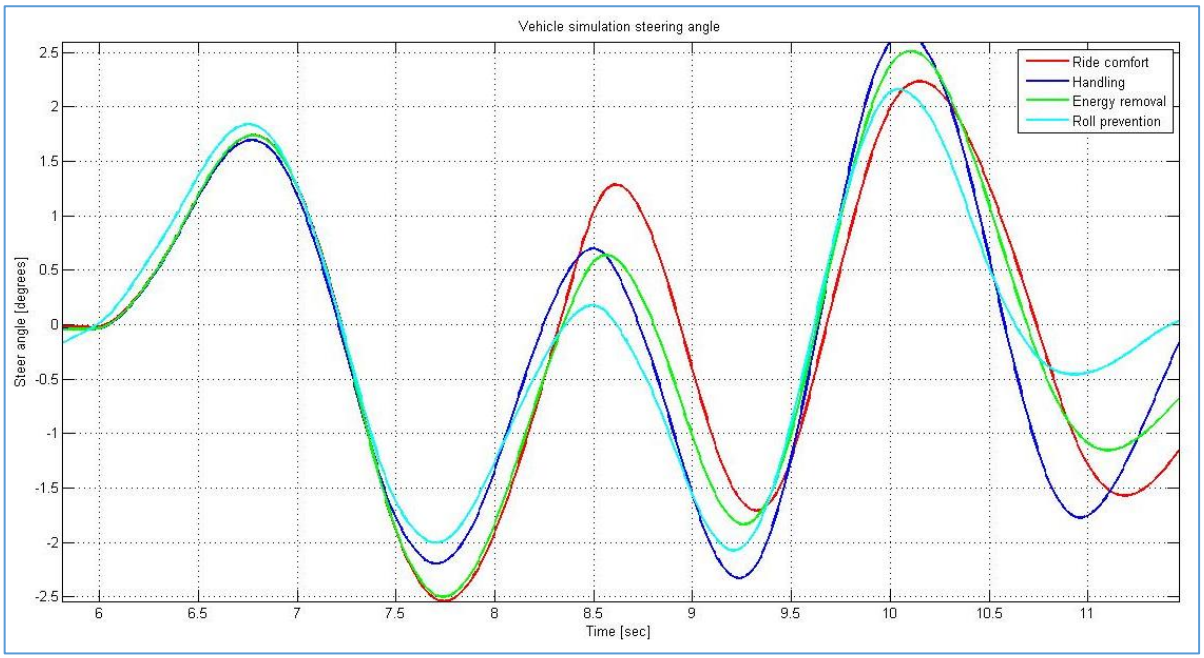

Figure 5.38: Double Lane Change at 80 km/h, steer input

The data shows that the rollover prevention algorithm generally required less steering angle input, thereby indicating greater vehicle controllability than the other configurations. There were also minor variances in the speeds for the different suspension settings, most likely due to lose of traction.

The model vehicle path is plotted in Figure 5.39 for the four modes:

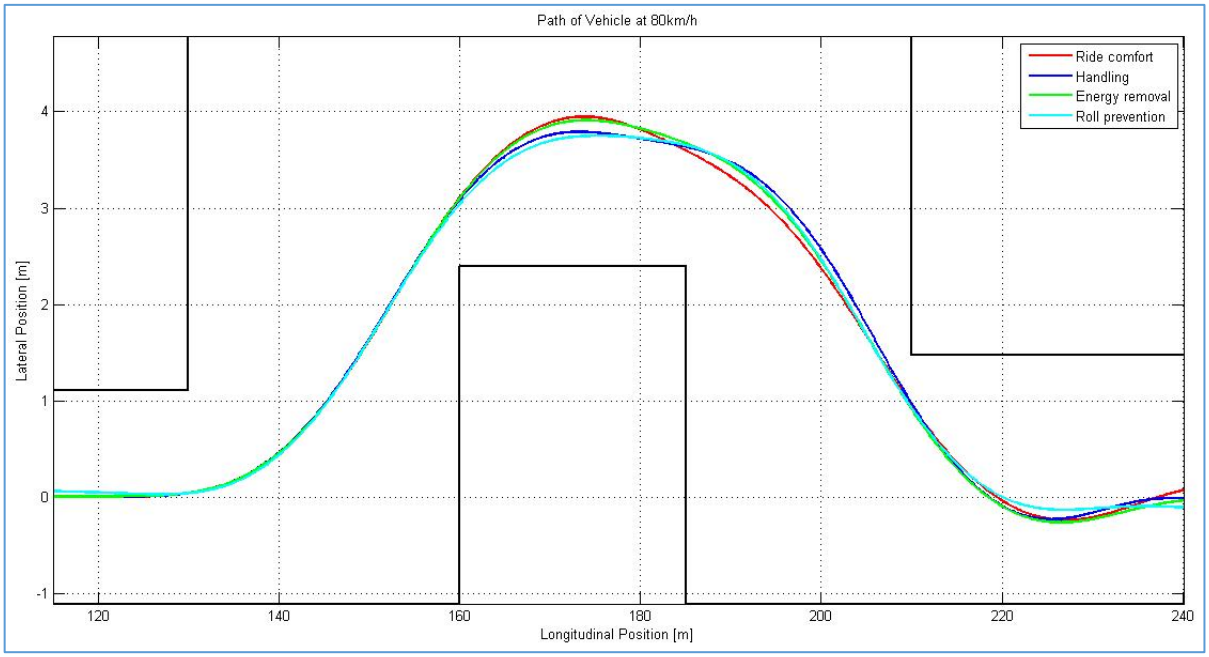

Figure 5.39: Double Lane Change at 80 km/h, vehicle path

The rollover prevention control algorithm presented the smoothest path thought the manoeuvre.

The dynamic parameters are presented in Figure 5.40:

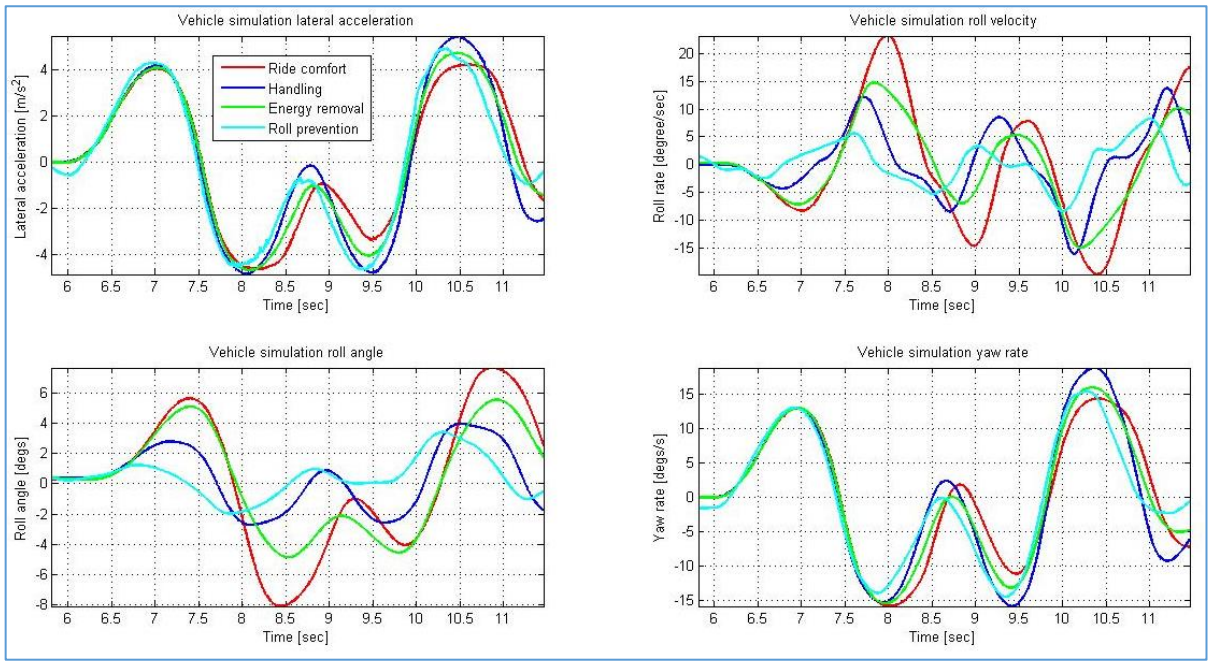

Figure 5.40: Double Lane Change at 80 km/h, lateral acceleration, roll rate, roll angle and yaw rate

The lateral acceleration for all tested configurations had similar results. The ride comfort mode exhibited the lowest overall lateral acceleration and the handling mode the highest overall lateral acceleration.

The smallest roll rate was exhibited by the rollover prevention control mode. It had a 52.6% reduction of maximum roll rate compared to the ride comfort mode, a 25.7% reduction of maximum roll rate compared to the energy removal mode and a 31.8% reduction of maximum roll rate compared to the handling mode. Reduction in the roll rate greatly reduces the risk of rollover from transient overshoot behaviour, providing strong confirmation that the designed rollover strategy is successful in minimising the threat of rollover.

Similarly, the control system gave the best results in terms of minimising the roll angle, showing a 13% improvement over the handling mode and a 56% improvement over the ride comfort mode with regard to maximum roll angle. These results confirm the importance of roll angle as a primary comparison criterion for the DLC. Optimizing the roll angle should reduce rollover tendency and improve safety. Roll angle also reflects on the handling of the vehicle since lower roll angles means the load is more evenly distributed. Lower roll angles are achieved through increasing the roll stiffness and reducing the CG height. Added roll angle adds a steering motion to the vehicle (roll steer) that steers the vehicle out of the corner.

The suspension displacements for each mode over each wheel are presented in Figure 5.41:

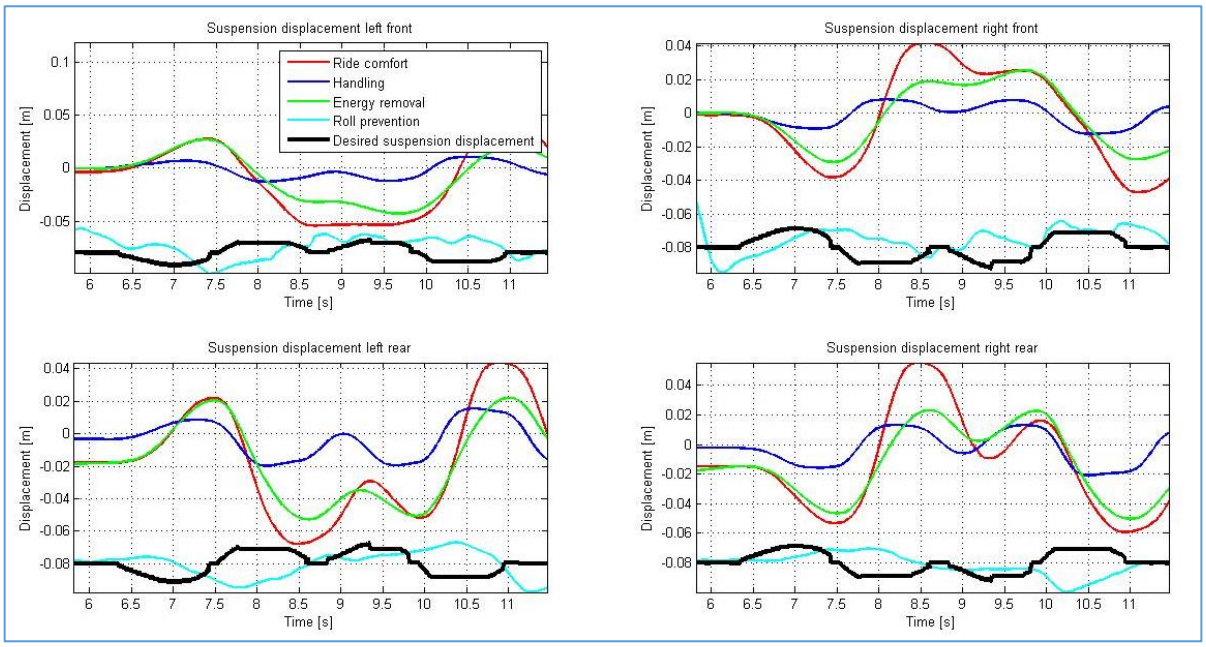

Figure 5.41: Double Lane Change at 80 km/h, suspension displacement

The data indicates that the control mode offered a significant improvement on suspension displacement compared to the other modes. Nevertheless, although the rollover prevention control is programmed to detect dynamic steering inputs and adjust the suspension height accordingly, the sudden inputs caused deviation from the desired heights, due to system limitations in adjustment rates.

The CG heights for the different modes are depicted in Figure 5.42. As in the previous simulations, the control model accessed maximum height reduction.

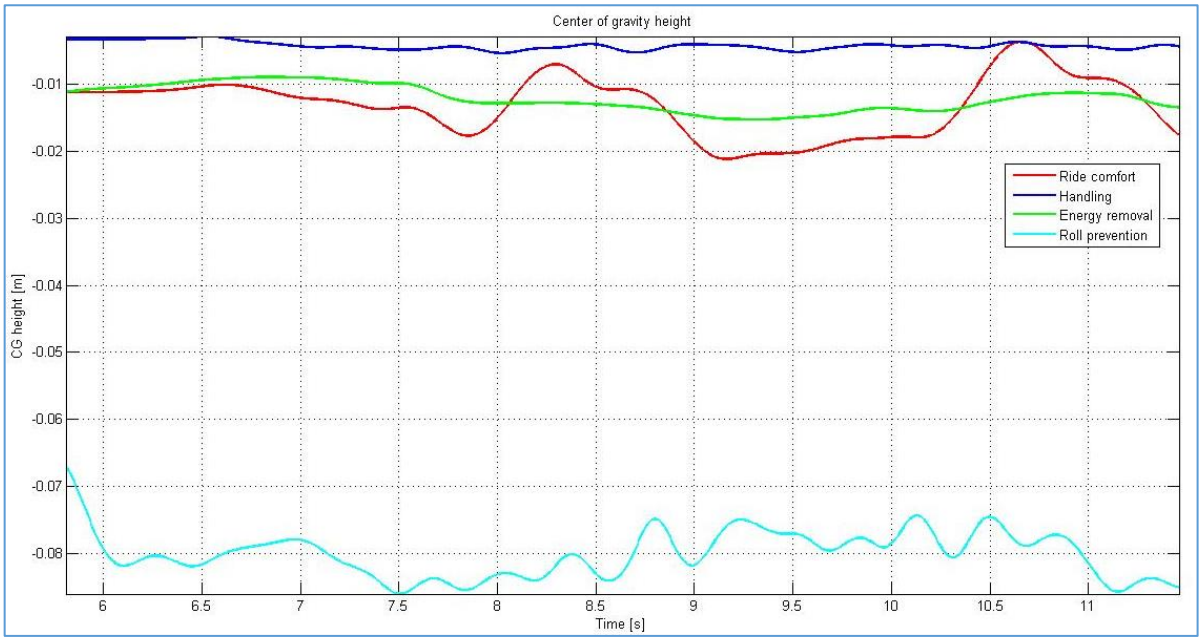

Figure 5.42: Double Lane Change at 80 km/h, CG height change

As the data shows, the CG height is maintained relatively constant at a reduction of 80mm, but the control system does appear to add some undesirable vertical oscillation. Refinement of the control

system in terms of ride comfort is beyond the scope of this study and is suggested as an avenue for future research.

The rollover index for the DLC manoeuvre was also investigated for the various modes and is presented in Figure 5.43:

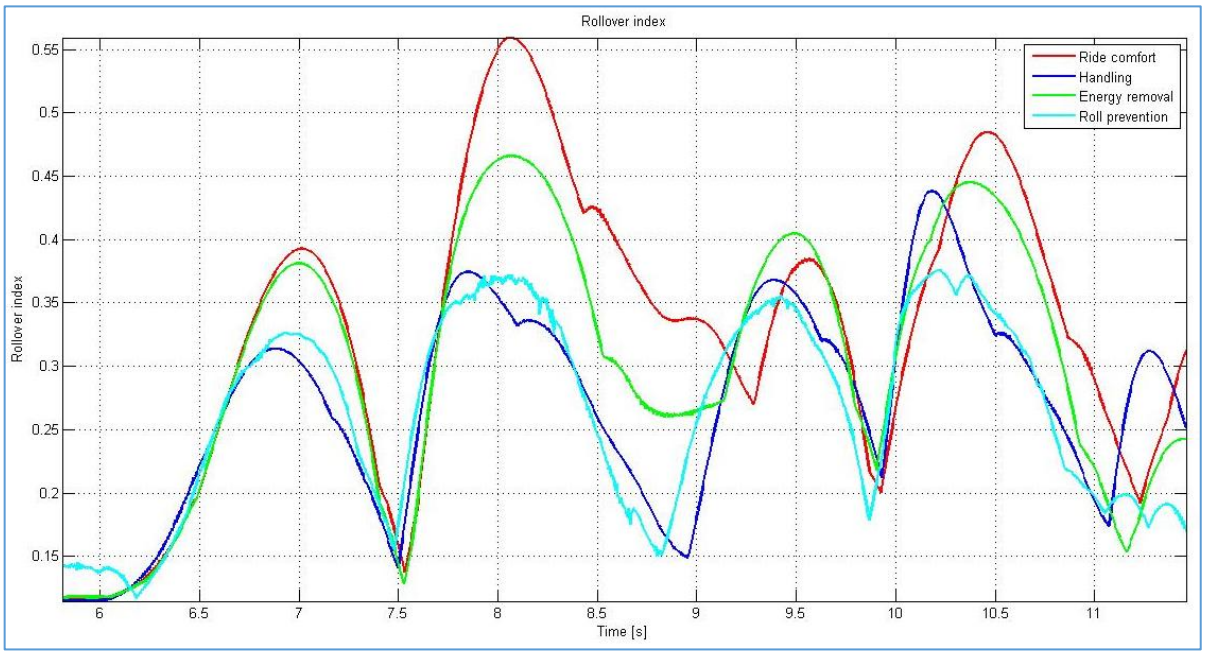

Figure 5.43: Double Lane Change at 80 km/h, rollover index from control system

According to the rollover index, the vehicle is far away from rollover for all modes. However, as the figure shows, a substantially lower index value was obtained for the handling and rollover prevention modes compared to the other two modes.

As noted in chapter 3.2.2, the index is compared in the study to the DSI and RPER. These are presented for the manoeuvre in Figure 3.44:

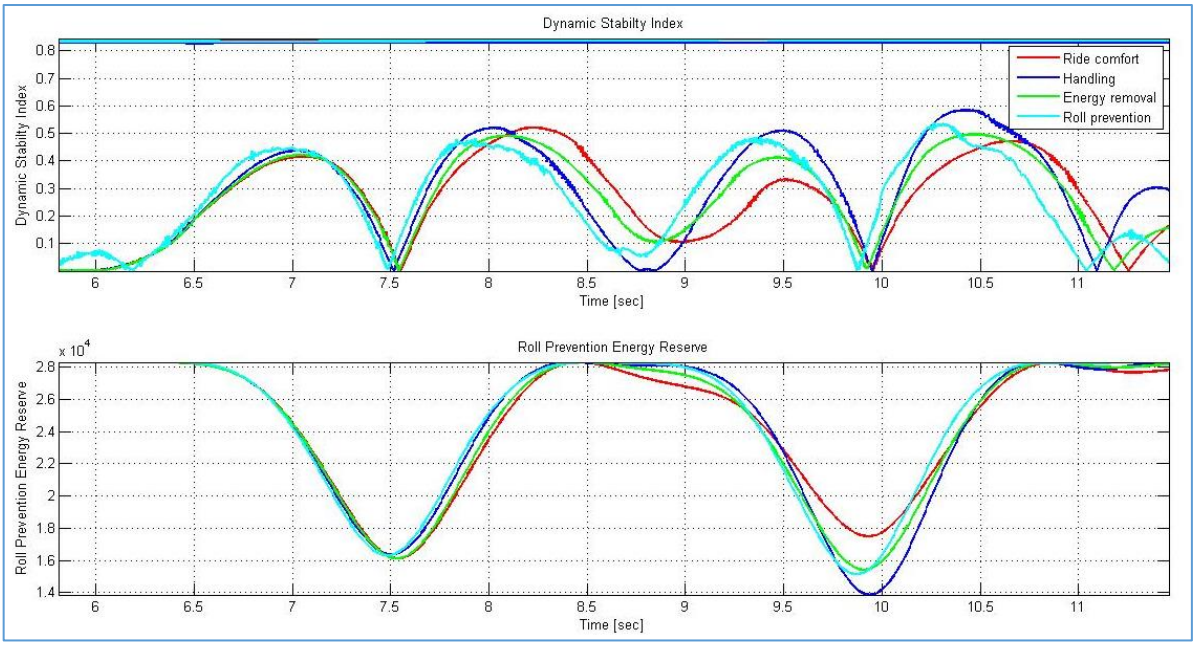

Figure 5.44: Double Lane Change at 80 km/h, DSI and RPER

The DSI also indicates rollover to be far away, but suggests that the handling mode is slightly more prone to rolling over. In contrast, during the validation simulations reported in chapter 4, it was observed that the handling mode substantially reduced rollover tendencies. This indicates that the derived rollover index gives a more realistic indication of the threat of rollover.

Although the RPER also reported no risk of rollover, it does not present a convenient graphical method of determining the degree of the threat of rollover, whereas the derived rollover index does.

5.4 Conclusion

Manoeuvres used to define some of the limits of the test vehicle with regard to rollover were discussed. The step-steer manoeuvre is used to investigate vehicle thresholds with regard to body roll angle, roll rate, lateral acceleration, yaw rate, speed and steering angle. The step-steer manoeuvre simulations are performed without the implementation of any control system. The findings from these simulations help define the rollover prevention algorithm. Simulation manoeuvres are also used to define the test vehicle for comparison between the original setup and the setup with the rollover prevention control in place. This evaluation test may be used in future to compare the test vehicle with other vehicles with regard to rollover.

Table 5-6 summarises the study results for the manoeuvres performed:

Table 5-6: Analysis of test manoeuvres

Test manoeuvre	Manoeuvre analysis	Result
Step-steer	Defining vehicle rollover parameters for roll angle, roll rate, yaw rate, lateral acceleration and wheel lift.	Improved performance
Fishhook 1B	Determining the vehicles propensity to rollover by evaluating the maximum maneuver speed. Evaluating the performance of the rollover prevention control system.	Improved performance
DLC	Evaluating the handling performance of the vehicle with the implement control system	Improved performance

Over 230 step-steer manoeuvre simulations were performed, allowing vehicle thresholds to be defined for roll angle, roll rate, lateral acceleration, yaw rate and suspension characteristics. The thresholds were derived from the suspension characteristics setting of those that exhibited the best with regard to vehicle ride comfort mode. The maximum wheel lift of the inner rear wheel exhibited the smoothest transition up until rollover for the ride comfort mode and roll rate exhibited the best indicator up until rollover for the other modes.

The propensity of the vehicle towards rollover was investigated with the Fishhook 1B test manoeuvre, regarded by the NHTSA to be the best test for observing vehicle rollover. The SIS steering angle was modified to exhibit stronger propensity to rollover. The control system significantly improved the vehicle dynamic response. The control strategy improved the maximum speed that the vehicle was able to execute the manoeuvre by 133% compared to ride comfort mode and by 64% compared to the handling mode, where the vehicle did not experience wheel lift of more than 2 inches. The implemented rollover prevention control strategy allowed the vehicle to experience speeds up to 140 km/h without the vehicle overturning.

The control system was investigated with DLC simulation with the highest speed being 80 km/h. The control system greatly reduces the body roll angle by a 13% improvement over the handling mode and by a 56% improvement over the ride comfort mode. The maximum roll rate was also significantly reduces with a 52.6% reduction in the ride comfort mode, a 25.7% reduction in the energy removal mode and a 31.8% reduction in the handling mode.

6 CONCLUSION AND RECOMMENDATIONS

6.1 Conclusion

This study set out to develop a rollover prevention control system for Sports Utility Vehicles which reduces the sprung mass centre of gravity height of the vehicle using slow active control. The control system has to be able to detect when the vehicle is close to the limit of rollover and set the suspension to aid the prevention of rollover.

The Vehicle Dynamics Group of the University of Pretoria have a Land Rover Defender 110 Sports Utility Vehicle that was used to develop the rollover prevention control system. The Vehicle Dynamics Group perform regular tests on the vehicle and most of the parameters and properties of the vehicle are known as well as a full vehicle ADAMS mathematical model of the vehicle was available for simulation.

A rollover detection algorithm was developed to report the response of the test vehicle to a manoeuvre with regard to rollover. The detection algorithm reports the propensity of rollover in terms of a roll index. The index was based on threshold of the test vehicle determined from step input simulations similar to constant radius manoeuvres. The index ranges from zero to one, where one is the rollover resistance limit of the vehicle. The control system applies one of three discrete suspension settings depending on the severity of the manoeuvre as well as lowering the ride height. The rollover prevention control system was evaluated using the Fishhook 1B manoeuvre as well as the ISO 3888 Double lane change manoeuvre **(ISO, 1975)**.

The rollover prevention control system and test vehicle were successfully modelled. The rollover prevention control system significantly improved the vehicle's response with regard to smooth flat on road untripped rollover. The rollover prevention control system improved the two wheel lift off speed of the vehicle through a Fishhook 1 B manoeuvre by 64% and the body roll angle of the vehicle through the Double Lane Change manoeuvre by 13% and the body roll rate by 25.7%.

6.2 Recommendation

Due to time limitations or exceeding the scope of the present project, the following improvements and further studies are made to improve performance and contribute towards the study of rollover prevention:

- Modelling of the hydraulic slow active suspension control was developed by **Van der Westhuizen (2012)**. Although some of the hydraulic circuit is modelled for simulation many of the components have been disregarded or simplified due to added complexity. However addition modelling of the system may account for internal fluid and pressure losses resulting in improved model accuracy.
- The PID controller in this study was optimised by trial and error to obtain acceptable compensation between fast response times and false activations for each individual strut. However the PID controller gains may still be further optimised to incorporate for ride comfort with optimisation undertaken in a more systematic manner
- A limitation of the present study was that the PID was designed in continuous-time but implemented in a discrete-time simulation, introducing instability in that the discrete controller values do not correspond to the continuous-time values. Therefore, a discrete-time controller is proposed for future research.

- For the dynamic mode, the PID controller could be replaced by an advance dynamic controller (such as a state space controller). The H_∞ control system could be used to synthesize stabilization with guaranteed performance, however it requires a good model of the system to be controlled and complex mathematical understanding (cf. Gasper et al., 2005). For example, **Jin et al. (2016)** investigate tripped and untripped vehicle rollover using an H-infinity controller to provide robustness to complex road conditions, the variation of the number of passenger, and other external interference. The H-infinity control operates in a stable environment and provides good control for the vehicle rollover system. The controller calculated the required anti-yaw torque to be provided by an Electro Hydraulic Brake (EHB) system. The controller effectively predicted and improved the stability of vehicle rollover for both untripped and special tripped situation.
- As this was part of a group project, the $4S_4$ suspension was the one used by default by the university Vehicle Dynamics team. However improved simulation results have been found using an interconnected suspension system (Smith & Walker 2004; Yao et al. 2015), and this use of such an interconnected system is proposed for future research.
- A simplified version of the Pacejka 89 tyre model was used in the present study since the study was undertaken as part of the university vehicle team's projects. However, it is suggested for future studies that the PAC2002 (or subsequent updates thereof) tyre model will deliver greater accuracy in results, especially for the double lane change (i.e. combined modes).
- The rollover detection algorithm may be greatly improved with the addition of a vehicle preview model. The preview model uses vehicle parameters and measured inputs such as steering angle and longitudinal vehicle speed to predict vehicle behaviour for a given preview. Accuracy is normal compensated for longer preview time. Preview vehicle models are readily available however are complex and require substantial time to be characterized for the test vehicle. Preview models allow for prediction of rollover before the event occurs. They are fundamental to overcoming system delays. Thus allowing for early prevention of rollover before the vehicle's critical limits are reached.
- The addition of other rollover prevention systems such as differential braking can also be incorporated into the rollover prevention algorithm. Most modern commercial vehicles are fitted with electronic braking making it an ideal addition. This will help prevent uncontrollable slide outs, allow for better path following and ultimately increase manoeuvre safety.
- The use of filters to attenuate the proportional effects is one of the classical trade-offs in handling control. This could be better tackled by designing a lead-lad controller using loop-shaping objectives.
- The relative error method **(Kat, 2012)** was used to quantify the accuracy of the simulation model, however it is common practice in model validation to use the normalised root mean square metric and thus is suggested as a consideration for future research.
- In the present study, the lateral stability was analysed by roll angle, roll rate, yaw rate, lateral acceleration and wheel lift However, calculating the relationship between the yaw rate and the vehicle sideslip angle would have been another efficient way of correlating lateral stability with rollover and is recommended for future research.
- Vehicle roll motion is strongly influence by suspension design and changing the hardpoint locations of the suspension can improve the vehicle roll motion. Suspension geometry is primarily characterized by toe angle, camber angle, roll centre height, caster angle and

kingpin inclination angle **(Shim & Velusamy 2011)**. These parameter can be set to improve the vehicle's rollover tendency by adjusting the understeer tendency. In the future, it is suggested to include detailed suspension kinematics optimization as well as to improve lateral and longitudinal force compliance. This may be done by modelling the rubber bushings in the suspension and steering sub-systems to alleviate metal-to-metal friction in kinematic motion **(Shim & Ghike, 2007; Shim & Velusamy, 2011).**

- The lateral load transfer ratio (LTR) describing rollover as a function of load distribution has been widely studies and can be used to improve rollover prediction **(cf. Imine et al., 2014; Zhang et al.,2017)** as well as control **(Jin et al., 2016)**. As the present study was already underway, these new advances could not be incorporated and are suggested for future research into rollover prediction. For example, **Jin et al. (2016)** used a modified LTR rollover index in conjunction with their improved H-infinity controller to detect untripped and special tripped situations using measured vertical accelerations of the sprung mass and unsprung mass, lateral acceleration and roll angle. The controller effectively predicted and improved the stability of vehicle rollover for both untripped and special tripped situation. **(Imine et al., 2014)** predicted heavy-vehicle rollover risk using a LTR rollover indicator. and a HOSM observer to estimate the vertical forces. The robustness is confirmed using zigzag and braking tests. The LTR is used to issue the driver a warning to reduce speed if the LTR exceeds to the limit (0.2). **(Zhang et al., 2017)** investigated the LTR in the roll phase plane for various ramp steering manoeuvres and derived a prediction model based on the contour line load transfer ratio (CL-LTR), defined using a ramp input lateral acceleration for static rollover and a step-input lateral acceleration for dynamic rollover for a 1 DOF roll model which they extended to a full vehicle model. The prediction of vehicle rollover threat is achieved by setting a prediction time and the vehicle is considered to be in danger of rollover if the time calculated for the CLRI is less than the selected prediction time
- The complexity of rollover prevention studies lies in the number of variables that need to be considered. Hence most studies to date focus on only a particular intervention. As knowledge in this field grows, it is envisaged that future studies will focus on investigating combination of interventions, i.e. integrated control mechanisms **(Gasper et al., 2017)**.

7 REFERENCES

Ackermann, J. and Odenthal, D. (1998), Robust steering control for active rollover avoidance of vehicles with elevated center of gravity. In *Proceedings of International Conference of Advances in Vehicle Control and Safety*, Amiens, France, July 1998.

Armscor Defence Institutes (2014), *Gerotek Test Facilities.* [Online] Available from: http://www.armscordi.com/SubSites/Gerotek1/Gerotek01_landing.asp [Accessed 19 June 2014].

Bauer, W. (2011), *Hydropneumatic Suspension Systems*, Heidelberg: Springer.

Botha, T. (2011), *High Speed Autonomous Off-Road Vehicle Steering*, University of Pretoria, Pretoria, http://upetd.up.ac.za/thesis/available/etd-11212011-125411/unrestricted/dissertation.pdf [Accessed 21 October 2013].

Chen, B. and Peng, H. (1999), A real-time rollover threat index for sports utility vehicles. In *Proceedings of the American Control Conference*. *San Diego, CA, USA, 2nd to 4th Jun 1999*. Piscataway: IEEE, 1233-1237.

Chen, B. and Peng, H. (2010), Differential-Braking-Based Rollover Prevention for Sport Utility Vehicles with Human-in-the-loop Evaluations. *Vehicle Systems Dynamics* 36:4-5, 359-389.

Clark, J. (2004), *Rollover Sensing Using Tire Pressure Sensors.* US 2005/0033549 A1.

Cronjé, P. and Els, P. (2009), Improving off-road vehicle handling using an active anti-roll bar. *Journal of Terramechanics* 47, 179-189.

Cronje, P. (2008), *Improving off-road vehicle handling using an active anti-roll bar*, Pretoria: University of Pretoria. http://upetd.up.ac.za/thesis/available/etd-11262009-011206/unrestricted/dissertation.pdf. [Accessed 21 October 2013].

Dukkipati, R., Pang, J., Qatu, M., Sheng, G. and Shuguang, Z. (2008), *Road Vehicle Dynamics*. USA: SAE International.

Eisele, D. and Peng, H. (2000), Vehicle Dynamics Control with Rollover Prevention for Articulated Heavy Trucks, In *Proceedings of AVEC.* Ann Arbor, MI: AVEC.

Els, P. (2006), *The Ride Comfort vs. Handling Compromise for Off-Road Vehicle.* Thesis Submitted in partial fulfilment of the Requirements of the University of Pretoria for the Degree of Doctor of Philosophy. Pretoria: University of Pretoria.

Ervin, R. (1998), Cooperative agreement to foster the deployment of a heavy vehicle intelligent dynamic stability enhancement system, University of Michigan Transportation Research Institute, Interim report, NHTSA -U.S. DOT Contract No. DTNH22-95-H-07002.

Farmer, C. (2004), Effect of electronic stability control on automobile crash risk. *Traffic Injury Prevention* 5:4, 317-325.

Forkenbrock, G., Garrott W., Heitz, M. and O'Harra B. (2002), *A Comprehensive Experimental Examination of Test Maneuvers That May Induce On-Road, Untripped, Light Vehicle Rollover - Phase*

IV of NHTSA's Light Vehicle Rollover Research Program. National Highway Traffic Safety Administration. DOT HS 809 513.

Forkenbrock, G., O'Harra, B. and Elsasser, D. (2004) *A Demonstration of the Dynamic Tests Developed for NHTSA's NCAP Rollover Rating System - Phase VIII of NHTSA's Light Vehicle Rollover Research Program.* National Highway Traffic Safety Administration. DOT HS 809 705.

Furukawa, Y., Yuhara, N., Sano, S., Takeda, H. and Matsushita, Y. (1989), A review of four-wheel steering studies from the viewpoint of vehicle dynamics and control. *Vehicle System Dynamics* 18:1-3, 151-186.

Gasper, P., Bokor, J. and Szaszi, I. (2004), The design of a combined control structure to prevent the rollover of heavy vehicles. *European Journal of Control* 10:2, 148-162.

Gasper, P., Szabo, Z. and Bokor, J. (2005), Brake control combined with prediction to prevent the rollover of heavy vehicles. *IFAC Proceedings* 38:1, 248-253.

Gasper, P., Szabo, Z., Bokor, J. and Nemeth, B. (2017), *Robust control design for active driver assistance systems.* Berlin: Springer.

Gillespie, T. (1992), *Fundamentals of Vehicle Dynamics*. Warrendale, PA: Society of Automotive Engineers.

Grip, H., Imsland, L., Johansen, T., Kalkkuhl, J., and Suissa A. (2009), *Vehicle Sideslip Estimation Design, implementation, and experimental validation.* IEEE CONTROL SYSTEMS MAGAZINE

Hac, A. (2002), Influence of Active Chassis Systems on Vehicle Propensity to Manoeuvre-Induced Rollovers. SAE paper 2002-01-0967.

Hac, A., Brown, T. and Martens, J. (2004), Detection of Vehicle Rollover. *SAE World Congress.* Detroit, Michigan, March 8-11 2004. Warrendale. SAE.

[ISO] International Organisation for Standardisation (1975), *International Organisation for Standardisation ISO 3888-1975: Road vehicles – test procedure for a severe lane – change manoeuvre*, ISO/TR 3888-1975.

Imine, H., Fridman, LM. and Madani, T. (2012), *Steering Control for Rollover Avoidance of Heavy Vehicles*. IEEE Transactions on Vehicular Technology 61:8, 3499-3509.

Imine H, Benallegue A, Madani T., and Srairi, S. (2014), Rollover risk prediction of heavy vehicle using high-order sliding-mode observer experimental results*. IEEE Trans Vehicle Technology* 63:6, 2533 – 2543.

Jazar, R. (2008), *Vehicle Dynamics Theory and Application*. Berlin: Springer.

Jin ZL., Zhang L., Zhang JL. and Khajepour, A. (2016), Stability and optimised H_∞ control of tripped and untripped vehicle rollover*. Vehicle Systems Dynamics* 54:10, 1405-1427.

Kat, C. (2012), Validation metric based on relative error, Mathematical and Computer Modelling of Dynamical Systems: Methods, Tools and Applications in Engineering and Related Sciences, 18:5, 487-520, DOI: 10.1080/13873954.2012.663392.

Lu, J. and Brown, T. (2004), Rollover Stability Control for an Automotive vehicle using Rear Wheel Steering and Brake Control. Unite States Patent. Patent No. US 6,799,092 B2.

Marine, M., Wirth, J. and Thomas, T. (1999), Characteristics of On-Road Rollovers, SAE paper No. 1999-01-0122.

Masato, A. (2009), *Vehicle Handling Dynamics-Theory and Application*. Butterworth: Heinemann.

Miege, A. and Cebon, D. (2011), Optimal roll control of an articulated vehicle: theory and model validation. *Vehicle System Dynamics* 43:12, 867-884.

MSC.Software (2013), *MSC.ADAMS Multibody Dynamics*. http://www.mscsoftware.com/Products/CAE-Tools/MSC.ADAMS.aspx. [Accessed: 8 October 2013].

[NHTSA] National Highway Traffic Safety Administration (2011), Rollover data special study final report. http://www.nhtsa.gov/search?q=rollover+data. [Accessed: 5 March 2013].

Nishio, A., Tozu, K., Yanguchi, H. Asano, K. and Amano, Y. (2001), Development of vehicle stability control system based on vehicle sideslip angle estimation. SAE paper No. 2001-01-0137.

[RTMC] Road Traffic Management Corporation (2009), *Road Traffic Report for the Calendar Year 2009*. http://www.arrivealive.co.za/documents/Year_2009_-_Road_Traffic_Report_-_V2.pdf. [Accessed: 6 October 2013].

Sampson, D. and Cebon, D. (1998), An investigation of roll control system design for articulated heavy vehicles. In *Proceedings of the 4th International Symposium on Advanced Vehicle Control, Nagoya, Japan*, pp 311–316. http://david.sampson.id.au/work/avec-1998.pdf. [Accessed: 4 February 2018].

Sampson, D. and Cebon, D. (2003a), Achievable roll stability of heavy road vehicles. In *Proc. Instn. Mech. Engineers, Part D. Automobile Engineering* 217:4, 269-287.

Samson, D. and Cebon, D. (2003b), Active roll control of single unit heavy road vehicles. *Vehicle System Dynamics* 40:4, 229-270.

Shim, T. and Ghike, C. (2007), Understanding the limitations of different vehicle models for roll dynamics studies. *Vehicle System Dynamics* 45:3, 191-216.

Shim, T. and Velusamy, P. (2011), Improvement of vehicle roll stability by varying suspension properties. *Vehicle System Dynamics* 49:1-2, 129-152.

Smith, W., Zhang, N. and Hu, W. (2011), Hydraulically interconnected vehicle suspension: handling performance. *Vehicle System Dynamics* 49:1-2, 87 – 106.

Stone Hydraulics (2012), *Pump Kits*, http://www.stonehydraulics.com/catalog/47-2007.pdf, [Accessed: 7 August 2012].

Thoresson, M. (2003), *Mathematical Optimisation of the Suspension System of an Off-Road Vehicle for Ride Comfort and Handling*. Thesis Submitted in partial fulfilment of the Requirements of University of Pretoria for the Degree of Master of Engineering. Pretoria: University of Pretoria.

Thoresson, M. (2007), *Efficient gradient-based optimisation of suspension characteristics for an off-road vehicle*, Unpublished PhD thesis, Pretoria: University of Pretoria. upetd.up.ac.za/thesis/available/etd-08042008-093103/. [Accessed 16 October 2013].

Uys, B. (2007), *Omrol van Veldvoertuie*. Thesis Submitted in partial fulfilment of the Requirements for the Degree of Master of Engineering in the Faculty of Engineering, Built Environment and Information Technology at the University of Pretoria. Pretoria: University of Pretoria.

Uys, P., Els, P., Thoresson, M., Voight, K., and Combrinck, W. (2006), Experimental determination of moments of inertia for an off-road vehicle in a regular engineering laboratory. *International Journal of Mechanical Engineering Education* 34:4, 291-314.

Uys, P., Els, P. and Thoresson, M. (2007), Suspension settings for optimal ride comfort of offroad vehicles travelling on roads with different roughness and speeds, *Journal of Terramechanics* 44, 163-175.

Van der Westhuizen, S. (2012), *Slow Active Suspension Control for Rollover Prevention.* Thesis Submitted in partial fulfilment of the Requirements for the Degree of Master of Engineering in the Faculty of Engineering, Built Environment and Information Technology at the University of Pretoria. Pretoria: University of Pretoria.

Whitehead, R., Travis, W., Bevly, D. and Flowers, G. (2004), A study of the effect of various vehicle properties on rollover propensity. SAE Paper No. 2004-01-2094.

Zhang, N., Wang, L. and Du, H. (2014), Motion-mode energy method for vehicle dynamics analysis and control. *Vehicle System Dynamics* 52:1, 1-25.

Zhang, XJ., Yang, Y., Guo, K., Lv, JM. and Peng, T. (2017), Contour line of load transfer ratio for vehicle rollover prediction*. Vehicle System Dynamics* 55:11, 1748-1763.

8 APPENDICES

8.1 Characteristics of hydraulic valves used in test vehicle circuit

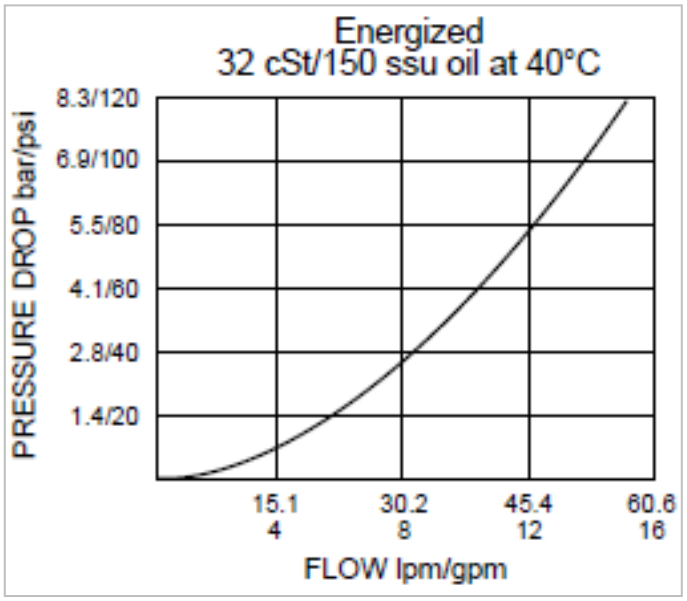

Figure 8.1: Performance graphs for the SV10-24 valve (Van der Westhuizen, 2012)

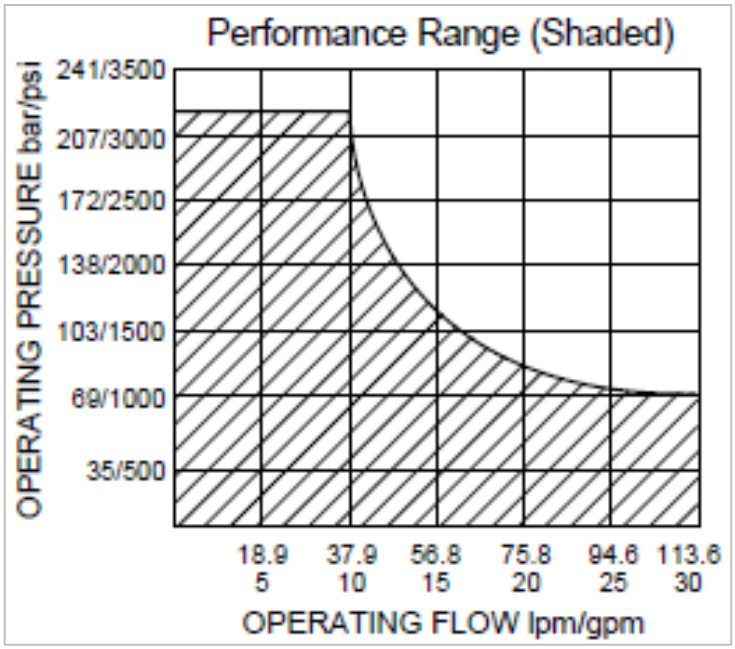

Figure 8.2: Performance graphs for the SV10-24 valve (Van der Westhuizen, 2012)

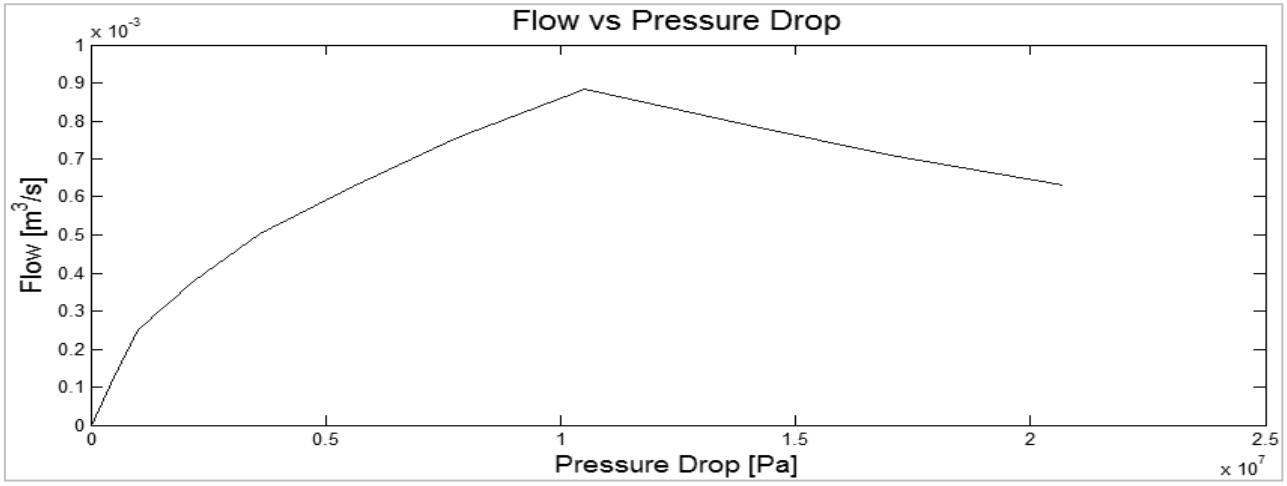

Figure 8.3: Flow vs. pressure drop for SV10-24 valve (Van der Westhuizen, 2012)

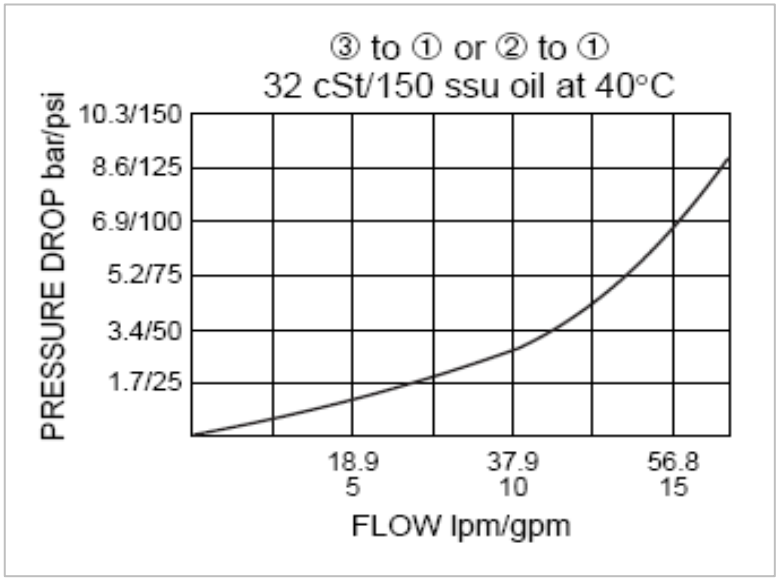

Figure 8.4: Flow vs. pressure for the SV12-33 directional valve (Van der Westhuizen, 2012)

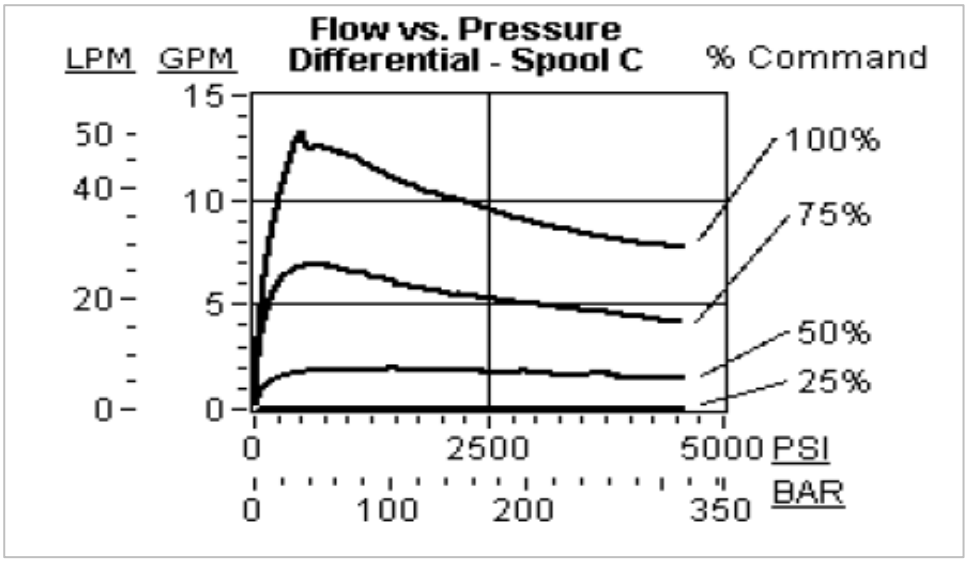

Figure 8.5: Flow vs. pressure for the FPCC proportional valve (Van der Westhuizen, 2012)

8.2 Validation plots for higher speeds

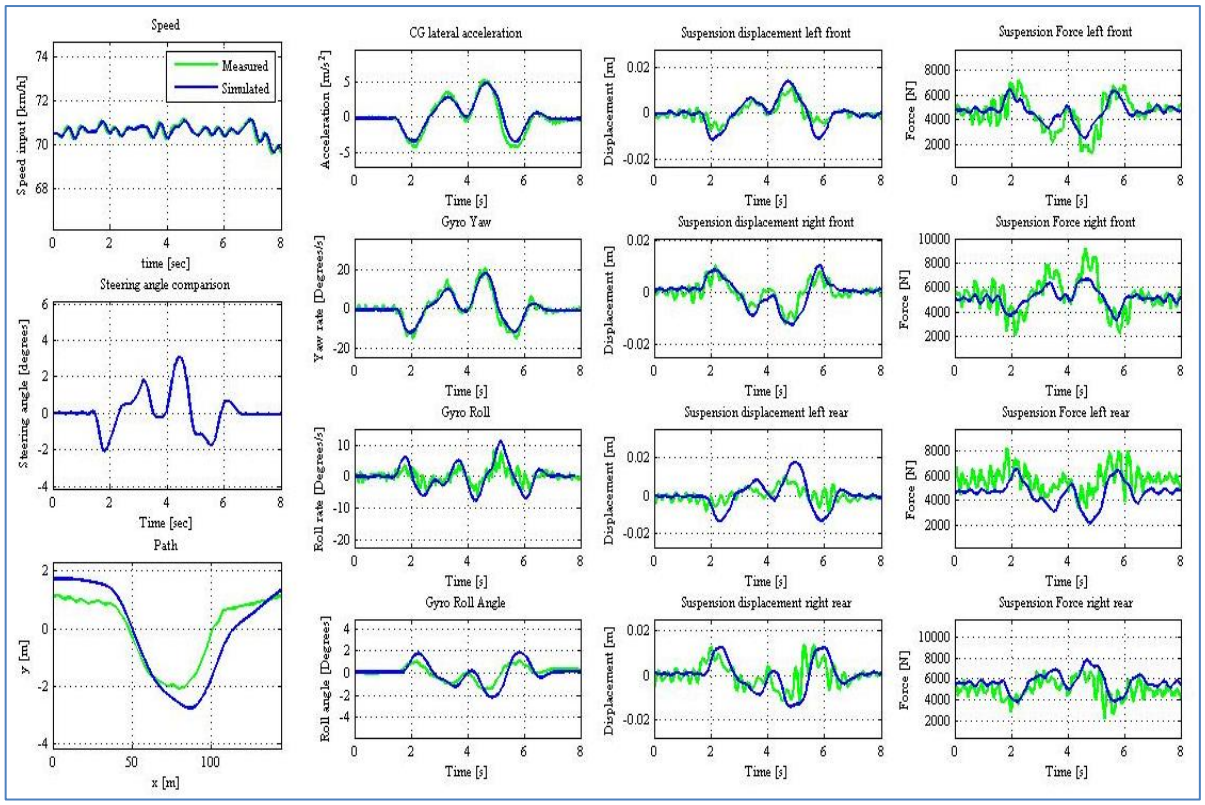

Figure 8.6: Validation DLC 71 km/h on handling suspension setting

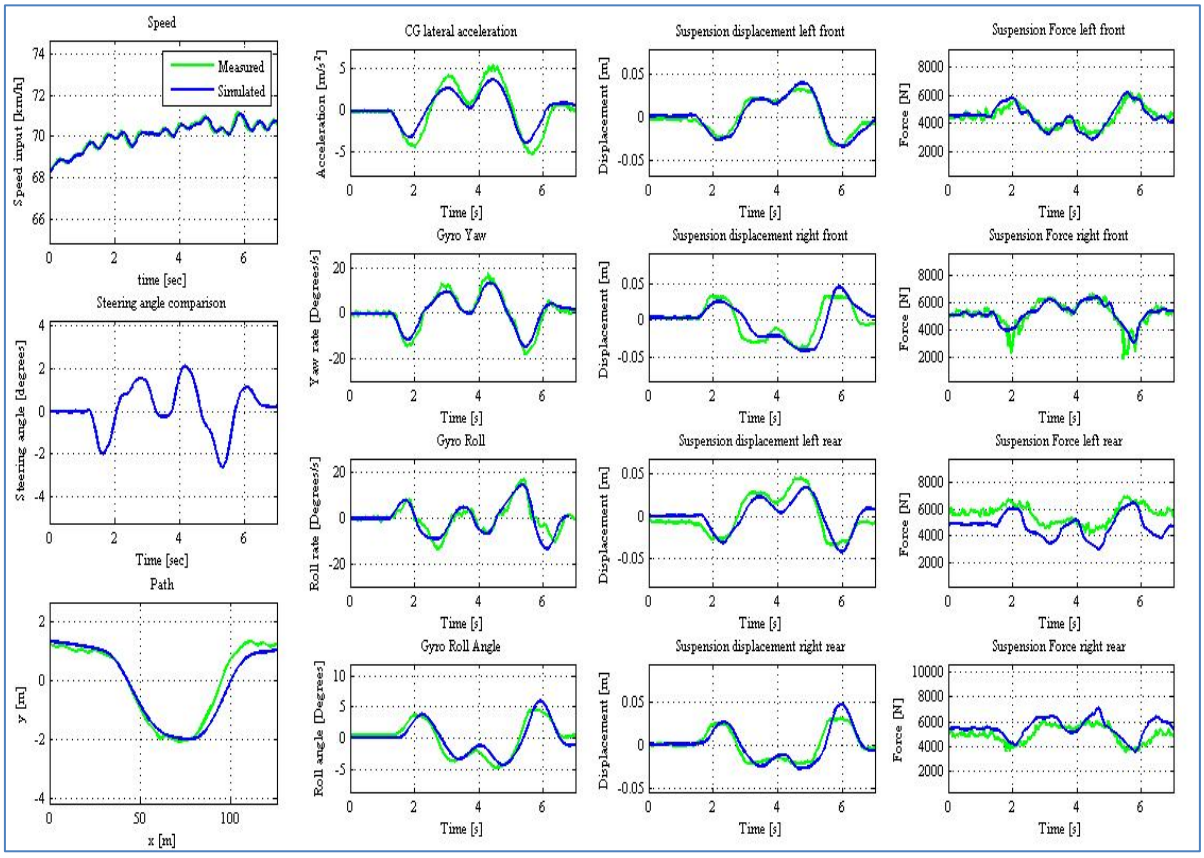

Figure 8.7: Validation DLC 71 km/h on ride comfort suspension setting

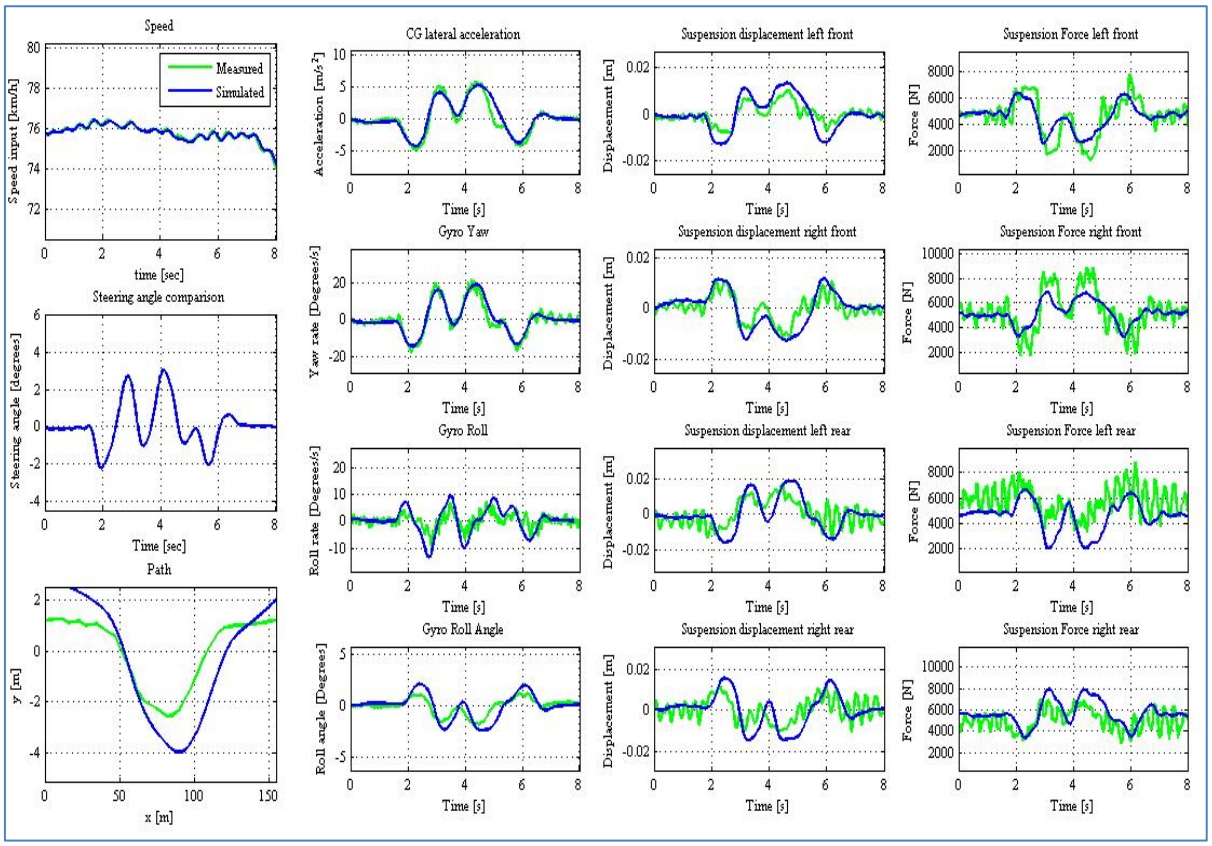

Figure 8.8: Validation DLC 76 km/h on handling suspension setting

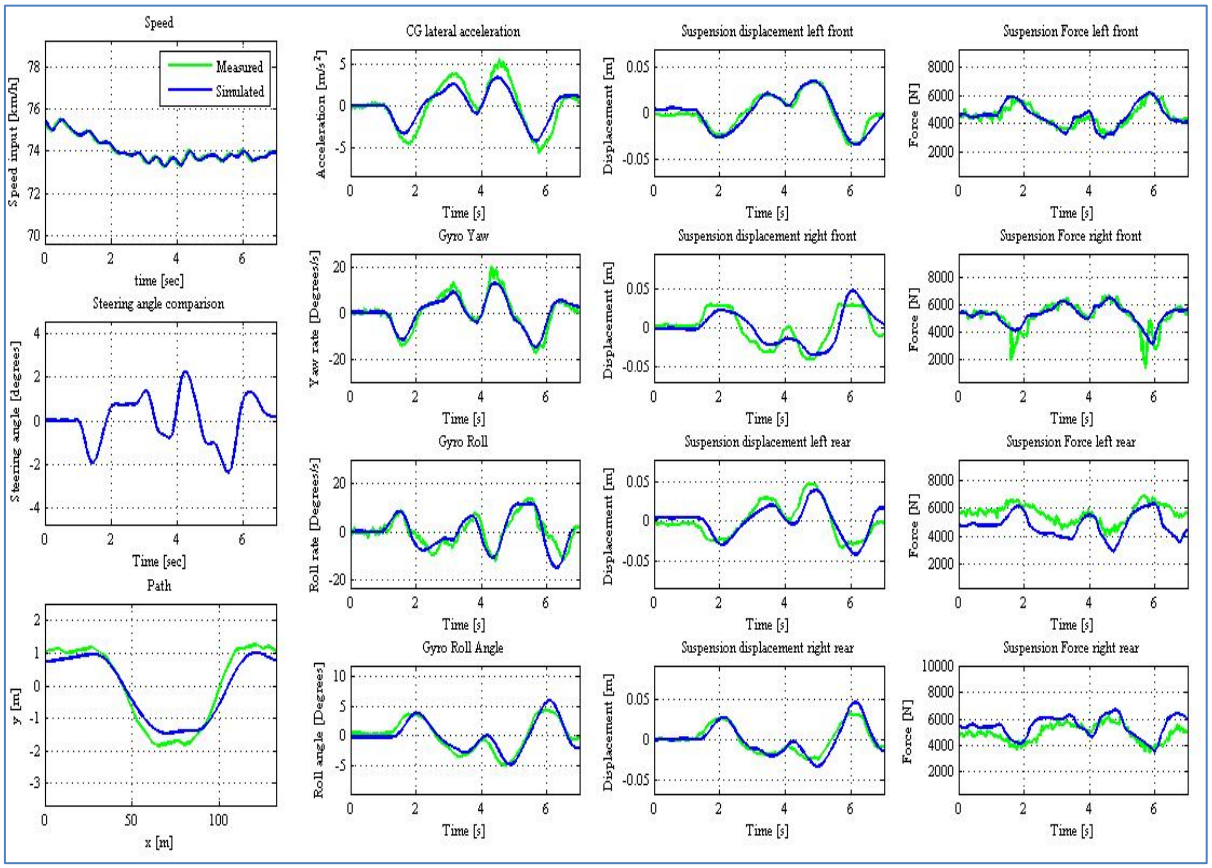

Figure 8.9: Validation DLC 74 km/h on ride comfort suspension setting

8.3 Comparison for Fishhook 1B maximum run speeds

8.3.1 Fishhook 1B at 36 km/h

8.3.1.1 Speed input

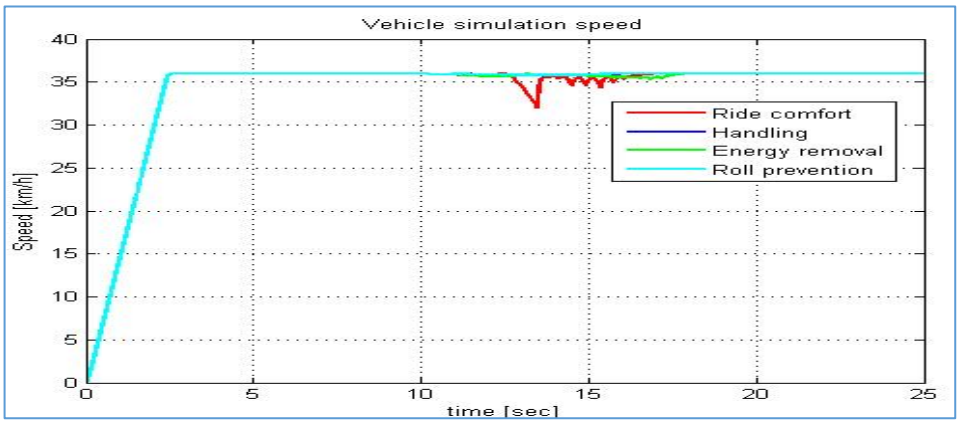

Figure 8.10: Fishhook 1B at 36 km/h, speed input

8.3.1.2 Steer angle

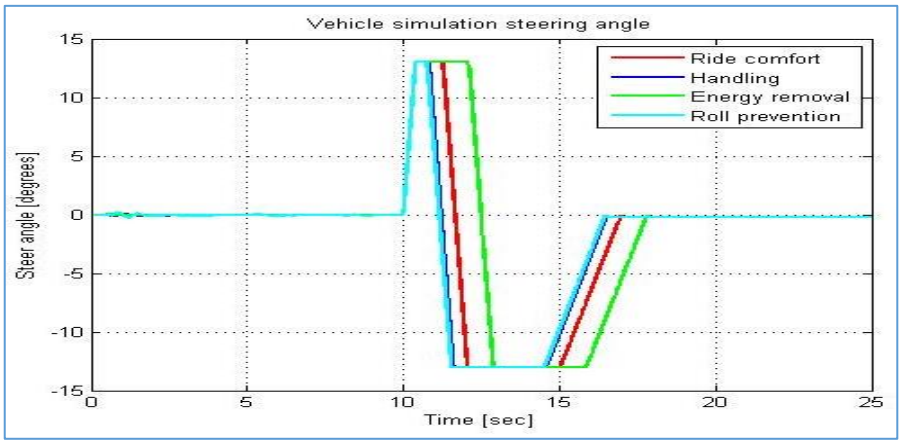

Figure 8.11: Fishhook 1B at 36 km/h, Steer angle

8.3.1.3 Vehicle path

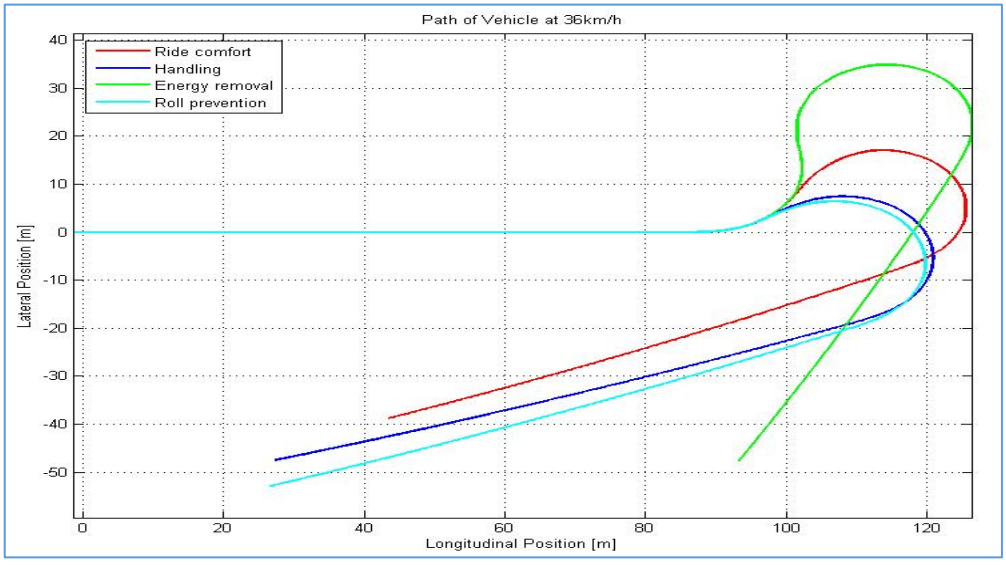

Figure 8.12: Fishhook 1B at 36 km/h, Vehicle path

8.3.1.4 Lateral acceleration, roll velocity, roll angle and yaw rate

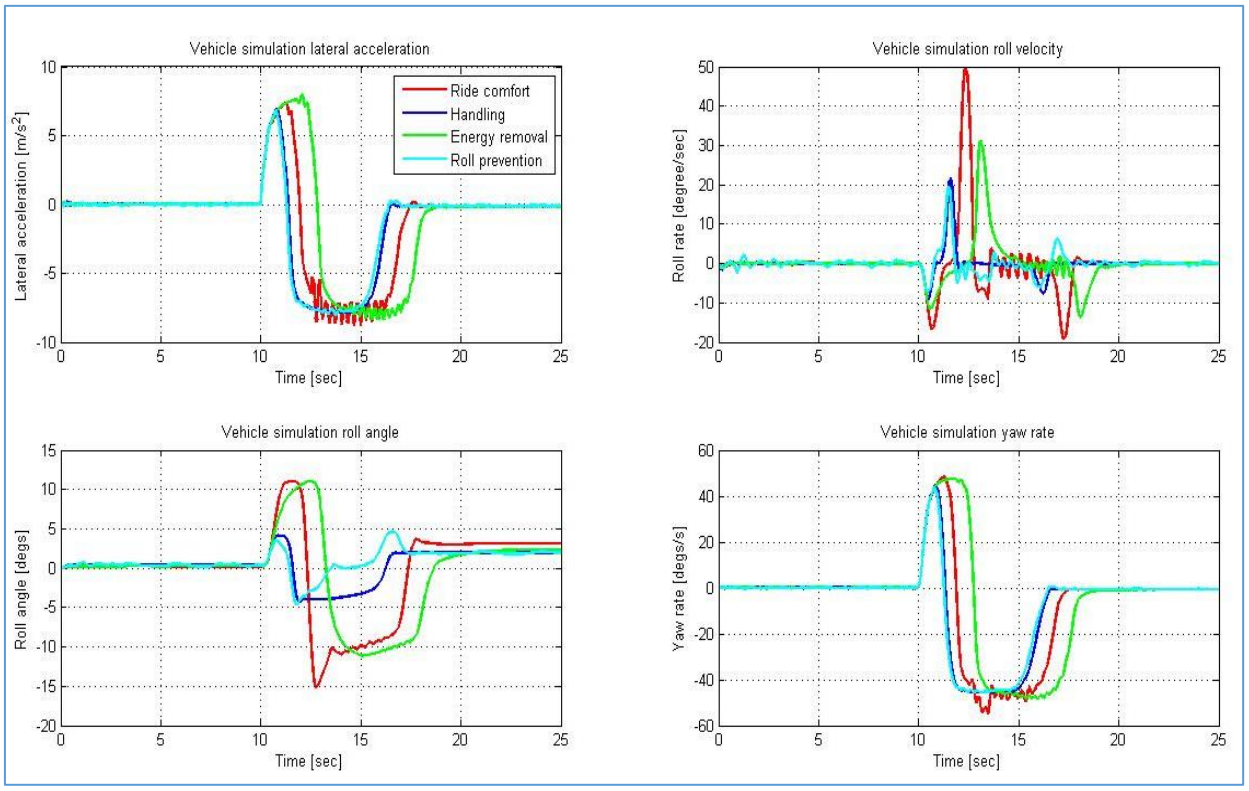

Figure 8.13: Fishhook 1B at 36 km/h, Lateral acceleration, roll velocity, roll angle and yaw rate

8.3.1.5 Wheel lift off

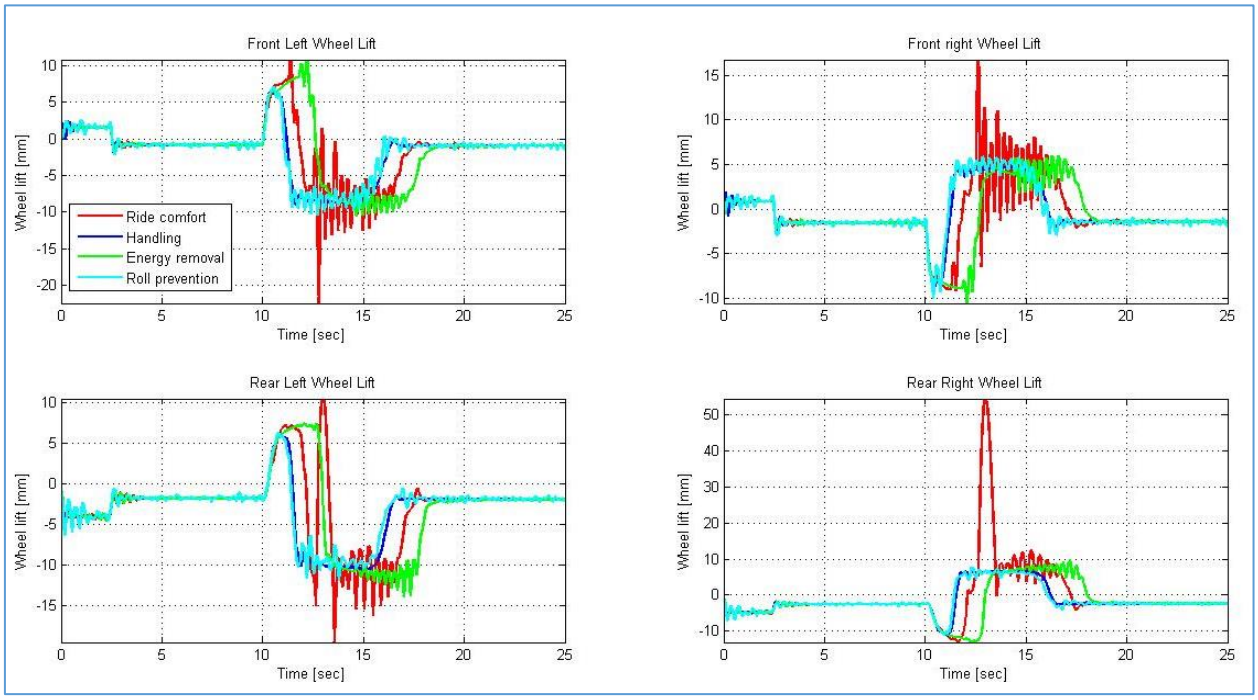

Figure 8.14: Fishhook 1B at 36 km/h, Wheel lift off

8.3.1.6 Suspension displacements

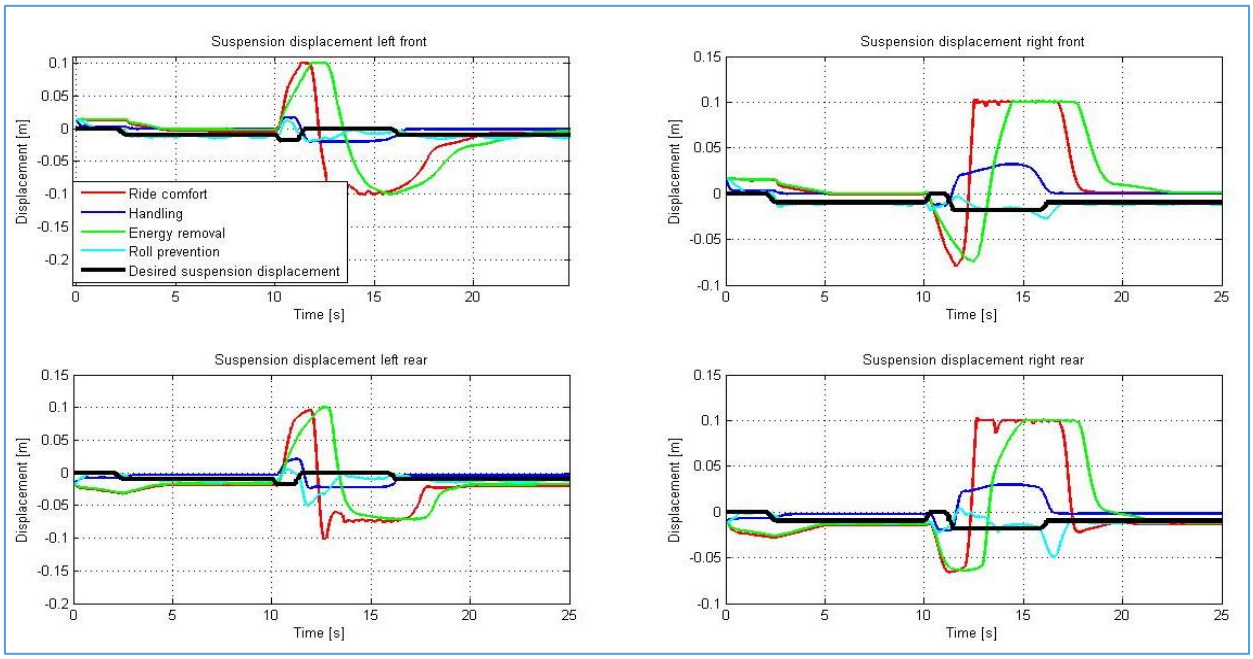

Figure 8.15: Fishhook 1B at 36 km/h, Suspension displacement

8.3.1.7 CG height change

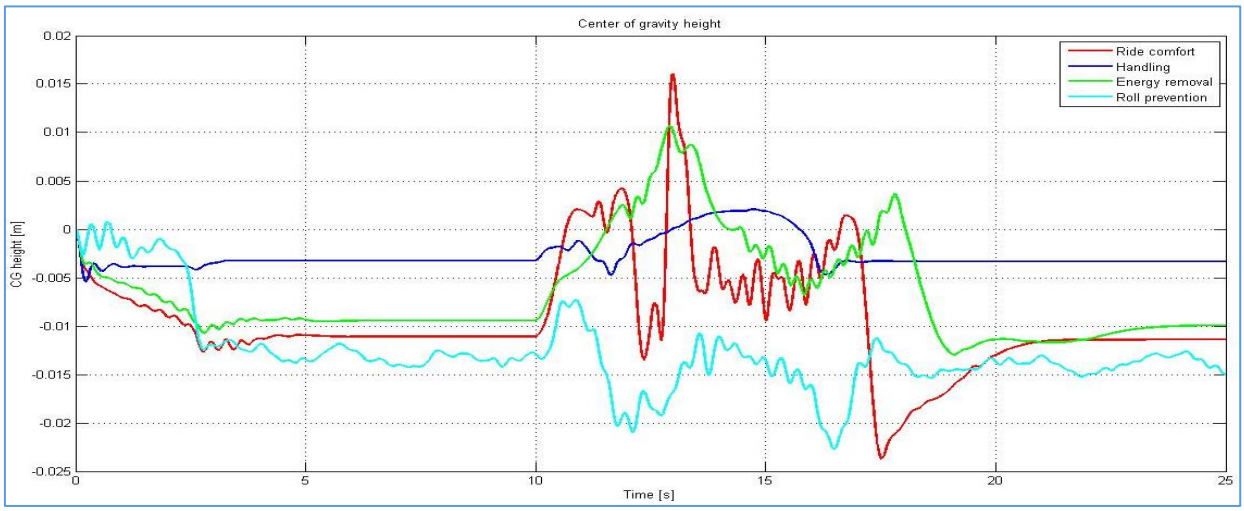

Figure 8.16: Fishhook 1B at 36 km/h, CG height change

8.3.1.8 Rollover index from control system

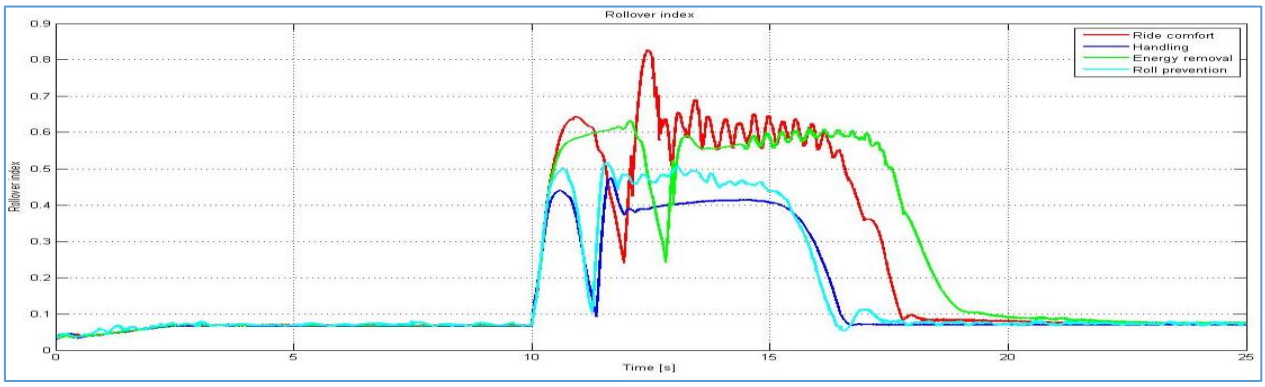

Figure 8.17: Fishhook 1B at 36 km/h, Rollover index from control system

8.3.1.9 DSI and RPER

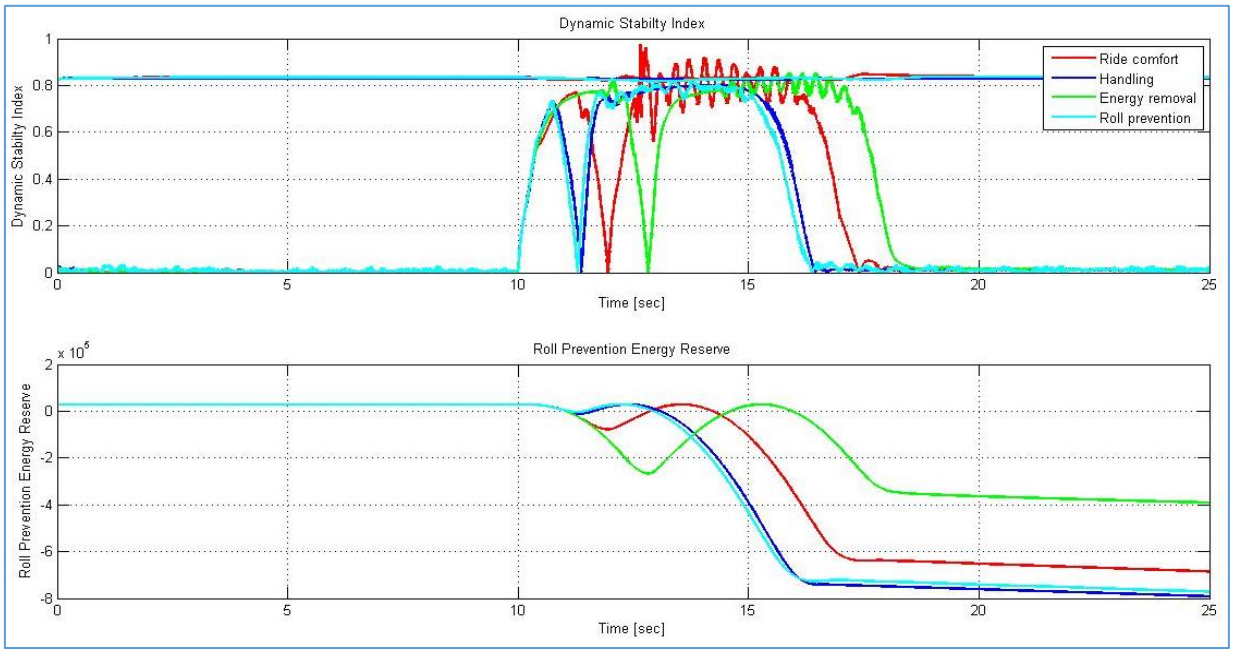

Figure 8.18: Fishhook 1B at 36 km/h, DSI and RPER

8.3.2 Fishhook 1B at 40 km/h

8.3.2.1 Speed input

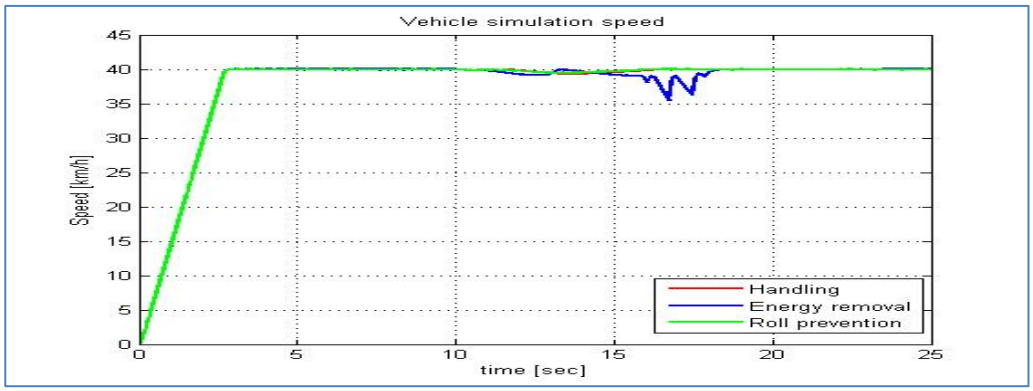

Figure 8.19: Fishhook 1B at 40 km/h, speed input

8.3.2.2 Steer angle

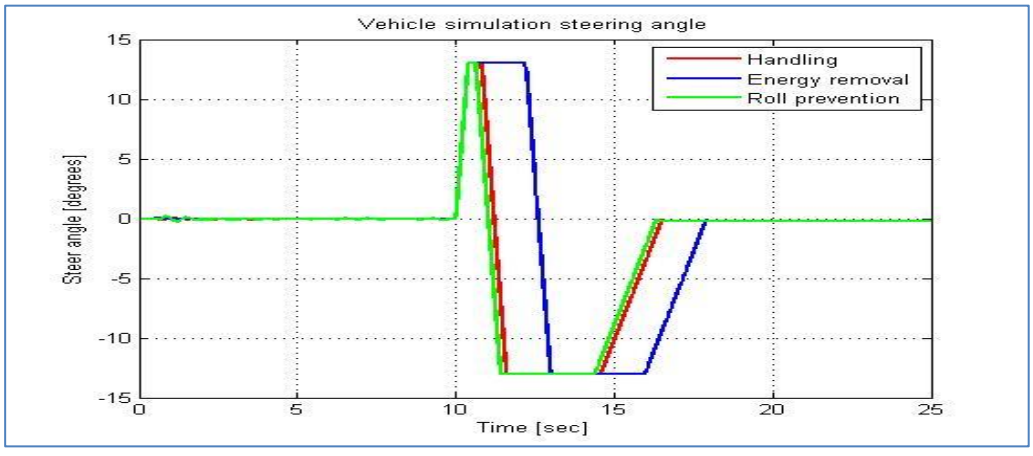

Figure 8.20: Fishhook 1B at 40km/h, Steer angle

8.3.2.3 Vehicle path

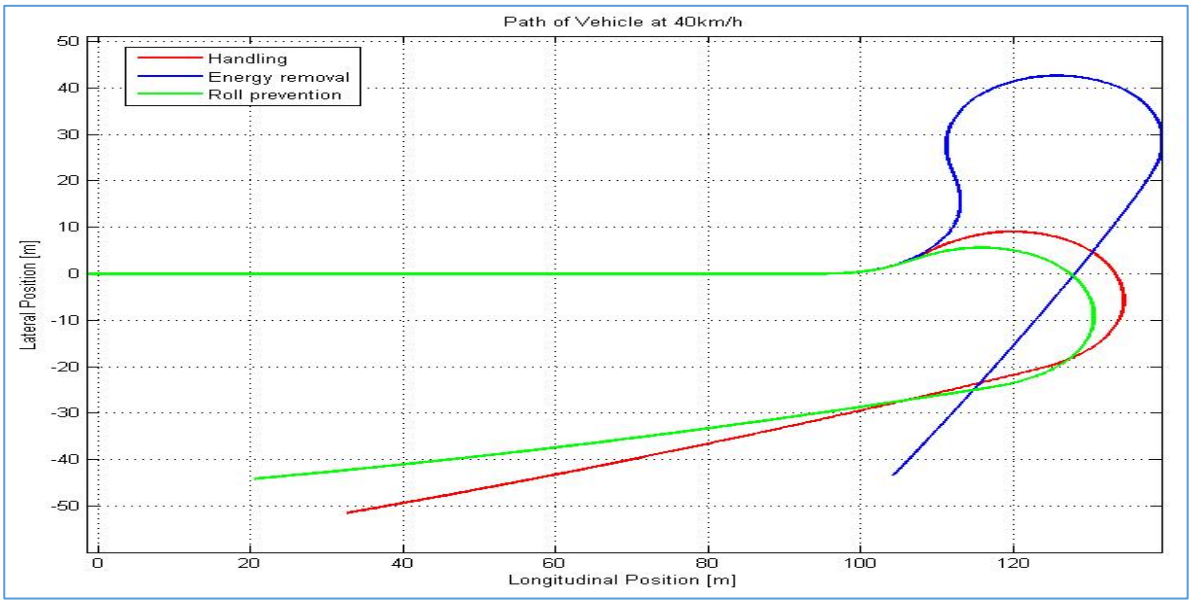

Figure 8.21: Fishhook 1B at 40km/h, Vehicle path

8.3.2.4 Lateral acceleration, roll velocity, roll angle and yaw rate

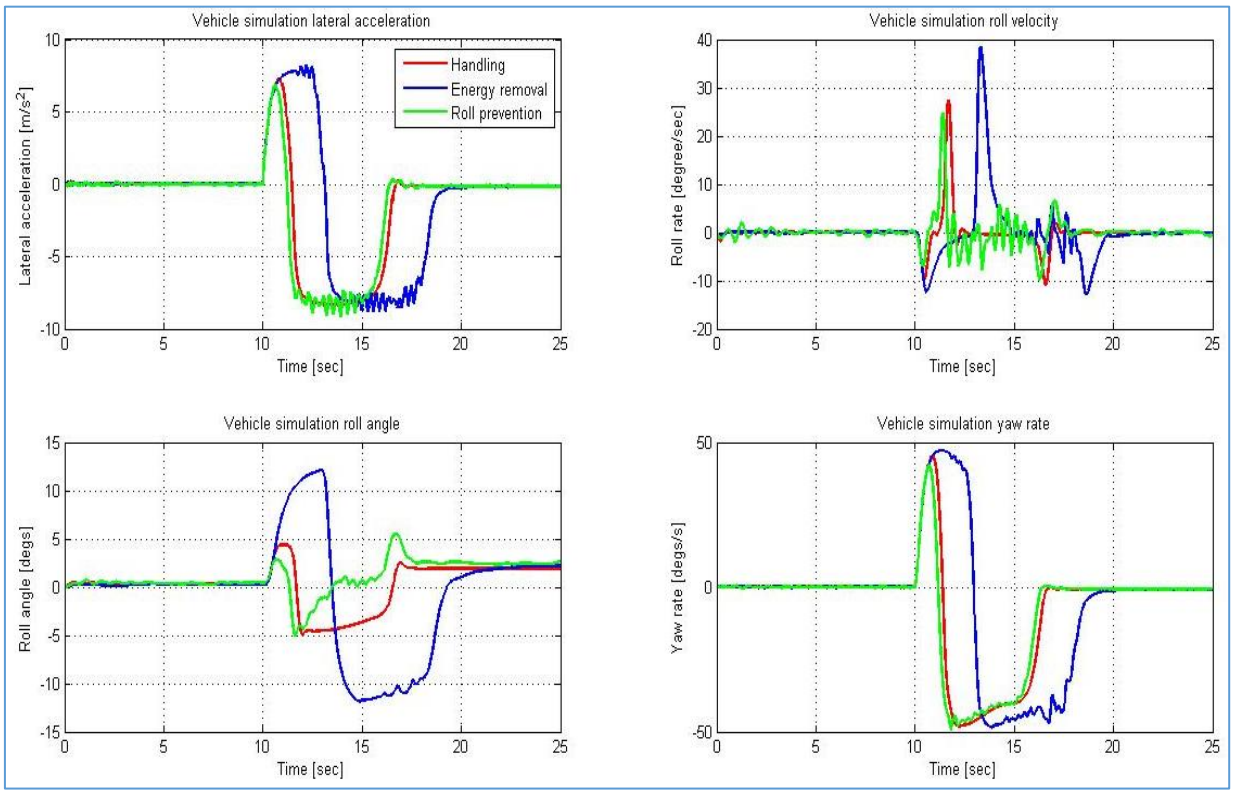

Figure 8.22: Fishhook 1B at 40km/h, Lateral acceleration, roll velocity, roll angle and yaw rate

8.3.2.5 Wheel lift off

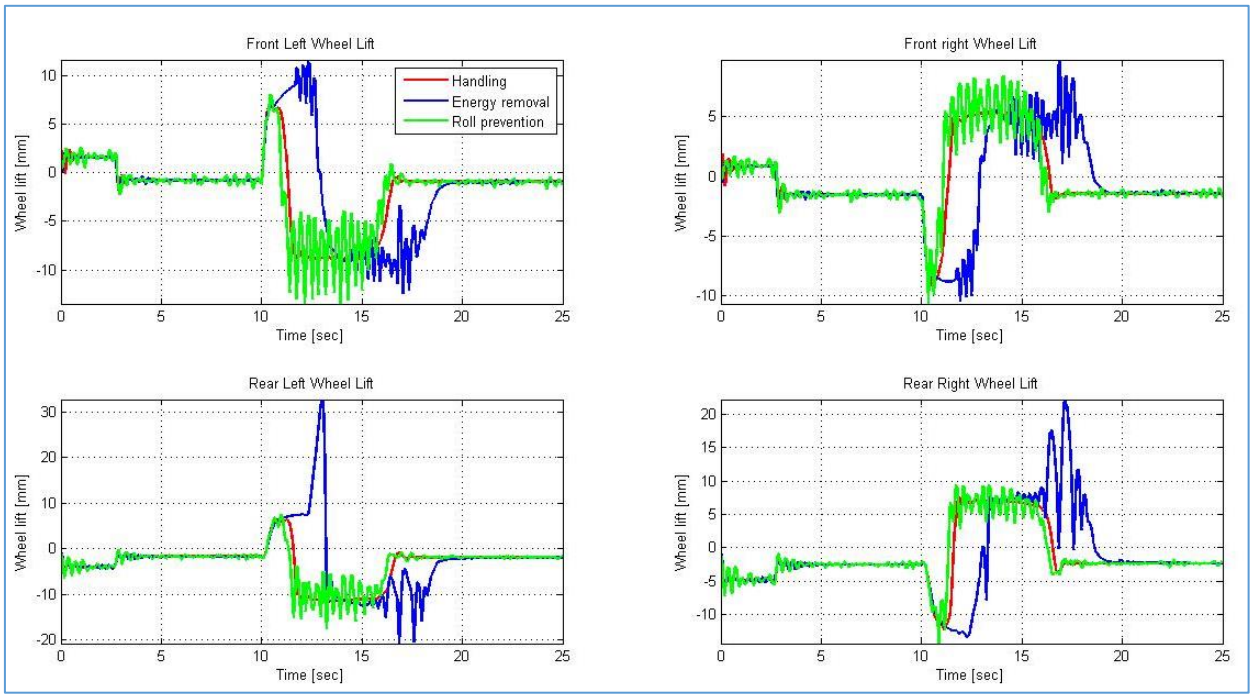

Figure 8.23: Fishhook 1B at 40km/h, Wheel lift off

8.3.2.6 Suspension displacements

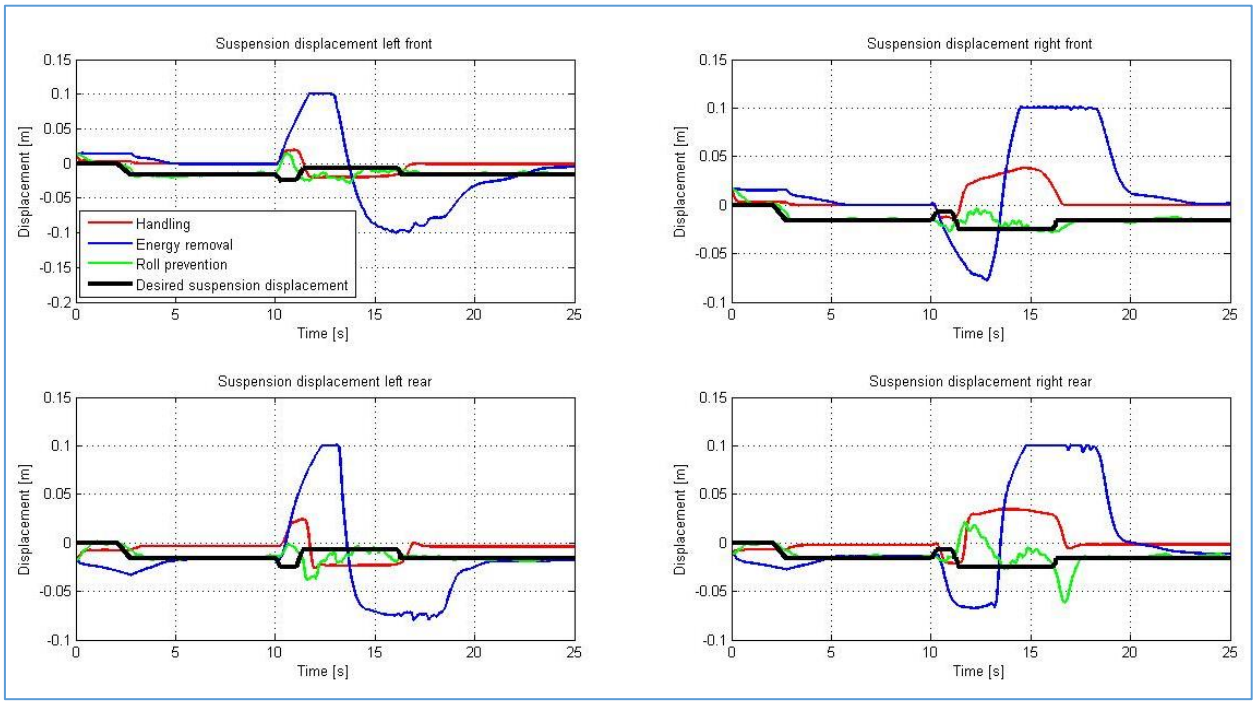

Figure 8.24: Fishhook 1B at 40km/h, Suspension displacement

8.3.2.7 CG height change

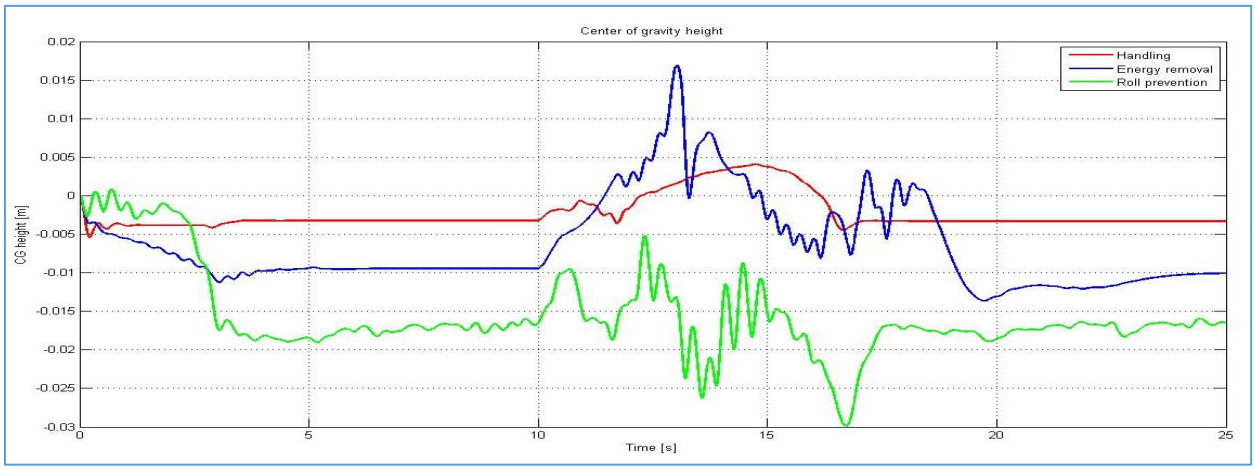

Figure 8.25: Fishhook 1B at 40km/h, CG height change

8.3.2.8 Rollover index from control system

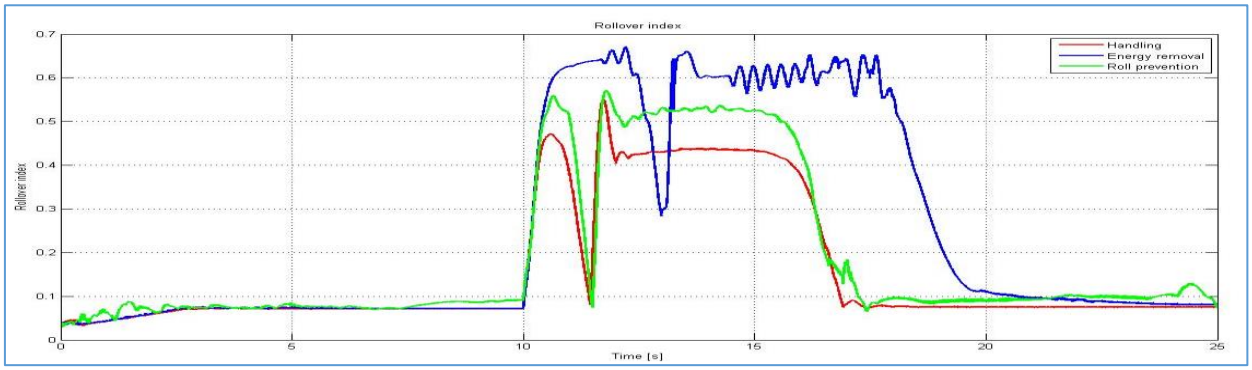

Figure 8.26: Fishhook 1B at 40km/h, Rollover index from control system

8.3.2.9 DSI and RPER

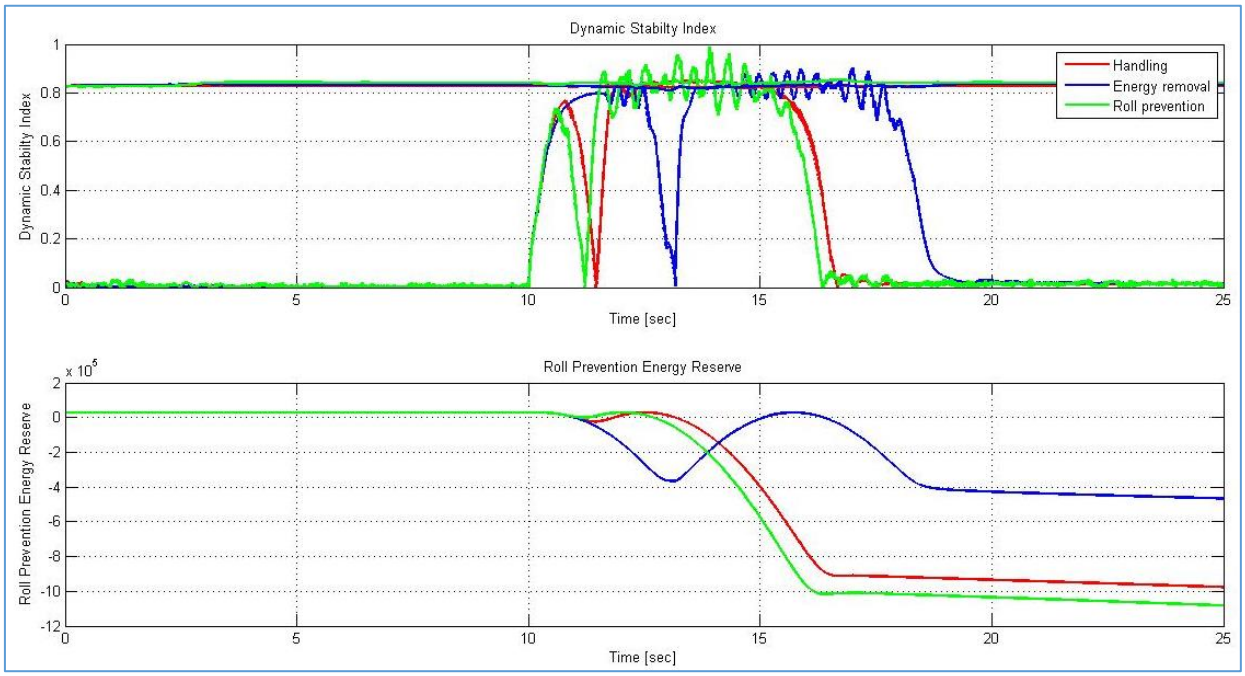

Figure 8.27: Fishhook 1B at 40km/h, DSI and RPER

8.3.3 Fishhook 1B at 50 km/h

8.3.3.1 Speed input

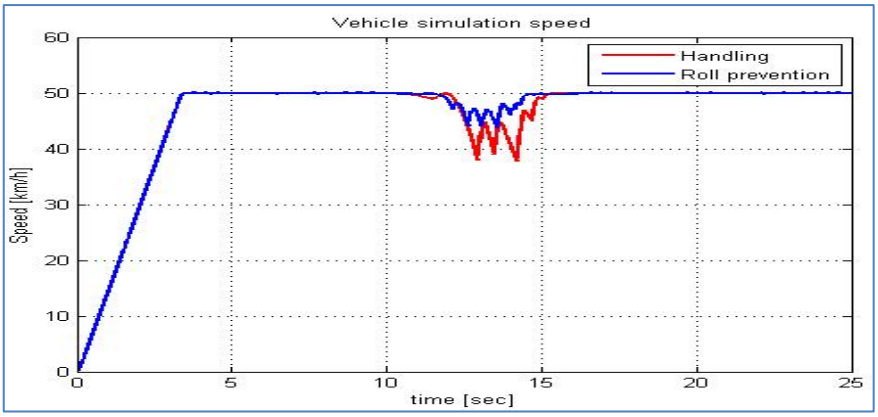

Figure 8.28: Fishhook 1B at 50 km/h, speed input

8.3.3.2 Steer angle

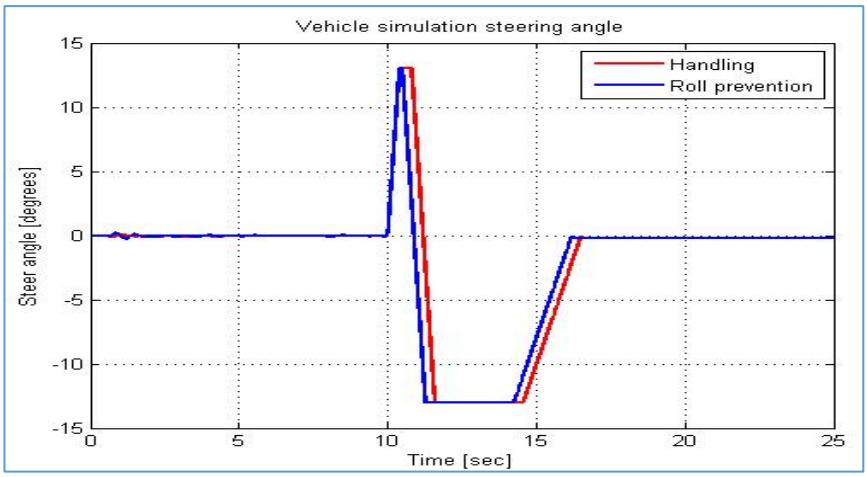

Figure 8.29: Fishhook 1B at 50km/h, Steer angle

8.3.3.3 Vehicle path

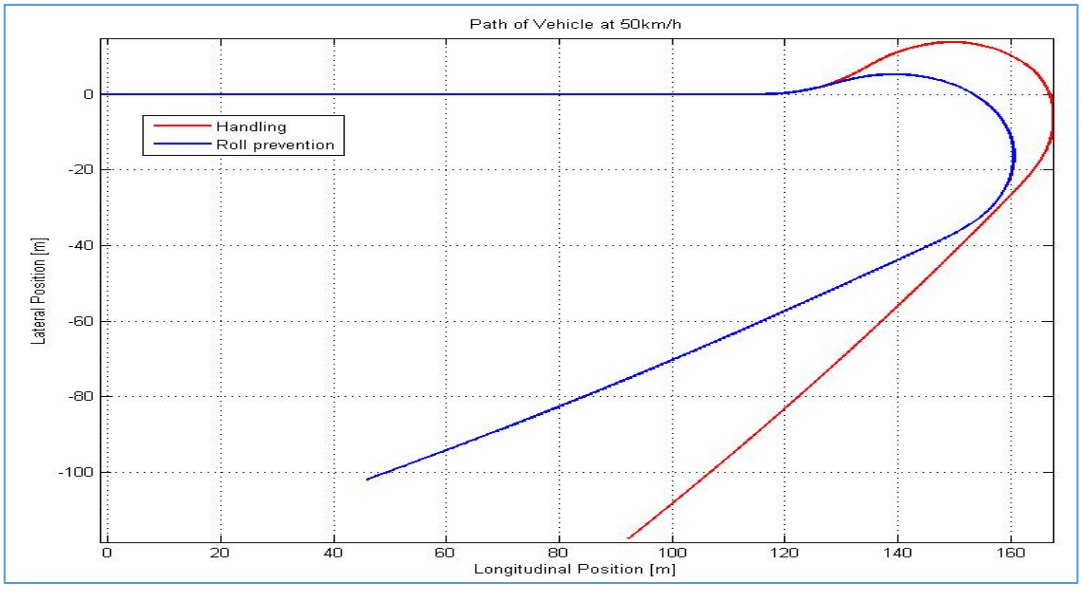

Figure 8.30: Fishhook 1B at 50km/h, Vehicle path

8.3.3.4 Lateral acceleration, roll velocity, roll angle and yaw rate

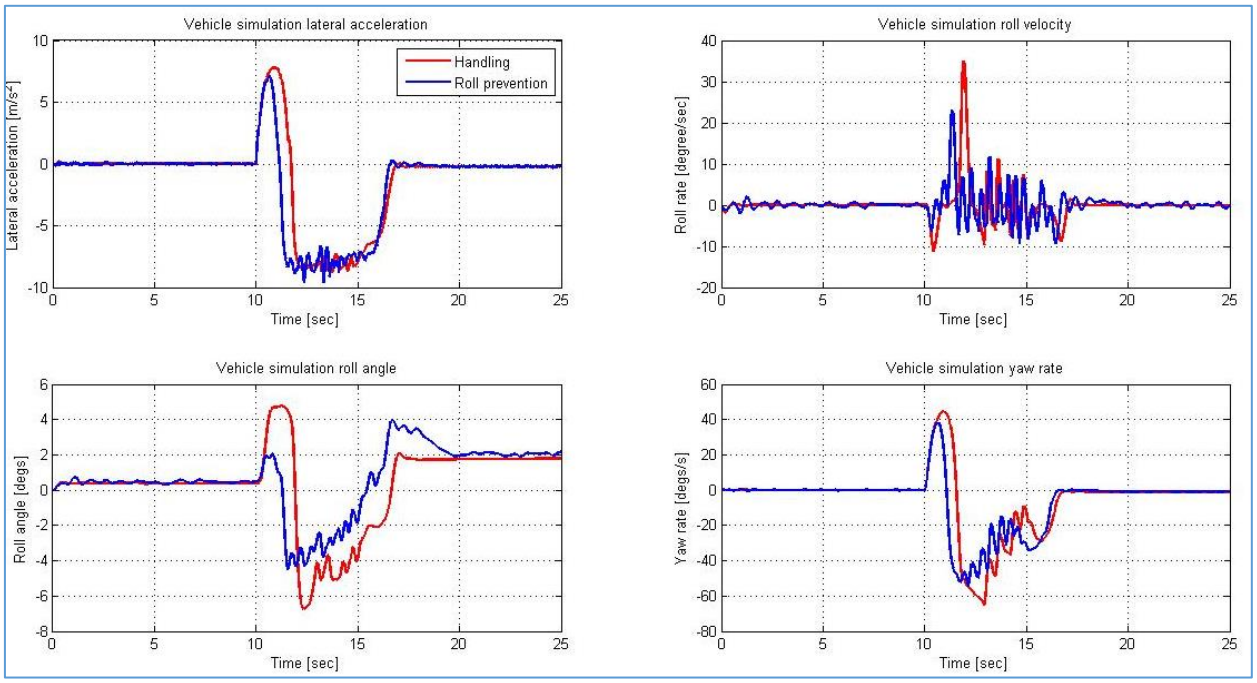

Figure 8.31: Fishhook 1B at 50km/h, Lateral acceleration, roll velocity, roll angle and yaw rate

8.3.3.5 Wheel lift off

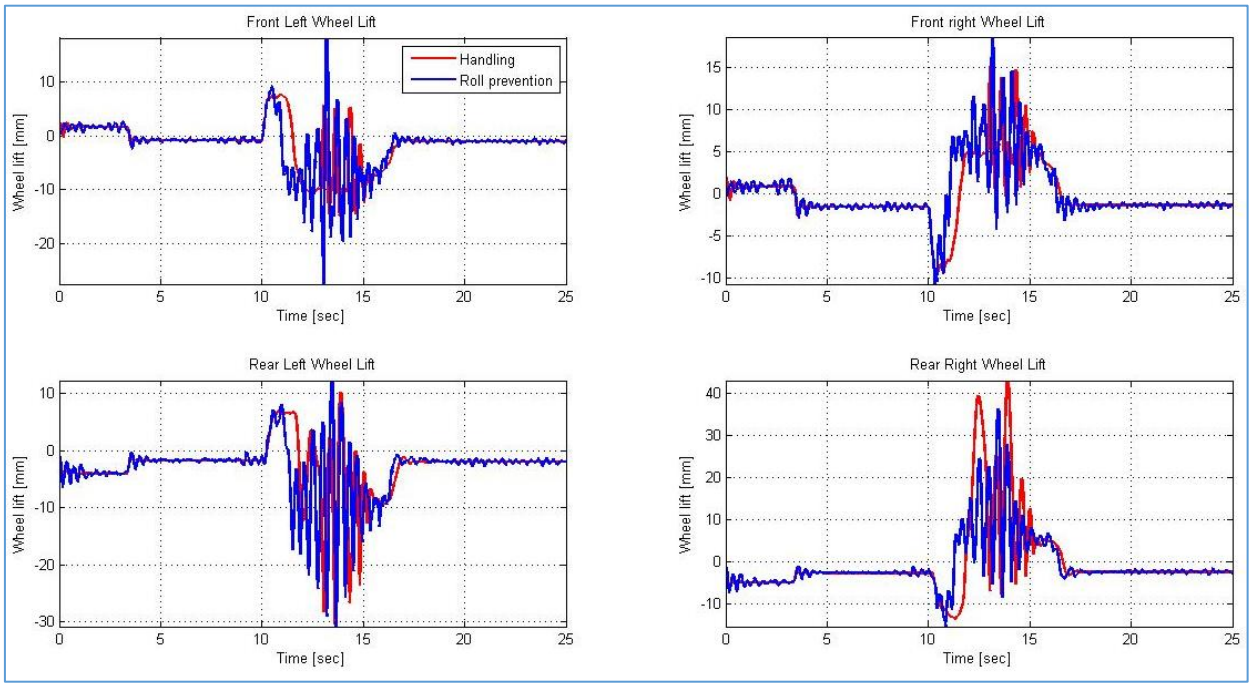

Figure 8.32: Fishhook 1B at 50km/h, Wheel lift off

8.3.3.6 Suspension displacements

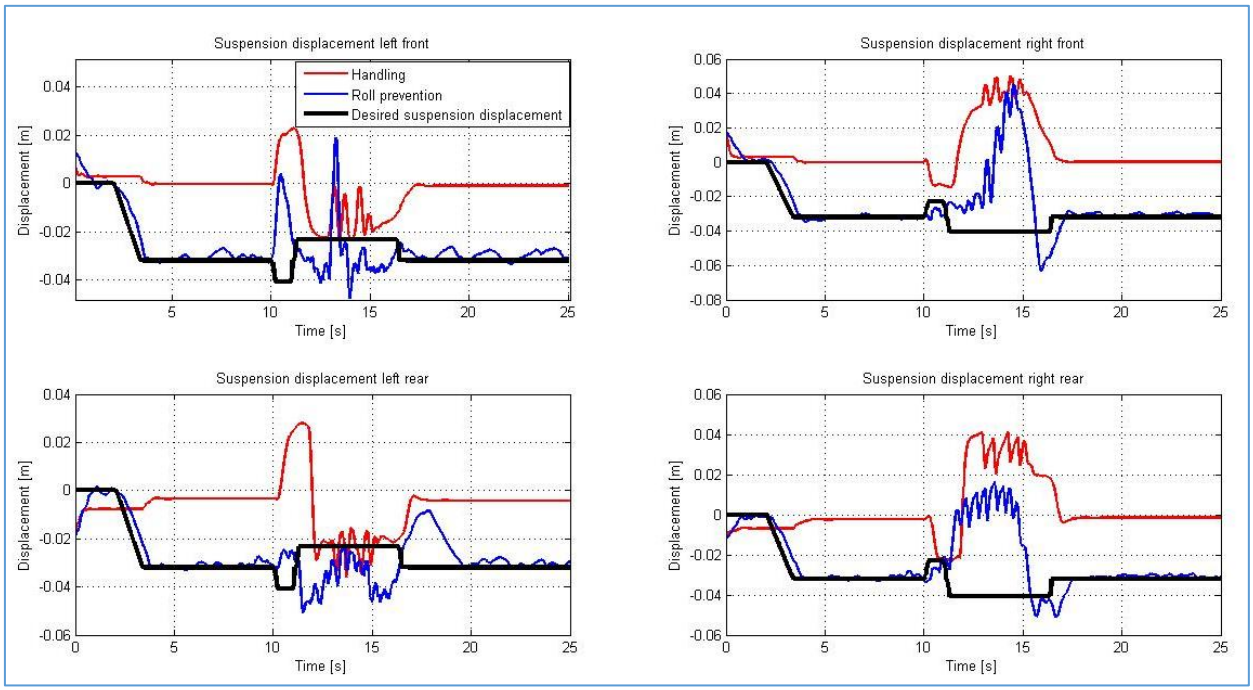

Figure 8.33: Fishhook 1B at 50km/h, Suspension displacement

8.3.3.7 CG height change

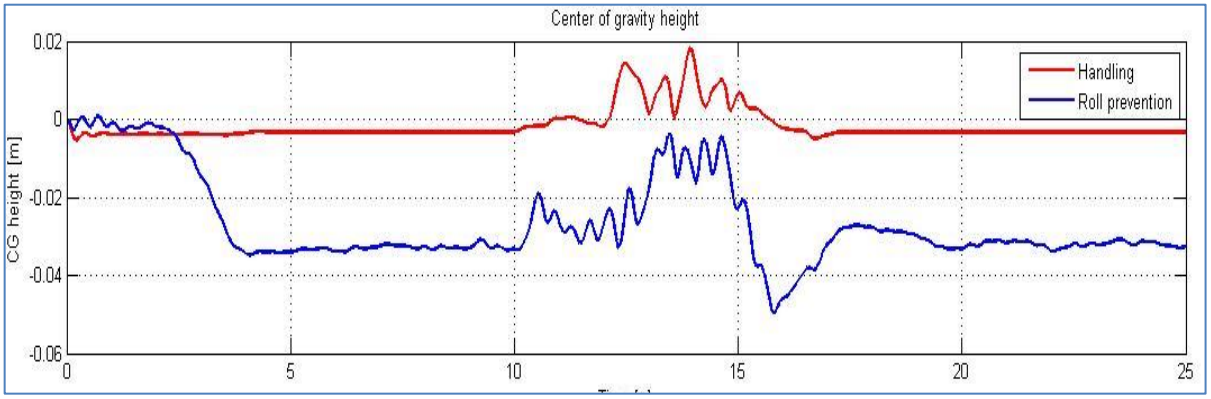

Figure 8.34: Fishhook 1B at 50km/h, CG height change

8.3.3.8 Rollover index from control system

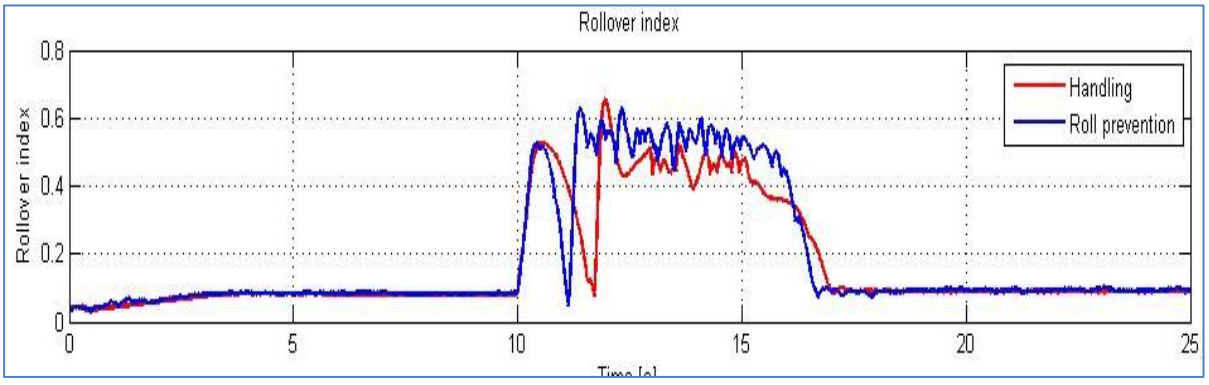

Figure 8.35: Fishhook 1B at 50km/h, Rollover index from control system

8.3.3.9 DSI and RPER

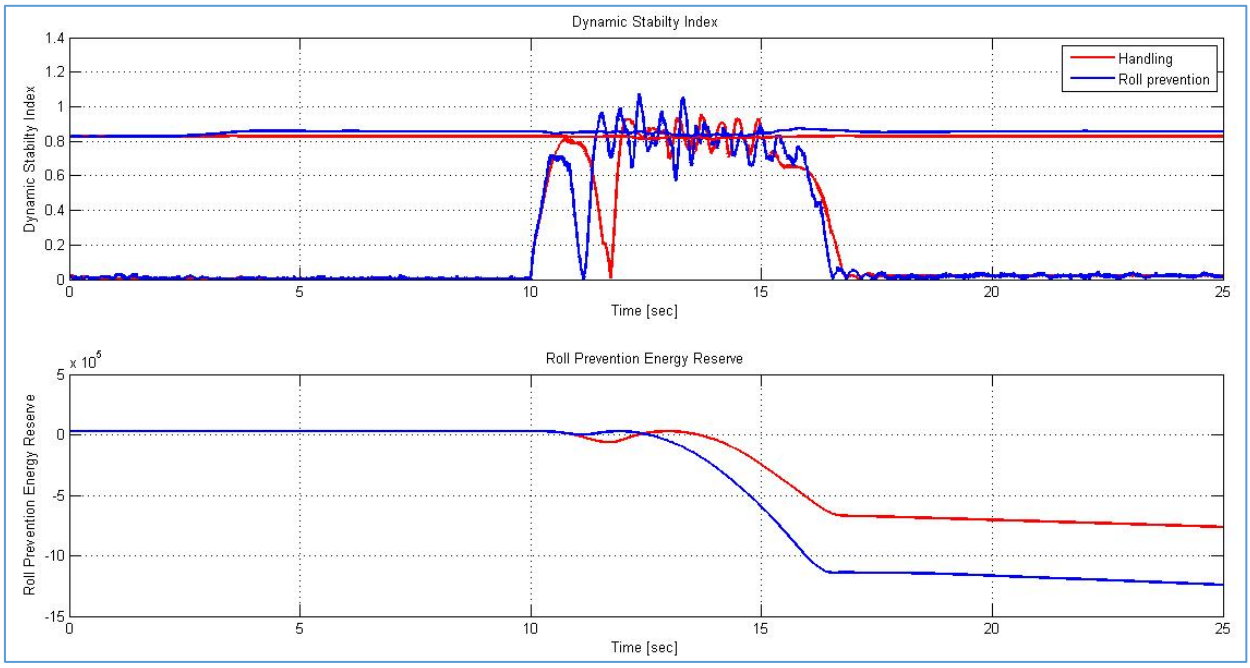

Figure 8.36: Fishhook 1B at 50km/h, DSI and RPER

8.4 Double Lane Change Simulation Results for 60 and 70 km/h

8.4.1 Double Lane Change at 60 km/h

8.4.1.1 Speed

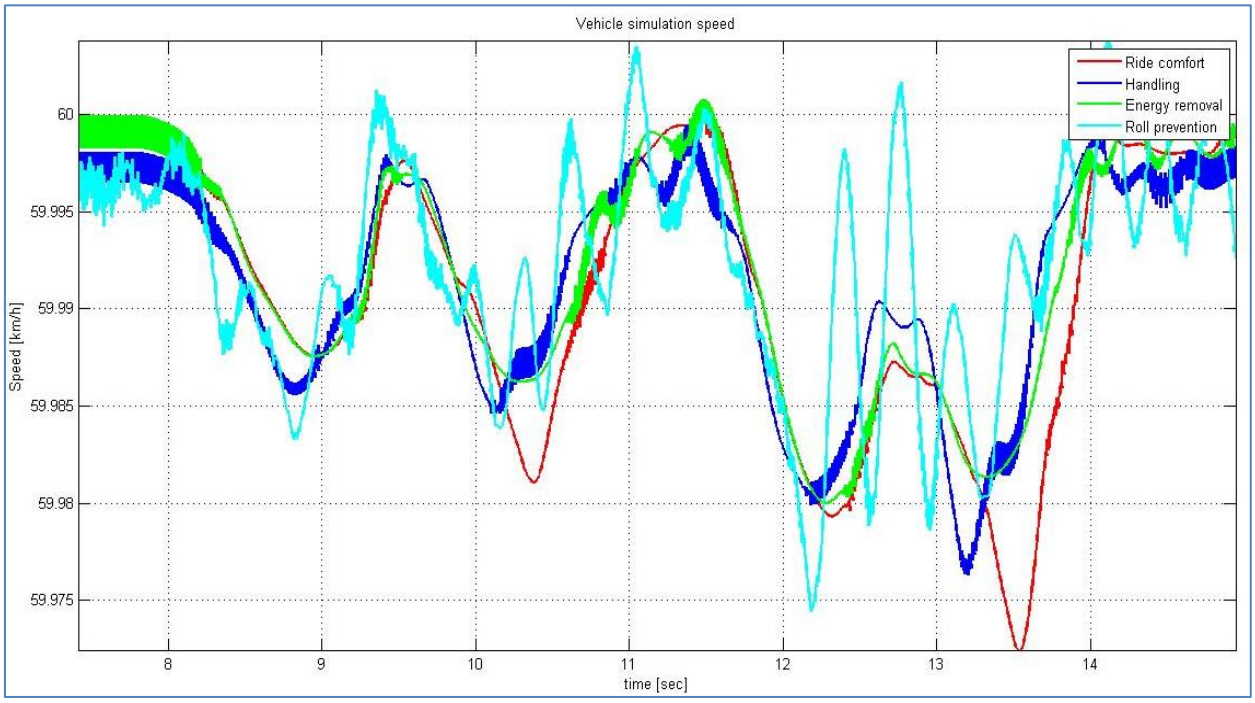

Figure 8.37: Double Lane Change at 60 km/h, speed

8.4.1.2 *Steer input*

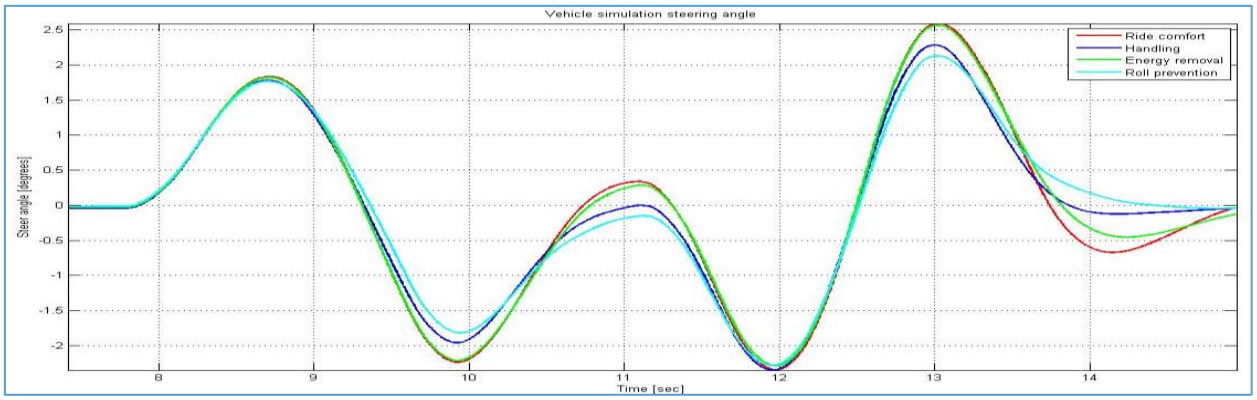

Figure 8.38: Double Lane Change at 60 km/h, steer input

8.4.1.3 *Vehicle path*

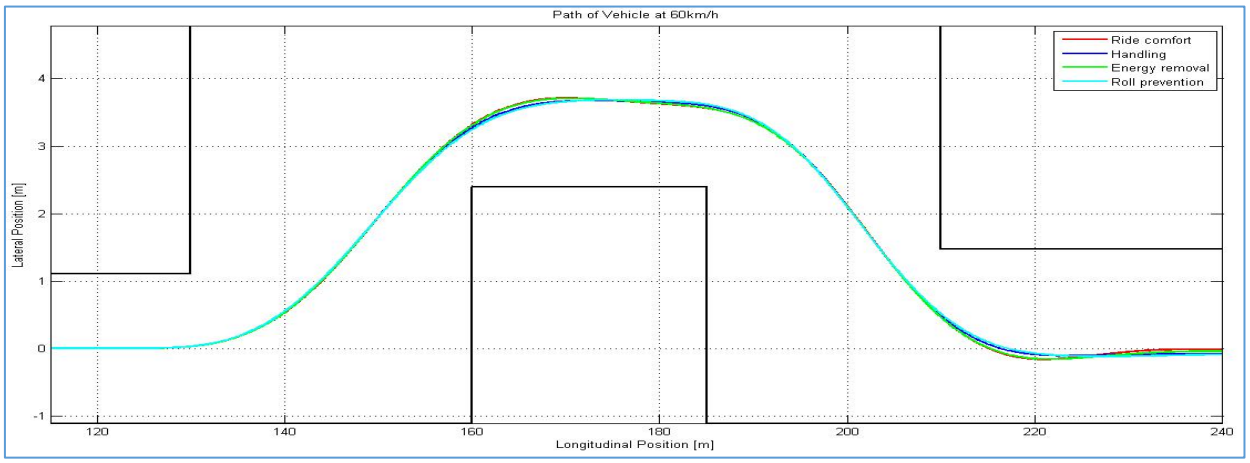

Figure 8.39: Double Lane Change at 60 km/h, vehicle path

8.4.1.4 ***Lateral** acceleration**, roll rate, roll angle and yaw rate***

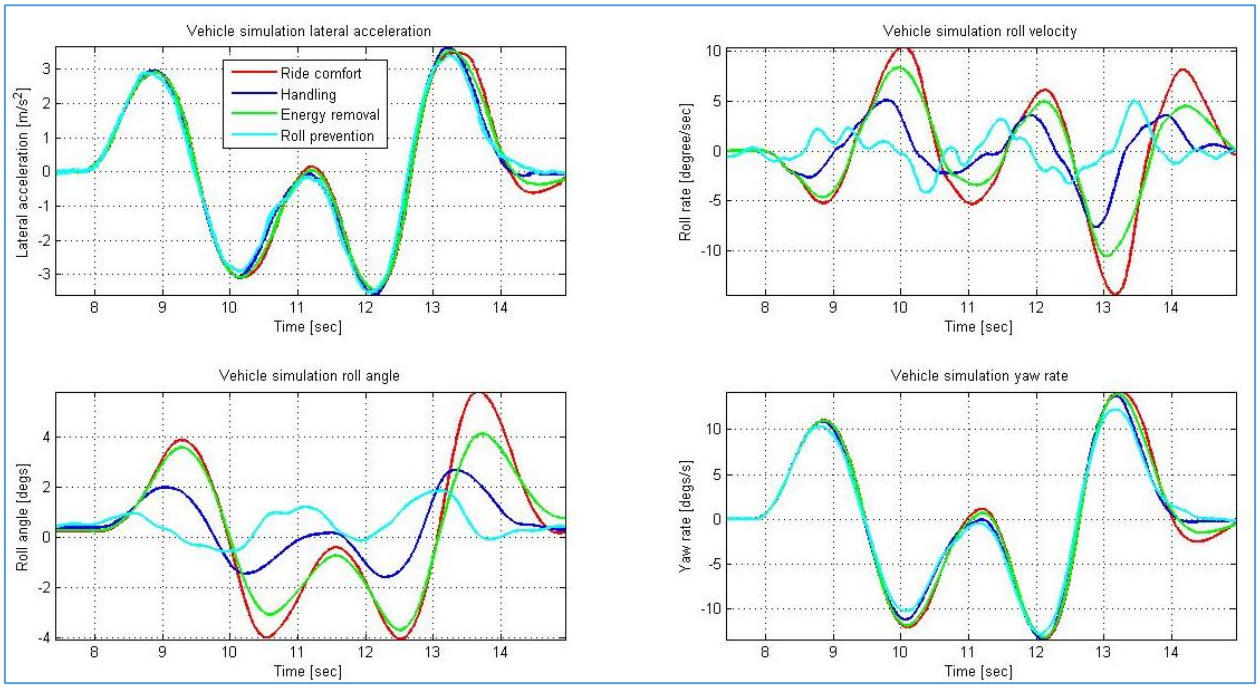

Figure 8.40: Double Lane Change at 60 km/h, lateral acceleration, roll rate, roll angle and yaw rate

8.4.1.5 Wheel lift

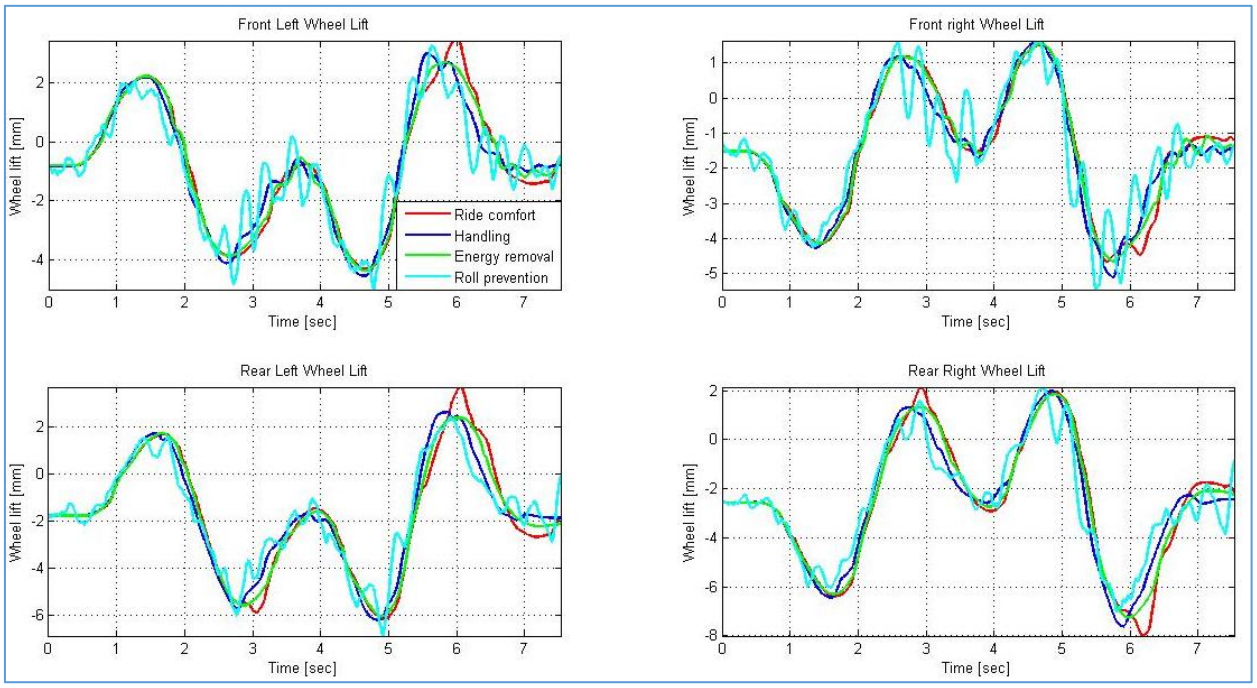

Figure 8.41: Double Lane Change at 60 km/h, wheel lift

8.4.1.6 Suspension displacement

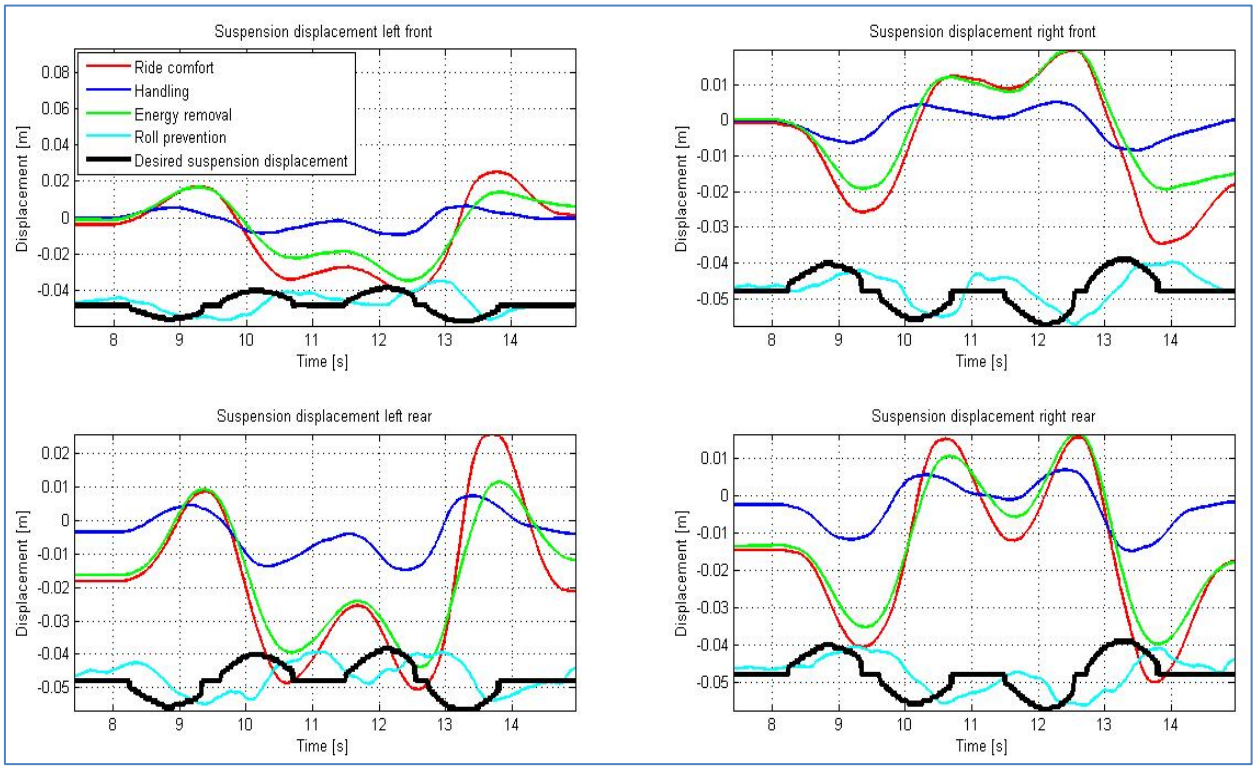

Figure 8.42: Double Lane Change at 60 km/h, suspension displacement

8.4.1.7 CG height change

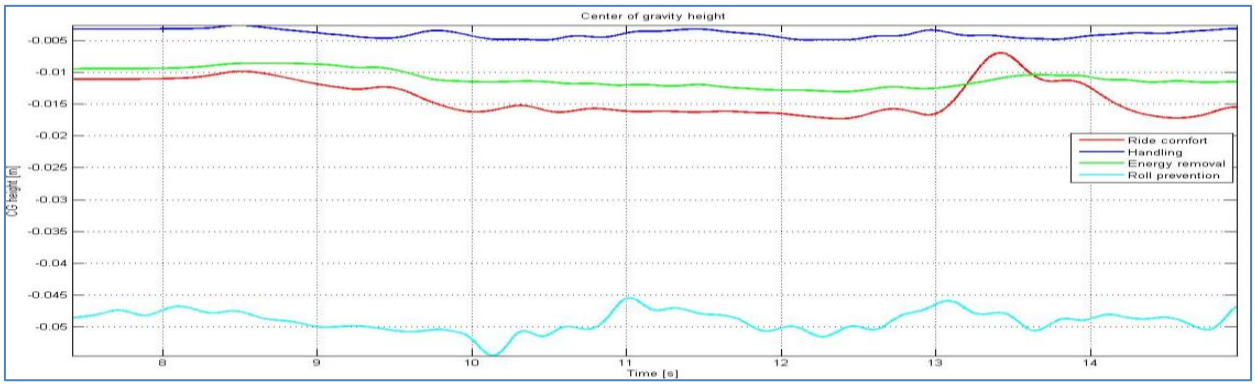

Figure 8.43: Double Lane Change at 60 km/h, CG height change

8.4.1.8 Rollover index from control system

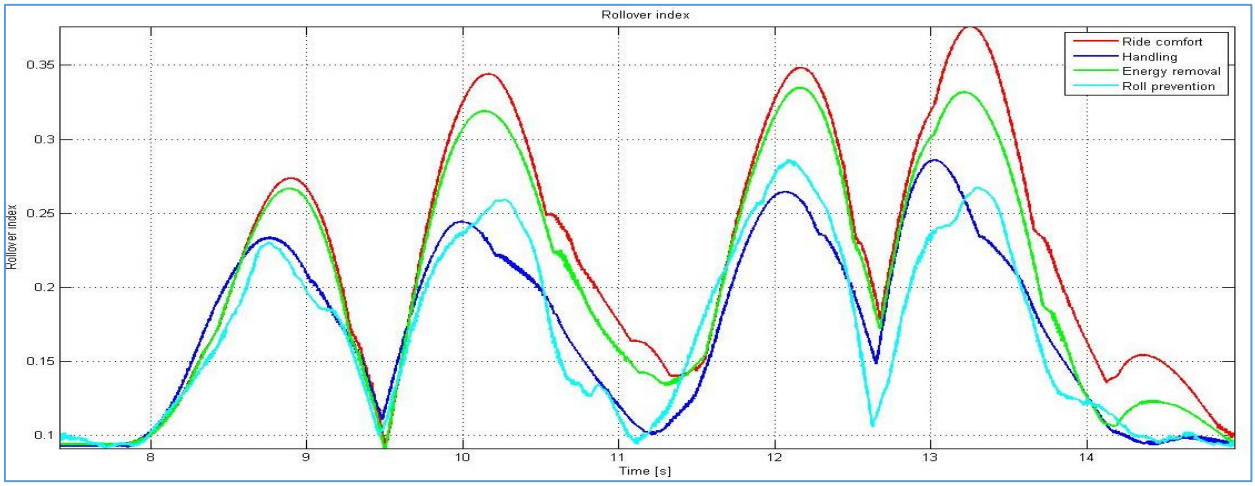

Figure 8.44: Double Lane Change at 60 km/h, rollover index from control system

8.4.1.9 DSI and RPER

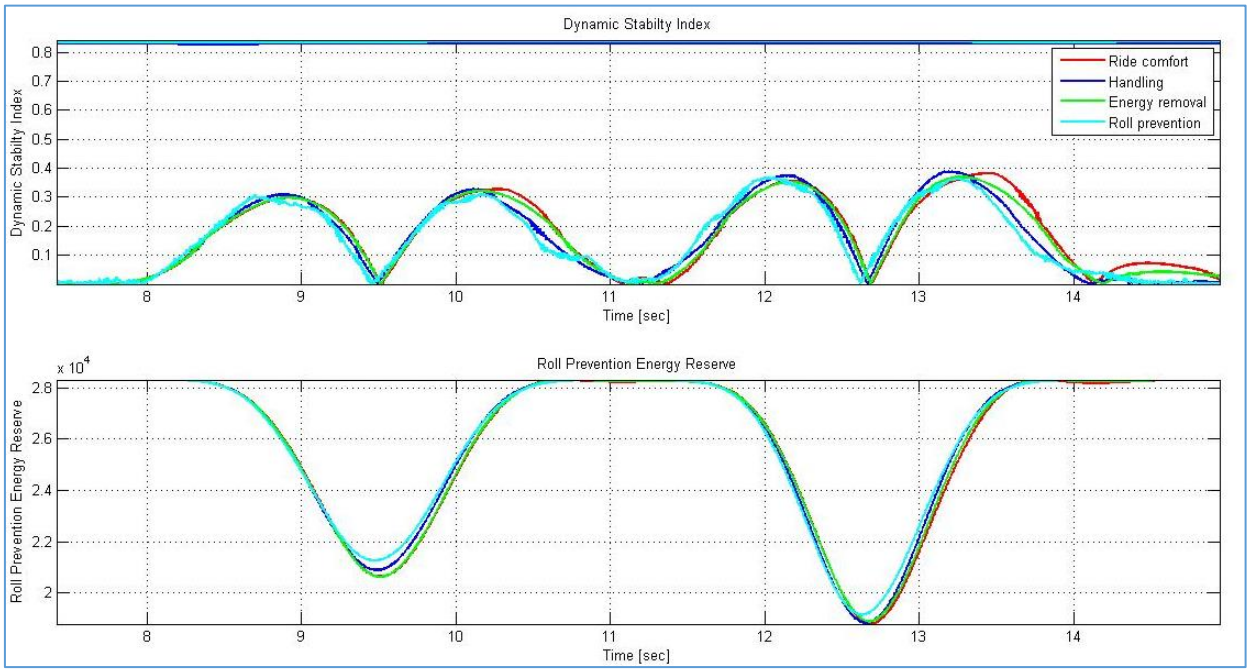

Figure 8.45: Double Lane Change at 60 km/h, DSI and RPER

8.4.2 Double Lane Change at 70 km/h

8.4.2.1 Speed

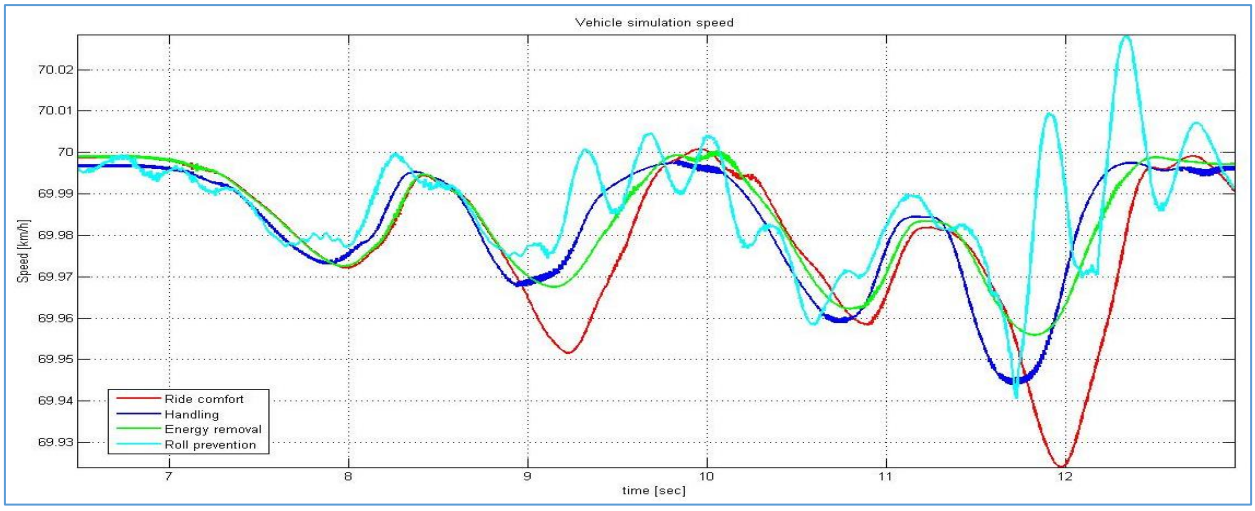

Figure 8.46: Double Lane Change at 70 km/h, speed

8.4.2.2 Steer input

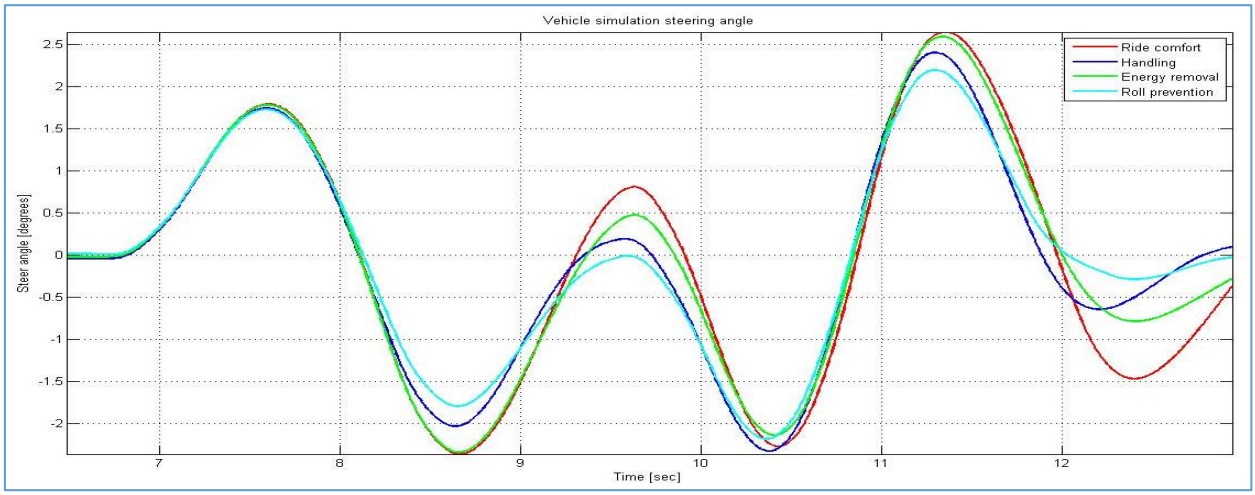

Figure 8.47: Double Lane Change at 70 km/h, steer input

8.4.2.3 Vehicle path

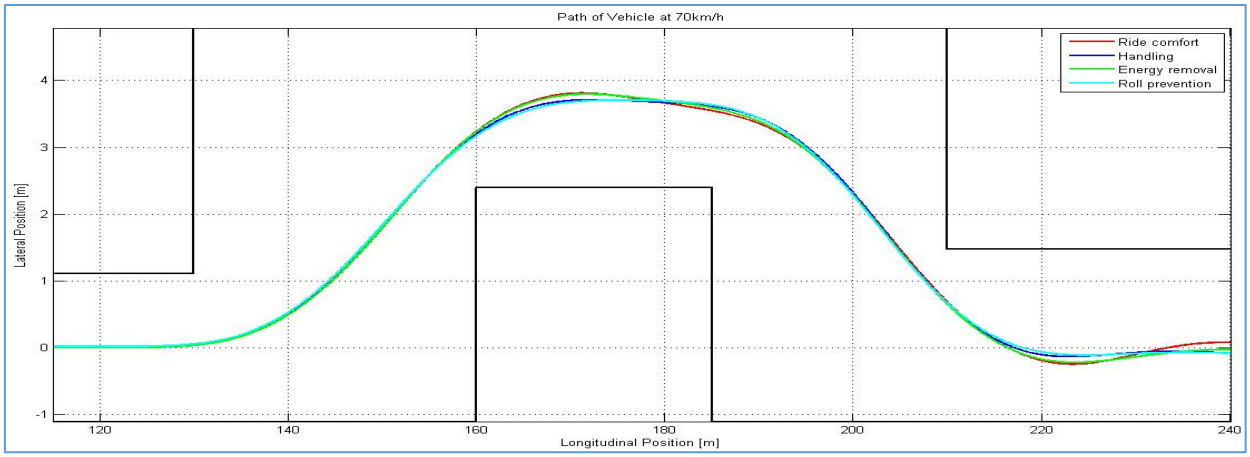

Figure 8.48: Double Lane Change at 70 km/h, vehicle path

8.4.2.4 Lateral acceleration, roll rate, roll angle and yaw rate

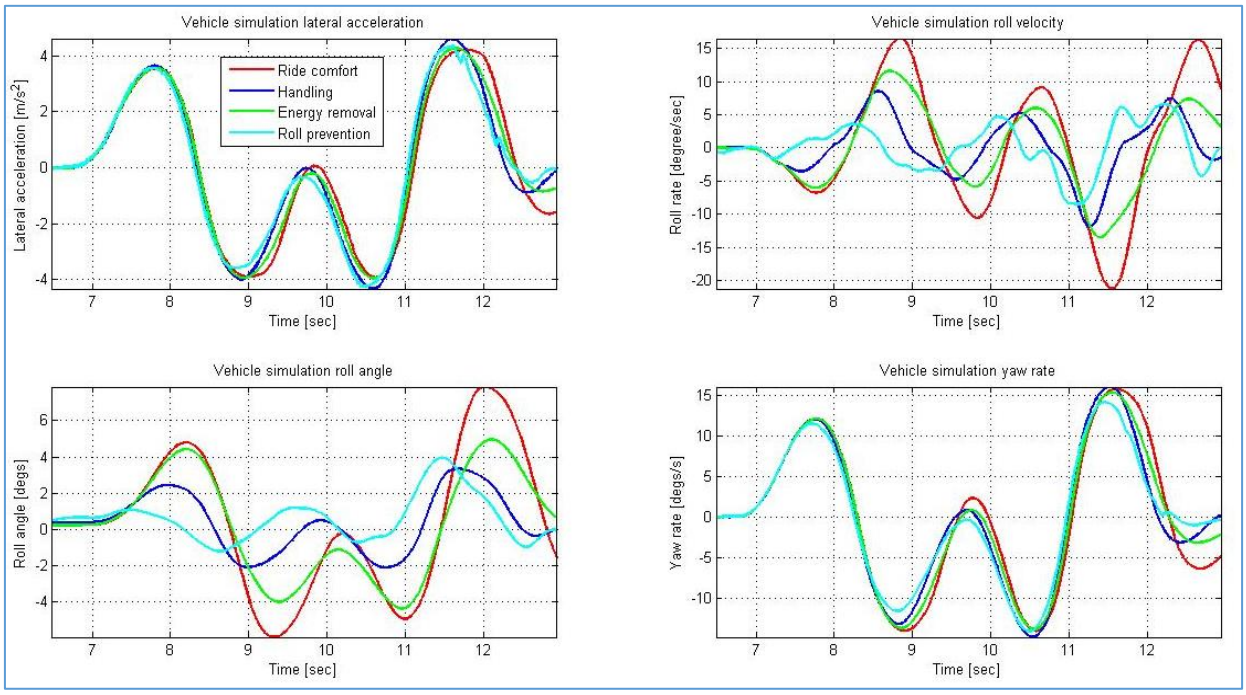

Figure 8.49: Double Lane Change at 70 km/h, lateral acceleration, roll rate, roll angle and yaw rate

8.4.2.5 Wheel lift

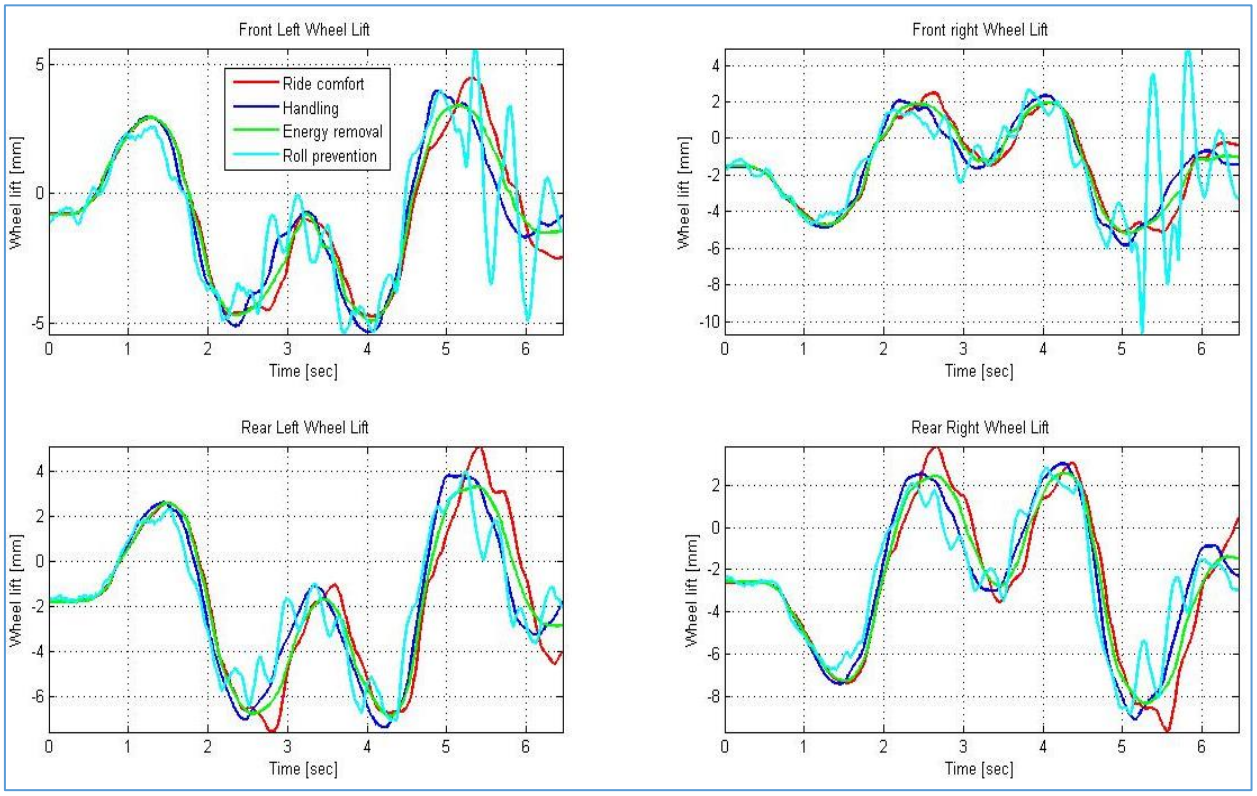

Figure 8.50: Double Lane Change at 70 km/h, wheel lift

8.4.2.6 Suspension displacement

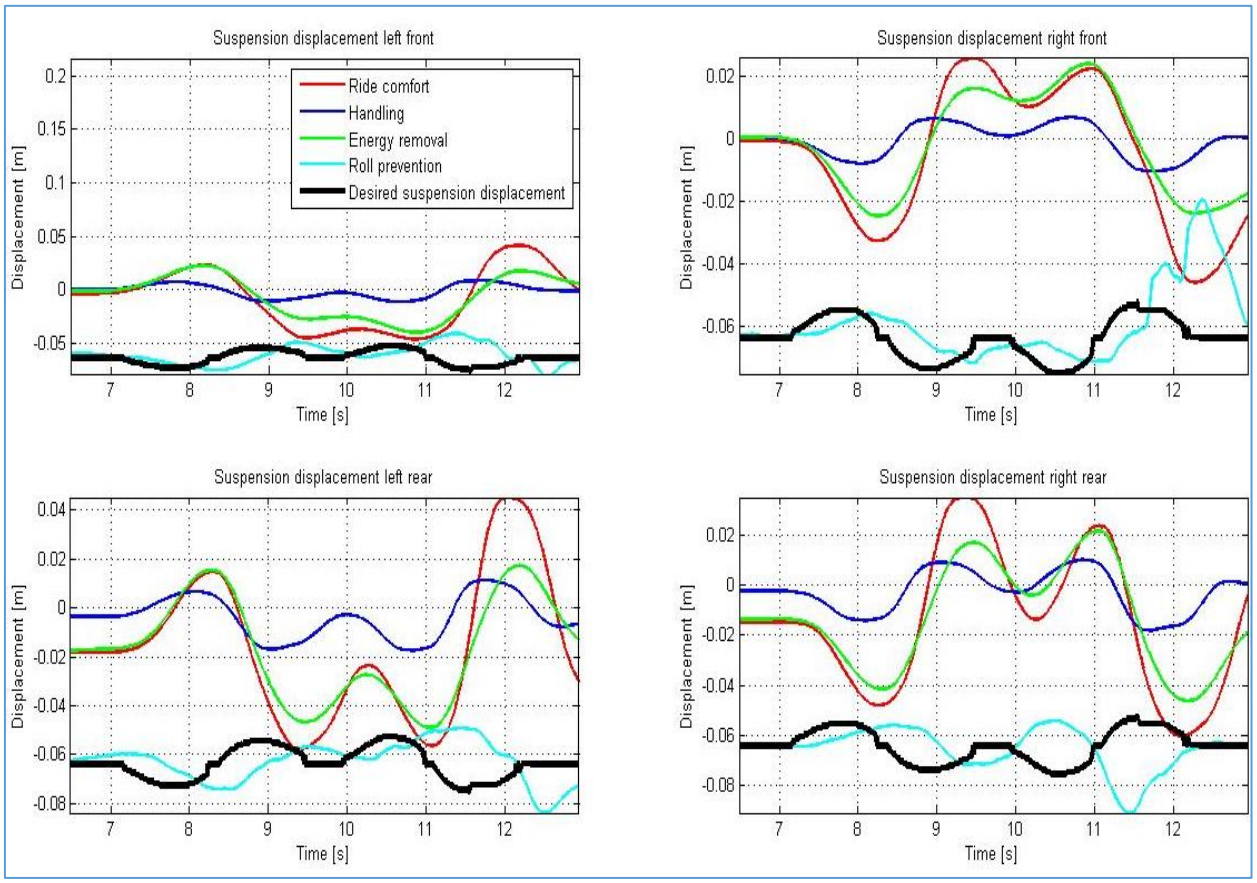

Figure 8.51: Double Lane Change at 70 km/h, suspension displacement

8.4.2.7 CG height change

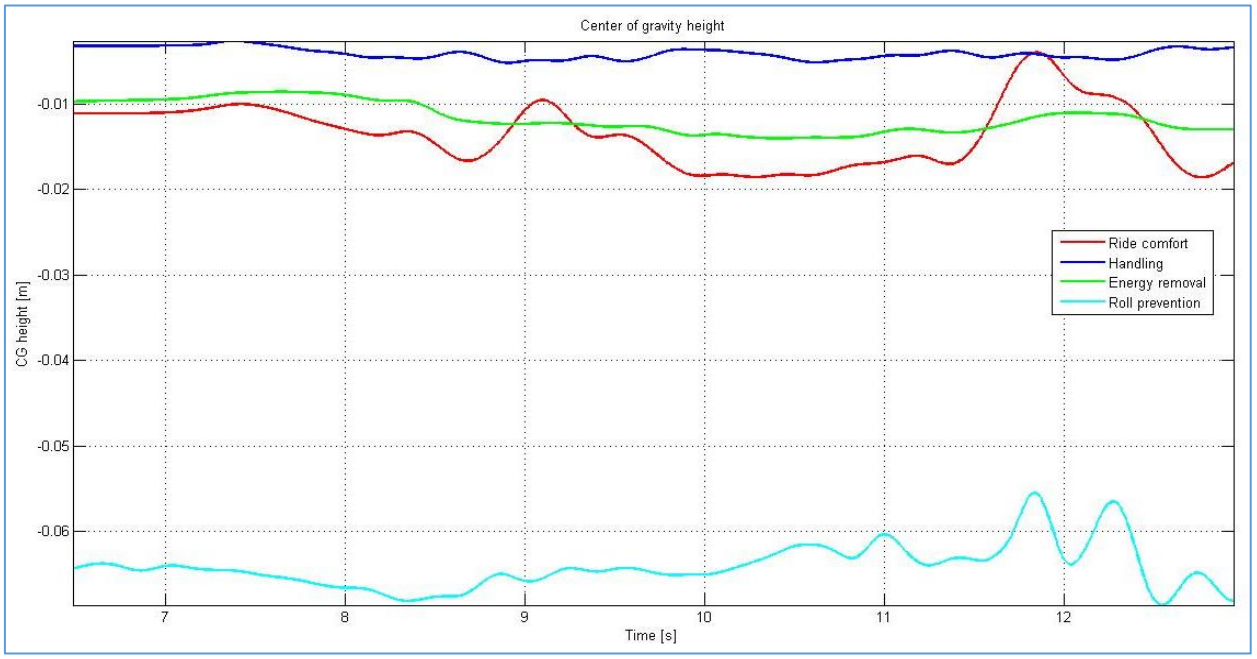

Figure 8.52: Double Lane Change at 70 km/h, CG height change

8.4.2.8 Rollover index from control system

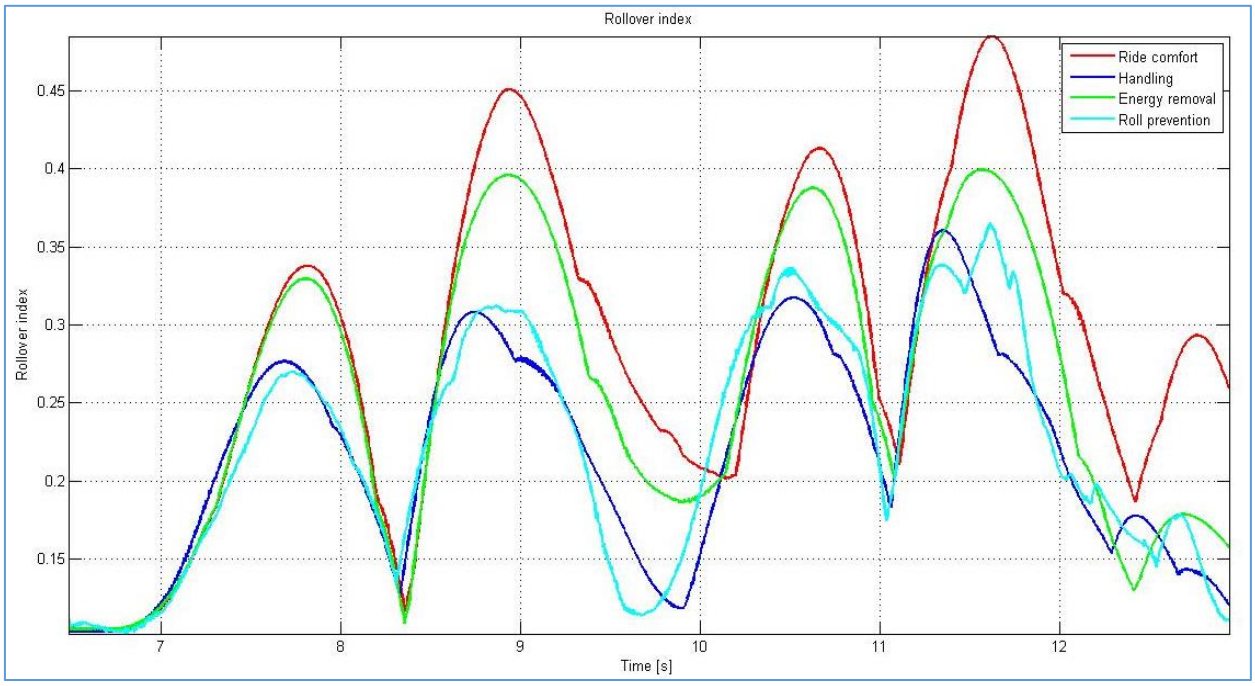

Figure 8.53: Double Lane Change at 70 km/h, Rollover index from control system

8.4.2.9 DSI and RPER

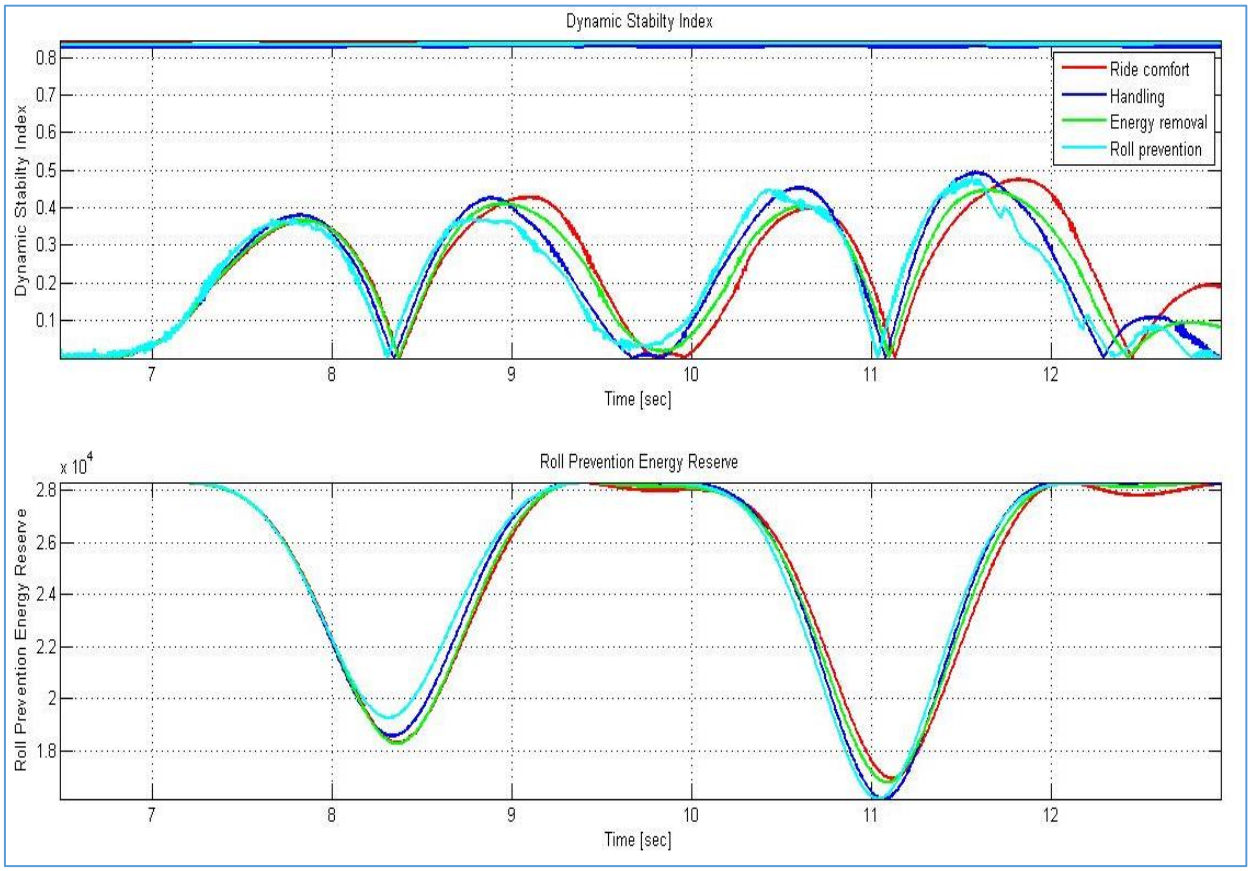

Figure 8.54: Double Lane Change at 70 km/h, DSI and RPER